frontiers | Research Topics

Therapeutic targets and clinical management of intermediate-advanced gastroenterological malignancies

Edited by
Hua Zhong and Yuanyuan Zheng

Published in
Frontiers in Medicine

ISSN 1664-8714
ISBN 978-2-8325-6872-9
DOI 10.3389/978-2-8325-6872-9

Generative AI statement
Any alternative text (Alt text) provided alongside figures in the articles in this ebook has been generated by Frontiers with the support of artificial intelligence and reasonable efforts have been made to ensure accuracy, including review by the authors wherever possible. If you identify any issues, please contact us.

About Frontiers

Frontiers is more than just an open access publisher of scholarly articles: it is a pioneering approach to the world of academia, radically improving the way scholarly research is managed. The grand vision of Frontiers is a world where all people have an equal opportunity to seek, share and generate knowledge. Frontiers provides immediate and permanent online open access to all its publications, but this alone is not enough to realize our grand goals.

Frontiers journal series

The Frontiers journal series is a multi-tier and interdisciplinary set of open-access, online journals, promising a paradigm shift from the current review, selection and dissemination processes in academic publishing. All Frontiers journals are driven by researchers for researchers; therefore, they constitute a service to the scholarly community. At the same time, the *Frontiers journal series* operates on a revolutionary invention, the tiered publishing system, initially addressing specific communities of scholars, and gradually climbing up to broader public understanding, thus serving the interests of the lay society, too.

Dedication to quality

Each Frontiers article is a landmark of the highest quality, thanks to genuinely collaborative interactions between authors and review editors, who include some of the world's best academicians. Research must be certified by peers before entering a stream of knowledge that may eventually reach the public - and shape society; therefore, Frontiers only applies the most rigorous and unbiased reviews. Frontiers revolutionizes research publishing by freely delivering the most outstanding research, evaluated with no bias from both the academic and social point of view. By applying the most advanced information technologies, Frontiers is catapulting scholarly publishing into a new generation.

What are Frontiers Research Topics?

Frontiers Research Topics are very popular trademarks of the *Frontiers journals series*: they are collections of at least ten articles, all centered on a particular subject. With their unique mix of varied contributions from Original Research to Review Articles, Frontiers Research Topics unify the most influential researchers, the latest key findings and historical advances in a hot research area.

Find out more on how to host your own Frontiers Research Topic or contribute to one as an author by contacting the Frontiers editorial office: frontiersin.org/about/contact

Therapeutic targets and clinical management of intermediate-advanced gastroenterological malignancies

Topic editors

Hua Zhong — University of Hawaii at Manoa, United States

Yuanyuan Zheng — Tongji University School of Medicine, China

Citation

Zhong, H., Zheng, Y., eds. (2025). *Therapeutic targets and clinical management of intermediate-advanced gastroenterological malignancies*.

Lausanne: Frontiers Media SA. doi: 10.3389/978-2-8325-6872-9

Table of contents

frontiers | Frontiers in Immunology

TYPE Original Research
PUBLISHED 10 April 2024
DOI 10.3389/fimmu.2024.1365834

OPEN ACCESS

EDITED BY
Hua Zhong,
University of Hawaii at Manoa, United States

REVIEWED BY
Zhiming Li,
Sun Yat-sen University Cancer Center (SYSUCC), China
Jichang Han,
Washington University in St. Louis, United States
Jinyong Pang,
University of South Florida, United States
Sisi Chen,
University of Pennsylvania, United States

*CORRESPONDENCE
Yantao Tian
tianyantao@cicams.ac.cn
Jianwei Liang
Liangjw1976@163.com

†These authors have contributed equally to this work

RECEIVED 05 January 2024
ACCEPTED 28 March 2024
PUBLISHED 10 April 2024

CITATION
Jiang Y, Hu H, Shao X, Li W, Lu Y, Liang J and Tian Y (2024) A novel web-based dynamic prognostic nomogram for gastric signet ring cell carcinoma: a multicenter population-based study.
Front. Immunol. 15:1365834.
doi: 10.3389/fimmu.2024.1365834

A novel web-based dynamic prognostic nomogram for gastric signet ring cell carcinoma: a multicenter population-based study

Yujuan Jiang[1†], Haitao Hu[1†], Xinxin Shao[1], Weikun Li[1], Yiming Lu[1], Jianwei Liang[2*] and Yantao Tian[1*]

[1]Department of Pancreatic and Gastric Surgery, National Cancer Center/National Clinical Research Center for Cancer/Cancer Hospital, Chinese Academy of Medical Sciences and Peking Union Medical College, Beijing, China, [2]Department of Colorectal Surgery, National Cancer Center/National Clinical Research Center for Cancer/Cancer Hospital, Chinese Academy of Medical Sciences and Peking Union Medical College, Beijing, China

Background: Gastric signet ring cell carcinoma (GSRCC) is a rare and highly malignant disease with a poor prognosis. To assess the overall survival (OS) and cancer-specific survival (CSS) of patients with GSRCC, prognostic nomograms were developed and validated using common clinical factors.

Methods: This retrospective cohort study included patients diagnosed with GSRCC between 2011 and 2018 from the National Cancer Center (n = 1453) and SEER databases (n = 2745). Prognostic nomograms were established by identifying independent prognostic factors using univariate and multivariate Cox regression analyses. The calibration curve and C-index were used to assess the predictions. The clinical usefulness of the survival prediction model was further evaluated using the DCA and ROC curves. The models were internally validated in the training cohort and externally validated in the validation cohort. Two web servers were created to make the nomogram easier to use.

Results: Patients with GSRCC were divided into training (*n* = 2938) and validation (*n* = 1260) cohorts. The nomograms incorporated six predictors: age, race, tumor site, tumor size, N stage, T stage, and AJCC stage. Excellent agreement was observed between the internal and exterior calibration plots for the GSRCC survival estimates. The C-index and area under the ROC curve were roughly greater than 0.7. Both nomograms had adequate clinical efficacy, as demonstrated by the DCA plots. Furthermore, we developed a dynamic web application utilizing the constructed nomograms available at https://jiangyujuan.shinyapps.io/OS-nomogram/ and https://jiangyujuan.shinyapps.io/DynNomapp-DFS/.

Conclusion: We developed web-based dynamic nomograms utilizing six independent prognostic variables that assist physicians in estimating the OS and CSS of patients with GSRCC.

KEYWORDS

gastric signet ring cell carcinoma, prognosis, dynamic nomogram, overall survival, cancer-specific survival

Introduction

Gastric cancer (GC) ranks fifth in incidence and fourth in cancer-related mortality, leading to approximately 768,793 deaths annually (1). Gastric signet ring cell carcinoma (GSRCC) is a unique type of GC characterized by abundant mucus, with the nucleus pushed to the side by intracytoplasmic mucin, representing 35–45% of new adenocarcinomas (2). Due to the underdevelopment of screening technologies in previous years, the majority of GSRCC patients were diagnosed with an advanced disease. The prognosis of GC patients has improved due to recent advancements in surgery, chemotherapy, radiation, targeted therapy, and immunotherapy; still, the 5-year survival rate of GSRCC is only about 32.1% (3). Notably, the biological behavior of GSRCC is significantly heterogeneous compared to that of non-GSRCCs, which can be attributed to the depth of tumor infiltration (4). GSRCC is typically an advanced tumor stage that is resistant to chemotherapy (2). Radical tumor resection (R0) is the most effective treatment for GSRCC. However, the R0 resection rate of GSRCC was significantly lower than that of non-GSRCC (56.0% vs. 74%, $P = 0.019$), and the postoperative peritoneal recurrence rate was much higher than that of non-GSRC (52.2% vs. 21.4%) (2). Hence, there is a need to improve the postoperative clinical outcomes of patients with GSRCC through individualized treatment.

Tumor-node-metastasis (TNM) staging is currently used to regularly estimate the prognosis of GC patients. However, due to the considerable genetic heterogeneity in GC, recurrence and mortality may differ significantly even among GC patients with similar TNM stage. Nomograms, which are commonly used for assessing cancer patient prognosis and personally predicting survival rates, are more suitable for clinical patient management than the TNM staging system. However, despite the establishment of several postoperative nomograms that have significantly contributed to the management of patients with GSRCC, some issues have arisen (5–8). First, these models focused solely on the overall postoperative survival and did not predict cancer-specific survival. Second, calibration tests, external model validations, and evaluations of the clinical usefulness of these models are lacking, making it difficult to assess their accuracy and practicability. Moreover, the traditional predictive models are not sufficiently simple. A web-based dynamic nomogram that calculates the probability of a disease is a more precise and practical tool than standard nomograms and some predictive models. To classify the prognosis of GSRCC patients, it is thus essential to create a straightforward, user-friendly, and reliable prognosis prediction model.

This study established two new postoperative web-based nomograms for patients with stage I-III GSRCC to predict 1-, 3-, and 5-year overall survival (OS) and cancer-specific survival (CSS).

Materials and methods

Study population

Patients diagnosed with GSRCC between 2011 and 2018 from the Surveillance, Epidemiology, and End Results (SEER) database (http://www.seer.cancer.gov) were identified using the SEER*Stat software (version 8.4.2). The eligibility criteria were as follows: (1) ICD-O-3 histology code of 8490, (2) site code of C16.0–16.9, (3) lack of other synchronous malignancies, (4) age between 20 and 80 years, and (5) radical surgical treatment. The exclusion criteria were as follows: (1) patients who did not undergo radical surgery, (2) patients who survived less than one month or had an unknown survival status, (3) patients with distant metastasis, and (4) patients with unclear clinicopathological characteristics such as TNM stage. Patients diagnosed with GSRCC between 2011 and 2018 at the National Cancer Center (NCC cohort) were included based on the above criteria. The patient screening process is illustrated in Figure 1. Ethical approval was obtained from the Ethics Committee of the National Cancer Center/Cancer Hospital, the Chinese Academy of Medical Science, and Peking Union Medical College (NCC2023C-657). Due to the retrospective nature of this study, informed consent was not required.

Prognostic variables

Patient variables such as age, sex, race, tumor size, tumor site, grade, AJCC TNM stage, pathological N stage, pathological T stage, survival time, and status were collected. All patients underwent restaging based on the criteria outlined in the AJCC on Cancer 8th edition staging manual. OS was the primary endpoint and was determined from the date of diagnosis until death from any cause or

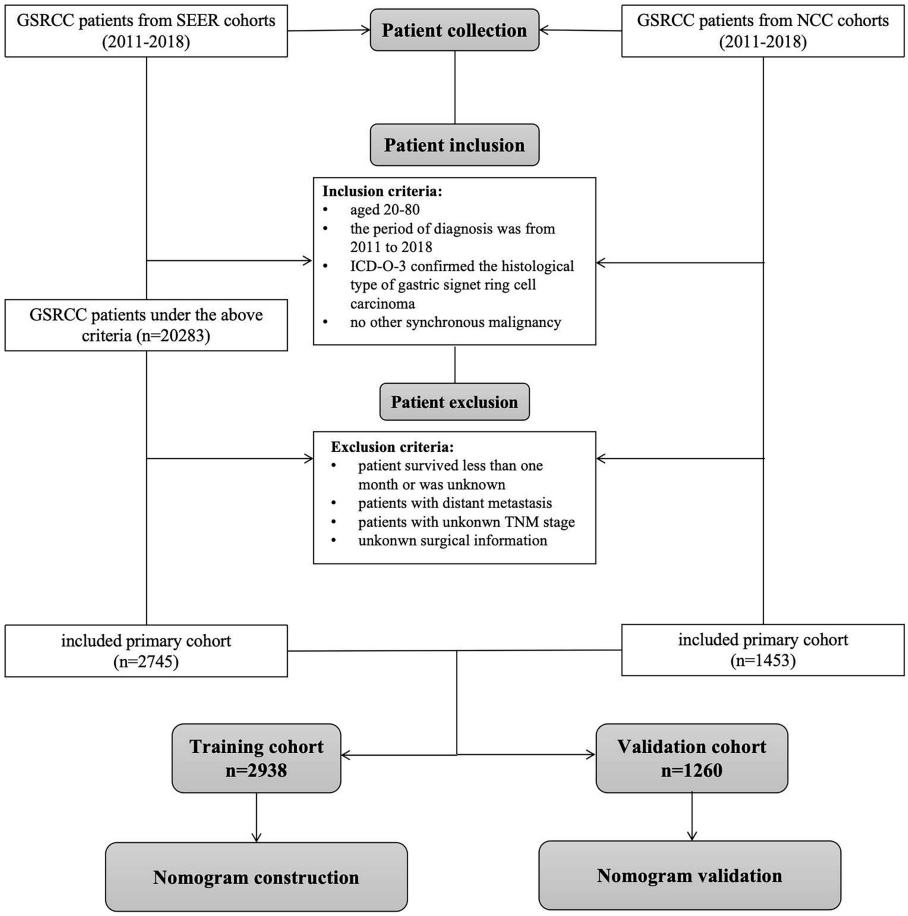

FIGURE 1
Flow chart of the construction and validation of the nomogram models.

last follow-up. CSS was the secondary endpoint and was selected from the date of diagnosis until GSRCC cancer-related death or last follow-up. In the SEER cohort, CSS is defined by the SEER cause-specific death category. In the NCC cohort, we carefully monitored every patient in the after surgery, and we included those who lost their lives due to GSRCC in the CSS survival analysis. Patients were categorized into two age groups: young (<60 years) and old (>60 years). The patient groups were stratified based on tumor size: <5 cm and >5 cm.

Establishment and validation of the nomogram

The patients were randomly assigned to the training (70%) and validation (30%) cohorts. Independent prognostic factors were chosen using a backward stepwise method with AIC to minimize information loss. Subsequently, a univariate Cox proportional hazard regression analysis was performed for the training cohort. Factors associated with a P value < 0.1 according to the univariate analysis were subsequently included in the multivariate Cox analysis to determine the hazard ratio (HR) and p-value for each independent prognostic variable. The factors with P <0.05 in COX multivariate regression analyses were considered independent risk factors for prognosis, and the prognostic prediction models were constructed on the basis of these factors. When building a multivariate regression model, we derive the regression coefficient β for each variable. The nomogram scores the variable with the largest regression coefficient in the regression model as 100 points. All other variables are converted using it as a criterion, e.g. β=2 with a score of 100. If the other variables β=1, the score is 1*100/2. After converting the regression coefficients to a 0–100 point scale based on multivariate analysis, we developed two prognostic nomograms to predict OS and CSS in patients with GSRCC using independent predictive variables. The accuracy of the nomograms was validated internally and externally using calibration curves. The C-index and area under the ROC curve (AUC) were used to evaluate the discriminative ability. To evaluate the models' clinical applicability, decision curve analysis (DCA) was used to calculate the net benefit at various threshold probabilities. The net benefit is defined as that true positive minus false positive. To put it succinctly, all patient death curves and none patient death curves were drawn as two references. DCA calculates the clinical benefit compared with the reference lines. The higher the net benefit, the more

10.3389/fimmu.2024.1365834

practical and effective the prediction model is in clinical practice. The patients were categorized into low- and high-risk groups based on the risk score calculated for each patient. Finally, Kaplan––Meier plots were generated to assess potential disparities in overall survival between the high- and low-risk patient groups.

Statistical analysis

Categorical variables are presented as numbers and percentages. Pearson's correlation analysis was used to ensure that there was no collinearity between the screened variables (Supplementary Figure 2). Univariable and multivariable Cox proportional hazards models were used to analyze DFS and OS, in which hazard ratios (HRs) and their 95% confidence intervals (CIs) were calculated. Survival analysis was performed using the Kaplan––Meier method and log-rank test. A two-tailed significance level of $P < 0.05$ (two-tailed) was used for all statistical tests. Statistical analysis was conducted using R (version 4.0.2 (https://www.r-project.org/). The "caret" package was used to partition the training and validation cohorts randomly. Dynamic nomogram models were constructed with the "rms" and "Dynnom" packages.

Results

Clinicopathological characteristics of patients

A total of 4198 patients diagnosed with GSRCC between 2011 and 2018 were included in this study and were randomly divided into two cohorts: the training cohort (n = 2938; 70%) and the validation cohort (n = 1260; 30%). Comprehensive descriptive statistics are presented in Table 1. Most patients were white (n = 1883; 44.9%) or male (n = 2416; 57.5%). More than half of the patients (51.0%) were in the older age group. Moreover, 2277 patients (54.2%) had a tumor size of ≤5 cm. The predominant grade was III (n =3423, 81.5%). Moreover, 1857 patients (44.2%) underwent surgery, 1126 (26.8%) underwent surgery plus chemotherapy, and 821 (19.6%) underwent surgery with neoadjuvant therapy. The gastric antrum, encompassing the pylorus, was the most common site of GSRCC (32.1%). The median follow-up duration for all patients was 45 months (IQR, 25–69 months).

Univariate and multivariate analysis of clinicopathological features

A ratio of 7:3 was used to randomly assign the patients to the training and validation cohorts. Preliminary univariate analysis of the training dataset revealed significant correlations (all $P < 0.1$) between OS and several variables including age, race, tumor size, tumor site, depth of invasion, pN, and AJCC stage. Subsequently, the predictive features that exhibited significant associations with OS in univariate

TABLE 1 The demographic and clinical characteristics of the patients with GSRCC in the SEER and NCC cohorts.

Factor	Total cohort (n = 4198)	SEER cohort (n = 2745)	NCC cohort (n = 1453)
Sex (%)			
Male	2416 (57.5%)	1468 (53.5%)	948 (65.2%)
Female	1782 (42.4%)	1277 (46.5%)	505 (34.8%)
Age			
≤60 years	2057 (49.0%)	1162 (42.3%)	895 (61.6%)
>60 years	2141 (51.0%)	1583 (57.7%)	558 (38.4%)
Race (%)			
Black	331 (7.9%)	331 (12.1%)	0
White	1883 (44.9%)	1883 (68.6%)	0
Chinese	1554 (37.0%)	101 (3.7%)	1453 (100%)
Other	430 (10.2%)	430 (15.7%)	0
Site (%)			
1/3 U	973 (23.2%)	628 (22.9%)	345 (23.7%)
1/3 M	428 (10.2%)	330 (12.0%)	98 (6.7%)
1/3 L	1349 (32.1%)	778 (28.3%)	571 (39.3%)
Curvature	761 (18.1%)	415 (15.1%)	346 (23.8%)
Total stomach	414 (9.9%)	329 (12.0%)	85 (5.9%)
others	273 (6.5%)	265 (9.7%)	8 (0.6%)
Size (%)			
≤5 cm	2277 (54.2%)	1268 (46.2%)	1009 (69.4%)
>5 cm	1921 (45.8%)	1477 (53.8%)	444 (30.6%)
Grade (%)			
I	34 (0.8%)	7 (0.3%)	27 (1.9%)
II	371 (8.8%)	58 (2.1%)	313 (21.5%)
III	3423 (81.5%)	2311 (84.2%)	1112 (76.5%)
IV	66 (1.6%)	65 (2.4%)	1 (0.1%)
NA	304 (7.2%)	304 (11.1%)	0
AJCC stage (%)			
IA	907 (21.6%)	568 (20.7%)	339 (23.3%)
IB	398 (9.5%)	276 (10.1%)	122 (8.4%)
IIA	442 (10.5%)	304 (11.1%)	138 (9.5%)
IIB	580 (13.8%)	400 (14.6%)	180 (12.4%)
IIIA	537 (12.8%)	387 (14.1%)	150 (10.3%)
IIIB	585 (13.9%)	375 (13.7%)	210 (14.5%)
IIIC	749 (17.8%)	435 (15.8%)	314 (21.6%)
pT stage (%)			
T1	1166 (27.8%)	751 (27.4%)	415 (28.6%)

(Continued)

10.3389/fimmu.2024.1365834

TABLE 1 Continued

Factor	Total cohort (n = 4198)	SEER cohort (n = 2745)	NCC cohort (n = 1453)
pT stage (%)			
T2	493 (11.7%)	320 (11.7%)	173 (11.9%)
T3	1232 (29.3%)	906 (33.0%)	326 (22.4%)
T4	1307 (31.1%)	768 (28.0%)	539 (37.1%)
pN stage (%)			
N0	1876 (44.7%)	1284 (46.8%)	592 (40.7%)
N1	759 (18.1%)	566 (20.6%)	193 (13.3%)
N2	575 (13.7%)	355 (12.9%)	220 (15.1%)
N3	988 (23.5%)	540 (19.7%)	448 (30.8%)
Therapy (%)			
surgery only	1857 (44.2%)	1664 (60.6%)	193 (13.3%)
surgery plus neo/chemo	392 (9.3%)	172 (6.3%)	220 (15.1%)
surgery plus chemo	1126 (26.8%)	678 (24.7%)	448 (30.8%)
surgery plus neo	821 (19.6%)	229 (8.3%)	592 (40.7%)
NA	2 (0.5%)	2 (0.1%)	0

pN, pathologic N stage; pT, pathologic T stage.
The tumor site was divided into 1/3 U (cardia, fundus, gastroesophageal junction), 1/3 M (body), 1/3 L (antrum, pylorus), curvature, total stomach, and other (gastric remnant, anastomosis, and linitis plastica) parts of the stomach. NA, not applicable.

analyses were subjected to multivariate Cox proportional hazards regression analysis. Multivariate analysis results indicated that only age (hazard ratio 1.60, 95% CI 1.45-1.76, P < 0.001), race (P < 0.05), tumor site (P < 0.05), tumor size (hazard ratio 1.80, 95% CI 1.62-2.00 P < 0.001), AJCC stage (P < 0.05), and pN stage (P < 0.001) were significantly associated with OS (Table 2). A forest plot illustrating the hazard ratios (HRs) and 95% confidence intervals (CIs) for OS based on the Cox proportional hazards regression analysis is presented in Supplementary Figure 1A.

In the training cohort, univariate analysis revealed that age, race, tumor size, tumor site, invasion depth, pN stage, and AJCC stage were associated with CSS in patients with GSRCC. Subsequent multivariate analysis identified age (hazard ratio 1.46, 95% CI 1.31-1.62, P < 0.001), race (P < 0.05), tumor site (P < 0.05), tumor size (hazard ratio 1.93, 95% CI 1.72-2.16, P < 0.001), AJCC stage (P < 0.001), and pN stage (P < 0.005) as independent factors (Table 3; Supplementary Figure 1B).

The nomograms for OS and CSS were established

We integrated age, race, tumor size, tumor site, AJCC stage, and pN stage to develop comprehensive prognostic nomograms for evaluating the OS and CSS probabilities of patients with

TABLE 2 Univariate and multivariate analyses of overall survival in the training cohort.

Factor	Univariate analyses		Multivariate analyses	
	p Value	HR (95% CI)	*p* Value	HR (95% CI)
Sex	0.143		0.266	
Male		Reference		Reference
Female		0.93 (0.84-1.02)		0.94 (0.85-1.04)
Age	**<0.001**		**<0.001**	
≤60 years		Reference		Reference
>60 years		1.73 (1.57-1.90)		1.60 (1.45-1.76)
Race				
Black		Reference		Reference
White	0.994	1(0.85-1.18)	**0.030**	0.84 (0.72-0.98)
Chinese	**<0.001**	0.34 (0.29-0.41)	**<0.001**	0.41 (0.34-0.49)
Other	**<0.001**	0.68 (0.55-0.83)	**0.001**	0.71 (0.57-0.87)
Site				
1/3 U		Reference		Reference
1/3 M	**<0.001**	0.62 (0.52-0.75)	0.606	0.95 (0.77-1.16)
1/3 L	**<0.001**	0.54 (0.48-0.62)	0.387	0.93 (0.80-1.09)
Curvature	**<0.001**	0.52 (0.45-0.61)	0.280	0.91 (0.76-1.08)
Total stomach	**0.010**	1.23 (1.05-1.45)	**<0.001**	1.39 (1.15-1.67)
others	**<0.001**	1.53 (1.28-1.82)	**0.023**	1.28 (1.03-1.58)
Size			**<0.001**	
≤5 cm		Reference		Reference
>5 cm	**<0.001**	2.85 (2.58-3.14)		1.80 (1.62-2.00)
Grade (%)				
I		Reference		Reference
II	0.730	1.28 (0.31-5.21)	0.985	1.01 (0.32-3.23)
III	0.097	3.23 (0.81-12.93)	0.461	1.54 (0.49-4.80)
IV	0.097	3.36 (0.80-14.01)	0.693	1.27 (0.39-4.20)
NA	0.064	3.74 (0.93-15.06)	0.286	1.87 (0.59-5.91)

(Continued)

10.3389/fimmu.2024.1365834

TABLE 2 Continued

Factor	Univariate analyses		Multivariate analyses	
	p Value	HR (95% CI)	*p* Value	HR (95% CI)
AJCC stage				
IA		Reference		Reference
IB	**<0.001**	1.57 (1.25-1.97)	**<0.001**	1.83 (1.35-2.47)
IIA	**<0.001**	1.85 (1.49-2.29)	**<0.001**	2.29 (1.53-3.41)
IIB	**<0.001**	2.58 (2.14-3.11)	**<0.001**	3.50 (2.21-5.54)
IIIA	**<0.001**	3.07 (2.55-3.70)	**<0.001**	4.22 (2.41-7.38)
IIIB	**<0.001**	4.08 (3.40-4.89)	**<0.001**	5.78 (3.19-10.46)
IIIC	**<0.001**	4.96 (4.18-5.89)	**<0.001**	8.04 (3.93-16.45)
pT stage				
T1		Reference		Reference
T2	**0.007**	1.31 (1.08-1.61)	0.146	0.80 (0.59-1.08)
T3	**<0.001**	2.73 (2.37-3.14)	0.626	0.91 (0.64-1.31)
T4	**<0.001**	3.43 (2.98-3.95)	0.389	0.82 (0.52-1.29)
pN stage				
N0		Reference		Reference
N1	**<0.001**	1.59 (1.39-1.82)	0.095	0.85 (0.70-1.03)
N2	**<0.001**	1.58 (1.36-1.83)	**0.002**	0.66 (0.51-0.86)
N3	**<0.001**	2.42 (2.15-2.73)	**0.007**	0.64 (0.46-0.89)
Therapy				
surgery only		Reference		
surgery plus neo/chemo	0.115	0.57 (0.47-0.68)		
surgery plus chemo	0.322	0.87 (0.78-0.97)		
surgery plus neo	0.979	1.00 (0.82-1.21)		
NA	0.751	1.25 (0.31-5.01)		

pN, pathologic N stage; pT, pathologic T stage; CI, confidence interval; HR, hazard ratio.
Bold represents significant statistical difference (P<0.05).
NA, not applicable.

TABLE 3 Univariate and multivariate analyses of cancer-specific survival in the training cohort.

Factor	Univariate analyses		Multivariate analyses	
	p Value	HR (95% CI)	*p* Value	HR (95% CI)
Sex	0.474		0.519	
Male		Reference		Reference
Female		0.96 (0.87-1.07)		0.97 (0.87-1.07)
Age	**<0.001**		**<0.001**	
≤60 years		Reference		Reference
>60 years		1.57 (1.41-1.73)		1.46 (1.31-1.62)
Race				
Black		Reference		Reference
White	**0.473**	0.94 (0.79-1.12)	**0.155**	0.88 (0.74-1.05)
Chinese	**<0.001**	0.40 (0.33-0.48)	**<0.001**	0.46 (0.37-0.56)
Other	**<0.001**	0.61 (0.48-0.76)	**0.004**	0.71 (0.56-0.90)
Site				
1/3 U		Reference		Reference
1/3 M	**<0.001**	0.67 (0.55-0.81)	0.741	0.96 (0.77-1.20)
1/3 L	**<0.001**	0.59 (0.52-0.68)	0.224	0.90 (0.77-1.06)
Curvature	**<0.001**	0.52 (0.44-0.61)	0.207	0.89 (0.73-1.07)
Total stomach	**0.004**	1.28 (1.08-1.51)	**0.003**	1.35 (1.10-1.64)
others	**<0.001**	1.55 (1.27-1.88)	**0.034**	1.27 (1.02-1.60)
Size	**<0.001**		**<0.001**	
≤5 cm		Reference		Reference
>5 cm		3.01 (2.71-3.35)		1.93 (1.72-2.16)
Grade (%)				
I		Reference		
II	0.989	0.99 (0.24-4.04)		
III	0.216	2.40 (0.60-9.61)		
IV	0.189	2.62 (0.62-11.02)		

(Continued)

10.3389/fimmu.2024.1365834

TABLE 3 Continued

Factor	Univariate analyses		Multivariate analyses	
	p Value	HR (95% CI)	*p* Value	HR (95% CI)
Grade (%)				
NA	0.105	3.18 (0.79-12.86)		
AJCC stage				
IA		Reference		Reference
IB	**0.004**	1.52 (1.15-2.01)	**<0.001**	1.91 (1.35-2.70)
IIA	**<0.001**	2.17 (1.70-2.77)	**<0.001**	2.94 (1.90-4.54)
IIB	**<0.001**	3.37 (2.71-4.19)	**<0.001**	4.85 (2.97-7.91)
IIIA	**<0.001**	4.23 (3.42-5.24)	**<0.001**	6.06 (3.35-10.95)
IIIB	**<0.001**	5.35 (4.34-6.59)	**<0.001**	8.66 (4.64-16.18)
IIIC	**<0.001**	6.89 (5.64-8.42)	**<0.001**	12.55 (5.94-26.53)
pT stage				
T1		Reference		Reference
T2	**0.001**	1.46 (1.16-1.83)	0.078	0.74 (0.53-1.03)
T3	**<0.001**	3.37 (2.85-3.98)	0.317	0.82 (0.56-1.21)
T4	**<0.001**	4.76 (4.05-5.61)	0.211	0.74 (0.46-1.19)
pN stage				
N0		Reference		Reference
N1	**<0.001**	1.94 (1.68-2.24)	0.173	0.87 (0.71-1.06)
N2	**<0.001**	1.91 (1.63-2.24)	**<0.001**	0.62 (0.47-0.81)
N3	**<0.001**	2.91 (2.55-3.30)	**0.002**	0.58 (0.42-0.82)
Therapy				
surgery only		Reference		
surgery plus neo/chemo	0.155	0.65 (0.54-0.78)		
surgery plus chemo	0.133	0.92 (0.81-1.03)		
surgery plus neo	0.981	1.00 (0.81-1.24)		
NA	0.155	0.72 (0.10-5.10)		

pN, pathologic N stage; pT, pathologic T stage; CI, confidence interval; HR, hazard ratio. NA, not applicable.

GSRCC, as depicted in Figure 2. The survival probabilities at 1, 3, and 5 years were computed graphically considering the individual patient's unique characteristics, resulting in an interactive function. After converting the regression coefficients to a 0–100 point scale based on multivariate analysis. A vertical line is drawn from the value of the prognostic factor to the "Points" axis to determine the risk points associated with each prognostic factor. Subsequently, a vertical line is traced from the "Total Points," representing the accumulation of risk points toward the final three axes, displaying the 1-year, 3-year, and 5-year survival rates, respectively, to determine the OS and CSS probability for a specific patient. To use the nomograms to predict the prognosis of an individual GSRCC patient, first determine the score for every variable based on the value on the topmost point row corresponding to its parameter.

For instance, we examined a patient of white ethnicity with upper gastric cancer (28 points) at TNM stage IIIA (82 points) and pN2 (18 points) with a tumor size ≤ 5 cm (30 points) and aged > 60 years (45 points). Consequently, the total number of risk points is 173, and the survival probability axis can be determined by drawing a vertical line. The 1-, 3-, and 5-year survival probabilities of the patients were 90.0%, 72.7%, and 68.0%, respectively. The length of each variable line in these nomograms indicates its contribution to prognosis. For instance, our nomograms showed that AJCC stage had the most prominent impact on both CSS and OS in GSRCC patients among the included clinical parameters. Furthermore, we developed a dynamic web application that utilizes the constructed nomograms (Figure 3). Hyperlinks (https://jiangyujuan.shinyapps.io/OS-nomogram/ and https://jiangyujuan.shinyapps.io/DynNomapp-DFS/) can be accessed.

Validation of the protein-associated prognostic model

The calibration plot, concordance index (c-index), area under the curve (AUC), and DCA curve were used to evaluate the performance of the predictive models in both the training and validation cohorts. Initially, calibration curves were constructed, revealing a close alignment between the actual outcomes of GSRCC patients in the training and validation cohorts and the 1-, 3-, and 5-year OS and CSS probabilities predicted by the nomogram models. These results indicated a high level of predictive accuracy (Figure 4). Second, the nomogram demonstrated favorable accuracy in predicting survival, as evidenced by c-index values of 0.735 ± 0.012 and 0.743 ± 0.012 for OS and CSS, respectively, in the training cohort, and 0.715 ± 0.019 and 0.719 ± 0.020, respectively, in the validation cohort. ROC curves were generated to assess the predictive sensitivity and specificity of the nomogram prediction models. For the training cohort, the 1-, 3-, and 5-year area under the curve (AUC) values for OS were 0.76, 0.82, and 0.81, respectively, and those for CSS were 0.76, 0.82, and 0.83, respectively. The area under the curve (AUC) values for the prediction models were consistently above 0.70 in the validation cohort (Figure 5).

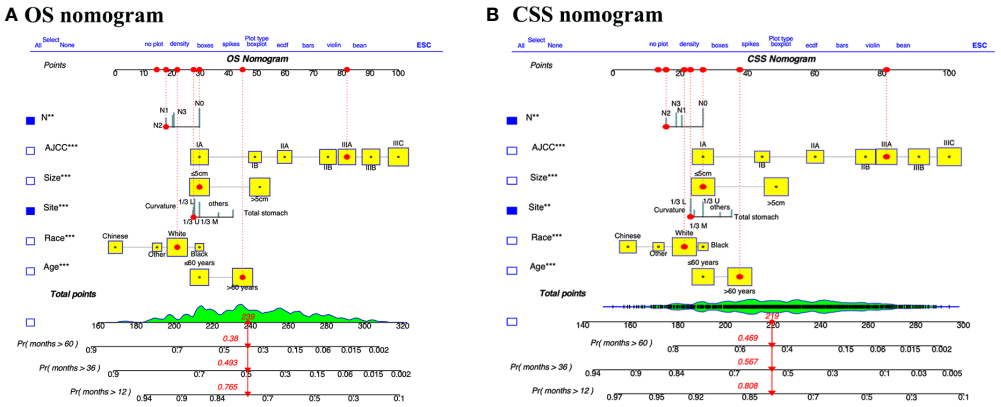

FIGURE 2
Dynamic nomograms for predicting the prognosis of patients with GSRCC. Nomograms for predicting the overall survival **(A)** and cancer specific survival **(B)** of GSRCC patients were created by integrating the six pivotal clinical prognostic factors. By drawing a vertical line straight upward from the factor's associated parameter to the points axis, one may find the score for each risk factor. The survival probability of GSRCC patients after one, three, and five years after surgery can then be obtained by adding the scores of all risk factors together and drawing a straight line from the total points axis to the OS or CSS axis.

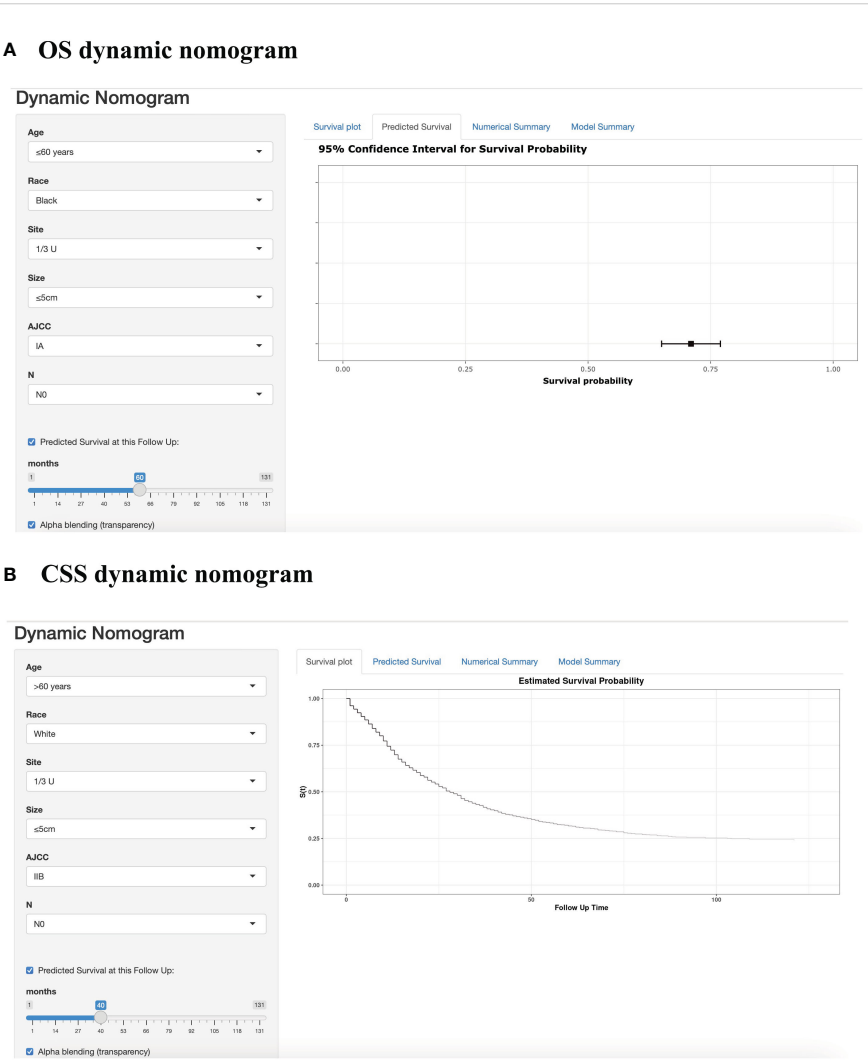

FIGURE 3
Web-based prognostic nomogram for patients with GSRCC. (Available at https://jiangyujuan.shinyapps.io/OS-nomogram/. and https://jiangyujuan.shinyapps.io/DynNomapp-DFS/.) **(A)** Overall survival. **(B)** Cancer-specific survival.

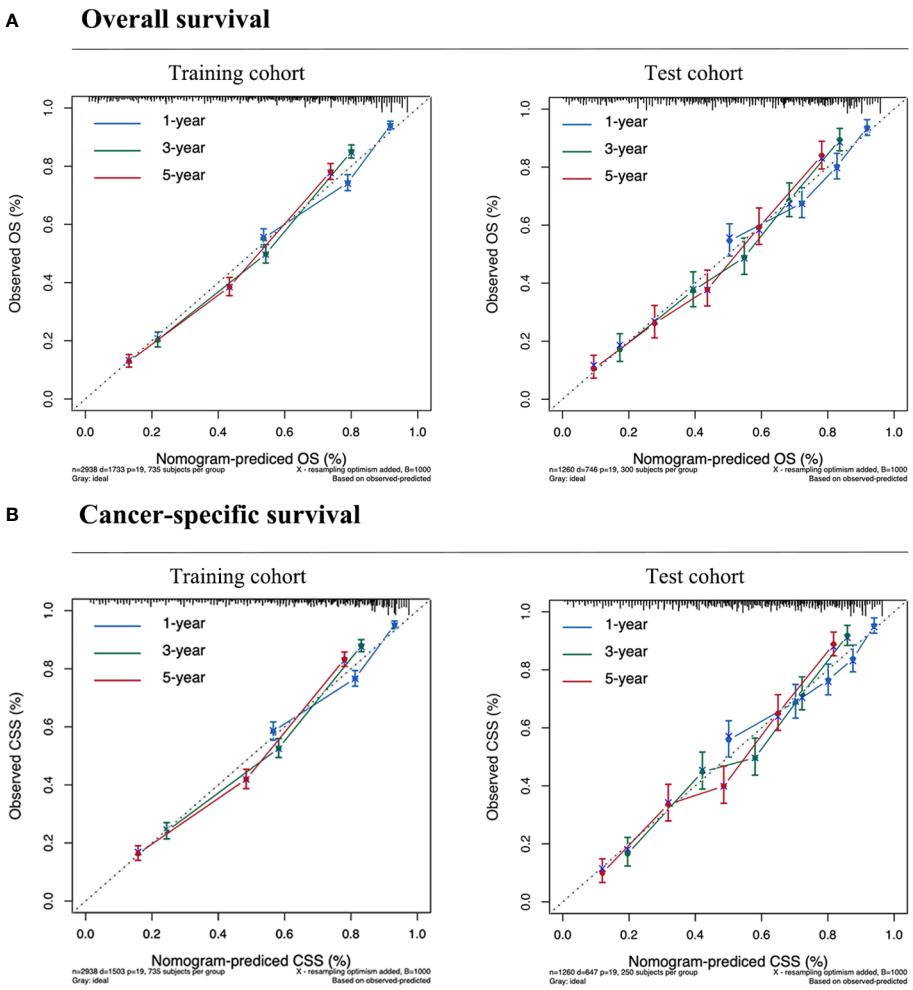

FIGURE 4
Calibration curves for predicting the survival of GSRCC patients. **(A)** Overall survival. **(B)** Cancer-specific survival. Our nomogram is represented by the solid line, while the ideal nomogram is represented by the 45-degree dotted line. The forecast is accurate if it falls on the 45-degree diagonal for the expected survival probability. The blue, green, and red lines represent 1, 3, and 5-year survival rates, respectively.

In summary, these findings substantiate the relatively high sensitivity and specificity of our nomogram models. Furthermore, DCA has frequently been employed to assess the clinical utility of nomograms. The nomograms outperformed conventional TNM staging and demonstrated a substantial positive net benefit in terms of mortality risk, as depicted in Figure 6. These findings indicate the significant clinical utility of nomograms in predicting the OS and CSS of patients with GSRCC.

Performance of the dynamic nomogram in stratifying patient risk status

Predictor variable scores were calculated using the nomogram and then combined to determine the total scores for individual patients. Patients with GSRCC were categorized into low- and high-risk groups based on their nomogram scores, using a threshold value of 125.0 points for the CSS nomogram and 157.0 points for the OS nomogram. Patients with scores exceeding the threshold were assigned to the high risk group. Survival analysis revealed that the probabilities of CSS ($P = 0.029$) and OS ($P = 0.024$) were significantly lower in the high-risk group than in the low-risk group, indicating the potential of these nomograms for risk stratification in GSRCC patients (Figure 7).

Discussion

GSRCC is a heterogeneous malignancy with a high risk of recurrence and death. For recurrent and metastatic GSRCC, there are currently few effective treatment options. To identify high-risk patients and implement early intervention and tailored treatment, it is crucial to create efficient prognostic prediction models. This study used data from the public SEER and NCC cohorts to develop and validate a predictive nomogram model for estimating the OS rate and CSS in patients with GSRCC. The nomograms incorporated six prognostic variables: age, race, tumor size, tumor site, N stage, and AJCC stage. Furthermore, a dynamic web application was

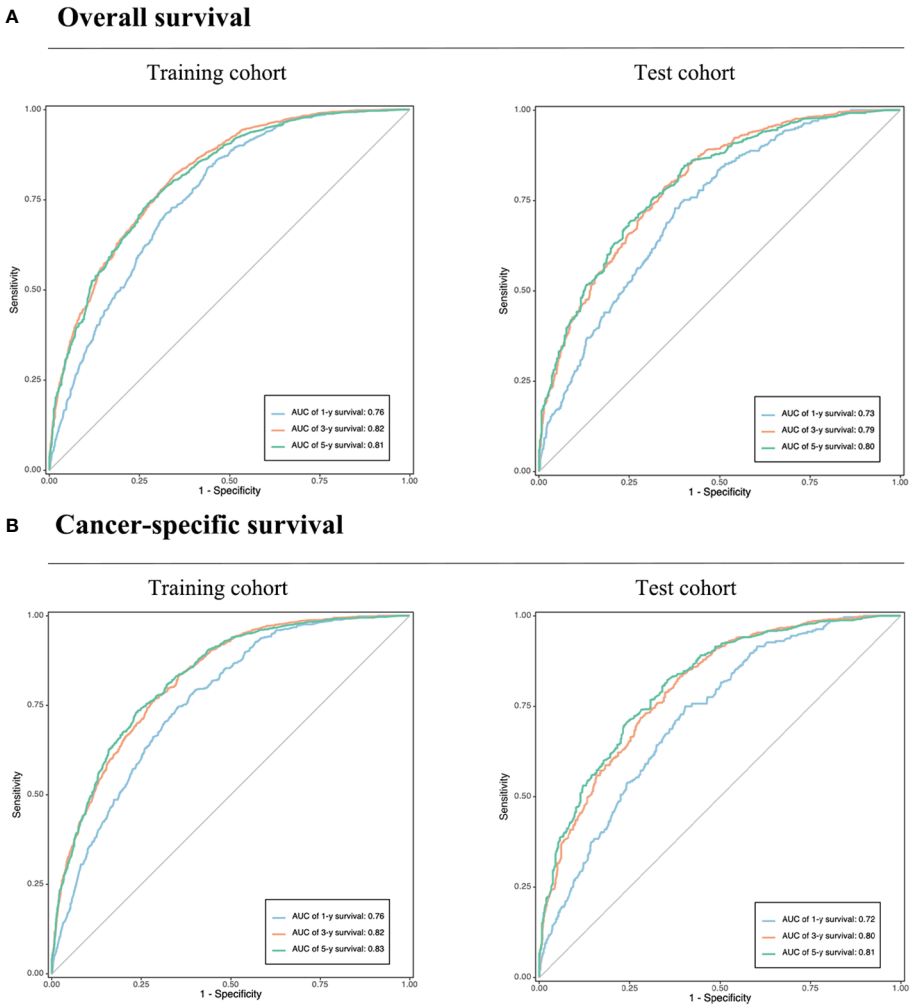

FIGURE 5
Validation of the prognostic nomograms using ROC curves. **(A)** Overall survival. **(B)** Cancer-specific survival. AUC, area under the curve. The blue, yellow, and green lines represent 1, 3, and 5-year survival rates, respectively.

developed to facilitate clinical decision making using these nomograms. The calibration of the nomograms demonstrated strong performance, with internal and external validations confirming their reliability. The OS and CSS nomograms also exhibited a C-index and AUC exceeding 0.7, indicating their effective discriminatory capability. Moreover, the decision curve analysis illustrated that our novel nomogram models provided a more significant net clinical benefit than the AJCC staging system across various threshold probabilities. These findings suggest that our nomograms could aid in developing tailored therapeutic strategies for the more effective treatment of patients with GSRCC.

This study focused on the GSRCC nomogram because of its controversial prognosis. Compared to other types of GC, GSRCC has unique tumorigenic properties and atypical epidemiological distribution (9). Zu et al. reported advanced GSRCC has a poorer prognosis than the other advanced gastric adenocarcinoma subtypes (10). The current staging system developed by the AJCC staging system for evaluating the prognosis of patients with AJCC staging system, cannot be used to effectively monitor GSRCC.

Only a few studies have revealed the prognostic factors of patients with GSRCC, and the related prognostic prediction models have been developed, although the models remain imperfect. For instance, the GSRCC prediction model that was presented by Liu et al. (5) and Zhang et al. (7) did not predict CSS; instead, it only addressed the OS. Nie et al. (8) only used data from the SEER database; hence, it is challenging to evaluate its accuracy and viability because there are insufficient external validations. Furthermore, a number of important clinicopathological parameters that have a substantial impact on patient survival—such as age, sex, and treatment type—are not taken into consideration by the GSRCC monitoring prediction models that are now in use. Therefore, further investigation is necessary to examine the factors influencing the long-term survival of patients with GSRCC and to develop valuable predictive models tailored to GSRCC. In this study, we conducted univariate and multivariate Cox regression analyses using extensive clinical data to identify independent risk factors for OS and CSS in patients with GSRCC.

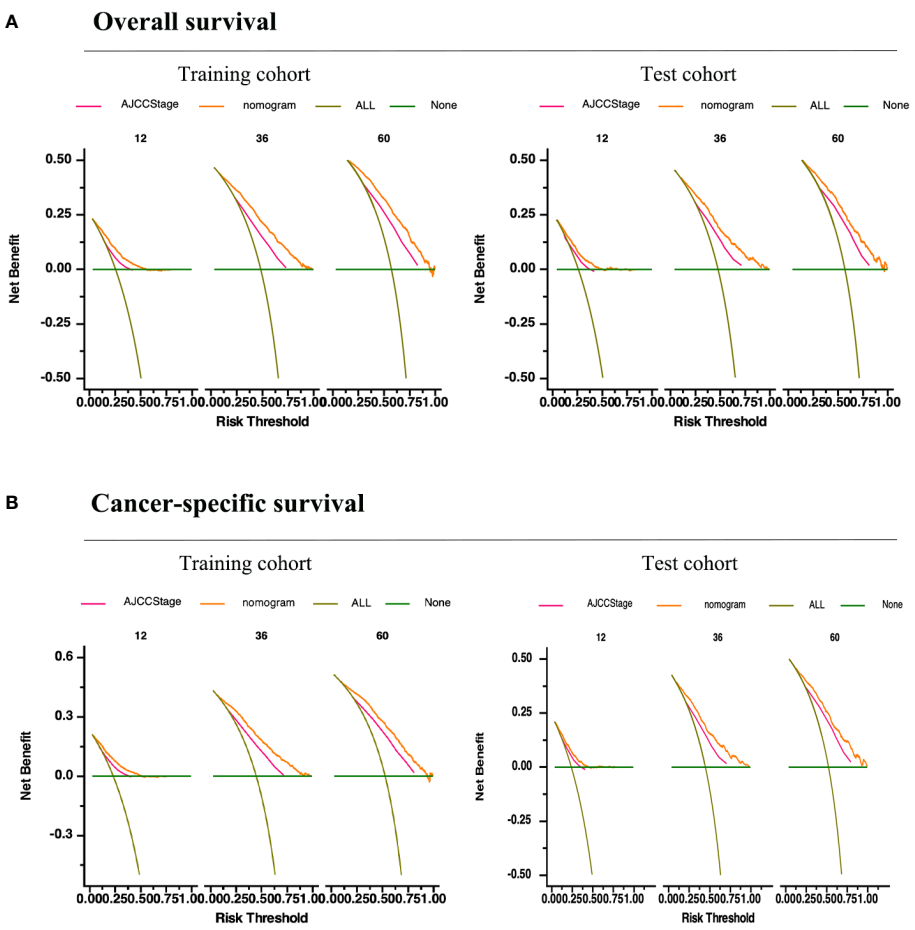

FIGURE 6
Validation of the prognostic nomograms using DCA curves. **(A)** Overall survival. **(B)** Cancer-specific survival. All, all the patients died or relapsed; None, no patients died or relapsed. The pink line represents the TNM staging and the yellow curve represents our prediction model.

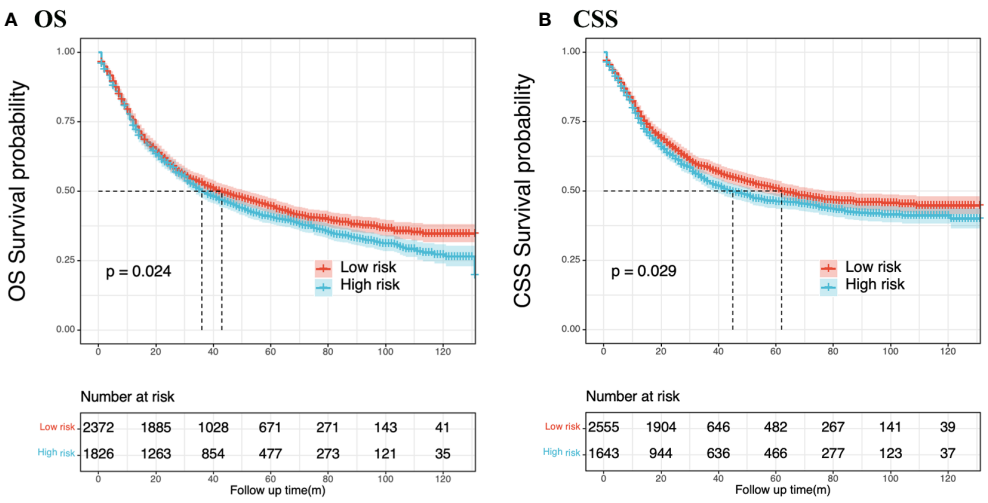

FIGURE 7
Nomogram-based risk stratification. GSRCC patients were divided into low- and high-risk subgroups by the nomogram score, and Kaplan-Meier survival analysis was performed to verify the clinical significance of the nomogram models. **(A)** Overall survival; **(B)** Cancer-specific cancer.

GSRCC is associated with advanced disease, with a higher incidence of patients at AJCC stage IV, more advanced T and N stages, and higher tumor grade. These findings are consistent with those of a previous study that reported a greater frequency of advanced-stage GSRCC than early-stage GSRCC (11). In line with the AJCC staging system, our newly developed nomogram demonstrated a significant influence of lymph node presence on predicting survival outcomes. Furthermore, the independent prognostic factors identified within the context of GSRCC included age, race, tumor size, and tumor site. Leveraging these variables as independent prognostic factors in a nomogram has the potential to enhance the predictive efficacy of the model. Previous reports have indicated that young patients with GSRCC with low-stage tumors who underwent radical surgery exhibited a more favorable prognosis than other GSRCC patients in terms of survival (12). Previous studies have indicated that older age and advanced tumor stage are associated with poorer OS. Ren et al. stated that age was the primary factor influencing survival, with individuals older than 74 years experiencing poorer survival than those younger than 45 years old (13). Chu et al. discovered that OS significantly deteriorates in patients older than 60 years (14). Our results are consistent with those of previous studies. Therefore, early detection, diagnosis, and treatment of tumors are crucial to enhance patient survival rates.

According to multivariate analysis, the identified optimal cutoff for tumor size was deemed a significant independent prognostic factor. Consequently, tumor size was incorporated into the nomogram. In a prior study, Im et al. reported that larger tumor size was an independent prognostic factor associated with poorer prognosis (15). A larger tumor size stimulates angiogenesis, leading to increased tumor cell proliferation. However, the underlying mechanism requires further investigation. Environmental factors, lifestyle, diet, and genetics significantly influence the development of gastric cancer. Wang et al. and Sun et al. reported that individuals of white and black ethnicities have poorer survival rates than individuals of other ethnic groups (16, 17). These findings are consistent with our results. Ethnic differences play an essential role in the occurrence and development of gastric cancer. In conclusion, these findings are consistent with those of the present study.

Nomograms are graphical tools that transform clinicopathological feature scores to predict the likelihood of clinical occurrence. Integrating patient data from other ethnic groups and cancer registries with the SEER database raises the possibility that this methodology can be universally used. According to previous research, nomograms offer a substantial likelihood of predicting the survival of patients with malignant tumors (18, 19), even surpassing the traditional TNM staging system (20). Currently, mature prognostic models for GSRCC that can be widely implemented in clinical practice are lacking. Our nomograms have the potential to be utilized for clinical and predictive assessments of patients with GSRCC, aiding individualized treatment planning.

The strength of our research lies in the two dynamic prediction models we successfully created and validated, one of which was used to predict GSRCC patients with CSS, and the other to forecast their OS. Additionally, we created two web-based predictive model applications. These devices will be put into practice by clinical surgeons and will be made convenient. Additionally, we included the SEER database and the NCC cohort. The two current prediction models are based on these two large databases, covering both Western and Eastern populations, so we believe that the models are universal and can predict the prognosis of gastric signet ring cell carcinoma in different populations to a large extent generalizability. Finally, our findings demonstrated that our nomograms had good clinical benefits and high discriminant and accurate predictive power. In addition, another outstanding advantage of our study is the simultaneous analysis of postoperative OS and CSS in patients with GSRCC. Currently, the majority of research has overlooked the examination of CSS in favor of concentrating more on the prognostic factors of postoperative OS in patients with GSRCC. CSS refers to death caused by a specific disease, and at this time, the concern about whether the cause of death is caused by a specific disease begins. If it is not due to a specific disease, it is not included in the outcome measures. It is a good indicator of the clinical benefit of a specific disease. In this work, we constructed prediction models based on both OS and CSS, which can assist physicians in recognizing the clinical factors affecting the postoperative survival of GSRCC patients globally, and also pay attention to the clinical prognostic factors that are actually associated with cancer.

However, our study had certain limitations. First, several important details, such as the surgical margin and technique, precise postoperative chemotherapy regimen and course, and patient's medical conditions, were missing from our study. Second, the retrospective nature of this study is another drawback that could lead to a recollection bias. Third, we excluded patients whose variables had uncertain data, to prevent selection bias. Further prospective studies are warranted in the future. Finally, another limitation of our study is that it only analyzes common clinicopathological factors and does not include molecular markers related to gastric cancer. In future studies, we will further incorporate molecular markers of gastric cancer such as Her-2, PD-1, and claudin18.2 to further enhance our prognostic prediction models.

In summary, using data from two sizable cohorts, we developed and validated two postoperative web-based nomograms to predict the 1-, 3-, and 5-year OS and CSS of patients with stage I–III GSRCC. We verified the great discriminating power, good consistency, and high clinical availability of the nomogram by comparing it with the AJCC staging system. The prediction models may offer useful prognostic data, such as a patient's probability of death and recurrence, making it easier to treat GSRCC with precision and individualization. This approach will assist physicians in managing patients with GSRCC after surgery. Nevertheless, the performance of the models needs to be validated by multicenter prospective studies in the future.

Data availability statement

The raw data supporting the conclusions of this article will be made available by the authors, without undue reservation.

Ethics statement

The studies involving humans were approved by ethics committee of the National Cancer Center/Cancer Hospital, the Chinese Academy of Medical Science, and Peking Union Medical College. The studies were conducted in accordance with the local legislation and institutional requirements. The participants provided their written informed consent to participate in this study.

Author contributions

YJ: Conceptualization, Writing – original draft. HH: Data curation, Writing – original draft. XS: Conceptualization, Writing – original draft. WL: Conceptualization, Methodology, Writing – original draft. YL: Conceptualization, Software, Writing – original draft. JL: Funding acquisition, Writing – review & editing. YT: Funding acquisition, Writing – review & editing.

Funding

The author(s) declare financial support was received for the research, authorship, and/or publication of this article. This work was supported by the National Natural Science Foundation of China (82072734) and the Beijing Hope Run Special Fund of the Cancer Foundation of China (LC2022L01).

Conflict of interest

The authors declare that the research was conducted in the absence of any commercial or financial relationships that could be construed as a potential conflict of interest.

Publisher's note

All claims expressed in this article are solely those of the authors and do not necessarily represent those of their affiliated organizations, or those of the publisher, the editors and the reviewers. Any product that may be evaluated in this article, or claim that may be made by its manufacturer, is not guaranteed or endorsed by the publisher.

Supplementary material

The Supplementary Material for this article can be found online at: https://www.frontiersin.org/articles/10.3389/fimmu.2024.1365834/full#supplementary-material

SUPPLEMENTARY FIGURE 1
Forest plots of multivariate Cox regression analysis for OS and CSS in patients with GSRCC.

SUPPLEMENTARY FIGURE 2
Pearson's correlation analysis was used to determine the correlations between the variables.

References

1. Sung H, Ferlay J, Siegel RL, Laversanne M, Soerjomataram I, Jemal A, et al. Global cancer statistics 2020: GLOBOCAN estimates of incidence and mortality worldwide for 36 cancers in 185 countries. *CA: A Cancer J Clin*. (2021) 71:209–49. doi: 10.3322/caac.21660

2. Li Y, Zhu Z, Ma F, Xue L, Tian Y. Gastric signet ring cell carcinoma: current management and future challenges. *Cancer Manage Res*. (2020) 12:7973–81. doi: 10.2147/CMAR.S268032

3. Kao YC, Fang WL, Wang RF, Li AF, Yang MH, Wu CW, et al. Clinicopathological differences in signet ring cell adenocarcinoma between early and advanced gastric cancer. *Gastric Cancer*. (2019) 22:255–63. doi: 10.1007/s10120-018-0860-8

4. Zhang L, Ma Y, Liu B. Prognostic performance of three lymph-node staging systems on gastric signet-ring-cell carcinoma. *Cancers*. (2023) 15:3170. doi: 10.3390/cancers15123170

5. Liu D, Ding R, Wang L, Shi E, Li X, Zhang C, et al. Novel nomogram to predict the overall survival of postoperative patients with gastric signet. *BMC Gastroenterol*. (2023) 23:284. doi: 10.1186/s12876-023-02915-z

6. Shao XX, Li XC, Lin ZJ, Ruan YJ, Lu GR, Wang WZ, et al. A prognostic model for survival in patients with gastric signet-ring cell carcinoma. *Digest Dis (Basel Switzerland)*. (2024). doi: 10.1159/000536454

7. Zhang S, Liu Y, Jiao Z, Li Z, Wang J, Li C, et al. Development and validation of a prognostic nomogram for gastric signet ring cell carcinoma: A multicenter population-based study. *Front Oncol*. (2021) 11:603031. doi: 10.3389/fonc.2021.603031

8. Nie D, Zheng H, An G, Li J. Development and validation of a novel nomogram for postoperative overall survival of patients with primary gastric signet-ring cell carcinoma: a population study based on SEER database. *J Cancer Res Clin Oncol*. (2023) 149:8593–603. doi: 10.1007/s00432-023-04796-x

9. Zhang ZS, Deng WY, Huang SL, Yang BF, Zhu FH, Jiang B, et al. Clinicopathological characteristics of signet-ring cell carcinoma derived from gastric fovelar epithelium. *J Digest Dis*. (2022) 23:396–403. doi: 10.1111/1751-2980.13120

10. Zu H, Wang H, Li C, Xue Y. Clinicopathologic characteristics and prognostic value of various histological types in advanced gastric cancer. *Int J Clin Exp Pathol*. (2014) 7:5692–700.

11. Efared B, Kadi M, Tahiri L, Lahmidani N, Hassani KM, Bouhaddouti HE, et al. Gastric signet ring cell carcinoma: A comparative analysis of clinicopathologic features. *Cancer Control: J Moffitt Cancer Center*. (2020) 27:1073274820976596. doi: 10.1177/1073274820976596

12. Lu M, Yang Z, Feng Q, Yu M, Zhang Y, Mao C, et al. The characteristics and prognostic value of signet ring cell histology in gastric cancer: A retrospective cohort study of 2199 consecutive patients. *Medicine*. (2016) 95:e4052. doi: 10.1097/MD.0000000000004052

13. Ren J, Niu G, Wang X, Song T, Hu Z, Ke C. Effect of age on prognosis of gastric signet-ring cell carcinoma: A SEER database analysis. *Med Sci Monit: Int Med J Exp Clin Res*. (2018) 24:8524–32. doi: 10.12659/MSM.911766

14. Chu Y, Mao T, Li X, Jing X, Ren M, Huang Z, et al. Predictors of lymph node metastasis and differences between pure and mixed histologic types of early gastric signet-ring cell carcinomas. *Am J Surg Pathol*. (2020) 44:934–42. doi: 10.1097/PAS.0000000000001460

15. Im WJ, Kim MG, Ha TK, Kwon SJ. Tumor size as a prognostic factor in gastric cancer patient. *J Gastric Cancer*. (2012) 12:164–72. doi: 10.5230/jgc.2012.12.3.164

16. Wang A, Squires MH 3rd, Melis M, Poultsides GA, Norton JA, Jin LX, et al. Stage-specific prognostic effect of race in patients with resectable gastric adenocarcinoma: an 8-institution study of the US gastric cancer collaborative. *J Am Coll Surgeons*. (2016) 222:633–43. doi: 10.1016/j.jamcollsurg.2015.12.043

17. Sun F, Sun H, Mo X, Tang J, Liao Y, Wang S, et al. Increased survival rates in gastric cancer, with a narrowing gender gap and widening socioeconomic status gap: A period analysis from 1984 to 2013. *J Gastroenterol Hepatol*. (2018) 33:837–46. doi: 10.1111/jgh.14024

18. Wang S, Ma K, Chen Z, Yang X, Sun F, Jin Y, et al. A nomogram to predict prognosis in malignant pleural mesothelioma. *World J Surgery*. (2018) 42(7):2134–42. doi: 10.1007/s00268-017-4424-6

19. Fang C, Wang W, Feng X, Sun J, Zhang Y, Zeng Y, et al. Nomogram individually predicts the overall survival of patients with gastroenteropancreatic neuroendocrine neoplasms. *British J Cancer*. (2017) 117(10):1544–50. doi: 10.1038/bjc.2017.315

20. Chen CL, Xue DX, Chen HH, Liang MZ, Lin DZ, Yu M, et al. Nomograms to predict overall and cancer-specific survival in gastric signet-ring cell carcinoma. *J Surg Res*. (2021) 266:13–26. doi: 10.1016/j.jss.2021.03.053

frontiers | Frontiers in Medicine

TYPE Original Research
PUBLISHED 23 May 2024
DOI 10.3389/fmed.2024.1403189

OPEN ACCESS

EDITED BY
Hua Zhong,
University of Hawaii at Manoa, United States

REVIEWED BY
Ting Gong,
University of Hawaii at Manoa, United States
Jie Xian,
University of California, San Diego, United States

*CORRESPONDENCE
Wei Gong
✉ gongwei@smu.edu.cn

†These authors have contributed equally to this work and share first authorship

RECEIVED 19 March 2024
ACCEPTED 06 May 2024
PUBLISHED 23 May 2024

CITATION
Li X, You L, Liu Q, He W, Cui X and Gong W (2024) A nomogram for predicting survival in patients with gastrointestinal stromal tumor: a study based on the surveillance, epidemiology, and end results database.
Front. Med. 11:1403189.
doi: 10.3389/fmed.2024.1403189

A nomogram for predicting survival in patients with gastrointestinal stromal tumor: a study based on the surveillance, epidemiology, and end results database

Xiaxi Li†, Lijuan You†, Qinghua Liu†, Wenhua He, Xiaobing Cui and Wei Gong*

Department of Gastroenterology, Shenzhen Hospital of Southern Medicine University, Shenzhen, China

Purpose: The objective of this investigation was to construct and validate a nomogram for prognosticating cancer-specific survival (CSS) in patients afflicted with gastrointestinal stromal tumor (GIST) at 3-, 5-, and 8-years post-diagnosis.

Methods: Data pertaining to patients diagnosed with GIST were acquired from the Surveillance, Epidemiology, and End Results (SEER) database. Through random selection, a training cohort (70%) and a validation cohort (30%) were established from the patient population. Employing a backward stepwise Cox regression model, independent prognostic factors were identified. Subsequently, these factors were incorporated into the nomogram to forecast CSS rates at 3-, 5-, and 8-years following diagnosis. The nomogram's performance was assessed using indicators such as the consistency index (C-index), the area under the time-dependent receiver operating characteristic curve (AUC), the net reclassification improvement (NRI), the integrated discrimination improvement (IDI), calibration curves, and decision-curve analysis (DCA).

Results: This investigation encompassed a cohort of 3,062 GIST patients. By analyzing the Cox regression model within the training cohort, nine prognostic factors were identified: age, sex, race, marital status, AJCC (American Joint Committee on Cancer) stage, surgical status, chemotherapy status, radiation status, and income status. The nomogram was subsequently developed and subjected to both internal and external validation. The nomogram exhibited favorable discrimination abilities, as evidenced by notably high C-indices and AUC values. Calibration curves confirmed the nomogram's reliability. Moreover, the nomogram outperformed the AJCC model, as demonstrated by enhanced NRI and IDI values. The DCA curves validated the clinical utility of the nomogram.

Conclusion: The present study has successfully constructed and validated the initial nomogram for predicting prognosis in GIST patients. The nomogram's performance and practicality suggest its potential utility in clinical settings. Nevertheless, further external validation is warranted.

KEYWORDS

surveillance, epidemiology, and end results, cancer-specific survival, nomogram, gastrointestinal stromal tumor, predicting survival

1 Introduction

Gastrointestinal stromal tumor (GIST) is a rare form of cancer that originates in the gastrointestinal tract (1). It primarily affects the connective tissue cells, known as stromal cells, found in the walls of the digestive system (2). GISTs can occur in various locations within the gastrointestinal tract, including the stomach, small intestine, and less commonly, the esophagus, colon, and rectum (3).

The incidence of GIST is relatively low compared to other gastrointestinal malignancies (4). However, it represents a distinct entity with unique characteristics that necessitate focused investigation and analysis (5). Despite its rarity, GIST has garnered significant attention due to its potential for aggressive behavior and variable clinical outcomes (6). To date, the understanding of GIST and its prognostic implications remains limited (7). To address this gap, researchers have explored potential risk factors and developed predictive models to aid in assessing patient prognosis and guiding treatment decisions (8).

One widely used tool in tumor prediction models is the nomogram, which provides a straightforward and accurate means of estimating a patient's chances of survival based on various clinical and demographic factors (9). While nomograms have been established for several cancer types, including tonsil, parotid-gland, and breast cancer (10–12), the development of a nomogram specifically designed for GIST is yet to be reported. Consequently, there exists a need to construct a comprehensive nomogram for GIST patients, utilizing pertinent data from reliable sources such as the Surveillance, Epidemiology, and End Results (SEER) database.

The aim of our study was to develop and evaluate a novel nomogram for GIST patients, utilizing the extensive data available in the SEER database. This nomogram would incorporate key demographic information, clinicopathologic features, and therapeutic approaches to provide a personalized and thorough estimation of patient survival probabilities. By analyzing relevant treatment modalities, our nomogram would offer clinicians a valuable tool for guiding treatment decisions and optimizing patient outcomes.

The development of a specialized nomogram for GIST patients represents a significant advancement in personalized medicine. By incorporating essential patient characteristics and treatment approaches, this nomogram surpasses conventional methods, providing clinicians with a comprehensive and tailored approach to predicting patient survival. Through our study, we aimed to enhance the understanding of GIST and contribute to improved clinical decision-making for this distinct malignancy.

2 Patients and methods

2.1 Data sources and research factors

The SEER database was utilized, employing the SEER*Stat software, to filter and extract the relevant data. While a portion of the SEER database is accessible to the public, additional access to the SEER plus database was requested for comprehensive data retrieval (13). Gastrointestinal stromal tumor (GIST) cases were collected by applying the histology/behavior codes from the third revision of the International Classification of Diseases for Oncology (ICD-O-3), specifically "8935/3: Stromal sarcoma, NOS" and "8936/3: Gastrointestinal stromal sarcoma." Furthermore, cases located in the digestive tract were selected for analysis.

Through a series of meticulous calculations and screenings using both univariate and multivariate Cox regression analyses, we identified a subset of these variables that demonstrated statistically significant associations with survival. The selection was guided by a rigorous statistical threshold to ensure that the included variables were not only statistically significant but also clinically meaningful. Age, race, sex, marital status, American Joint Committee on Cancer (AJCC) stage, income, summary of stage, surgery status, radiotherapy status, and chemotherapy status. Given the substantial multicollinearity arising from the inclusion of all these factors, the analysis focused solely on the AJCC staging system. The primary outcome variable of interest was cancer-specific survival (CSS). As the SEER database used in this study does not contain personally identifiable information, patient-informed consent was not required.

The selection of patients for analysis was based on the availability of complete baseline and survival data. The seventh edition of the AJCC staging system was adopted. Following the aforementioned methodology, an initial cohort of 16,794 GIST patients diagnosed between 2000 and 2019 was identified. After excluding patients with any missing information, a final cohort of 3,062 GIST patients was included in the study (14). To assess the model, these patients were randomly divided into a training cohort (70%) and a validation cohort (30%), with R software (version 4.2.0[1]) utilized for the analysis. Figure 1 provides a visual representation of the data screening process.

2.2 Nomogram and statistical analysis

The assignment of subjects to training and validation groups was followed by a log-rank test, which revealed no statistically significant difference between the groups. Baseline characteristics of each variable in the study cohort were subsequently summarized using SPSS Statistics software (version 27.0, IBM SPSS, Chicago, IL, USA). The presentation of other variable data was in the form of frequencies and percentages, while age at diagnosis was expressed as a median and interquartile range (IQR) value.

Nomograms were employed to estimate the probabilities of cancer-specific survival (CSS) at 3, 5, and 8 years for patients with GIST, and Cox regression analysis was conducted to identify factors associated with CSS in GIST ($p = 0.05$). Following the development of the nomogram, an evaluation of the model was undertaken using a set of metrics. Two metrics, namely the concordance index (C-index) and the area under the curve (AUC) of the time-dependent receiver operating characteristic (ROC), were utilized to assess the model's discrimination capabilities. However, despite the common use of AUC and C-index, their improvements were found to be insignificant when compared to the existing model. To determine whether the new model exhibited superiority, two relatively recent metrics, the Net Reclassification Improvement (NRI) and the Integrated Discriminant Improvement (IDI), were additionally employed. While IDI considers multiple thresholds for assessing overall model performance, NRI primarily evaluates the prediction capacity of the old and new models

1 http://www.r-project.org

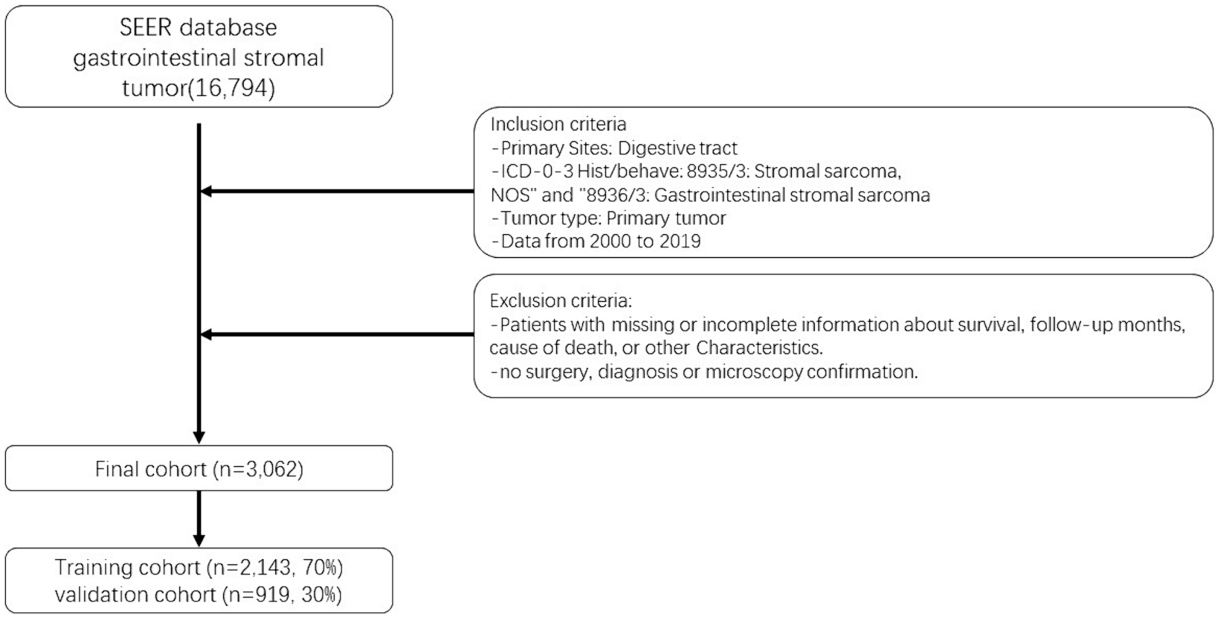

FIGURE 1
Flow chart of patient selection.

at a specific threshold level (15, 16). These two markers are better understood and more applicable in clinical settings.

Furthermore, a calibration plot was generated to visually depict the variation between predicted and actual values. The level of model calibration indicates the consistency between predicted and observed outcomes. Improved model consistency is evident when the calibration curve aligns closely with the 45-degree reference line. Lastly, decision curve analysis (DCA) curves were employed to evaluate the clinical validity of the model. The abscissa and ordinate of the DCA curve represent the model's threshold probability and net benefit, respectively. A higher net benefit indicates an increased utility of the model (17).

All statistical analyses were conducted using the R software package and SPSS Statistics. The fundamental characteristics of the cohort were characterized using SPSS Statistics. Subsequently, R software was utilized to randomly assign data to training and validation groups, and the log-rank test was performed. Various R packages, including survival, rms, foreign, survival ROC, nricens, and DCA packages, were employed for Cox regression analysis, proportional hazards construction testing, nomogram development, and assessment. Statistical significance was defined as two-sided probability values with $p < 0.05$.

3 Results

3.1 General characteristics

After randomizing 3,062 patients into 2 cohorts, applying the log-rank test yielded a probability value ($p = 0.5$) that indicated no significant difference between these cohorts. The fundamental demographic and clinical characteristics of the two cohorts were then described using SPSS, as shown in Table 1. In the training cohort, the median age at diagnosis was 65 years (IQR 54–77 years), while in the validation cohort, it was 64 years (IQR 55–73 years). The gender distribution and surgery were fairly even. The majority of patients in the training and validation cohorts were white (68.36 and 69.31%, respectively) and married (60.9 and 58.65%). AJCC stage I was seen in the majority of cases. The majority of patients were not treated with radiation or chemotherapy. Most patients earn about $60,000 to $74,999 a year.

3.2 Constructing a nomogram using the training cohort

Following a multivariate Cox stepwise regression analysis ($p < 0.05$), nine variables were identified as significant factors. These variables, along with their hazard ratios (HR) and p-values, are presented in Table 2. Age at diagnosis demonstrated a significant association with cancer prognosis (HR 1.051, $p < 0.0001$), while sex exhibited a protective effect (HR 0.667, $p < 0.0001$). The variable of race revealed a higher hazard ratio for black individuals compared to white individuals (HR 1.412, $p < 0.0001$). Marital status also played a role, with married individuals having a lower hazard ratio compared to those who were single (HR 0.688, $p < 0.0001$). The AJCC stage variable demonstrated notable associations with disease prognosis. Specifically, AJCC stage II had a higher hazard ratio compared to AJCC stage I (HR 1.249, $p = 0.0608$), AJCC stage III exhibited a significantly increased hazard ratio (HR 2.408, $p < 0.0001$), and AJCC stage IV showed the highest hazard ratio (HR 3.247, $p < 0.0001$) when compared to AJCC stage I.

Treatment-related factors were also found to be significant predictors. Patients who did not receive or had unknown radiation therapy had a lower hazard ratio compared to those who underwent radiation therapy (HR 0.728, $p < 0.0001$). Similarly, patients without

TABLE 1 Demographic and clinical characteristics of the 2 cohorts of patients.

Variable	Training cohort (%)	Validation cohort (%)
N	2,143	919
Age of diagnosis	65 (54–74)	64 (55–73)
Sex		
Male	1,103 (51.47)	473 (51.47)
Female	1,040 (48.53)	446 (48.53)
Race		
White	1,465 (68.36)	637 (69.31)
Black	370 (17.27)	152 (16.54)
Other	308 (14.37)	130 (14.15)
Marital status		
Single	369 (17.22)	170 (18.5)
Married	1,305 (60.9)	539 (58.65)
DSW	469 (21.89)	210 (22.85)
AJCC stage		
I	1,025 (47.83)	458 (49.84)
II	373 (17.41)	145 (15.78)
III	354 (16.52)	157 (17.08)
IV	391 (18.25)	159 (17.3)
Summary of Stage		
Localized	1,517 (70.79)	664 (72.25)
Regional	255 (11.9)	101 (10.99)
Distant	371 (17.31)	154 (16.76)
Radiation		
Yes	8 (0.37)	10 (1.09)
No/unknow	2,135 (99.63)	909 (98.91)
Chemotherapy		
Yes	960 (44.8)	383 (41.68)
No/unknow	1,183 (55.2)	536 (58.32)
Surgery		
Yes	1917 (89.45)	831 (90.42)
No/unknow	226 (10.55)	88 (9.58)
Income		
< $35,000, $35,000–$44,999	212 (9.89)	66 (7.18)
$45,000–$59,999	472 (22.03)	221 (24.05)
$60,000–$74,999	775 (36.16)	338 (36.78)
$75,000+	684 (31.92)	294 (31.99)

TABLE 2 Selected variables by multivariate Cox stepwise regression analysis.

	Multivariate analysis		
Variable	HR	95% CI	*p*-value
Age of diagnosis	1.051	1.045–1.057	<0.0001
Sex			
Male	reference		
Female	0.667	0.579–0.768	<0.0001
Race			
White	reference		
Black	1.412	1.19–1.676	<0.0001
Other	0.941	0.757–1.169	0.5805
Marital status			
Single	reference		
Married	0.688	0.571–0.83	<0.0001
DSW	0.987	0.801–1.215	0.8997
AJCC stage			
I	reference		
II	1.249	0.99–1.576	0.0608
III	2.408	1.952–2.971	<0.0001
IV	3.247	2.259–4.668	<0.0001
Summary of Stage			
Localized	reference		
Regional	1.208	0.957–1.525	0.1126
Distant	1.375	0.979–1.931	0.0658
Radiation			
Yes	reference		
No/unknow	0.728	0.398–1.331	0.0302
Chemotherapy			
Yes	reference		
No/unknow	1.484	1.27–1.734	<0.0001
Surgery			
Yes	reference		
No/unknow	1.979	1.648–2.376	<0.0001
Income			
< $35,000, $35,000–$44,999	reference		
$45,000–$59,999	0.999	0.787–1.268	0.9903
$60,000–$74,999	0.81	0.644–1.018	0.0711
$75,000+	0.71	0.558–0.905	0.0056

or with unknown chemotherapy had a higher hazard ratio than those who received chemotherapy (HR 1.484, $p < 0.0001$). Moreover, individuals who did not undergo or had unknown surgical intervention exhibited an increased hazard ratio compared to those who underwent surgery (HR 1.979, $p < 0.0001$). Income level was identified as a significant variable, with an income of $75,000 or more associated with a lower hazard ratio when compared to an income less than $35,000 or between $35,000 and $44,999 (HR 0.71, $p < 0.0001$). These findings highlight the impact of age, sex, race, marital status, AJCC stage, treatment modalities, and income level on the prognosis of patients with gastrointestinal stromal tumor (GIST).

The final nomogram, depicted in Figure 2, provides a comprehensive visualization of the multiple regression model for predicting cancer-specific survival (CSS) probabilities based on the relevant factors identified earlier. Among these factors, AJCC stage

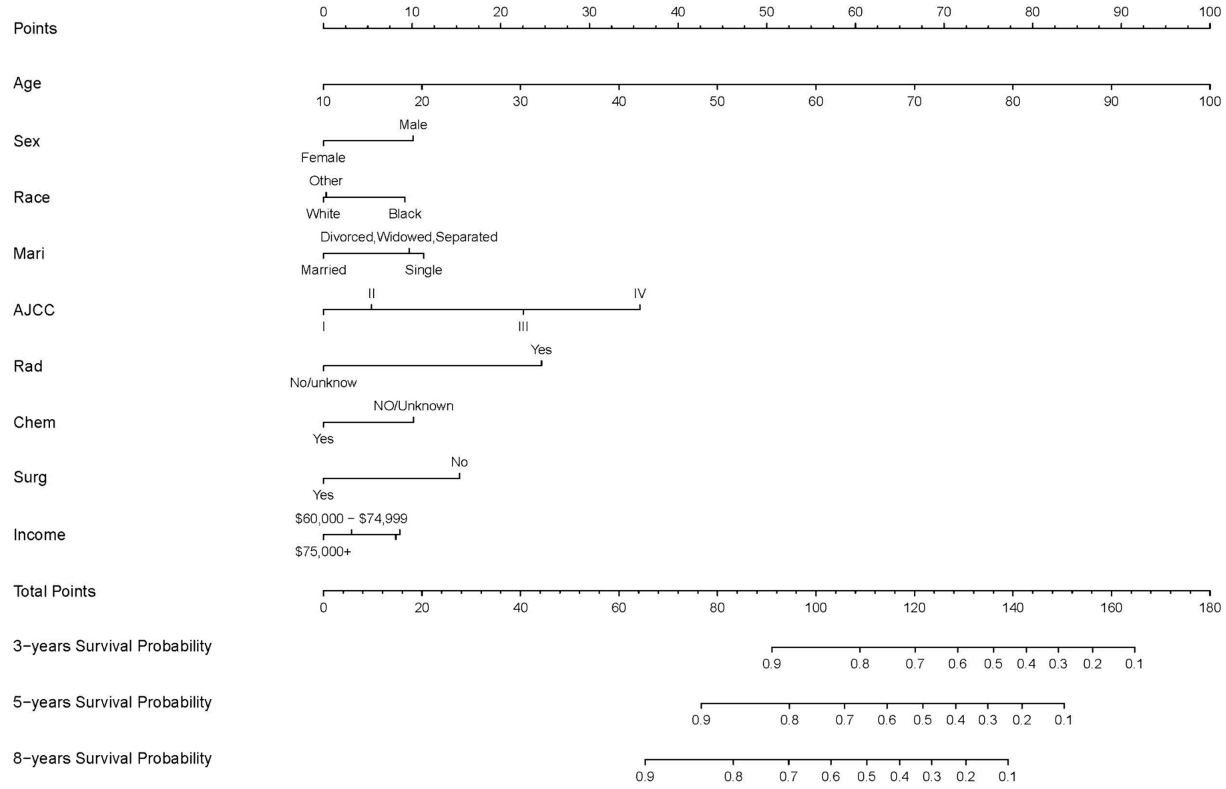

FIGURE 2
Nomogram predicting 3-, 5-, and 8-years CSS probability. Mari, marital status; Surg, surgery status; Rad, radiotherapy status; Chem, chemotherapy status.

exerts the most significant influence on the survival rate, followed by surgery, race, chemotherapy, age at diagnosis, marital status, income, and sex. This figure shows scores at the top for different patient signs. Each patient's scores are added together to get a total score. This total score matches up with the chances of dying in 3, 5, or 8 years, shown at the bottom of the nomogram. This helps doctors and patients see how likely it is that someone might die within these times. The nomogram serves as a practical tool for clinicians to estimate an individual patient's prognosis based on the identified risk factors.

3.3 Evaluating the nomogram using the validation cohort

The performance of the nomogram model was assessed using the concordance index (C-index) and the area under the receiver operating characteristic (ROC) curve (AUC). In the training cohort, the C-index for the nomogram model was determined to be 0.764, indicating a good discriminatory ability to predict cancer-specific survival. Similarly, the validation cohort yielded a C-index of 0.76, further confirming the reliability of the model's predictive capacity.

To evaluate the model's discriminative power at different time points, ROC curves were constructed for 3, 5, and 8 years. The AUC values were then calculated as performance metrics. In the training cohort, the AUC values for years 3, 5, and 8 were found to be 0.789, 0.792, and 0.801, respectively. These values indicate a favorable ability of the model to differentiate between patients with different CSS probabilities at each time point. Similarly, in the validation cohort, the AUC values were 0.773, 0.796, and 0.778 for years 3, 5, and 8, respectively, further validating the model's predictive accuracy (Figure 3).

To further assess the nomogram's performance, additional metrics such as the Net Reclassification Improvement (NRI) and Integrated Discrimination Improvement (IDI) were employed. In the training cohort, the NRI values for the 3-, 5-, and 8-year CSS probabilities were 0.584 (95% CI 0.462–0.689), 0.641 (95% CI 0.543–0.729), and 0.663 (95% CI 0.598–0.777), respectively. Similarly, in the validation cohort, the NRI values were 0.569 (95% CI 0.347–0.721), 0.672 (95% CI 0.494–0.883), and 0.681 (95% CI 0.507–0.87). These NRI values indicate that the nomogram provides improved reclassification of patients into appropriate risk categories compared to the existing model.

The IDI values, which also assess the improvement in prediction performance, were found to be statistically significant in both the training and validation cohorts. In the training cohort, the IDI values for the 3-, 5-, and 8-year CSS probabilities were 0.095, 0.126, and 0.145, respectively ($p < 0.001$). Similarly, in the validation cohort, the IDI values were 0.091, 0.130, and 0.150 ($p < 0.001$). These results further demonstrate the enhanced predictive ability of the nomogram compared to the existing model.

To evaluate the calibration of the nomogram, calibration plots were generated. A calibration plot shows how closely the predictions from the nomogram match actual patient results, which is key for its use in clinical settings. The calibration plots for the 3-, 5-, and

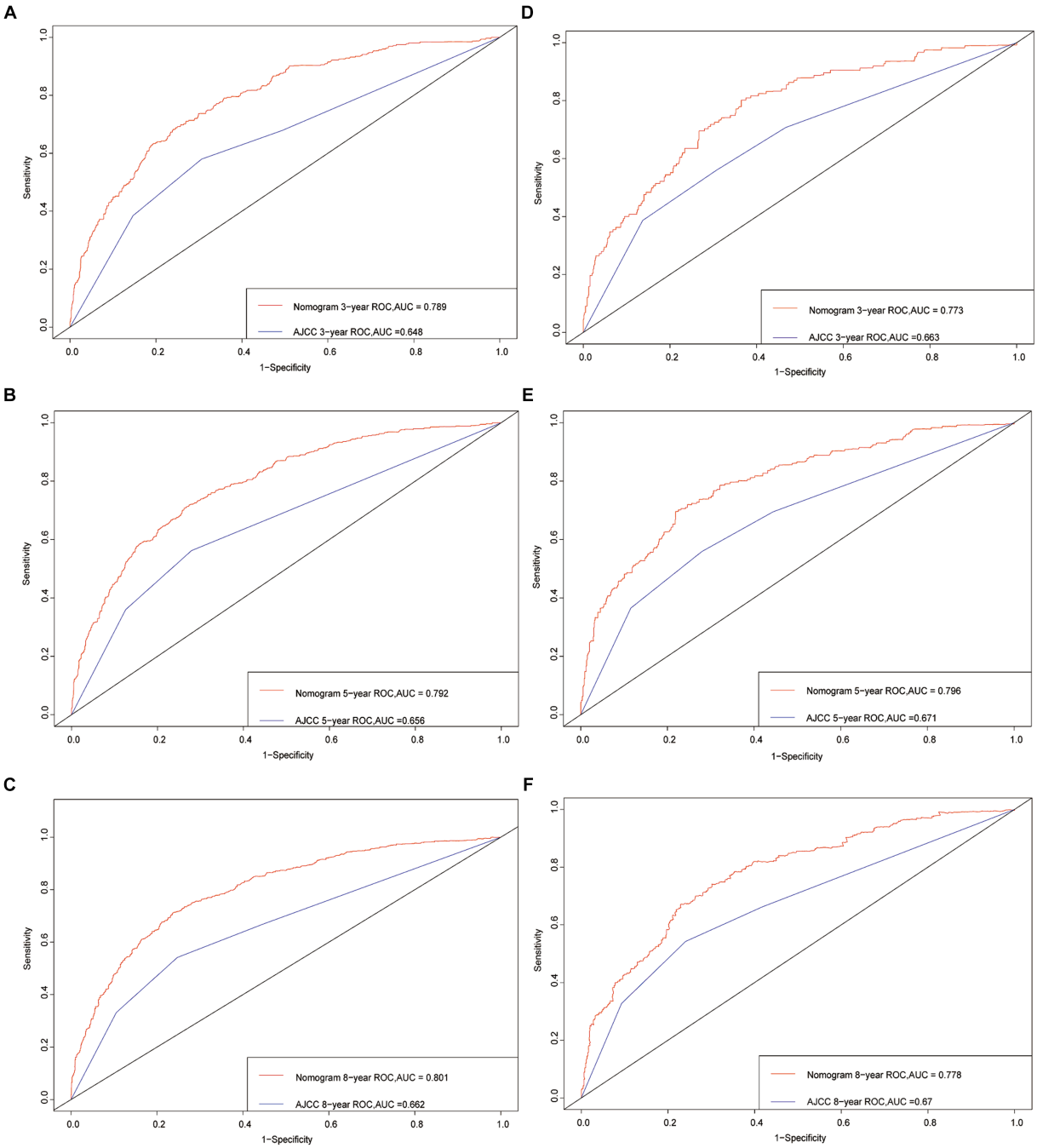

FIGURE 3
Receiver operating characteristic curves. The area under the ROC curve (AUC) for 3-, 5-, and 8-year CSS probability of the training cohort **(A–C)** and validation cohort **(D–F)**.

8-year CSS probabilities in Figure 4 show a close alignment between the predicted probabilities and the ideal 45-degree reference line. This indicates a high level of calibration, suggesting that the nomogram accurately estimates the survival probabilities for GIST patients.

Overall, the NRI, IDI, and calibration plot analyses provide evidence for the nomogram's discriminative ability, improved reclassification of patients, and accurate calibration, respectively, further supporting its reliability and clinical utility.

Finally, to assess the clinical validity of the nomogram, Decision Curve Analysis (DCA) curve was constructed. This analysis shows the range of probabilities at which the nomogram provides a net benefit, supporting its use in making clinical decisions. Figure 5 displays the survival probability curves for the new nomogram model compared to the AJCC model. Notably, the survival probability curves for the new model consistently surpass those of the AJCC model across the 3-, 5-, and 8-year time frames. This indicates that utilizing the new nomogram to predict CSS probabilities provides

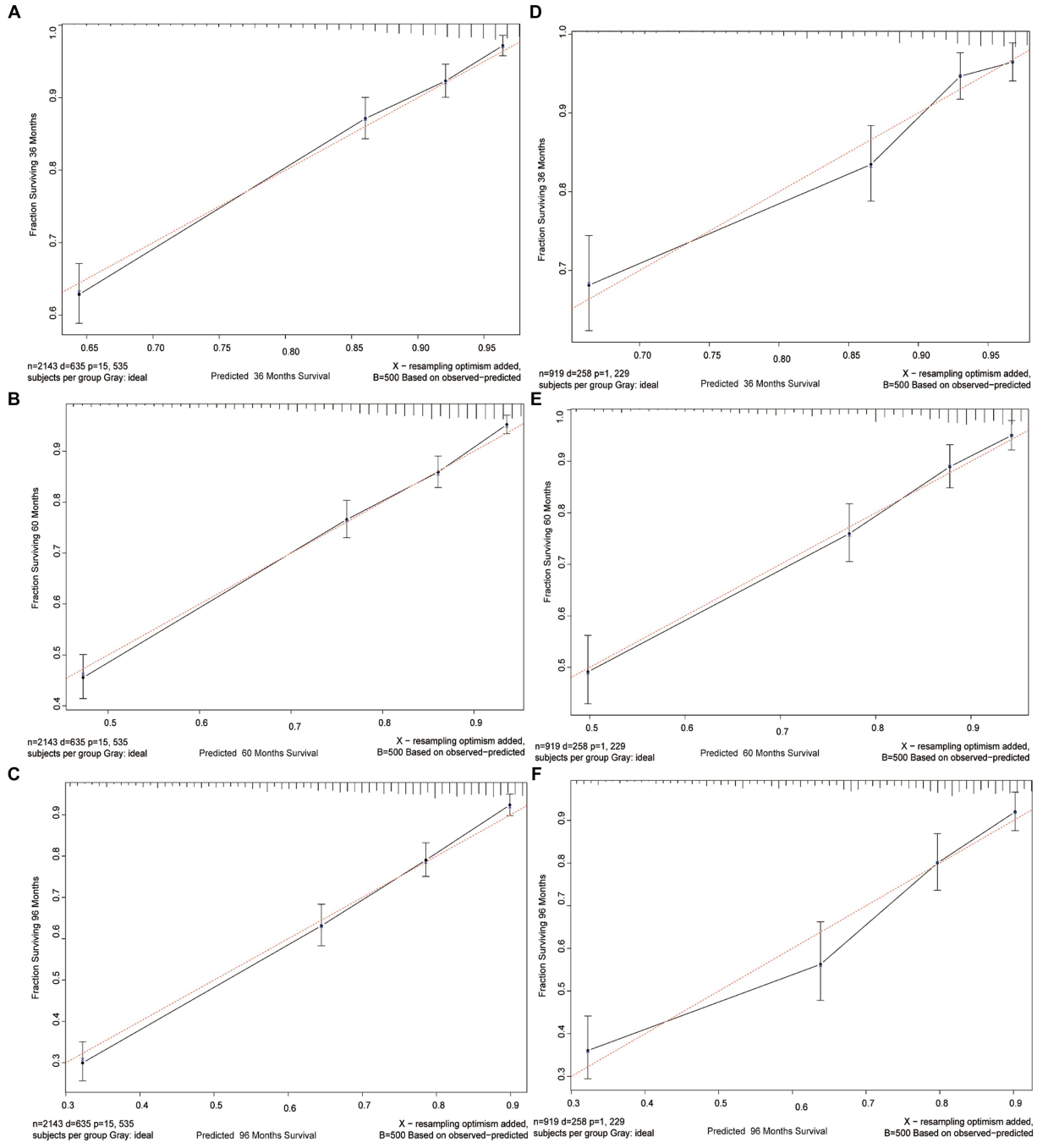

FIGURE 4
Calibration curves. Calibration curves for 3-, 5-, and 8-years CSS probability depict the calibration of each model in terms of the agreement between the predicted probabilities and observed outcomes of the training cohort **(A–C)** and validation cohort **(D–F)**.

greater overall benefits compared to relying solely on the AJCC staging system.

4 Discussion

The development of a specialized nomogram for patients diagnosed with gastrointestinal stromal tumors (GIST) signifies a noteworthy stride in the realm of personalized medicine. GIST, a rare form of malignancy primarily affecting the connective tissue cells in the gastrointestinal tract, has garnered considerable attention due to its potential for aggressive behavior and the varying clinical outcomes it presents (18). However, our comprehension of GIST and its prognostic implications remains limited, underscoring the imperative for comprehensive predictive models (19).

Nomograms have become a ubiquitous tool in cancer prediction models, providing a straightforward and accurate means of estimating survival probabilities based on a range of clinical and demographic

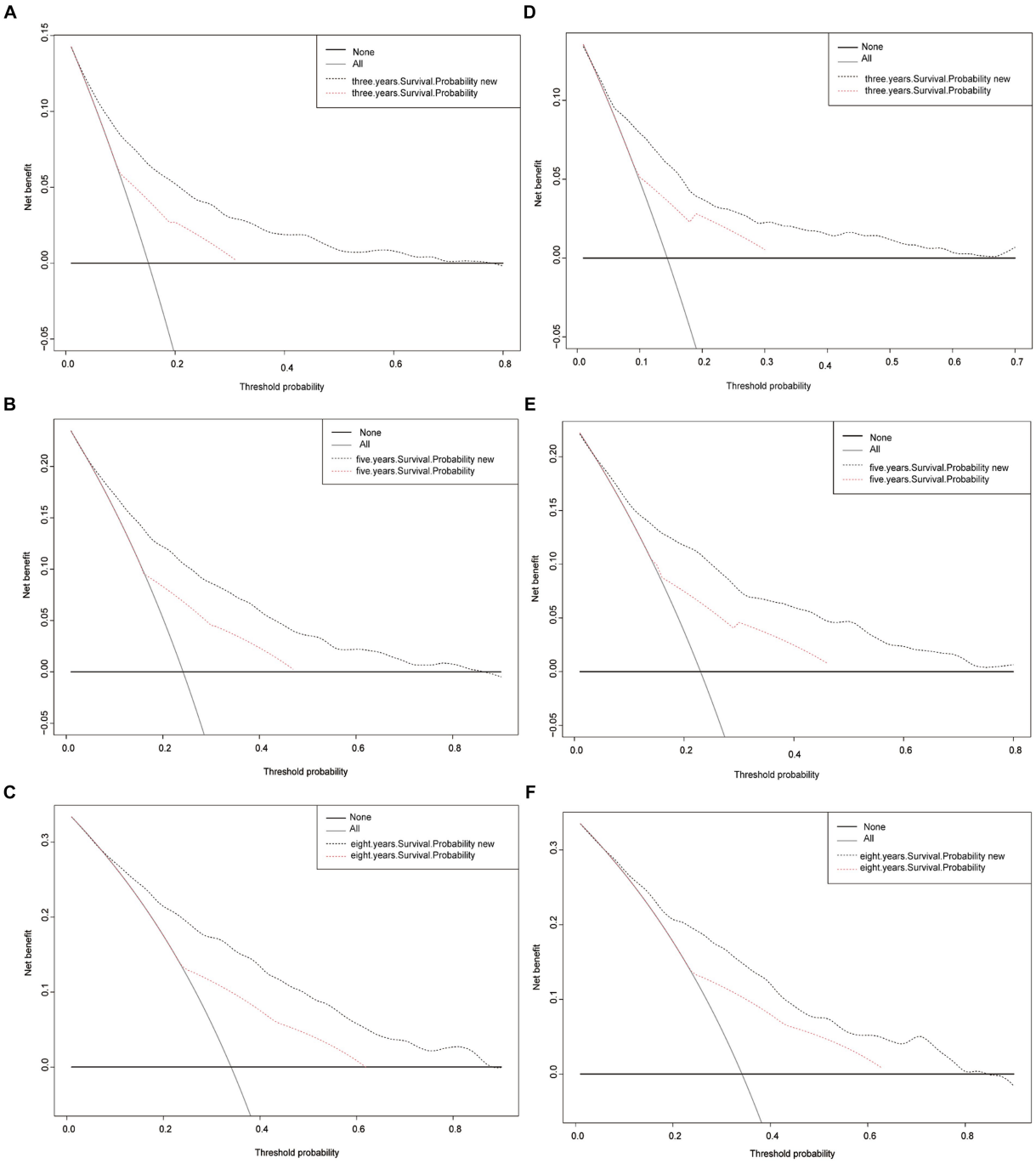

FIGURE 5
Decision curve analysis curves. Decision curve analysis of the training cohort **(A–C)** and validation cohort **(D–F)** for 3-, 5-, and 8-years CSS probability.

factors (9). Notwithstanding, the absence of a tailored nomogram specifically designed for GIST patients had been conspicuous prior to the inception of this study. Recognizing this void, the researchers sought to leverage the extensive data within the Surveillance, Epidemiology, and End Results (SEER) database, specifically pertaining to GIST cases, with the intention of bridging this gap and equipping clinicians with an invaluable tool for prognostication and guiding treatment decisions (20).

Backward stepwise selection in Cox regression models effectively addresses potential overfitting by iteratively removing the least significant predictors, thus simplifying the model and enhancing its generalizability. This method begins with a full model, including all potential predictors, and eliminates those with the highest p-values, typically based on the Wald test, indicating their low statistical significance (often using a threshold such as $p > 0.05$ or $p > 0.10$). The process continues until removing further variables would significantly worsen the model fit, assessed using criteria like the Akaike Information Criterion (AIC) or the Bayesian Information Criterion (BIC). These criteria help balance the model's complexity against its goodness of fit, ensuring the final model is

robust, not overly complex, and retains all necessary predictors for accurate predictions. This systematic reduction of predictors minimizes overfitting, making the model more applicable to new data.

The outcomes of this investigation demonstrated the successful construction and validation of a nomogram specifically tailored for predicting prognosis in GIST patients. This nomogram ingeniously incorporated nine indispensable prognostic factors, encompassing age, sex, race, marital status, American Joint Committee on Cancer (AJCC) stage, surgical status, chemotherapy status, radiation status, and income status (21, 22). These factors were meticulously identified through a backward stepwise Cox regression model, thereby illuminating their profound significance in delineating patient outcomes. The nomogram exhibited a commendable ability to discriminate, substantiated by high values of the C-index and the area under the receiver operating characteristic curve (AUC) (23, 24). The calibration curves further validated the nomogram's reliability, while the net reclassification improvement (NRI) and integrated discrimination improvement (IDI) values unequivocally showcased its superiority over the existing AJCC model. Furthermore, the decision curve analysis (DCA) curves provided additional validation of the nomogram's clinical utility (25). In the training cohort, the Net Reclassification Improvement (NRI) revealed noteworthy advancements in accurately classifying Conditional Survival Probability (CSS) at 3, 5, and 8 years, with increments of 58.4, 64.1, and 66.3%, respectively. Similarly, the validation cohort exhibited substantial increases of 56.9, 67.2, and 68.1% ($p < 0.001$). Another crucial metric, the Integrated Discrimination Improvement (IDI), complements the NRI by considering diverse threshold values and reflecting the overall enhancement of the model. The IDI values further substantiate that the novel model surpasses the AJCC model in predictive efficacy for CSS probabilities at 3, 5, and 8 years. Specifically, the new model demonstrates improvements of 9.5, 12.6, and 14.5% in the training cohort, and 9.1, 13, and 15% in the validation cohort ($p < 0.001$).

The development of this nomogram represents a substantial contribution to the realm of personalized medicine in the context of GIST. By assimilating essential patient characteristics and treatment approaches, the nomogram surpasses conventional methods, endowing clinicians with a comprehensive and bespoke approach to prognostication and treatment decision-making. The nomogram's notable performance and practicality augur its potential utility in diverse clinical settings.

Nevertheless, it is incumbent upon us to acknowledge the limitations inherent in this study. The nomogram's development and validation were based on data procured exclusively from the SEER database, which may not fully encapsulate the diversity and nuances of GIST patients encountered in real-world clinical practice. Hence, external validation is paramount to evaluate the generalizability and robustness of the nomogram. The SEER database, while a crucial resource for cancer research, has several limitations including geographic and demographic representation, as it covers only about 34.6% of the U.S. population and may not adequately represent all racial or ethnic groups. It also lacks detailed variables on lifestyle, genetics, and environmental factors, as well as comprehensive treatment data, limiting the scope of research on cancer etiology and treatment outcomes. Furthermore, it is worth noting that this study predominantly focused on cancer-specific survival (CSS) as the primary outcome variable, without considering other pivotal endpoints such as overall survival or recurrence-free survival.

5 Conclusion

In summary, drawing upon a substantial retrospective population, we have successfully constructed the pioneering nomogram for estimating 3-, 5-, and 8-year cancer-specific survival (CSS) probabilities in patients diagnosed with gastrointestinal stromal tumors (GIST). This innovative nomogram integrates a comprehensive array of demographic and clinicopathological characteristics. Rigorous validation and assessment protocols have underscored the utility and user-friendliness of this model, empowering physicians with a valuable resource to inform their clinical decision-making for individual patients. Notably, the nomogram has demonstrated its capacity to provide meaningful and advantageous recommendations. Moving forward, our aspirations encompass the development of more intricate nomograms, drawing from a broader range of data sources, with the aim of further enriching the predictive capabilities of these models.

Data availability statement

The datasets presented in this study can be found in online repositories. The names of the repository/repositories and accession number(s) can be found at: https://seer.cancer.gov.

Author contributions

XL: Conceptualization, Methodology, Writing – review & editing, Data curation, Writing – original draft. LY: Data curation, Methodology, Writing – review & editing. QL: Data curation, Methodology, Writing – review & editing. WH: Data curation, Writing – review & editing. XC: Data curation, Writing – review & editing. WG: Conceptualization, Methodology, Supervision, Writing – review & editing.

Funding

The author(s) declare that financial support was received for the research, authorship, and/or publication of this article. Shenzhen Science and Technology Program (JCYJ20220530154013031), Guangdong Province Grassroots Science Popularization Action Plan (20240205).

Acknowledgments

We thank all SEER database staff and scientists.

Conflict of interest

The authors declare that the research was conducted in the absence of any commercial or financial relationships that could be construed as a potential conflict of interest.

Publisher's note

References

1. Søreide K, Sandvik OM, Søreide JA, Giljaca V, Jureckova A, Bulusu VR. Global epidemiology of gastrointestinal stromal tumours (GIST): a systematic review of population-based cohort studies. *Cancer Epidemiol*. (2016) 40:39–46. doi: 10.1016/j.canep.2015.10.031

2. Nannini M, Rizzo A, Indio V, Schipani A, Astolfi A, Pantaleo MA. Targeted therapy in SDH-deficient GIST. *Ther Adv Med Oncol*. (2021) 13:175883592110232. doi: 10.1177/17588359211023278

3. Mantese G. Gastrointestinal stromal tumor: epidemiology, diagnosis, and treatment. *Curr Opin Gastroenterol*. (2019) 35:555–9. doi: 10.1097/MOG.0000000000000584

4. Blay JY, Kang YK, Nishida T, von Mehren M. Gastrointestinal stromal tumours. *Nat Rev Dis Primers*. (2021) 7:22. doi: 10.1038/s41572-021-00254-5

5. Asija AP, Mejia AV, Prestipino A, Pillai MV. Gastrointestinal stromal Tumors: a review. *Am J Ther*. (2016) 23:e550–7. doi: 10.1097/MJT.0b013e3182a1be76

6. Miettinen M, Lasota J. Gastrointestinal stromal tumors: review on morphology, molecular pathology, prognosis, and differential diagnosis. *Arch Pathol Lab Med*. (2006) 130:1466–78. doi: 10.5858/2006-130-1466-GSTROM

7. Kelly CM, Gutierrez Sainz L, Chi P. The management of metastatic GIST: current standard and investigational therapeutics. *J Hematol Oncol*. (2021) 14:2. doi: 10.1186/s13045-020-01026-6

8. Brinch CM, Aggerholm-Pedersen N, Hogdall E, Krarup-Hansen A. Medical oncological treatment for patients with gastrointestinal stromal tumor (GIST) - a systematic review. *Crit Rev Oncol Hematol*. (2022) 172:103650. doi: 10.1016/j.critrevonc.2022.103650

9. Balachandran VP, Gonen M, Smith JJ, DeMatteo RP. Nomograms in oncology: more than meets the eye. *Lancet Oncol*. (2015) 16:e173–80. doi: 10.1016/S1470-2045(14)71116-7

10. Li C, Yang J, Zheng S, Xu F, Han D, Bai L, et al. Establishment and validation of a nomogram for tonsil squamous cell carcinoma: a retrospective study based on the SEER database. *Cancer Control*. (2020) 27:1073274820960481. doi: 10.1177/1073274820960481

11. Xu F, Feng X, Zhao F, Huang Q, Han D, Li C, et al. Competing-risks nomograms for predicting cause-specific mortality in parotid-gland carcinoma: a population-based analysis. *Cancer Med*. (2021) 10:3756–69. doi: 10.1002/cam4.3919

12. Xu F, Yang J, Han D, Huang Q, Li C, Zheng S, et al. Nomograms for estimating cause-specific death rates of patients with inflammatory breast cancer: a competing-risks analysis. *Technol Cancer Res Treat*. (2021) 20:153303382110163. doi: 10.1177/15330338211016371

13. Yang J, Li Y, Liu Q, Li L, Feng A, Wang T, et al. Brief introduction of medical database and data mining technology in big data era. *J Evid Based Med*. (2020) 13:57–69. doi: 10.1111/jebm.12373

14. Wu WT, Li YJ, Feng AZ, Li L, Huang T, Xu AD, et al. Data mining in clinical big data: the frequently used databases, steps, and methodological models. *Mil Med Res*. (2021) 8:44. doi: 10.1186/s40779-021-00338-z

15. Steyerberg EW, Vickers AJ, Cook NR, Gerds T, Gonen M, Obuchowski N, et al. Assessing the performance of prediction models: a framework for traditional and novel measures. *Epidemiology*. (2010) 21:128–38. doi: 10.1097/EDE.0b013e3181c30fb2

16. Parikh CR, Coca SG, Thiessen-Philbrook H, Shlipak MG, Koyner JL, Wang Z, et al. Postoperative biomarkers predict acute kidney injury and poor outcomes after adult cardiac surgery. *J Am Soc Nephrol*. (2011) 22:1748–57. doi: 10.1681/ASN.2010121302

17. Vickers AJ, Cronin AM, Elkin EB, Gonen M. Extensions to decision curve analysis, a novel method for evaluating diagnostic tests, prediction models and molecular markers. *BMC Med Inform Decis Mak*. (2008) 8:53. doi: 10.1186/1472-6947-8-53

18. Wada R, Arai H, Kure S, Peng WX, Naito Z. "wild type" GIST: Clinicopathological features and clinical practice. *Pathol Int*. (2016) 66:431–7. doi: 10.1111/pin.12431

19. Ford SJ, Gronchi A. Indications for surgery in advanced/metastatic GIST. *Eur J Cancer*. (2016) 63:154–67. doi: 10.1016/j.ejca.2016.05.019

20. Doll KM, Rademaker A, Sosa JA. Practical guide to surgical data sets: surveillance, epidemiology, and end results (SEER) database. *JAMA Surg*. (2018) 153:588–9. doi: 10.1001/jamasurg.2018.0501

21. Coe TM, Fero KE, Fanta PT, Mallory RJ, Tang CM, Murphy JD, et al. Population-based epidemiology and mortality of small malignant gastrointestinal stromal Tumors in the USA. *J Gastrointest Surg*. (2016) 20:1132–40. doi: 10.1007/s11605-016-3134-y

22. Ma GL, Murphy JD, Martinez ME, Sicklick JK. Epidemiology of gastrointestinal stromal tumors in the era of histology codes: results of a population-based study. *Cancer Epidemiol Biomarkers Prev*. (2015) 24:298–302. doi: 10.1158/1055-9965.EPI-14-1002

23. LeDell E, van der Laan MJ, Petersen M. AUC-maximizing ensembles through Metalearning. *Int J Biostat*. (2016) 12:203–18. doi: 10.1515/ijb-2015-0035

24. Hanley JA, McNeil BJ. A method of comparing the areas under receiver operating characteristic curves derived from the same cases. *Radiology*. (1983) 148:839–43. doi: 10.1148/radiology.148.3.6878708

25. Vickers AJ, van Calster B, Steyerberg EW. A simple, step-by-step guide to interpreting decision curve analysis. *Diagn Progn Res*. (2019) 3:18. doi: 10.1186/s41512-019-0064-7

frontiers | Frontiers in Medicine

TYPE Original Research
PUBLISHED 23 October 2024
DOI 10.3389/fmed.2024.1463041

OPEN ACCESS

EDITED BY
Hua Zhong,
University of Hawaii at Manoa, United States

REVIEWED BY
Peng Wang,
Coriell Institute for Medical Research, United States
Peng Zhang,
Albert Einstein College of Medicine, United States

*CORRESPONDENCE
Jie Wei
✉ w_j_doc@163.com

RECEIVED 11 July 2024
ACCEPTED 30 September 2024
PUBLISHED 23 October 2024

CITATION
Du X, Ji Y, Qin W and Wei J (2024) Clinical efficacy of Endostar continuous infusion combined with concurrent chemoradiotherapy in the treatment of oesophageal squamous cell carcinoma. *Front. Med.* 11:1463041. doi: 10.3389/fmed.2024.1463041

Clinical efficacy of Endostar continuous infusion combined with concurrent chemoradiotherapy in the treatment of oesophageal squamous cell carcinoma

Xinglong Du, Yuting Ji, Wenqiang Qin and Jie Wei*

Department of Radiotherapy, The Affiliated Chuzhou Hospital of Anhui Medical University, Chuzhou, China

Objective: To evaluate the effectiveness and safety of concurrent chemoradiotherapy using Endostar continuous infusion for treating oesophageal squamous cell carcinoma (OSCC).

Method: A total of 62 patients with oesophageal carcinoma were divided into three groups: the Endostar continuous infusion group (n=27), the Endostar intravenous drip group (n=21) and the concurrent chemoradiotherapy group (n=14). All patients underwent oesophageal radiotherapy (56–60Gy) alongside concurrent chemotherapy (4mg of raltitrexed +100mg of oxaliplatin, two cycles). In the Endostar continuous infusion group, 210mg of Endostar was administered via infusion once every 3weeks for 72h, repeated for two cycles. The Endostar intravenous drip group received a dosage of 15mg/day of Endostar, administered once daily for 14days, repeated for two cycles. The objective response rate (ORR) (complete remission + partial remission), progression-free survival (PFS), 2-year overall survival (2y-OS) and adverse reactions were observed.

Results: In the Endostar continuous infusion, intravenous drip and concurrent chemoradiotherapy groups, the ORR was 100, 95.2 and 78.6%, respectively ($p < 0.05$). There was a statistically significant difference between the continuous infusion and concurrent chemoradiotherapy groups ($p < 0.05$). However, there was no statistically significant difference between the continuous infusion and intravenous drip groups or the intravenous drip and concurrent chemoradiotherapy groups ($p > 0.05$). The continuous infusion and intravenous drip groups had higher PFS rates than the concurrent chemoradiotherapy group ($p < 0.05$). Regarding the 2y-OS rate, no statistically significant difference was observed among the three groups ($p > 0.05$). Furthermore, there was no statistically significant difference in adverse reactions among the groups ($p > 0.05$).

Conclusion: Concurrent chemotherapy based on endostatin is effective and safe in the treatment of OSCC. Continuous 3-day Endostar infusion treatment can significantly enhance both short-and long-term therapy efficacy in patients while maintaining a high level of safety.

KEYWORDS

Endostar, continuous infusion, concurrent chemoradiotherapy, oesophageal squamous cell carcinoma, clinical efficacy

1 Introduction

Concurrent chemoradiotherapy has emerged as the primary approach for the radical treatment of oesophageal carcinoma, notably extending survival time (1). Raltitrexed, which is capable of inhibiting thymidylate synthase with minimal side effects, is increasingly incorporated into concurrent chemotherapy regimens for oesophageal cancer, yielding enhanced efficacy (2, 3). Currently, the standard approach to treating oesophageal cancer typically involves a combination of concurrent chemoradiotherapy alongside immunotherapy and targeted anti-angiogenesis medications (4, 5). Angiogenesis is pivotal in the progression, invasion and metastasis of malignant solid tumors. Consequently, anti-angiogenesis therapy holds significant promise in treating various tumor types. As a result, there is a growing focus on incorporating anti-vascular drugs into the comprehensive management of oesophageal cancer. Approximately 95% of cases of oesophageal carcinoma in China are squamous cell carcinomas (6). Since patients with oesophageal carcinoma have varying degrees of dysphagia, most small-molecule anti-angiogenic drugs cannot be taken orally.

Endostar is an innovative recombinant human endostatin injection, a new generation of biologics that has shown significant potential in the field of cancer treatment. Its therapeutic mechanism primarily relies on the inhibition of tumor angiogenesis (7), a critical component of tumor growth and metastasis. By specifically targeting vascular endothelial growth factor (VEGF), Endostar blocks the binding of VEGF to its receptors, thereby inhibiting the proliferation of vascular endothelial cells and effectively reducing the formation of new blood vessels (8). This process not only cuts off the tumor's supply of nutrients, limiting its growth, but also reduces the risk of tumor cells migrating to other parts of the body through blood vessels to form metastatic tumors. Additionally, it can work synergistically with other treatment modalities, such as chemotherapy and radiotherapy, to enhance their efficacy. Clinical studies have shown promising results for Endostar in various cancer types, including lung cancer, nasopharyngeal carcinoma and gastric cancer (9–11). Pan-target anti-angiogenesis modulates the dynamic equilibrium of angiogenesis within the tumor microenvironment, facilitating its normalization. This normalization enhances chemotherapy sensitivity, consequently impeding tumor growth and metastasis, leading to objectively prolonged patient survival time (12, 13). When combined with chemoradiotherapy, Endostar has demonstrated improved efficacy in treating lung cancer (14) and nasopharyngeal cancer (15), as well as other tumor types, alleviating concerns about bleeding associated with squamous cell carcinoma. Moreover, it has relatively few side effects and relatively high safety levels (16, 17). Endostar has a half-life of 8–12 h. The traditional route of administration of Endostar is 7.5 mg/m^2 via intravenous drip for 3–4 h per day for 14 consecutive days. However, the traditional use of intravenous drip causes large fluctuations in drug concentration and limits the compliance of patients with long-term administration of Endostar. Studies have shown that the anti-tumor effect of Endostar is time-and concentration-dependent, and its anti-tumor effect will increase with the extension of medication time and the increase of blood drug concentration within a certain range. Kisker (18) found that after a single intraperitoneal injection of Endostar to mice, the drug in the tumor tissue was quickly cleared within 2 h. Moreover, continuous administration through a micro-osmotic pump can keep the blood drug concentration stable for a long time, and the same anti-tumor effect can be obtained with one-eighth of the dose of a single injection. This may be due to the continuous intravenous pumping of Endostar, which allows the drug solution to be continuously and evenly infused, prolongs the infusion time and can maintain a stable blood drug concentration, such that the drug can continue to act on the endothelial cells of the new blood vessels, thereby achieving a better anti-tumor effect. Clinical studies have indicated that the continuous intravenous infusion of recombinant human endostatin yields superior outcomes compared with intravenous drip treatment (19–21), without an associated increase in side effects.

In the treatment of locally advanced oesophageal squamous cell carcinoma (LA-OSCC), concurrent chemoradiotherapy has become the standard treatment plan. With the rise of immunotherapy, researchers have begun to explore new combined treatment plans to improve therapeutic outcomes. Recently, a single-center, open-label phase II study demonstrated the potential of Endostar in combination with envafolimab (a PD-L1 checkpoint inhibitor) and concurrent chemoradiotherapy for the treatment of LA-OSCC. In this study, patients received 50.4 Gy of radiotherapy, chemotherapy with paclitaxel liposome and carboplatin, and treatments with Endostar and envafolimab. Preliminary results showed that this combined treatment plan has good tolerability and controllable toxicity, and all patients experienced a reduction in target lesion size, with an objective response rate (ORR) of 100% and an endoscopic complete remission rate of 88.9%. These promising results provide strong support for the ongoing phase II study and offer new therapeutic hope for patients with LA-OSCC (22).

However, there has been no study reporting the efficacy of Endostar continuous infusion combined with raltitrexed-based concurrent chemoradiotherapy in the treatment of OSCC. Therefore, this study reports the efficacy and safety of Endostar continuous infusion combined with concurrent chemoradiotherapy in treating this disease.

2 Information and methodology

2.1 Inclusion criteria

The inclusion criteria for patients were as follows: (1) aged 45–75 years; (2) pathological confirmation of squamous cell carcinoma; (3) ability to tolerate concurrent chemoradiotherapy; (4) no previous history of bleeding and concomitant diseases; (5) routine physical examination, blood routine, liver function, kidney function and other auxiliary examinations not contraindicated by radiotherapy and chemotherapy; and (5) informed consent obtained and signed prior to treatment. The exclusion criteria were as follows: (1) severe underlying diseases and unable to tolerate concurrent chemotherapy; (2) a history of significant peptic ulcer; and (3) a history of previous bleeding. The general information collected included age, location, differentiation, tumor stage and angiographic classification. Tumor staging was performed using the Union for International Cancer Control (UICC) guidelines (2002 edition).

2.2 General information

A total of 62 patients (38 men and 24 women) with OSCC admitted to the department of radiotherapy between February 2017 and December 2020 were randomly divided into three groups. The patients' ages ranged from 45 to 75 years, with a median age of 63.0 and an average age of 63.60 ± 7.34. The distribution skewness was −0.283 ± 0.304, which conformed to a normal distribution. The ages provided were those at the time of the patient's initial radiation treatment. In addition, the time between the first diagnosis and first radiation treatment for all patients did not exceed 3 months. Patients were randomly assigned to either the Endostar continuous infusion group, the Endostar intravenous drip group or the concurrent chemoradiotherapy group based on the day of the week of admission. Patients admitted on Monday and Thursday were assigned to the Endostar continuous infusion group, those admitted on Tuesday and Friday were assigned to the Endostar intravenous drip group and those admitted on Wednesday and Saturday were assigned to the concurrent chemoradiotherapy group. None of the patients assigned to these groups had received any anti-tumor treatment prior to the therapy. Ethical approval for this study was obtained from the institutional ethical committee. The treatment choice for the randomly assigned patients was independent of both gender and age. The general treatments administered to the enrolled patients are detailed in Table 1.

2.3 Methods

All patients underwent radiotherapy alongside concurrent chemotherapy based on raltitrexed. The concurrent chemoradiotherapy group received radiotherapy combined with concurrent chemotherapy alone. The Endostar continuous infusion group received Endostar administered via a pump in addition to concurrent chemoradiotherapy. The Endostar intravenous drip group received Endostar administered intravenously via a drip in addition to concurrent chemoradiotherapy.

2.3.1 Radiotherapy

The patient's position was fixed with thermoplastic film, and enhanced computed tomography (CT) simulation localisation was performed. The image was uploaded to the Pinnacle intensity-modulated radiation therapy (IMRT) system. The target area was delineated based on the CT scan image, gastroscopy and oesophagography. Gross tumor volume (GTV) delineated the focus of oesophageal carcinoma, whereas nodal GTV (GTVn) included enhanced CT images of metastatic lymph nodes. Clinical target volume (CTV) encompassed both GTV and GTVn, extending the upper and lower ends of GTVn outward by 0.5 cm and incorporating the corresponding lymph node drainage area with a 0.6-cm margin at each end. Planning gross tumor volume (PGTV) comprised GTV and GTVn, with the upper and lower ends of GTV extended by 3–5 cm and the upper and lower ends of GTVn extended outward by 0.5 cm, along with an additional extension of 0.5 cm on the anterior, posterior, left and right sides. Planning target volume underwent a three-dimensional (3D) CTV expansion of 0.5 cm, followed by adjustments to organs at risk, such as large blood vessels and vertebral bodies. In terms of prescription dose, 95% of PGTV received 50.4–60 Gy in 1.8–2 Gy fractions over 28–30 fractions, and 95% of PGTV received 59.92 Gy in 2.14 Gy fractions over 28 fractions. The maximum dose to organs at risk was as follows: spinal cord, maximum <40 Gy; lungs, V20 < 28%; and heart, V40 < 30%. Routine segmentation occurred once per day, five times per week. Following the completion of the radiotherapy plan, the deputy chief physician confirmed and verified the treatment dose before execution. The treatment was administered using a Siemens accelerator (6MV-X IMRT; Siemens AG, Munich, Germany).

2.3.2 Chemotherapy

All patients received concurrent chemotherapy based on raltitrexed. The first week of radiotherapy was followed by 4 mg of raltitrexed +100 mg of oxaliplatin and was repeated for 3 weeks, completing two cycles.

2.3.3 Nutritional support and other treatments

Raltitrexed (Nanjing Zhengda Tianqing Pharmaceutical Co., Ltd., Nanjing, China) was administered at a dose of 2 mg per vial, whereas oxaliplatin (Jiangsu Hengrui Pharmaceutical Co., Ltd., China; Jinan Qilu Pharmaceutical Co., Ltd., China) was given at a dose of 100 mg per vial.

2.3.4 Targeted therapy

The Endostar continuous infusion group received 210 mg of endostatin +102 mL of normal saline (NS) at the beginning of the first day of radiotherapy for 72 h once every 3 weeks, totalling two cycles. The Endostar intravenous drip group received 15 mg of endostatin +500 mL of NS intravenously for 3 h from the first day of radiotherapy once daily for 14 consecutive days, followed by 7 days of rest, completing two cycles. Endostar was used at a concentration of 15 mg/mL (First Sound Pharmaceutical, Jiangsu, China).

2.4 Observation index and judging standard

The TNM staging was performed for all patients using the UICC guidelines (2002 edition) staging system. Enhanced CT and oesophagography were performed within 1–2 months of radiotherapy. Wan et al. (23) initially proposed the efficacy standard for oesophageal carcinoma, categorizing oesophageal lesions as either in complete remission (CR), in partial remission (PR), stable (SD) or progressive (PD) based on oesophagography. Mediastinal lymph nodes were identified as complete response (CR), partial response (PR), SD or PD using chest CT according to the World Health Organization's RECIST1.1 criteria. The overall therapeutic effect was judged in combination with the changes in oesophageal lesions and mediastinal lymph nodes. If the results of the two tests were not completely consistent, this study adopted the lowest therapeutic effect as the comprehensive therapeutic effect result (see Table 2). The ORR was defined as including the comprehensive therapeutic effect results of CR and PR. For long-term effects, the median progression-free survival (mPFS) and the median 2-year overall survival (median 2y-OS) were observed. The mPFS was defined as the point prior to which 50% of the patients had not shown disease progression after the start of radiation therapy. The median 2y-OS was defined as the number of patients who survived at least 2 years after the start of radiation treatment. Adverse reactions to the chemotherapy drugs

TABLE 1 Patient general information.

	ENDOSTAR continuous infusion group ($n = 27$)	ENDOSTAR intravenous drip group ($n = 21$)	Concurrent chemoradiotherapy group ($n = 14$)	χ^2/F value	p value
Male	16 (59%)	13 (62%)	9 (64%)	0.103	$p = 0.950$
Female	11 (41%)	8 (38%)	5 (36%)		
Age	63.22 ± 1.01	64.09 ± 1.12	63.57 ± 2.07	1.043	$p = 0.439$
Smoking					
Yes	18 (67%)	14 (67%)	10 (71%)	0.112	$p = 0.945$
No	9 (33%)	7 (33%)	4 (29%)		
Alcohol drinking					
Yes	20 (74%)	15 (71%)	11 (79%)	0.224	$p = 0.894$
No	7 (26%)	6 (29%)	3 (21%)		
TNM stage					
Stage II	4 (15%)	4 (19%)	3 (21%)	0.369	$p = 0.985$
Stage III	17 (63%)	13 (62%)	8 (57%)		
Stage IV	6 (22%)	4 (19%)	3 (22%)		
Highly differentiated	8 (30%)	6 (29%)	4 (29%)	0.321	$p = 0.988$
Intermediate differentiation	15 (56%)	11 (52%)	7 (50%)		
Low differentiation	4 (14%)	4 (19%)	3 (21%)		
≤6 cm	19 (70%)	16 (76%)	10 (71%)	0.213	$p = 0.899$
>6 cm	8 (30%)	5 (24%)	4 (29%)		
Medullary type	20 (74%)	18 (86%)	10 (71%)	7.465	$p = 0.280$
Ulcer type	2 (7%)	0 (0%)	1 (7%)		
Narrow type	2 (7%)	1 (5%)	1 (7%)		
Intracavity type	3 (12%)	2 (9%)	2 (14%)		

10.3389/fmed.2024.1463041

10.3389/fmed.2024.1463041

TABLE 2 Comparison of short-term efficacy among three groups.

	ENDOSTAR continuous infusion group ($N = 27$)	ENDOSTAR intravenous drip group ($N = 21$)	Concurrent chemotherapy group ($N = 14$)
CR	9/27 (33.3%)	6/21 (28.6%)	3/14 (21.4%)
PR	18/27 (66.7%)	14/21 (66.7%)	8/14 (57.1%)
SD	0/27 (0)	1/21 (4.8%)	3/14 (21.4%)
ORR (%)	100	95.2	78.6

The p- value for comparison between the 3 groups was $p = 0.031$ ($p < 0.05$). Comparisons between subgroups require a corrected P value of P′. P′ ENDOSTAR continuous infusion group/Concurrent chemotherapy group = 0.014 ($p' < 0.017$), P′ ENDOSTAR continuous infusion group / ENDOSTAR intravenous drip group = 0.508 ($p' > 0.017$), P′ ENDOSTAR intravenous drip group/Concurrent chemotherapy group = 0.143 ($p' > 0.017$).

were assessed according to the Common Terminology Criteria for Adverse Events (CTCAE) 4.0 standard (May 2009), and the Radiation Therapy Oncology Group's (RTOG) acute radiation injury grading standard (24) was used to assess the side effects of radiation therapy.

The ORR included the CR and PR, and the lowest curative effect was taken as the standard. Progression-free survival and 2y-OS were observed during telephone and outpatient follow-ups of 24 months. The side effects of radiotherapy were assessed according to the May 2009 CTCAE 4.0 criteria for adverse reactions to chemotherapy and the RTOG's acute radiation injury grading criteria (24).

2.5 Follow-up

Telephone and outpatient follow-ups were conducted for all patients following radiotherapy and chemotherapy. Follow-up examinations were performed every 3 months in the first year and every 4–5 months in the second year. The follow-up indices included alleviation of eating obstruction, oesophagography and chest CT imaging. All patients were followed up for 24 months, and the deadline for follow-up was December 2022. One patient died from an accidental incident and two died from heart disease; none of the patients were lost to follow-up, with a 100% follow-up rate.

2.6 Statistical methods

All results were analyzed using the SPSS 25.0 statistical software. The mean ± standard error was used to summarize the measurement data, and the ORR was expressed as a percentage. Patient data and adverse drug reactions were analyzed using the chi-square (χ^2) test. The ORR was assessed using analysis of variance with a random block design. The PFS and 2y-OS were evaluated for differences in survival using the Breslow test. Kaplan–Meier survival curves were subsequently constructed, with a significance level (α) set at 0.05.

3 Results

3.1 Comparison of short-term efficacy

The CR, PR and SD were 9 (33.30%), 18 (66.7%) and 0 (0%), respectively, in the Endostar continuous infusion group. The CR, PR and SD were 6 (28.6%), 14 (66.7%) and 1 (4.8%), respectively, in the Endostar intravenous drip group. In the concurrent chemoradiotherapy group, the CR, PR and SD were 3 (21.4%), 8 (57.1%) and 3 (21.4%), respectively. The ORRs of the three groups were 100, 95.2 and 78.6%, respectively, and the difference among the three groups was statistically significant ($p = 0.031$). The ORR of the Endostar continuous infusion group (100%) was significantly higher than that of the concurrent chemoradiotherapy group (78.2%) ($p = 0.014$). There was no significant difference between the continuous infusion and intravenous drip groups or between the intravenous drip and concurrent chemoradiotherapy groups ($p > 0.05$; see Table 2).

3.2 Survival analysis

3.2.1 Progression-free survival

The mPFS was 19.9 [95% confidence interval (CI): 18.39–21.42] months in the Endostar continuous infusion group, 17.7 (95% CI: 16.46–18.87) months in the Endostar intravenous drip group and 15.6 (95% CI: 14.3–16.84) months in the concurrent chemoradiotherapy group, and the difference was statistically significant ($p = 0.003$). Following correction using the Bonferroni method, the intergroup significance level was set at $\alpha = 0.017$. Further analysis between the two groups revealed a statistical difference between the Endostar continuous infusion group and the concurrent chemotherapy group ($p < 0.017$), but there was no statistically significant difference between the intravenous drip group and the concurrent chemotherapy group or between the continuous infusion group and the intravenous drip group ($p > 0.017$; see Figure 1).

3.2.2 Two-year overall survival

The median 2y-OS response rate was 20.35 (95% CI: 17.77–22.93), 17.7 (95% CI: 16.46–18.87) and 16.6 (95% CI: 15.32–17.83) months in the Endostar continuous infusion, Endostar intravenous drip and concurrent chemotherapy groups, respectively, and the difference was not statistically significant ($p = 0.090$). Following correction with the Bonferroni method, the intergroup significance level was set at $\alpha = 0.017$. Further analysis found no statistical difference between the Endostar continuous infusion and concurrent chemotherapy groups, between the intravenous drip and concurrent chemotherapy groups or between the Endostar continuous infusion and intravenous drip groups ($p > 0.017$; see Figure 2).

3.3 Adverse reactions

The major adverse events were radiation oesophagitis (grades I–II and III–IV), decreased neutrophil counts and fatigue, and neutropenia was managed with CSF3. Thrombocytopenia treatment with interleukin 11 and thrombopoietin was successfully completed. During that period, one case of III–IV grade hypertension was relieved by adjusting the dose of antihypertensive drugs, and the treatment was resumed. One case in each group of grade I–II haematemesis was found in all three groups, and no radiation pneumonitis occurred in any of the three groups (see Table 3).

4 Discussion

This study concluded that Endostar continuous infusion combined with concurrent chemoradiotherapy can improve the ORR of oesophageal carcinoma. Inhibition of the VEGF-related signaling pathway may promote the efficacy of radiotherapy for this type of carcinoma (25). Fan et al. (26) found that Endostar combined with concurrent chemoradiotherapy increased the ORR of OSCC ($p = 0.026$). The ORR of concurrent chemoradiotherapy with Endostar and tetrandrine for recurrent oesophageal cancer was 66.7%, significantly surpassing that of the control group (39.3%) ($p < 0.05$) (27). In a study by Liang (28), which included 62 patients with advanced ovarian cancer, the findings indicated that there was no difference in the overall response rate between the paclitaxel/platinum plus Endostar intravenous infusion and intravenous infusion regimens ($p > 0.05$). However, some clinical studies have revealed that the ORR of Endostar continuous infusion is better than that of intravenous infusion. Zhang et al. (21) reported 100 cases of advanced non-small cell lung carcinoma cancer (NSCLC) treated with Endostar continuous infusion and infusion combined with platinum-containing dual-drug chemotherapy. The results demonstrated that the intravenous infusion of ORR ($p = 0.026$) and disease-control rate ($p = 0.017$) were superior to intravenous infusion. In the present study, the ORR was 95.2 and 78.2% in the Endostar intravenous drip and concurrent chemoradiotherapy groups, respectively, and there was no statistically significant difference ($p > 0.05$). These results differ from those of existing clinical studies. The absence of a statistical difference between the two groups may be attributed to an increased likelihood of random error due to the smaller number of patients in both groups. However, there was a significant difference between the Endostar continuous infusion and concurrent chemotherapy groups ($p = 0.036$). It may be advantageous to explore cumulative differences between the Endostar continuous infusion and Endostar intravenous drip groups, as well as between the intravenous and concurrent chemoradiotherapy groups.

This study found that there was a significant difference in mPFS between the three groups, and subgroup analysis showed that the difference in PFS between the Endostar continuous infusion group and the concurrent chemotherapy group was significant. It is suggested that Endostar combined with radiotherapy and chemotherapy can enhance the PFS of patients, with continuous infusion potentially offering more pronounced benefits. A retrospective analysis suggested that concurrent chemoradiotherapy combined with Endostar injection can improve the 3-year PFS rate of patients with locally advanced nasopharyngeal carcinoma (29). Another study suggested that the PFS of patients with nasopharyngeal cancer treated with concurrent chemoradiotherapy plus Endostar was significantly longer than that of concurrent chemoradiotherapy by approximately 4 months (30). However, in the present study, there was no significant difference between the Endostar continuous infusion group and the Endostar intravenous drip group, or between the Endostar intravenous drip group and the concurrent chemotherapy group, which is different from the results of published studies. A previous study suggested that continuous infusion of Endostar combined with chemotherapy may decrease the risk of locally advanced disease compared with intravenous drip, and the mPFS of NSCLC increased from 4.4 to 8.0 months ($p = 0.019$) (16). Xu et al. found that the PFS of 40 patients with intermediate-to-advanced NSCLC treated by the two routes of Endostar combined with a gemcitabine/cisplatin (GP) regimen was 7.5 and 5.9 months, respectively ($p < 0.05$) (31). A real-world analysis assessing the effectiveness of Endostar combined with chemotherapy in treating 54 cases of non-driver gene mutation NSCLC revealed that the mPFS of 7-day continuous infusion was superior to that of 14-day intravenous drip (6 vs. 4.5 months) (32).

The difference in our results can be attributed to the study's design, which involved comparing three groups using two subgroups. This

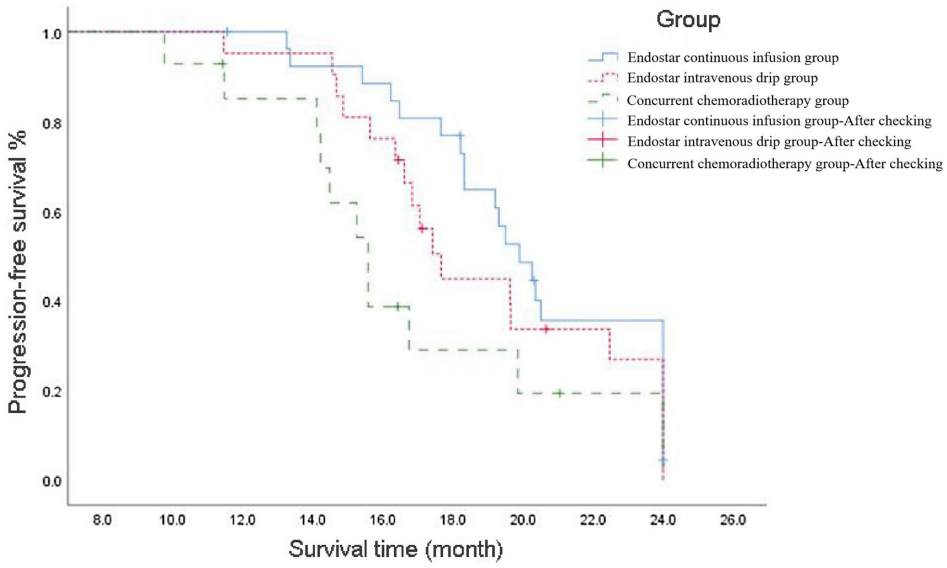

FIGURE 1
Progression-free survival curve of ENDOSTAR continuous infusion group, ENDOSTAR intravenous drip group and concurrent chemotherapy group. The curves depict the rates at which patients in each group maintained disease progression-free status over time since the commencement of treatment.

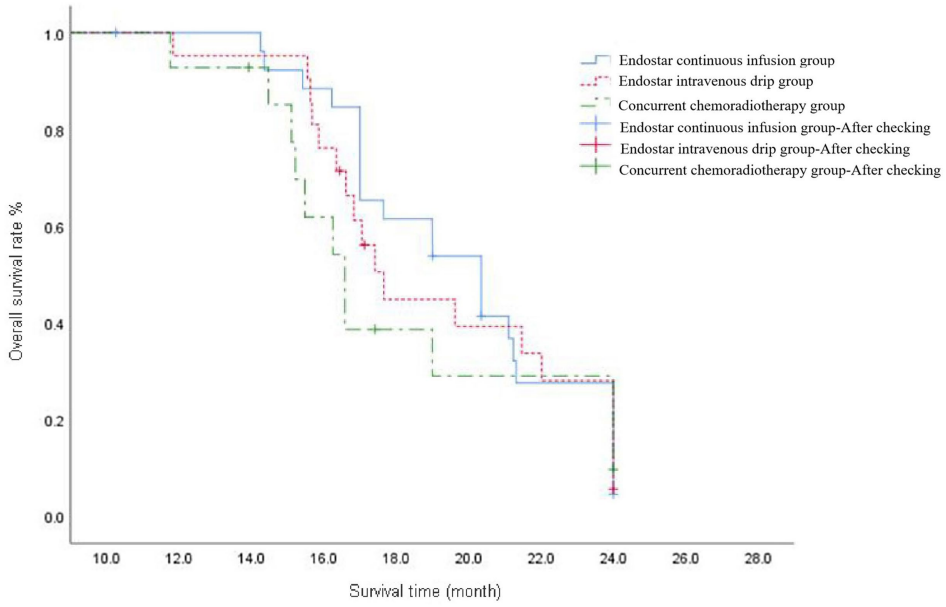

FIGURE 2
The overall survival curve of ENDOSTAR continuous infusion group, ENDOSTAR intravenous drip group and concurrent chemotherapy group. The curves reflect the survival conditions of patients in each group from the start of treatment until the end of follow-up.

TABLE 3 The adverse reactions of 62 cases of esophageal carcinoma with different therapeutic schemes.

Adverse reactions	ENDOSTAR continuous infusion Group		ENDOSTAR intravenous drip group		Concurrent chemoradiotherapy group		X^2 value	*p*- value
	I-II	III-IV	I-II	III-IV	I-II	III-IV		
Thrombocytopenia	7	2	6	2	4	1	0.017	0.895
Less neutrophil	14	3	11	3	10	2	0.021	0.796
Vomiting blood	1	0	1	0	1	0	0	1.000
High blood pressure	7	1	8	0	1	0	−0.111	0.288
Radiation esophagitis	24	3	16	5	12	2	0.083	0.241
Hoarse voice	4	0	2	0	0	0	−0.286	0.439
Hard to breathe	1	0	1	0	1	0	0	1.000
Fatigue	23	4	18	3	12	2	−0.004	0.958
Nausea/vomiting	17	2	18	1	10	2	−0.032	0.589

contrasts with other clinical studies, which typically compare only two groups. Furthermore, this study's statistical test employed $p < 0.017$ as the threshold for test significance, whereas other studies typically used $p < 0.05$ as the criterion for significance. Moreover, the limited number of cases and short follow-up time may have introduced experimental bias.

This study suggests that whether or not Endostar is used, and irrespective of whether it is administered via continuous infusion or intravenous drip, there were no benefits in terms of the 2y-OS ($p = 0.196$). Moreover, the study did not demonstrate that the use of Endostar in combination with chemoradiotherapy can significantly improve long-term survival rates compared with chemoradiotherapy alone. Endostar also showed no significant benefit in the 2y-OS of patients with other tumors. The OS of recombinant human endostatin combined with a GP regimen and GP regimen alone was 12.7 and 12.3 months in 40 patients with advanced NSCLC, respectively ($p > 0.05$) (31). No prolonged OS was seen in a real-world study of the efficacy of chemotherapy combined with recombinant human endostatin following 7-day continuous infusion and 14-day intravenous infusion in 54 patients with NSCLC ($p = 0.111$) (32).

In the present study, radiation-induced oesophagitis, neutrophil levels, fatigue and vomiting were the primary adverse events. These adverse reactions (graded >3) occurred in 16.0% (10/62), 14.5% (9/62), 12.9% (8/62) and 8.1% (5/62) of patients, respectively. No oesophageal perforation or severe haematemesis occurred. The study assessed whether Endostar was used in combination and whether the drug was administered continuously over 3 days or infused intravenously over 14 days without causing life-threatening side effects. The results showed that Endostar is safe and reliable. Additionally, Endostar can be considered safe and manageable in other cancer combinations. A 3-day regimen of continuous intravenous infusion of recombinant

human endostatin combined with chemotherapy was found to have a manageable adverse effect and an acceptable safety profile in 127 patients with solid tumors (33). A phase II study of Endal plus etoposide/cisplatin in 22 patients with small-cell carcinoma found that all patients tolerated the treatment. The main adverse reactions were myelosuppression, proteinuria, nausea and vomiting, and the incidence of grade 3 and 4 adverse reactions was 7.2%. No treatment-related deaths occurred (34). Endostar combined with chemoradiotherapy can further expand the benefits of treating the population with OSCC and, for more extensive cases, improve effective and safe treatment opportunities.

This study provides important insights in the field of concurrent chemoradiotherapy for OSCC. Based on this study, the use of Endostar combined with chemotherapy and radiotherapy for OSCC may have a range of potential long-term effects on patients. First, we discovered that combining Endostar with chemotherapy and radiotherapy yields notable efficacy and safety in treating this carcinoma type. Specifically, continuous infusion of Endostar notably enhances ORRs and PFS rates, offering fresh therapeutic avenues for clinical practice. Although no statistically significant difference in 2y-OS was found in this study, the improved treatment effect may help prolong patient survival. This result may be limited by sample size or follow-up time. Improved treatment efficacy and longer survival may reduce patients' symptoms and complications, thereby improving their quality of life. Second, this study emphasizes the importance of personalized treatment approaches. By comparing various regimens, it was found that continuous Endostar infusion outperforms intravenous administration and simple chemoradiotherapy. This highlights the need to tailor treatments based on individual patient characteristics and pathology, ultimately improving treatment outcomes and survival rates. In addition, as an anti-angiogenic drug, Endostar may help reduce tumor recurrence and metastasis by inhibiting tumor angiogenesis, providing patients with longer-term disease control. However, although the side effects of Endostar were controllable in this study, the unknown long-term side effects that may be caused by long-term use need to be managed through continuous monitoring and evaluation. This study highlights the need for improved treatment options. Finally, this study may provide new directions for future research on Endostar and other anti-angiogenic drugs in OSCC, and even other types of cancer, to explore their long-term effects and optimal use strategies.

Despite our progress, limitations persist, including sample size constraints and short follow-up periods. Therefore, future research should prioritize enlarging the sample size, and further research involving more diverse populations and extended follow-up durations is needed to validate our findings and explore novel therapeutic strategies and drugs.

In summary, Endostar combined with raltitrexed-based concurrent chemoradiotherapy is safe and effective for the treatment of OSCC. Furthermore, 3D continuous infusion can improve the ORR and PFS rate. A 3-day continuous infusion of Endostar constitutes a short treatment duration, associated with mild adverse reactions, meaning it may offer an effective and safe approach to treating OSCC.

Data availability statement

The original contributions presented in the study are included in the article/supplementary material, further inquiries can be directed to the corresponding authors.

Ethics statement

The studies involving humans were approved by ethics committee of The Affiliated Chuzhou Hospital of Anhui Medical University. The studies were conducted in accordance with the local legislation and institutional requirements. The participants provided their written informed consent to participate in this study.

Author contributions

XD: Conceptualization, Formal analysis, Funding acquisition, Supervision, Writing – original draft, Writing – review & editing. YJ: Data curation, Investigation, Writing – review & editing. WQ: Data curation, Investigation, Writing – review & editing. JW: Formal analysis, Investigation, Writing – review & editing.

Funding

The author(s) declare that financial support was received for the research, authorship, and/or publication of this article. This study was supported by 2021 Clinical Science Fund of Anhui Medical University (2021xkj204).

Conflict of interest

The authors declare that the research was conducted in the absence of any commercial or financial relationships that could be construed as a potential conflict of interest.

Publisher's note

References

1. Cooper JS, Guo MD, Herskovic A, Macdonald JS, Martenson JA, Al-Sarraf M, et al. Chemoradiotherapy of locally advanced esophageal cancer: long-term follow-up of a prospective randomized trial (RTOG 85-01). Radiation Therapy Oncology Group. *JAMA*. (1999) 281:1623–7. doi: 10.1001/jama.281.17.1623

2. Zhou WB, Xu J, Li YX, Dai SB, Yao J, Zhang H, et al. The short-term effect of concurrent radiotherapy with RETETROXOL and cisplatin in the treatment of advanced esophageal carcinoma. *Cancer Res Clin*. (2017) 29:693–5. doi: 10.3760/cma.j.issn.1006-9801.2017.10.011

3. Xia YY, Wang L, Song DA, Li SQ, Jiang XD. A phase II clinical study of concurrent radiotherapy combined with Retetrose and oxaliplatin in the treatment of advanced esophageal cancer. *Chin J Clin Oncol*. (2014) 41:716–9. doi: 10.3969/j.issn.1000-8179.20140440

4. Shi JZ, Zhang YJ, Wang JZ, Li JB, Li ZX. Anlotinib combined with Chemoradiotherapy exhibits significant therapeutic efficacy in esophageal squamous cell carcinoma. *Front Oncol*. (2020) 10:995. doi: 10.3389/fonc.2020.00995

5. Ge XL, Wang YD, Wen W, Zhu HC, Ye HX, Yang X, et al. Recombinant human endostatin combined with definitive chemoradiotherapy for patients with locally advanced esophageal carcinoma. *Int J Clin Exp Med*. (2016) 9:20137–44.

6. Chen F, Xu B, Li J, Yang X, Gu J, Yao X, et al. Hypoxic tumour cell-derived exosomal mi R-340-5p promotes radioresistance of oesophageal squamous cell carcinoma via KLF10. *J Exp Clin Cancer Res*. (2021) 40:38. doi: 10.1186/s13046-021-01834-9

7. Li Y, Yi Y, Lin A, Luo P, Zhang J. A comparison of the efficacy of antiangiogenic agents combined with chemotherapy for the treatment of non-small cell lung cancer: a network meta-analysis. *Cancer Cell Int*. (2020) 20:548. doi: 10.1186/s12935-020-01639-4

8. Wang YB, Liu JH, Song ZM. Effects of recombinant human endostatin on the expression of vascular endothelial growth factor in human gastric cancer cell line MGC-803. *Biomed Rep*. (2013) 1:77–9. doi: 10.3892/br.2012.3

9. Jiang W, Sun W, Li W, Gao J, Wang H, Zhou W, et al. Real-world treatment pattern and comprehensive comparative effectiveness of Endostar plus different chemotherapy in advanced patients with non-small cell lung cancer. *Sci Rep*. (2022) 12:10841. doi: 10.1038/s41598-022-14222-w

10. Jin T, Jiang F, Jin QF, Piao YF, Chen XZ. Endostar combined with gemcitabine and cisplatin chemotherapy for patients with metastatic nasopharyngeal carcinoma: an update. *Transl Oncol*. (2018) 11:286–91. doi: 10.1016/j.tranon.2018.01.002

11. Liang J, Dai W, Li Z, Liang X, Xiao M, Xie C, et al. Evaluating the efficacy and microenvironment changes of HER2 + gastric cancer during HLX02 and Endostar treatment using quantitative MRI. *BMC Cancer*. (2022) 22:1033. doi: 10.1186/s12885-022-10136-y

12. Ma J, Waxman DJ. Combination of antiangiogenesis with chemotherapy for more effective cancer treatment. *Mol Cancer Ther*. (2008) 7:3670–84. doi: 10.1158/1535-7163.MCT-08-0715

13. Ansari MJ, Bokov D, Markov A, Jalil AT, Shalaby MN, Suksatan W, et al. Cancer combination therapies by angiogenesis inhibitors; a comprehensive review. *Cell Commun Signal*. (2022) 20:49. doi: 10.1186/s12964-022-00838-y

14. Lv Y, Jiang R, Ma C, Li J, Wang B, Sun L, et al. Clinical observation of recombinant human vascular Endostatin durative transfusion combined with window period arterial infusion chemotherapy in the treatment of advanced lung squamous carcinoma. *Zhongguo Fei Ai Za Zhi*. (2015) 18:500–4. doi: 10.3779/j.issn.1009-3419.2015.08.05

15. Li Y, Jin F, Wu W, Long J, Gong X, Chen G, et al. Clinical results of recombinant human endostatin combined with chemoradiotherapy for locally advanced nasopharyngeal carcinoma. *Zhonghua Zhong Liu Za Zhi*. (2015) 37:128–32.

16. Zhu J, Chen G, Niu K, Feng Y, Xie L, Qin S, et al. Efficacy and safety of recombinant human endostatin during peri-radiotherapy period in advanced non-small-cell lung cancer. *Future Oncol*. (2022) 18:1077–87. doi: 10.2217/fon-2021-1239

17. Tan A, Wang H, Nong L, Jia Y, Liu Y, Zhong W, et al. Efficacy and safety of continuous infusion of Rh-endostatin combined with platinum-based chemotherapy for advanced triple-negative breast cancer. *Ann Palliat Med*. (2021) 10:12101–12. doi: 10.21037/apm-21-2624

18. Kisker O, Becker CM, Prox D, Fannon M, D'Amato R, Flynn E, et al. Continuous administration of endostatin by intraperitoneally implanted osmotic pump improves the efficacy and potency of therapy in a mouse xenograft tumor model. *Cancer Res*. (2001) 61:7669–74.

19. Pang LR, Chen J, Lu JE, Huang J, Li H, Xu CH, et al. Different administration methods of recombinant human endostatin combined with GP regimen in the treatment of advanced non-small cell lung cancer. *Mod Pract Med*. (2015) 27:255–6. doi: 10.3969/j.issn.1671-0800.2015.02.071

20. Meng M. Effect of two infusion methods of Endol combined with chemotherapy in the treatment of advanced non-small cell lung cancer. *J Clin Med*. (2017) 37:3.

21. Zhang MR, Cao DD, Ge W. Comparison of efficacy and safety of Endu intravenous continuous pumping and infusion combined with platinum-containing double-drug chemotherapy in the treatment of advanced non-small cell lung cancer. *J Pract Oncol*. (2022) 36:20–5. doi: 10.11904/j.issn.1002-3070.2022.01.004

22. Wang X, Li B. Two-stage phase II study of Envafolimab combined with Endostar and concurrent Chemoradiotherapy in treatment of Unresectable locally advanced esophageal squamous cell carcinoma: preliminary results of stage 1. *Int J Radiat Oncol Biol Phys*. (2022) 114:e166–7. doi: 10.1016/j.ijrobp.2022.07.1045

23. Wan J, Xiao AQ, Gao SZ, Gao BZ, Wang YD, Zhou DA. Evaluation criteria for short-term efficacy after radiotherapy for esophageal cancer: an analysis of 1000 cases. *Chin J Radiat Oncol*. (1989) 4:3–5.

24. Cox JD, Stetz J, Pajak TF. Toxicity criteria of the radiation therapy oncology group (RTOG) and the European Organization for Research and Treatment of Cancer (EORTC). *Int J Radiat Oncol Biol Phys*. (1995) 31:1341–6. doi: 10.1016/0360-3016(95)00060-C

25. Liu GF, Chang H, Li BT, Zhang Y, Li DD, Liu Y, et al. Effect of recombinant human endostatin onradiotherapy for esophagus cancer. *Asian Pac J Trop Med*. (2016) 9:86–90. doi: 10.1016/j.apjtm.2015.12.017

26. Fan RT, Liu Y, Wang X, Sun YY, Wu J. Clinical observation of Endu combined with chemoradiotherapy in the treatment of advanced esophageal cancer. *Chin J Pract Med*. (2014) 41:13–5. doi: 10.3760/cma.j.issn.1674-4756.2014.06.005

27. Tian Q, Fan RT, Zhang CF, Hu JG, Wang X. Efficacy of Tighio combined with recombinant human endostatin in the treatment of recurrent esophageal cancer by reradiotherapy. *Henan Med Res*. (2018) 27:200–2. doi: 10.3969/j.issn.1004-437X.2018.02.004

28. Liang L. Clinical study of recombinant human endostatin Endol combined with TP regimen in the treatment of advanced ovarian cancer. *Chin Med Guide*. (2017) 15:2.

29. Yin Y, Zhou Z, Li Z, Shen M, Qin Y, Yang C, et al. Efficacy of concurrent chemoradiotherapy plus Endostar compared with concurrent chemoradiotherapy in the treatment of locally advanced nasopharyngeal carcinoma: a retrospective study. *Radiat Oncol*. (2022) 17:135. doi: 10.1186/s13014-022-02104-4

30. Xu L, Li D, Ji J, Chen Z, Tang X, Chen D, et al. Recombinant human endostatin injection (Endostar) combined with PF chemotherapy and sequential intensity-modulated radiotherapy is tolerable and improves prognosis of locally advanced nasopharyngeal carcinoma: a randomized, open, multicenter phase II clinical study. *Am J Cancer Res*. (2022) 12:4622–36.

31. Xu J, Chen B, Cao JM, Jia SC, Hu XB, Zhang LJ, et al. Clinical study of recombinant human endostatin combined with gemcitabine and cisplatin in the treatment of advanced non-small cell lung cancer. *J Clin Oncol*. (2011) 16:709–14. doi: 10.3969.j.issn.1009-0460.2011.08.010

32. Wang Z, Zhang H, Zhou C, Long X, Guan R, Yang N, et al. Real-world outcomes of various regimens of recombinant human endostatin combined with chemotherapy in non-driver gene mutation advanced non-small cell lung cancer. *Cancer Med*. (2019) 8:1434–41. doi: 10.1002/cam4.2014

33. Song JF, Peng H, Peng XQ, Wu XL, Jian D, Luo H, et al. Observation and analysis of adverse effects of 3 days continuous intravenous pump focused on human endostatin combination regimen in treatment of solid tumors. *Cancer Prog*. (2019) 19:5. doi: 10.11877/j.issn.1672-1535.2021.19.11.12

34. Zhao Y, Zhang X, Jin C, Yu X, Zhang M, Cao Y, et al. Efficacy and safety of endostatin in combination with chemotherapy in small cell lung cancer: a phase 2 single-arm multicenter open-label trial. *Ann Palliat Med*. (2021) 10:3277–85. doi: 10.21037/apm-21-443

frontiers | Frontiers in Medicine

TYPE Systematic Review
PUBLISHED 22 November 2024
DOI 10.3389/fmed.2024.1507739

OPEN ACCESS

EDITED BY
Hua Zhong,
University of Hawaii at Manoa, United States

REVIEWED BY
Laixing Zhang,
University of California, Los Angeles, United States
Nan Zhang,
St. Jude Children's Research Hospital, United States

*CORRESPONDENCE
Yong-hui Jia
✉ jiayonghui729@163.com

RECEIVED 08 October 2024
ACCEPTED 11 November 2024
PUBLISHED 22 November 2024

CITATION
Li A-j, Jiang H-y and Jia Y-h (2024) Statin exposure and risk of colorectal cancer in patients with inflammatory bowel disease: a systematic review and meta-analysis.
Front. Med. 11:1507739.
doi: 10.3389/fmed.2024.1507739

Statin exposure and risk of colorectal cancer in patients with inflammatory bowel disease: a systematic review and meta-analysis

Ai-juan Li[1], Hai-yin Jiang[2] and Yong-hui Jia[1]*

[1]Pharmacy Department, The 960th Hospital of PLA, Jinan, China, [2]State Key Laboratory for Diagnosis and Treatment of Infectious Diseases, Collaborative Innovation Center for Diagnosis and Treatment of Infectious Diseases, The First Affiliated Hospital, College of Medicine, Zhejiang University, Hangzhou, China

Background: While epidemiological studies have linked statin use to a reduced risk of advanced colorectal adenomas, its impact on colorectal cancer (CRC) risk in patients with inflammatory bowel disease (IBD) remains unclear. To our knowledge, no meta-analysis to date has specifically examined this association. Therefore, we conducted a systematic review and meta-analysis of the available observational studies to investigate the risk of CRC associated with statin use in IBD patients.

Methods: We searched three databases for articles published in English before September 2024, focusing on the protective effects of statins against CRC in IBD patients. We calculated multivariate odds ratios (ORs) and their 95% confidence intervals (CIs) to assess this association. A random-effects meta-analysis was conducted using the generic inverse variance method.

Results: The meta-analysis included 4 studies encompassing 22,250 IBD patients, 6,712 of whom were statin users. The methodological quality of three of the studies was deemed high. We found a significantly lower risk of CRC in statin users compared to non-users, with a pooled relative risk of 1.88 (95% CI 1.54–2.30). Sensitivity analyses confirmed the consistency of these findings.

Conclusion: Statin use appears to be associated with a reduced risk of CRC in patients with IBD. However, given the limited number of studies available, further prospective research with large sample size is necessary to confirm the potential chemopreventive role of statins in this population.

KEYWORDS

lipid-lowering, colon, rectum, neoplasm, cancer

Introduction

Inflammatory bowel disease (IBD) encompasses a group of immune-mediated disorders that exhibit a relapsing–remitting course, including ulcerative colitis (UC), Crohn's disease (CD), and IBD-unclassified colitis (IBD-U) (1). The global incidence of IBD is on the rise, presenting significant economic and social challenges to healthcare systems due to its high prevalence, early onset, and the requirement for lifelong treatment (2). IBD is associated with various complications such as anemia, stenosis, abscesses, and fistulas (3). Notably, colorectal

cancer (CRC) represents a significant morbidity factor in IBD patients, with studies showing an estimated 2-fold increased risk compared to the general population (4). This risk is further elevated in patients with concomitant primary sclerosing cholangitis (5, 6). Recognizing the risk factors for CRC in IBD could aid in preventing the disease and guiding targeted interventions.

Statins are primarily prescribed to treat hypercholesterolemia and reduce cardiovascular morbidity and mortality (7). Beyond their lipid-lowering effects, statins have demonstrated anti-proliferative, anti-inflammatory, and anti-neoplastic properties in numerous preclinical studies (8–10). As a result, research has suggested a potential benefit of statins in reducing cancer incidence. In terms of CRC risk in the general population (11, 12), meta-analyses of observational studies have indicated a modest reduction in CRC risk, though randomized controlled trials have not shown significant benefits (13). Subsequently, several studies (14–17) have explored the link between statin use and CRC risk in patients with IBD. In the earliest study, Samadder et al. found no protective effect of statins against CRC. Similar results were reported in a U.S.-based hospital analysis. However, two larger population-based studies identified an inverse association between statin use and CRC. These findings raise the question of whether statin use is linked to a reduced risk of CRC in the IBD population.

In light of the growing prevalence of IBD and widespread use of statins, we conducted a systematic review and meta-analysis to evaluate the relationship between statin use and CRC risk among IBD patients. This review aimed to support the development of evidence-based clinical guidelines and inspire further research in this area.

Methods

Search strategy

This systematic review and meta-analysis was conducted in accordance with the PRISMA (Preferred Reporting Items for Systematic Reviews and Meta-Analyses) guidelines. We conducted a comprehensive search in PubMed and Embase databases for studies published up to September 10, 2024. Our search terms included combinations of "inflammatory bowel disease," "IBD," "Crohn's disease," "CD," "ulcerative colitis," "UC," "statin(s)," "HMG-CoA reductase inhibitor(s)," "simvastatin," "atorvastatin," "pravastatin," "fluvastatin," "rosuvastatin," "lovastatin," and terms related to colorectal conditions such as "colon," "rectal," "colorectal," along with "cancer," "tumor," "carcinoma," and "neoplasm." In addition, a manual search of the reference lists of the retrieved articles was conducted.

Inclusion criteria

The inclusion criteria of our study followed the PICO (Population, Intervention, Comparison, Outcome) framework: (1) Population: patients diagnosed with IBD; (2) Intervention: statin use; (3) Comparison: non-use of statins; (4) Outcome: incidence of CRC. Randomized controlled trials (RCTs), cohort studies, and case–control studies were included, while case series, case reports, animal studies, editorials, and reviews were excluded.

Data extraction and quality assessment

Data from the included studies were extracted and summarized in an Excel spreadsheet. Extracted information included the first author, publication year, study design, study location, subject characteristics (age and IBD type), methods for assessing IBD, the number of IBD patients exposed and unexposed to statins, CRC definitions, statistical adjustments for confounders, and study quality assessment.

Each article was independently evaluated using the Newcastle-Ottawa Quality Assessment Scale (NOS) (18), as recommended by the Cochrane Collaboration for assessing the quality of observational studies. A score higher than 7 points indicated a high-quality study.

Statistical analysis

Statistical analyses were conducted using Stata 12.0 software (Stata Corp., College Station, TX, USA). Heterogeneity was assessed using the I^2 statistic, with $I^2 > 50\%$ indicating significant heterogeneity (19). In cases of significant heterogeneity, random-effects models were applied. The risks of CRC were expressed as odds ratios (ORs) with 95% confidence intervals (CI) for case–control studies, and as relative risks (RRs) or hazard ratios (HRs) with 95% CIs for cohort studies (20). ORs were treated as approximations of RRs or HRs due to the rarity of CRC in all populations. Fixed-effect models were used when no significant heterogeneity was found. A funnel plot was not generated because <10 studies were included (21). A 2-sided test was performed, and $p < 0.05$ was considered statistically significant.

Results

Search results

We identified 262 studies from two databases using relevant keywords. After screening titles and abstracts, 32 duplicates and 220 studies were excluded, leaving 10 for full-text review. Six studies were excluded due to multiple reasons. Ultimately, four studies involving patients with IBD were included in our analysis. The selection process was further refined by addressing potential duplicates (due to shared databases and common co-authors) and by excluding case reports. Figure 1 provides a flow diagram outlining the literature search and selection process.

Characteristics of included studies

Table 1 summarizes the characteristics of the included studies: two were conducted in North America, one in Europe, and one in Asia. These studies were published between 2011 and 2023, with sample sizes ranging from 60 to 11,001 participants. Of the four studies, three were cohort studies and one was a case–control study. Based on methodological quality assessments, three studies were deemed high quality, while one was categorized as low quality. Supplementary Tables S1, S2 provide detailed score breakdowns.

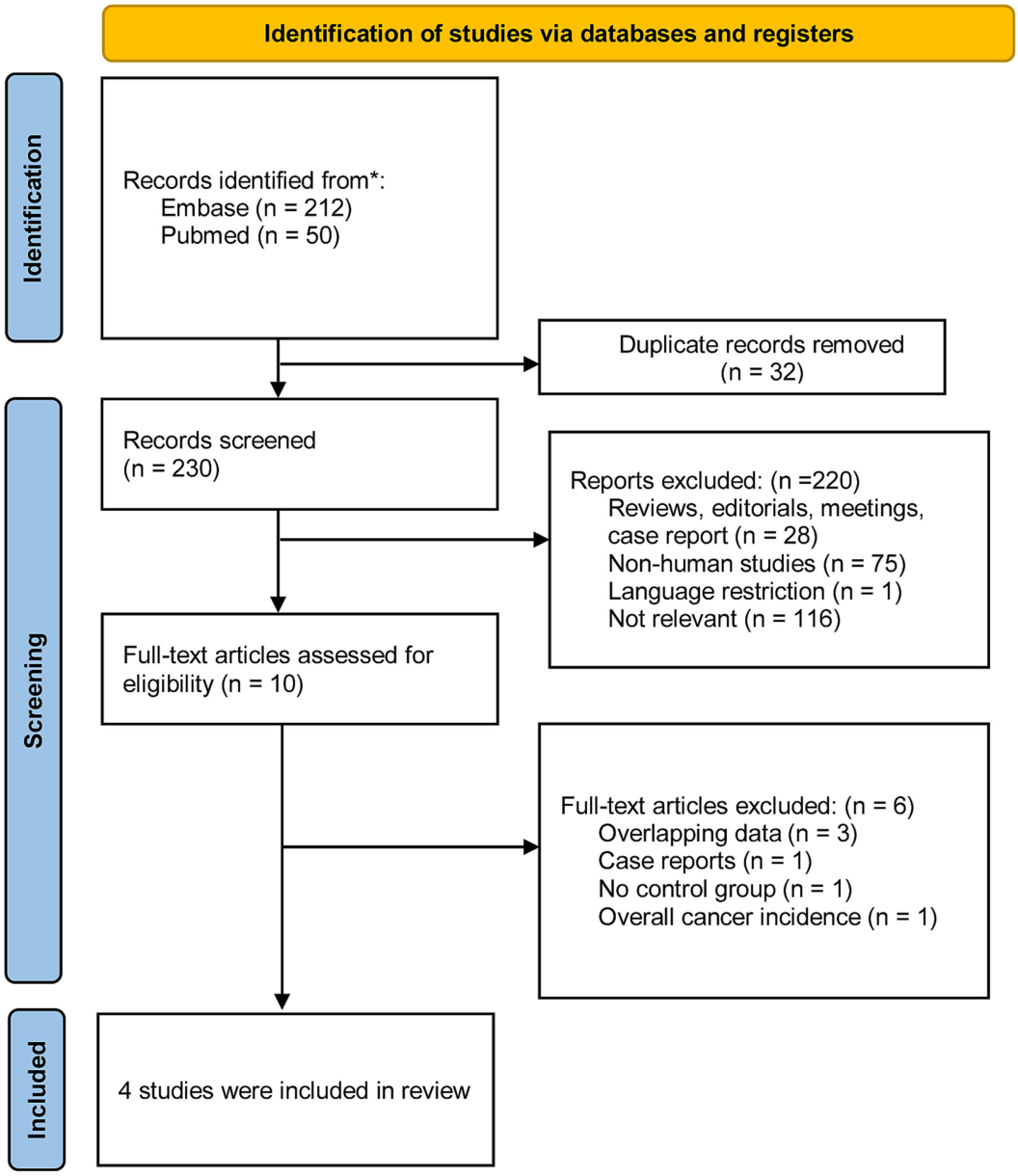

FIGURE 1
Flow chart of the search process and study selection.

Meta-analysis

We analyzed 4 studies, comprising 6,712 statin-exposed and 15,537 unexposed patients with IBD, to assess the risk of CRC associated with statin use. The combined OR for CRC was 0.53 (95% CI 0.31–0.92; $p = 0.024$), indicating a protective effect, although there was significant heterogeneity ($I^2 = 65.7\%$) (Figure 2). When the analysis was limited to three high-quality cohort studies, the protective effect of statins on CRC risk remained consistent (OR = 0.58, 95% CI 0.35–0.97, $p = 0.037$; $I^2 = 69.1\%$). Sensitivity analysis showed no substantial change in the pooled risk estimates; the pooled ORs for CRC ranged from 0.41 to 0.58.

Further analysis by type of IBD revealed that statin-exposed UC patients had a lower risk of CRC (OR = 0.58, 95% CI 0.46–0.73, $p < 0.001$; $I^2 = 0\%$) (Figure 3A), whereas no significant protective effect was observed in CD patients (OR = 0.55, 95% CI 0.04–7.02, $p = 0.649$; $I^2 = 94.9\%$) (Figure 3B). In sex-based analyses, a protective effect was seen in male IBD patients exposed to statins (OR = 0.49, 95% CI 0.27–0.88, $p = 0.018$; $I^2 = 74.2\%$) (Figure 3C), but not in female patients (OR = 0.56, 95% CI 0.17–1.17, $p = 0.122$; $I^2 = 70.3\%$) (Figure 3D).

Discussion

This is the first meta-analysis to investigate the association between statin use and the risk of CRC in patients with IBD. Our findings suggest a significantly reduced risk of CRC in statin users

TABLE 1 Characteristics of the included studies.

Author, year	Location, setting	Study design/ Study period	IBD assessment	Statin exposure assessment	No. of IBD	Age (year)	CRC assessment	Adjustment (Yes/no)	NOS
Samadder et al., 2011	Israel, population-based	Case-control, 1998–2004	Self-Reported	Questionnaire	60 (exposure 6) (no-exposure 54)	exposure 70 no-exposure 70	One pathologist confirmed diagnoses	Age, sex, ethnic group, presence or absence of sports participation, level of vegetable consumption, smoking status, and history of colorectal cancer in a first-degree relative	6
Ananthakrishnan et al., 2016	USA, population-based	Cohort, 1998–2010	ICD-9-CM	Electronic medical record system	1,1,001 (exposure 1,376) (no-exposure 9,625)	exposure 67 no-exposure 42	ICD-9	Age, sex, smoking, smoking status, ethnic group, drug use, primary sclerosing cholangitis, duration of inflammatory bowel disease	9
Shah et al., 2019	USA, hospital-based	Cohort, 2005–2016	ICD-9 and/or ICD-10	Medical record review	643 (exposure 57) (no-exposure 585)	exposure 59 no-exposure 39.4	ICD-9 and/or ICD-10	Statin use, age, sex, primary sclerosing cholangitis, duration of inflammatory bowel disease, mean inflammatory score, number of colonoscopies, thiopurine exposure and biologic exposure	6
Sun et al., 2023	Sweden, population-based	Cohort, 2006–2019	ICD-10	Electronic medical record system	10,546 (exposure 5,273) (no-exposure 5,273)	exposure 51 no-exposure 51	ICD-9	Propensity score matching	9

compared to non-users, even after adjusting for potential confounding factors. However, due to the limited number of included studies, caution is warranted when interpreting these results.

The exact pharmacological mechanisms behind the antitumor effects of statins are not yet fully understood, but several explanations have been proposed. One of the primary mechanisms involves the inhibition of HMG-CoA reductase, the enzyme statins target to lower cholesterol. This inhibition reduces mevalonate synthesis, which is essential for cholesterol production (22). Interestingly, disruptions caused by statins in the mevalonate synthesis pathway inhibit cancer growth and lead to apoptotic cell death, and the depletion of cholesterol may inhibit cancer cell growth (23). Additionally, statins may inhibit the synthesis of isoprenoids, which are essential lipid attachments for intracellular signaling molecules, such as Rho, Rac, and Cdc42 (24). These related-proteins are overpresented in CRC and are associated with tumor invasion. Furthermore, statins may reduce the formation of aberrant crypt foci and polyps, and reduce tumor metastasis (25). Non-HMG-CoA-related effects of statins include anti-proliferative actions, regulation of cell adhesion, antioxidant properties, and anti-inflammatory effects (26). Finally, several reports have demonstrated that the use of statins may reshape the balance of gut microbiota in patients with hyperlipidemia and favors the growth of species whose metabolites may exert anti-inflammatory effects as *Bifidobacterium* (27). The anti-tumor effect of *Bifidobacterium* has been proved in *in vitro* and *in vivo* (28, 29).

Chronic intestinal inflammation is thought to play a critical role in the development of CRC (30). Persistent inflammation in IBD patients increases the risk of colorectal neoplasia and its long-term consequences, including CRC. A meta-analysis by Lutgens et al. (4) reported that IBD patients have a 70% higher risk of CRC compared to the general population. Since 2010, several meta-analyses (11, 12) based on observational studies have shown a lower CRC risk in the general population. Given the high incidence of CRC in IBD and the potential antitumor effects of statins, it is important to explore further the association between statin use and CRC risk in IBD patients.

Although the potential protective effects of statins on CRC in IBD are biologically plausible, the studies included in our meta-analysis reported inconsistent results, which is reflected in the significant clinical heterogeneity observed. A key source of this heterogeneity is the variation in sample sizes. Two studies reporting no protective effect of statins enrolled only 703 IBD patients and identified 44 CRC cases, making it reasonable to speculate that their findings may be influenced by small sample sizes. In contrast, the other 2 studies, with a combined total of 21,545 IBD patients, observed a protective role for statins in CRC prevention.

Previous meta-analysis (31) have demonstrated that colonoscopy can effectively reduce the incidence of CRC. In one of the included studies, Shah et al. explored the relationship between statin use and CRC in a cohort of IBD patients undergoing regular colorectal surveillance, which may have minimized the observed protective effect of statins. Additionally, the statin-exposed group in this study were older than the unexposed group, which is notable since CRC incidence increases with age. This uneven age distribution may have masked the effect of statins.

Other factors, such as exposure to chemopreventive agents, IBD medications, IBD severity, and the presence of primary sclerosing

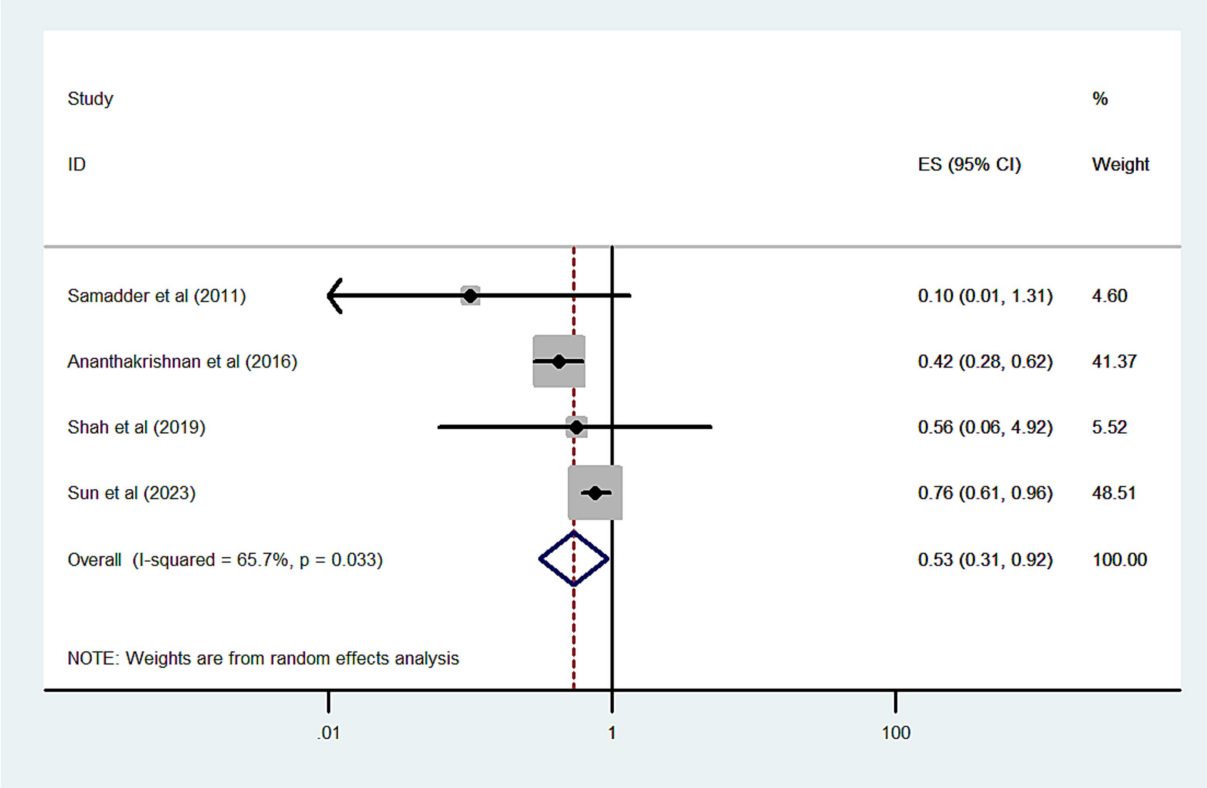

FIGURE 2
Forest plot of the overall risk of CRC in relation to exposure to statin among patients with IBD.

cholangitis, have also been associated with CRC development in IBD patients (32–34). However, the studies included in our meta-analysis adjusted for these confounding variables to varying degrees. The failure to account for these important factors in some studies may have influenced the strength and reliability of their conclusions.

This is the first and most comprehensive systematic review and meta-analysis to investigate the risk of CRC in statin users with IBD. However, our study has some limitations, particularly regarding unknown confounders. Given ethical and practical constraints, conducting RCTs to evaluate the chemopreventive effects of statins on CRC risk is not feasible. Future well-designed studies that account for additional variables, such as smoking status, chronic comorbidities, and other medication use, are needed to examine further this association. Second, another limitation is the high heterogeneity with respect to the characteristics of the included studies, and finding sources of heterogeneity is one of the most important goals of meta-analysis. In the present meta-analysis, this heterogeneity could not be explained by the sensitivity, or subgroup analyses based on type of IBD or gender. The existence of clinical heterogeneity would be the source of statistical heterogeneity in the results. One included study (14) observed a significant duration-dependent benefit. With respect to statin type, previous meta-analysis (35) showed a significant association between lipophilic statin use and CRC risk and a null association between hydrophilic statin use and CRC risk among the general population. However, the included studies provided limited data on the dose, duration, and type of statins used, preventing us from conducting further analyses about how these factors might influence CRC risk. Third, the number of eligible studies and the sample size of IBD patients and CRC cases were relatively small, which may have affected the accuracy of our findings. These results should be interpreted with caution, and more clinical and basic research is needed to confirm the potential protective effects of statins in IBD patients. Fourth, we were unable to assess the causal relationship between statin use and CRC risk, which would provide a deeper understanding of the association. Finally, most of the included studies were conducted in Western countries, limiting the generalizability of our findings to other populations.

In conclusion, our results suggest that statin use is associated with a reduced risk of CRC in patients with IBD, indicating potential for statins as a chemopreventive agent in this population. However, these findings need to be confirmed through larger, well-designed prospective studies.

Data availability statement

The original contributions presented in the study are included in the article/Supplementary material, further inquiries can be directed to the corresponding author.

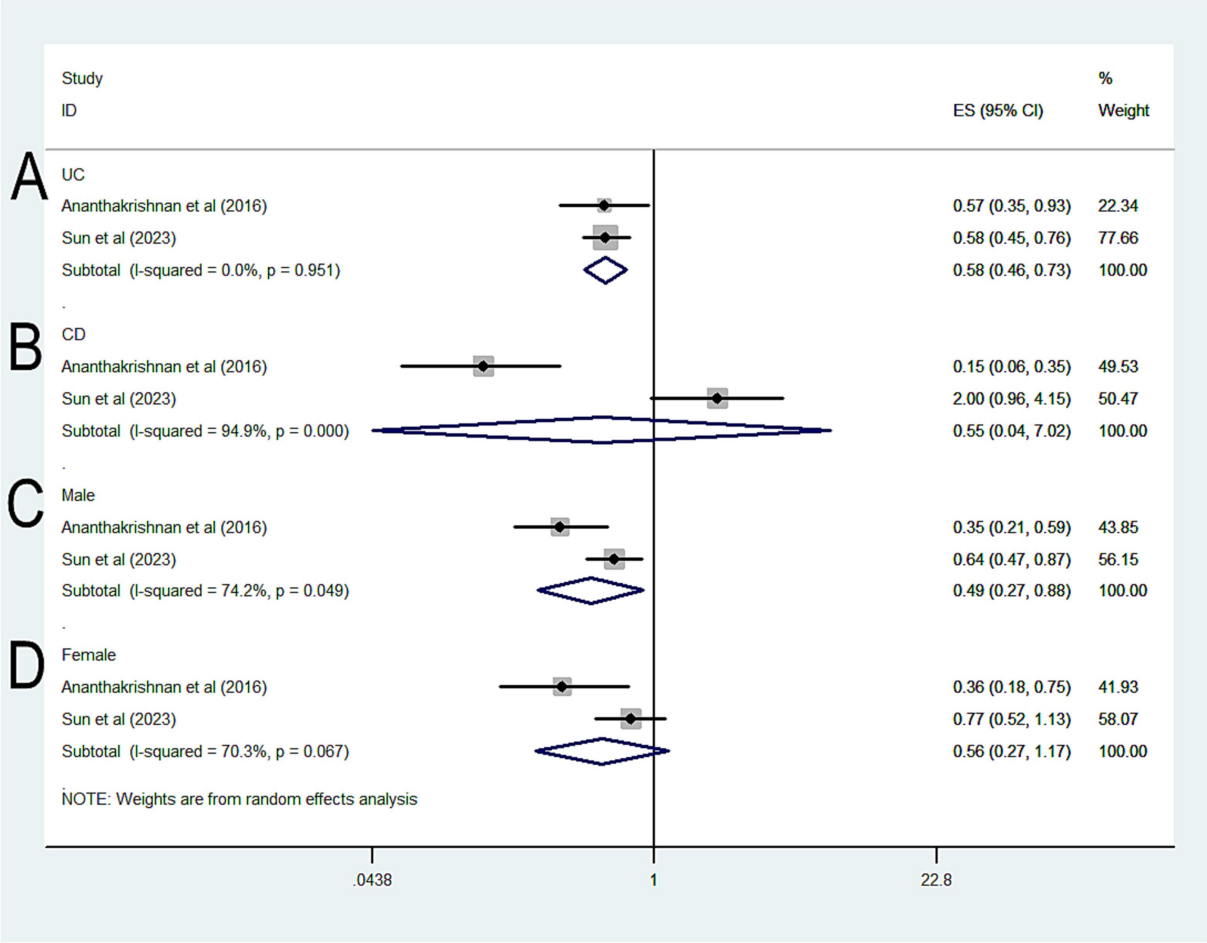

FIGURE 3
Forest plot of the overall risk of CRC in relation to exposure to statin among patients with IBD **(A)** UC; **(B)** CD; **(C)** Male; **(D)** Female.

Author contributions

A-jL: Conceptualization, Data curation, Investigation, Software, Writing – original draft. H-yJ: Methodology, Project administration, Resources, Supervision, Writing – review & editing. Y-hJ: Formal analysis, Project administration, Validation, Visualization, Writing – original draft, Writing – review & editing.

Funding

The author(s) declare that no financial support was received for the research, authorship, and/or publication of this article.

Conflict of interest

The authors declare that the research was conducted in the absence of any commercial or financial relationships that could be construed as a potential conflict of interest.

Generative AI statement

The author(s) declare that no Gen AI was used in the creation of this manuscript.

Publisher's note

Supplementary material

The Supplementary material for this article can be found online at: https://www.frontiersin.org/articles/10.3389/fmed.2024.1507739/full#supplementary-material

References

1. Baumgart DC, Sandborn WJ. Inflammatory bowel disease: clinical aspects and established and evolving therapies. *Lancet*. (2007) 369:1641–57. doi: 10.1016/S0140-6736(07)60751-X

2. Ng SC, Shi HY, Hamidi N, Underwood FE, Tang W, Benchimol EI, et al. Worldwide incidence and prevalence of inflammatory bowel disease in the 21st century: a systematic review of population-based studies. *Lancet*. (2017) 390:2769–78. doi: 10.1016/S0140-6736(17)32448-0

3. Argollo M, Gilardi D, Peyrin-Biroulet C, Chabot JF, Peyrin-Biroulet L, Danese S. Comorbidities in inflammatory bowel disease: a call for action. *Lancet Gastroenterol Hepatol*. (2019) 4:643–54. doi: 10.1016/S2468-1253(19)30173-6

4. Lutgens MW, van Oijen MG, van der Heijden GJ, Vleggaar FP, Siersema PD, Oldenburg B. Declining risk of colorectal cancer in inflammatory bowel disease: an updated meta-analysis of population-based cohort studies. *Inflamm Bowel Dis*. (2013) 19:789–99. doi: 10.1097/MIB.0b013e31828029c0

5. Brentnall TA, Haggitt RC, Rabinovitch PS, Kimmey MB, Bronner MP, Levine DS, et al. Risk and natural history of colonic neoplasia in patients with primary sclerosing cholangitis and ulcerative colitis. *Gastroenterology*. (1996) 110:331–8. doi: 10.1053/gast.1996.v110.pm8566577

6. Soetikno RM, Lin OS, Heidenreich PA, Young HS, Blackstone MO. Increased risk of colorectal neoplasia in patients with primary sclerosing cholangitis and ulcerative colitis: a meta-analysis. *Gastrointest Endosc*. (2002) 56:48–54. doi: 10.1067/mge.2002.125367

7. Chou R, Cantor A, Dana T, Wagner J, Ahmed AY, Fu R, et al. Statin use for the primary prevention of cardiovascular disease in adults: updated evidence report and systematic review for the US preventive services task force. *JAMA*. (2022) 328:754–71. doi: 10.1001/jama.2022.12138

8. Bedi O, Dhawan V, Sharma PL, Kumar P. Pleiotropic effects of statins: new therapeutic targets in drug design. *Naunyn Schmiedeberg's Arch Pharmacol*. (2016) 389:695–712. doi: 10.1007/s00210-016-1252-4

9. Bryniarski KL, den Dekker W, Legutko J, Gasior P, Tahon J, Diletti R, et al. Role of lipid-lowering and anti-inflammatory therapies on plaque stabilization. *J Clin Med*. (2024) 13:3096. doi: 10.3390/jcm13113096

10. Ji L, Liu C, Yuan Y, Gao H, Tang ZX, Yang Z, et al. Key roles of rho GTPases, YAP, and mutant P53 in anti-neoplastic effects of statins. *Fundam Clin Pharmacol*. (2020) 34:4–10. doi: 10.1111/fcp.12495

11. Jeong GH, Lee KH, Kim JY, Eisenhut M, Kronbichler A, van der Vliet HJ, et al. Effect of statin on Cancer incidence: an umbrella systematic review and Meta-analysis. *J Clin Med*. (2019) 8:819. doi: 10.3390/jcm8060819

12. Lytras T, Nikolopoulos G, Bonovas S. Statins and the risk of colorectal cancer: an updated systematic review and meta-analysis of 40 studies. *World J Gastroenterol*. (2014) 20:1858–70. doi: 10.3748/wjg.v20.i7.1858

13. Chen Z, Wu P, Wang J, Chen P, Fang Z, Luo F. The association of statin therapy and cancer: a meta-analysis. *Lipids Health Dis*. (2023) 22:192. doi: 10.1186/s12944-023-01955-4

14. Sun J, Halfvarson J, Bergman D, Ebrahimi F, Roelstraete B, Lochhead P, et al. Statin use and risk of colorectal cancer in patients with inflammatory bowel disease. *EClinicalMedicine*. (2023) 63:102182. doi: 10.1016/j.eclinm.2023.102182

15. Samadder NJ, Mukherjee B, Huang SC, Ahn J, Rennert HS, Greenson JK, et al. Risk of colorectal cancer in self-reported inflammatory bowel disease and modification of risk by statin and NSAID use. *Cancer*. (2011) 117:1640–8. doi: 10.1002/cncr.25731

16. Shah SC, Glass J, Giustino G, Hove JRT, Castaneda D, Torres J, et al. Statin exposure is not associated with reduced prevalence of colorectal neoplasia in patients with inflammatory bowel disease. *Gut Liver*. (2019) 13:54–61. doi: 10.5009/gnl18178

17. Ananthakrishnan AN, Cagan A, Cai T, Gainer VS, Shaw SY, Churchill S, et al. Statin use is associated with reduced risk of colorectal Cancer in patients with inflammatory bowel diseases. *Clin Gastroenterol Hepatol*. (2016) 14:973–9. doi: 10.1016/j.cgh.2016.02.017

18. Higgins J.P., Cochrane handbook for systematic reviews of interventions version 5.1.0. The Cochrane collaboration. Available at: https://cochrane-handbook.org/. (2014)

19. Higgins JP, Thompson SG, Deeks JJ, Altman DG. Measuring inconsistency in meta-analyses. *BMJ*. (2003) 327:557–60. doi: 10.1136/bmj.327.7414.557

20. Egger M, Davey Smith G, Schneider M, Minder C. Bias in meta-analysis detected by a simple, graphical test. *BMJ*. (1997) 315:629–34. doi: 10.1136/bmj.315.7109.629

21. Lau J, Ioannidis JP, Terrin N, Schmid CH, Olkin I. The case of the misleading funnel plot. *BMJ*. (2006) 333:597–600. doi: 10.1136/bmj.333.7568.597

22. Pikoulis E, Margonis GA, Angelou A, Zografos GC, Antoniou E. Statins in the chemoprevention of colorectal cancer in established animal models of sporadic and colitis-associated cancer. *Eur J Cancer Prev*. (2016) 25:102–8. doi: 10.1097/CEJ.0000000000000152

23. Wong WW, Dimitroulakos J, Minden MD, Penn LZ. HMG-CoA reductase inhibitors and the malignant cell: the statin family of drugs as triggers of tumor-specific apoptosis. *Leukemia*. (2002) 16:508–19. doi: 10.1038/sj.leu.2402476

24. Lochhead P, Chan AT. Statins and colorectal cancer. Clinical gastroenterology and hepatology. *J Am Gastroenterol Ass*. (2013) 11:109–18. doi: 10.1016/j.cgh.2012.08.037

25. Terdiman JP, Steinbuch M, Blumentals WA, Ullman TA, Rubin DT. 5-Aminosalicylic acid therapy and the risk of colorectal cancer among patients with inflammatory bowel disease. *Inflamm Bowel Dis*. (2007) 13:367–71. doi: 10.1002/ibd.20074

26. Demierre MF, Higgins PD, Gruber SB, Hawk E, Lippman SM. Statins and cancer prevention. *Nat Rev Cancer*. (2005) 5:930–42. doi: 10.1038/nrc1751

27. She J, Sun L, Yu Y, Fan H, Li X, Zhang X, et al. A gut feeling of statin. *Gut Microbes*. (2024) 16:2415487. doi: 10.1080/19490976.2024.2415487

28. Kosumi K, Hamada T, Koh H, Borowsky J, Bullman S, Twombly TS, et al. The amount of Bifidobacterium genus in colorectal carcinoma tissue in relation to tumor characteristics and clinical outcome. *Am J Pathol*. (2018) 188:2839–52. doi: 10.1016/j.ajpath.2018.08.015

29. Lee DK, Jang S, Kim MJ, Kim JH, Chung MJ, Kim KJ, et al. Anti-proliferative effects of *Bifidobacterium adolescentis* SPM0212 extract on human colon cancer cell lines. *BMC Cancer*. (2008) 8:310. doi: 10.1186/1471-2407-8-310

30. Laine L, Kaltenbach T, Barkun A, McQuaid KR, Subramanian V, Soetikno R. SCENIC international consensus statement on surveillance and management of dysplasia in inflammatory bowel disease. *Gastrointest Endosc*. (2015) 81:489–501.e26. doi: 10.1016/j.gie.2014.12.009

31. Wang D, Xu Q, Dai S, Zhang Y, Ding F, Ji L. Effects of sigmoidoscopy screening (including colonoscopy) on colorectal cancer: a meta-analysis based on randomized controlled trials. *Prev Med Rep*. (2024) 39:102636. doi: 10.1016/j.pmedr.2024.102636

32. Brandaleone L, Dal Buono A, Gabbiadini R, Marcozzi G, Polverini D, Carvello M, et al. Hereditary colorectal Cancer syndromes and inflammatory bowel diseases: risk management and surveillance strategies. *Cancers*. (2024) 16:2967. doi: 10.3390/cancers16172967

33. Axelrad JE, Rubin DT. The Management of Colorectal Neoplasia in patients with inflammatory bowel disease. *Clin Gastroenterol Hepatol*. (2024) 22:1181–5. doi: 10.1016/j.cgh.2024.01.030

34. Fatakhova K, Rajapakse R. From random to precise: updated colon cancer screening and surveillance for inflammatory bowel disease. *Transl Gastroenterol Hepatol*. (2024) 9:27. doi: 10.21037/tgh-23-36

35. Liu Y, Tang W, Wang J, Xie L, Li T, He Y, et al. Association between statin use and colorectal cancer risk: a meta-analysis of 42 studies. *Cancer Causes Control*. (2014) 25:237–49. doi: 10.1007/s10552-013-0326-6

frontiers | Frontiers in Medicine

TYPE Original Research
PUBLISHED 06 December 2024
DOI 10.3389/fmed.2024.1486750

OPEN ACCESS

EDITED BY
Hua Zhong,
University of Hawaii at Manoa, United States

REVIEWED BY
Peng Wang,
Coriell Institute for Medical Research, United States
Shunian Xiang,
Admera Health, United States
Ling Xiao,
Harvard Medical School, United States

*CORRESPONDENCE
Ran Wei
✉ weiran@sysucc.org.cn
Shengping Li
✉ lishengp@mail.sysu.edu.cn

†These authors have contributed equally to this work

RECEIVED 26 August 2024
ACCEPTED 20 November 2024
PUBLISHED 06 December 2024

CITATION
Qin D, Xi P, Huang K, Jiang L, Yao Z, Wei R and Li S (2024) Nomogram for predicting post-progression-free survival in patients with recurrent pancreatic ductal adenocarcinoma after radical surgery: a retrospective analysis.
Front. Med. 11:1486750.
doi: 10.3389/fmed.2024.1486750

Nomogram for predicting post-progression-free survival in patients with recurrent pancreatic ductal adenocarcinoma after radical surgery: a retrospective analysis

Dailei Qin†, Pu Xi†, Kewei Huang†, Lingmin Jiang, Zehui Yao, Ran Wei* and Shengping Li*

State Key Laboratory of Oncology in South China, Guangdong Provincial Clinical Research Center for Cancer, Sun Yat-sen University Cancer Center, Guangzhou, China

Background: Radical resection is the only curative method for patients with pancreatic adenocarcinoma (PDAC). However, nearly 85% of PDAC patients suffer from local or distant recurrence within 5 years after curative resection. The progression of recurrent lesions accelerates the mortality rate in PDAC patients. However, the influence of clinicopathological factors on post-progression-free survival (PPFS), defined as the period from tumor recurrence to the timing of the progression of recurrent lesions, has rarely been discussed. The present study aimed to explore the independent prognostic factors for PPFS and construct a nomogram for PPFS prediction.

Materials and methods: The 200 recurrent PDAC patients were divided into training and validation groups by leave-one-out cross-validation. The patients' clinicopathological characteristics were compared through a chi-square test. Meanwhile, these factors were enrolled in the univariate and multivariate COX regression to find the independent prognostic factors of PPFS. Moreover, the Kaplan–Meier survival analysis based on the independent prognostic factors was performed. Finally, we constructed a nomogram model for PPFS prediction, followed by an effectiveness examination.

Results: PDAC patients who received multi-agent chemotherapy after surgery showed a longer PPFS than the single-agent chemotherapy group. PDAC patients who received multi-agent chemotherapy after recurrence showed a similar PPFS compared to the single-agent chemotherapy group. Local recurrence with distant metastases, early recurrence, lympho-vascular invasion, higher T stage, and higher N stage predicted shorter PPFS in recurrent PDAC patients. Finally, a nomogram to indicate the progression of recurrent lesions was constructed.

Conclusion: Multi-agent chemotherapy is recommended for PDAC patients after surgery. Meanwhile, single-agent chemotherapy also deserves consideration after tumor recurrence. Moreover, the nomogram could be used in PPFS prediction.

KEYWORDS

nomogram, recurrence, chemotherapy, pancreatic adenocarcinoma, post-progression-free survival

Introduction

PDAC is the major component of pancreatic cancer (1, 2). As reported in previous research, the 5-year overall survival rate of PDAC is less than 10% (3). Moreover, PDAC was expected to become the second leading cause of cancer-related death by 2030 (4). So far, radical resection has been the only curative method for PDAC (5). Unfortunately, even though the adjuvant chemotherapy has been performed, nearly 85% of resected cases eventually experience tumor recurrence (6, 7). The relationship between the clinicopathological factors and tumor recurrence in PDAC has been explored previously. In detail, PDAC patients who received adjuvant chemotherapy achieved longer progression-free survival and overall survival compared to untreated patients (8, 9). However, the restriction effect of chemotherapy on recurrent PDAC has been rarely discussed.

The advancement of recurrent lesions was defined as follows: at least 20% increase in maximum diameter of the primary recurrent lesions, or detection of any new recurrent lesions in the distant tissue. Meanwhile, the period from tumor recurrence to the timing of the progression of recurrent lesions was defined as PPFS. The progression of relapse lesions reflects the weakness of the anti-tumor immune system and the production of circulating tumor cells, predicting poor prognosis (10–12). According to the NCCN guidelines, a change to an alternate chemotherapy regimen is usually recommended for recurrent PDAC patients. However, there lacked of a definite chemotherapeutic regimens for recurrent PDAC patients in the NCCN guidelines (13). Therefore, exploring independent prognostic factors of PPFS and further creating an analysis tool to predict the risk of PPFS is crucial for developing suitable adjuvant chemotherapy regimens for recurrent PDAC patients.

Several prediction models have been used to estimate the overall survival or progression-free survival of PDAC patients (14–16). Some independent factors in these models such as tumor markers or chemotherapy regimens were only collected before or soon after surgeries. The updated data after tumor recurrence were scarcely mentioned. Moreover, previous partial research only recorded whether PDAC patients received chemotherapy or not, the detailed classification of chemotherapy regimens has rarely been established. However, the PPFS of recurrent PDAC patients is greatly impacted by characteristics of relapse lesions rather than primary tumor features. Therefore, prior nomogram models may be less effective for PPFS prediction. Considering the lack of a specific predictive model for PPFS estimation, it was necessary to build a novel nomogram model for recurrent PDAC patients.

In order to ensure the quality and reliability of data analysis, all participants were screened by their clinical and pathologic features. The flow chart has been established in Figure 1. Finally, a total of 200 recurrent PDAC patients were collected from 394 surgically resected cases with pancreatic cancer.

Materials and methods

Patient's enrollment and grouping

A total of 394 patients who underwent radical resection for PDAC from January 2008 to December 2019 were collected from medical records (Figure 1). Pancreaticoduodenectomy and distal pancreatectomy are the main type of radical resection (17, 18). Tumoral resectability was investigated by a professional multidisciplinary team for PDAC based on imaging findings from computed tomography (CT), magnetic resonance imaging (MRI), and positron emission tomography-CT (PET-CT). Three chief physicians skilled in pancreaticoduodenectomy and distal pancreatectomy performed all of the surgeries included in this study. The attending clinician and resident physician were also required to participate in the surgical procedure. Furthermore, open, laparoscopic, and robotic surgery was chosen according to the clinical tumor state with consent obtained from patients.

The inclusion criteria concluded as follows: (1) histopathological examination reveals a definite diagnosis of PDAC, (2) diagnosed with tumor recurrence postoperatively according to the results of CT, tumor markers, and biopsy pathology, (3) the medical records were available, (4) Patients received multiagent chemotherapy: modified-FOLFIRINOX, FOLFIRINOX (oxaliplatin, Irinotecan, calcium folinate, fluorouracil), AG (nab-paclitaxel, gemcitabine), GS (gemcitabine, tegafur), (5) Patients received single-agent chemotherapy: Gemcitabine or tegafur, (6) Patients never received chemotherapy. On the contrary, the exclusion criteria were represented as follows: (1) patients with a second tumor before surgery, (2) patients who received neoadjuvant chemotherapy, (3) patients without R0 resection (the margin for R0 resection was described as 1.5–2 mm in the previous study) (19), (4) lost follow-up, (5) the number of dissected lymph nodes was no more than 15.

The patients enrolled in the present study were subsequently divided into training and validation group by leave-one-out cross-validation (LOOCV) method. In detail, one patient was enrolled into validation group each time, while the rest of patients served as a training group. Then, the accuracy of this model was recorded from analysis tool. The above procedure was repeated until all of the patients were tested as a validation sample. The final grouping schemes was determined by the average accuracy.

The consent to use the medical records has been obtained from all of patients enrolled in the present study. The Ethics Committee approved the retrospective study. This study was registered with www.researchregistry.com. This work has been reported according to the STROCSS (Strengthening the Reporting of Cohort Studies in Surgery) criteria (20).

Collection of clinicopathological characteristics

The clinicopathological factors included in this research were chosen based on the results of previous prognostic analyses (9, 14). It is worth mentioning that some of the factors were acquired at the time points after tumor recurrence because the present study focused on the progression of relapse lesion in PDAC patients. In detail, the pathological diagnosis was acquired from experienced pathologists, including the tumor size, tumor differentiation, lymph node metastasis, microvascular invasion, lymph vascular invasion, and adjacent organ invasion. Moreover, several inflammation indices, such as the neutrophil-to-lymphocyte ratio (NLR) and platelet-to-lymphocyte ratio (PLR), were involved in this study. Besides, this study also registered clinical factors such as age, gender, serum levels of carbohydrate antigen 19-9 (CA19-9), and carcinoembryonic antigen (CEA) after confirmation of tumor recurrence. Moreover, the key features of tumor

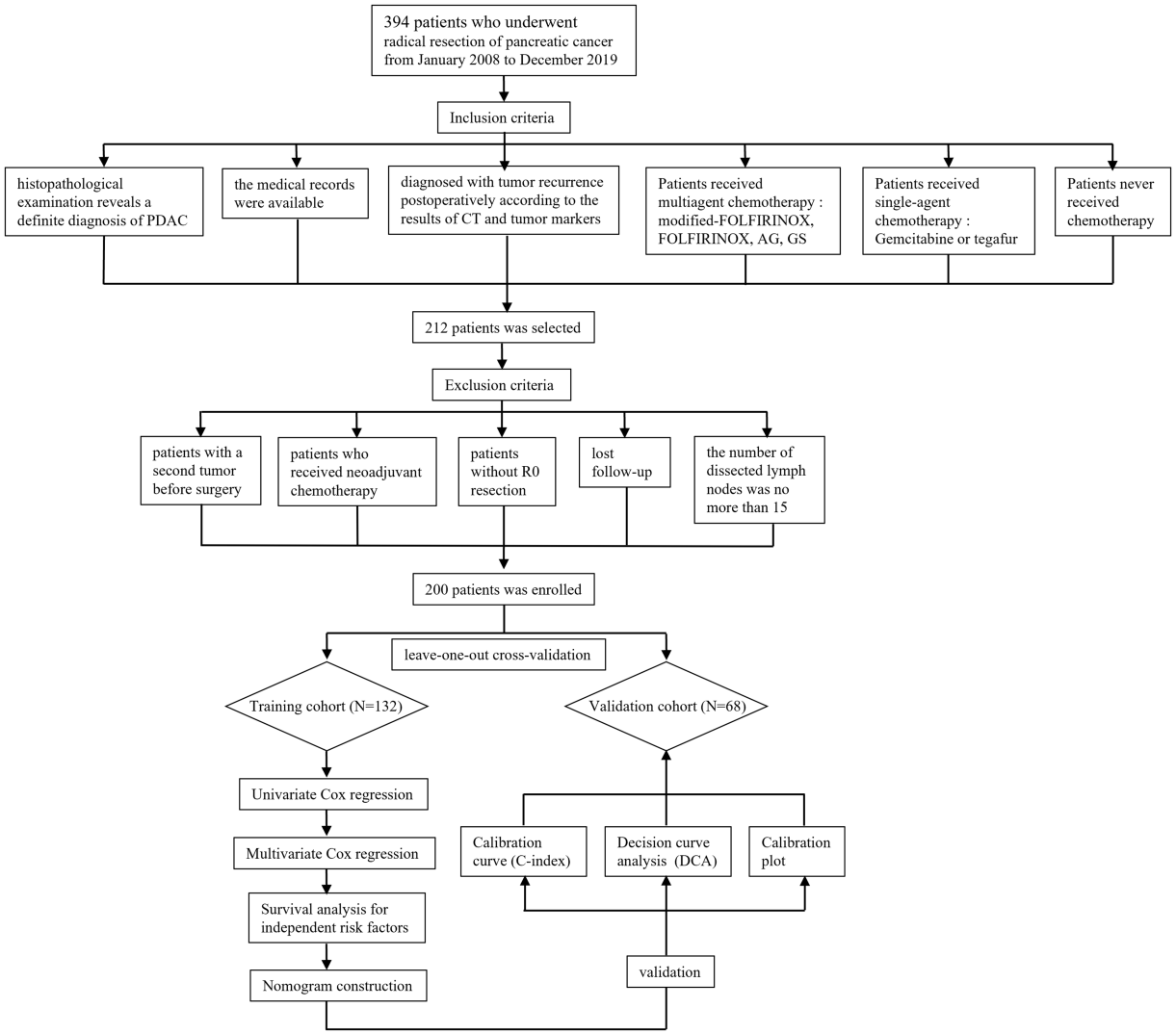

FIGURE 1
Flow chat of patients' enrollment and study design.

recurrence were also registered in this research, including time to recurrence (the cut-off value to define early and late recurrence was one year after surgery) and recurrence patterns (the definition of different relapse patterns referred from the research by Groot) (7, 21).

Development and classification criteria of chemotherapy regimens

The chemotherapy regimens mentioned in the present study were applied after radical surgery or tumor recurrence according to the recommendation from NCCN (2021 Ver2.0) guidelines for PDAC respectively (13). Meanwhile, the patients' will and Eastern Cooperative Oncology Group Performance Status (ECGO PS) were considered before developing the chemotherapy schema. The modified-FOLFIRINOX or FOLFIRINOX were the preferred option for PDAC patients in better physical condition or ECGO PS range from 0 to 1 point. If patients had a poor overall physical condition (ECGO PS range from 2 to 5 point), gemcitabine or tegafur will be recommended. AG or GS chemotherapy schema were usually applied in recurrent PDAC patients who were not sensitive to FOLFIRINOX chemotherapy schema. Furthermore, the chemotherapy regimens were divided into three levels through the variety of drug utilization. Firstly, the patients who never received chemotherapy after surgery or tumor recurrence were classified as "untreated." Then, the patients who got only gemcitabine or tegafur therapies were defined as "single-agent chemotherapy." Finally, the patients who underwent modified-FOLFIRINOX or FOLFIRINOX, AG, GS chemotherapy schema were categorized as "multi-agent chemotherapy."

Follow-up and outcome adjudication

The follow-up began at the time of tumor recurrence after radical surgery. The patients were recommended to undergo outpatient review every 3 months. Meanwhile, abdominal and chest CT, CA19-9, and CEA were performed regularly after surgery. If the outpatient review were unavailable for some patients, telephone contact would

be the alternative method. The endpoint of the present study was progression in recurrent lesions, which is defined as follows: (A) ≥20% increase in maximum diameter of the primary recurrent lesions, (B) or detection of any new recurrent lesions in the distant tissue. The outcome adjudication was made after the imaging examination or pathology diagnosis during follow-up.

Statistical analysis

The comparison of clinicopathological characteristics between the early and late recurrent groups was conducted using the chi-square test. The relationship between clinicopathological factors and PPFS was investigated using Kaplan–Meier methods. In detail, the log-rank test was utilized when the survival curve was not crossed, while the landmark analysis was applied when the survival curve was crossed. Multivariate Cox regression analysis was used to detect the independent prognostic factors for PPFS after completing the study of univariate Cox regression. The concordance indexes (C-indexes), calibration plots, and decision curve analyses (DCA) were utilized to compare the predictive ability between the nomogram and TNM-stage prediction models. A two-tailed $p < 0.05$ was considered statistically significant in the present study. All statistical analyses were conducted using SPSS software version 22 and R software version 4.2.2 (R Development Core Team; http://www.r-project.org). Moreover, the R packages "getsummary, tidyverse, survival, plyr, broom, forestmodel, ggplot2, rms, survminer, and ggDCA" were used in this research.

Results

Patient's clinicopathological characteristics

A total of 394 PDAC patients received radical surgery between January 2008 and December 2019, while 212 cases of them were eventually diagnosed with tumor recurrence. Meanwhile, 12 recurrent PDAC patients were eliminated from the research according to the exclusion criteria as follows: patients with a second tumor before surgery (2 cases), patients who received neo-adjuvant chemotherapy (1 case), patients without R0 resection (1 case), lost follow-up (6 cases), the number of dissected lymph nodes was less than 15 (2 cases). At last, 200 recurrent PDAC patients were enrolled in the present study. Subsequently, the 200 patients were divided into a training cohort (132 cases) and a validation cohort (68 cases) by the 200 recurrent PDAC patients were divided into training and validation groups by LOOCV. For the training cohort, the median PPFS was 5.25 months. For the validation cohort, the median PPFS was 5.25 months. The clinicopathological characteristics of the two groups were established in Table 1. Based on the results of the chi-square test, T stage, TNM stage, tumor differentiation, chemotherapy after recurrence, and recurrence patterns showed a significant difference between the training and validation cohorts.

Prognostic factors for PPFS

As shown in Table 2, 18 factors were enrolled into univariate Cox regression in the training cohort. As the results showed, 11 factors were described to be correlated with PPFS: tumor differentiation, T stage, N stage, time to recurrence, CA19-9, NLR, adjacent organ invasion, lymph vascular invasion, recurrence pattern, chemotherapy after surgery, chemotherapy after recurrence. Consequently, these factors were enrolled into the multivariate Cox regression, and the results were established in Table 3. The T stage, N stage, time to recurrence, Lymph vascular invasion, recurrence pattern, chemotherapy after surgery, chemotherapy after recurrence were considered as independent prognostic factors for PPFS in recurrent PDAC patients.

Survival analysis for independent prognostic factors

The patients who received multi-agent therapy showed better PPFS than patients treated with single-agent therapy ($p = 0.009$) (Figure 2A). Meanwhile, the patients treated with multi-agent or single-agent chemotherapy regiments after tumor relapse were estimated to have a similar prognosis ($p = 0.011$) (Figure 2B). The PDAC patients in the T1 stage had a finer prognosis than patients in the T2 or T3 stage ($p = 0.011$) (Figure 2C). Worse outcomes are observed in patients with higher N stages ($p = 0.005$) (Figure 2D). The patients with local recurrence had the best prognosis among the four relapse patterns mentioned in this study ($p = 0.038$) (Figure 2E). PDAC patients with late recurrence had a relatively better prognosis than early recurrent patients ($p = 0.019$) (Figure 2F). Finally, positive lymph vascular invasion in PDAC patients predicted worse outcomes when compared with negative lymph vascular invasion ($p = 0.026$) (Figure 2G).

Construction and validation of a nomogram for PPFS prediction

As shown in Figure 3, a specific nomogram for PPFS prediction in patients with PDAC was built on independent prognostic factors. The recurrence patterns are the factor that displayed the most prominent effect in this model, followed by the lymph vascular invasion, T-stage, N-stage, chemotherapy after recurrence, chemotherapy after surgery, and time to recurrence. Furthermore, to detect the accuracy of the nomogram model, the calibration plots were produced, demonstrating a high conformity between the actual and predictive PPFS in both training and validation groups (Figure 4). Meanwhile, to assess the discriminatory ability between the nomogram and TNM stage system, the C-index was calculated based on the training cohort and validation cohort; as shown in Table 4, the C-index of the nomogram model was significantly higher than that in the TNM stage in both training and validation cohort. Finally, the decision curve analysis was fabricated to compare the clinical benefits of the nomogram and the TNM stage system (Figure 5). It means that the nomogram built in the present study could be more beneficial for clinical prediction than the TNM stage system.

Discussion

PDAC was a lethal disease in which micro-metastatic lesions occurred in the early stage of carcinogenesis (22). Therefore, nearly 85% of the PDAC patients who received radical surgery would suffer from tumor relapse in the early postoperative period (6, 7). Tumor

10.3389/fmed.2024.1486750

TABLE 1 Clinicopathological characteristics of PDAC patients in the training and validation cohort.

Characteristic	Training, *N* = 132	Validation, *N* = 68	*p*-value
Gender			0.7
Female	80 (61%)	43 (63%)	
Male	52 (39%)	25 (37%)	
Age			0.3
<60	42 (32%)	27 (40%)	
≥60	90 (68%)	41 (60%)	
Tumor site			>0.9
Head	103 (78%)	53 (78%)	
Body and Tail	29 (22%)	15 (22%)	
T stage			**<0.001**
T1	7 (5.3%)	14 (21%)	
T2	54 (41%)	14 (21%)	
T3	71 (54%)	40 (59%)	
N stage			0.064
N0	28 (21%)	19 (28%)	
N1	51 (39%)	33 (49%)	
N2	53 (40%)	16 (24%)	
TNM stage			**0.033**
I	15 (11%)	12 (18%)	
II	64 (48%)	41 (60%)	
III	53 (40%)	15 (22%)	
Tumor differentiation			**0.005**
Well-Moderate	34 (26%)	31 (46%)	
Poor	98 (74%)	37 (54%)	
Adjacent organ invasion			0.2
Absence	52 (39%)	21 (31%)	
Presence	80 (61%)	47 (69%)	
Microvascular invasion			0.4
Absence	67 (51%)	39 (57%)	
Presence	65 (49%)	29 (43%)	
Lymph vascular invasion			0.12
Absence	85 (64%)	36 (53%)	
Presence	47 (36%)	32 (47%)	
Perineural invasion			0.5
Absence	27 (20%)	17 (25%)	
Presence	105 (80%)	51 (75%)	
Chemotherapy after surgery			>0.9
Untreated	52 (39%)	25 (37%)	
Single-agent therapy	57 (43%)	31 (46%)	
Multi-agent therapy	23 (17%)	12 (18%)	
Chemotherapy after recurrence			**<0.001**
Untreated	47 (36%)	15 (22%)	
Single-agent therapy	29 (22%)	37 (54%)	
Multi-agent therapy	56 (42%)	16 (24%)	

(Continued)

TABLE 1 (Continued)

Characteristic	Training, *N* = 132	Validation, *N* = 68	*p*-value
Recurrence patterns			**0.006**
Local	13 (9.8%)	18 (26%)	
Lung only	29 (22%)	9 (13%)	
Liver only	35 (27%)	22 (32%)	
Local and distant	55 (42%)	19 (28%)	
Time to recurrence			0.9
Early recurrence	89 (67%)	45 (66%)	
Late recurrence	43 (33%)	23 (34%)	
CA199 (U/ml)			0.5
<35	31 (23%)	19 (28%)	
≥35	101 (77%)	49 (72%)	
CEA (ng/ml)			0.8
<5	61 (46%)	33 (49%)	
≥5	71 (54%)	35 (51%)	
NLR			0.078
<224.65	38 (29%)	28 (41%)	
≥224.65	94 (71%)	40 (59%)	
PLR			0.3
<2.28	88 (67%)	50 (74%)	
≥2.28	44 (33%)	18 (26%)	

The bold values represents *p*-values less than 0.05.

recurrence was portrayed as a crucial time point for PDAC patients since 80% of them may die from tumor recurrence or metastasis during the next five years (23, 24). Moreover, the advancement of recurrent lesions was also demonstrated as another primary concern, from which the alternative chemotherapy regimen should be considered for restricting the growth of recurrent lesions (13, 25). Therefore, exploring the factors independently influencing the PPFS and precisely predicting the PPFS through the nomogram model was essential for developing alternative chemotherapy regimens and improving patient outcomes. However, the correlation between the clinicopathological factors and PPFS has not been explored clearly. The present study determined that lymph vascular invasion, N stage, T stage, recurrence patterns, time to recurrence, chemotherapy after surgery, and chemotherapy after recurrence were independent prognostic factors for PPFS. Furthermore, we also constructed a nomogram based on those independent prognostic factors with favorable predictive capacity.

Since the high invasive capacity of PDAC, micro-metastatic lesions and residual tumor foci commonly co-existed in the same patient (22, 26, 27), adjuvant chemotherapy was imminent after radical resection (28–31). The preceding research declared that chemotherapy inhibited tumor progression and metastasis (32–35). However, the tumor-inhibiting effect of chemotherapy on the relapse lesions had been rarely discussed before. The present study found that PDAC patients received multi-agent chemotherapy after surgery showed better PPFS than patients received single-agent chemotherapy. Meanwhile, we also found that multi-agent chemotherapy and single-agent chemotherapy had similar efficacy in limiting the progression of relapse foci. Drug-tolerant tumor cells was fundamental for drug-resistant clones and contribute to relapse and disease progression (36). It means that the resistance to chemotherapy was significantly strengthened in the recurrent lesion compared with the primary tumor. Meanwhile, the progression of recurrent lesions was too fast to be restricted by the chemotherapeutic agent (37, 38). Therefore, the superiority of the multi-agent regimen was masked when compared with the single-agent schema in recurrent PDAC patients (39–43). Based on the results of the present study, we argue that multi-agent chemotherapy brings more survival benefits to PDAC patients after radical surgery compared with a single-agent scheme. However, single-agent chemotherapy regimens should also be recommended for recurrent PDAC patients with poor chemotherapy tolerance to reduce the toxic side effects of chemotherapeutic agents (44, 45).

In previous research, lymph node metastasis was explained as an essential predictor for tumor progression (46–49). Meanwhile, the consensus in the Japanese Pancreatic Society also cited that confirmation of N9 and N16 lymph node metastasis was intimately linked with tumor relapse and distant metastasis (14). Similarly, the higher N stage and positive lymph vascular invasion portended early advancement of recurrent lesions in the present research. Dissemination into the lymphatic system was the major routes for PDAC metastasis (50). Meanwhile, lymph node metastasis was an initial step in PDAC metastasis. It was also crucial for determination of clinical staging, prognosis and survival in PDAC patients (51, 52). Therefore, recurrent PDAC patients with lymph vascular invasion or lymph node metastasis may benefit from chemotherapy for inhibiting the relapse lesion progression.

TABLE 2 The results of univariate cox regression in the training cohort.

Characteristics	HR	*p*	CI	Characteristics	HR	*p*	CI
Gender				Perineural invasion			
Male	Ref			Absence	Ref		
Female	0.86	0.412	0.59 – 1.24	Presence	1.18	0.473	0.75 – 1.83
Age				Microvascular invasion			
<60	Ref			Absence	Ref		
≥60	1.01	0.956	0.68 – 1.5	Presence	1.1	0.603	0.77 – 1.58
Tumor site				Adjacent organ invasion			
Head	Ref			Absence	Ref		
Body and Tail	1.28	0.264	0.83 – 1.97	Presence	1.47	**0.044**	1.01 – 2.14
Tumor differentiation				Lymph vascular invasion			
Well-Moderate	Ref			Absence	Ref		
Poor	1.68	**0.019**	1.09 – 2.59	Presence	1.54	**0.026**	1.05 – 2.25
T stage				Recurrence patterns			
T1	Ref			Local	Ref		
T2	2.85	**0.019**	1.19 – 6.81	Lung only	3.42	**0.011**	1.32 – 8.86
T3	3.47	**0.005**	1.47 – 8.17	Liver only	3.64	**0.007**	1.41 – 9.39
N stage				Local and distant	3.31	**0.011**	1.32 – 8.31
N0	Ref			Chemotherapy after surgery			
N1	1.51	0.108	0.91 – 2.51	Untreated	Ref		
N2	2.19	**0.002**	1.34 – 3.57	Single-agent therapy	0.65	**0.035**	0.44 – 0.97
Time to recurrence				Multi-agent therapy	0.45	**0.005**	0.26 – 0.78
Early recurrence	Ref			Chemotherapy after recurrence			
Late recurrence	0.61	**0.020**	0.41 – 0.92	Untreated	Ref		
CA199				Single-agent therapy	0.63	0.081	0.38 – 1.06
<35	Ref			Multi-agent therapy	0.54	**0.003**	0.36 – 0.82
≥35	1.64	**0.033**	1.04 – 2.59				
CEA							
<5	Ref						
≥5	1.27	0.214	0.87 – 1.85				
PLR							
<2.28	Ref						
≥2.28	0.91	0.629	0.61 – 1.35				
NLR							
<224.65	Ref						
≥224.65	1.57	**0.036**	1.03 – 2.38				

The bold values represents *p*-values less than 0.05.

The T stage represented the tumor diameters measured by the pathologists, indicating the tumor burden. Moreover, it has also been estimated as the reference standard for chemotherapeutic efficacy (13, 53, 54). The probability that a cancer contains drug-resistant clones depended on the size of the tumor (55). In this study, we found that the higher T stage was one of the independent prognostic factors for PPFS, portending a shorter PPFS. The residual disease of PDAC patients after surgery my cause tumor recurrence or relapse lesions progression. Hence, the radiotherapy or nano knife against the resection margin may reduce the local recurrence rate in PDAC patients with large tumor volumes.

Different recurrence patterns of PDAC patients are usually linked with diverse post-progression survival (7, 21, 56). In the earlier study, the local and distant recurrence pattern heralded the poorest post-progression survival among the four abovementioned recurrence patterns (7). The present study also estimated that the local and distant recurrence patterns predicted poorer PPFS compared to the local recurrence patterns. The late tumor stage may be one of the most important causes leading to this result (7, 57). Therefore, PDAC patients with local and distant recurrence are warranted to received chemotherapy when compared with local recurrent cases.

TABLE 3 The results of multivariate cox regression in the training cohort.

Characteristics	HR	*p*	CI	Characteristics	HR	*p*	CI
Tumor differentiation				Adjacent organ invasion			
Well-Moderate	Ref			Absence	Ref		
Poor	1.09	0.753	0.64 – 1.87	Presence	0.99	0.9613	0.63 – 1.56
T stage				Lymph vascular invasion			
T1	Ref			Absence	Ref		
T2	3.23	**0.017**	1.24 – 8.42	Presence	4.21	**0.001**	2.42 – 7.33
T3	3.86	**0.010**	1.39 – 10.71	Recurrence patterns			
N stage				Local	Ref		
N0	Ref			Lung only	4.77	**0.004**	1.65 – 13.82
N1	2.43	**0.007**	1.28 – 4.62	Liver only	5.02	**0.002**	1.79 – 14.06
N2	2.59	**0.002**	1.43 – 4.7	Local and distant	5.11	**0.002**	1.84 – 14.18
Time to recurrence				Chemotherapy after surgery			
Early recurrence	Ref			Untreated	Ref		
Late recurrence	0.54	**0.035**	0.3 – 0.96	Single-agent therapy	0.64	0.058	0.4 – 1.02
CA199				Multi-agent therapy	0.36	**0.003**	0.18 – 0.7
<35	Ref			Chemotherapy after recurrence			
≥35	1.18	0.559	0.68 – 2.07	Untreated	Ref		
NLR				Single-agent therapy	0.57	0.058	0.32 – 1.02
<224.65	Ref			Multi-agent therapy	0.48	**0.002**	0.3 – 0.77
≥224.65	0.67	0.169	0.38 – 1.18				

The bold values represents *p*-values less than 0.05.

Last but not least, we investigated the relationship between the time to recurrence and PPFS. The results declared that PDAC patients with late relapse had exclusively longer PPFS compared with the early relapse patients. In the previous research, early recurrence reflected the malignant phenotype of PDAC (8, 14, 58). Most of the early relapse patients were combine with late tumor stage, poorer tumor differentiation, and stronger drug-resistant effect, causing a more rapid progression of recurrent lesions (7, 59, 60). Therefore, chemotherapy-only may be not enough to restrain the tumor progression in early recurrent PDAC patients. Combination therapies may be more suitable for early recurrent cases. In detail, secondary surgery could be performed in PDAC patients with isolated local recurrent or oligometastatic lesions. Besides this, radiofrequency ablation or radiation therapy combined with chemotherapy could be another option for early recurrent patients with multiple metastases.

The development of recurrent lesions was a crucial time point for replacing chemotherapy schemes according to the NCCN guidelines (13). Furthermore, individualized intervention for PDAC patients should be managed based on the risk of relapse lesions advancement. Therefore, precise prediction for PPFS is essential for clinical decision-making. After statistical analysis, our research selected several independent prognostic factors from high-dimensional radiological and pathological variables. Furthermore, we also constructed a nomogram for PPFS prediction based on those independent prognostic factors. The results of contrast analysis (the calibration curve, DCA, and C-index) between the training and validation cohort demonstrated this nomogram system's strong predictive and discriminative power. Thus, clinicians can precisely assess the risk of progression in relapse lesions for PDAC patients by using the nomogram system fabricated in this study.

There are still some limitations to the present study. First, this study adopted a single-center retrospective design. The regional difference of clinical practices might affect the extrapolation of the results in our current analysis. A multi-center control study was needed to better estimate the predictive capacity of the nomogram constructed in the present study. Meanwhile, a major potential bias in this analysis is selection bias. For example, there was a lower readmission probability in the PDAC patients with history of stroke or coronary artery disease because of the higher surgical risk when compared with PDAC patients with better physical condition. It may limit the predictive power of the nomogram in the PDAC patients with poor physical status.

Hence, to minimize such bias, we inflated the sample size by including the resected PDAC patients from 2008 to 2019, and we also set strict inclusion criteria and exclusion criteria for screening. On the other hand, some variables, such as serum total bilirubin levels, C-reactive protein, and albumin, had not been included in this research. It was beneficial to explore the impact of nutritional status and inflammatory response on the progression of relapse lesions in PDAC patients. Meanwhile, some of the characteristics were only vaguely described during the information collection. For example, the specific chemotherapy regimens and the lymph node metastasis group had not been displayed in detail. The involvement of the characteristics mentioned above could further refine the predictive effect of the nomogram. For instance, more precise results would be established in future exploration

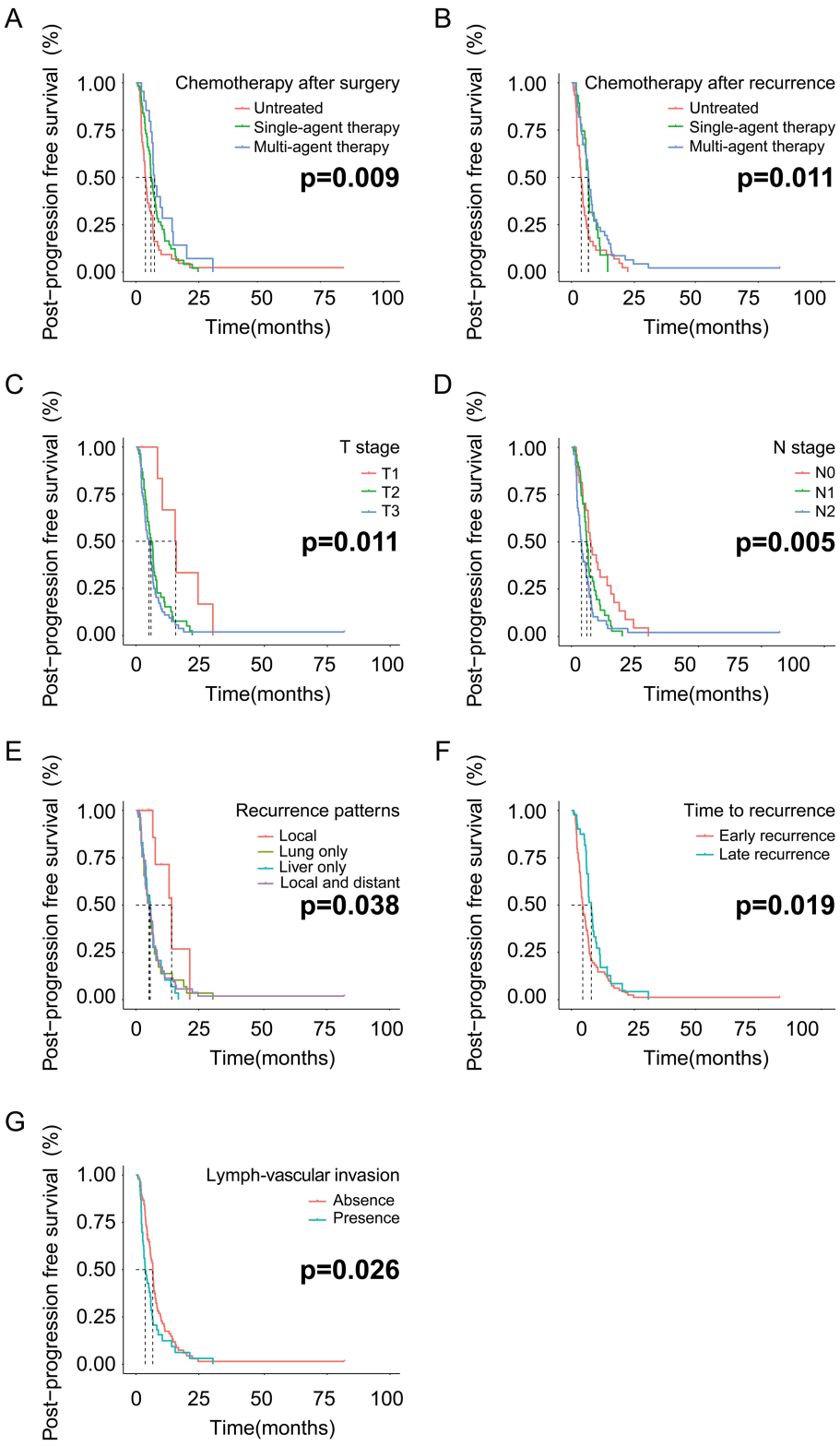

FIGURE 2
The PPFS analysis based on the independent risk factors in the training cohort. **(A)** PPFS analysis based on chemotherapy after surgery; **(B)** PPFS analysis based on chemotherapy after recurrence; **(C)** PPFS analysis based on T stage; **(D)** PPFS analysis based on N stage. **(E)** PPFS analysis based on recurrence patterns; **(F)** PPFS analysis based on time to recurrence; **(G)** PPFS analysis based on lymph vascular invasion.

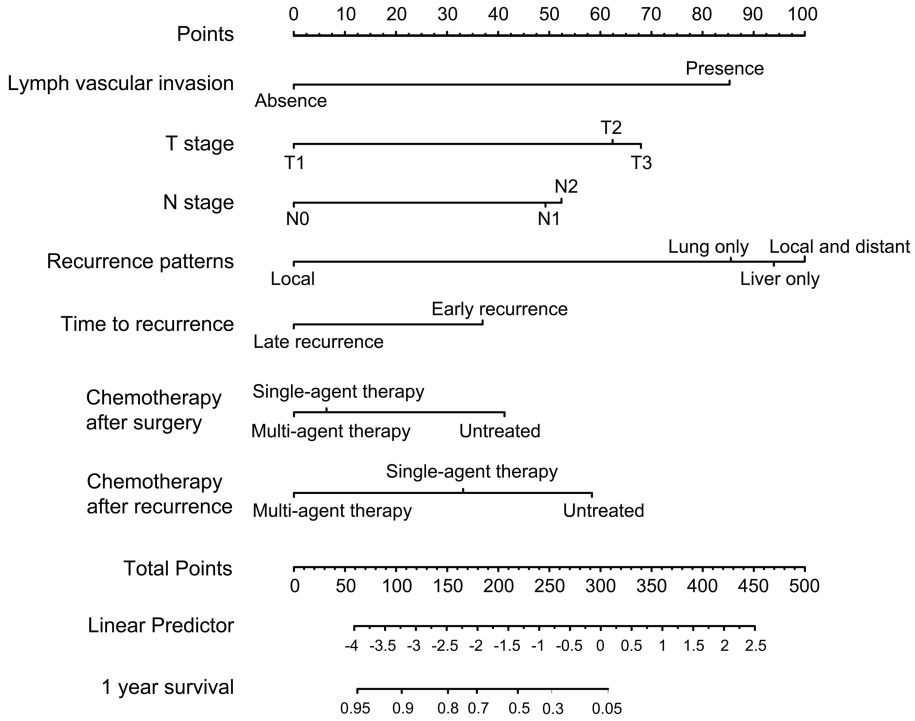

FIGURE 3
Nomogram for predicting the 1-year PPFS rates of PDAC patients after radical resection in the training cohort.

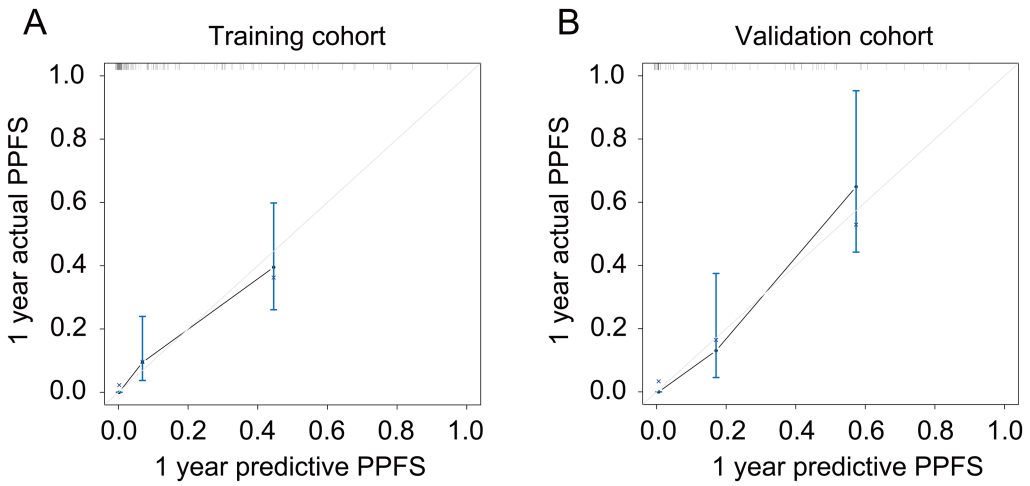

FIGURE 4
The calibration plot for predicting PPFS rates in recurrent PDAC. **(A)** The calibration plot for predicting the 1-year PPFS rates in the training cohort; **(B)** The calibration plot for predicting the 1-year PPFS rates in the validation cohort.

when a larger sample size was available. Finally, some modified described methods for lymph node metastasis, such as lymph node ratio and log odds of positive lymph nodes, have already been proposed in some research (61). However, we still referred to the description of lymph node metastasis from the AJCC guidelines in the present study. More persuasive results would be available if future research could apply the modified methods to lymph node metastasis discrimination.

TABLE 4 Comparison of the C-index between nomogram and TNM stage.

Cohort	Model	C-index
Validation cohort	Nomogram	0.739
	TNM stage	0.726
Training cohort	Nomogram	0.609
	TNM stage	0.596

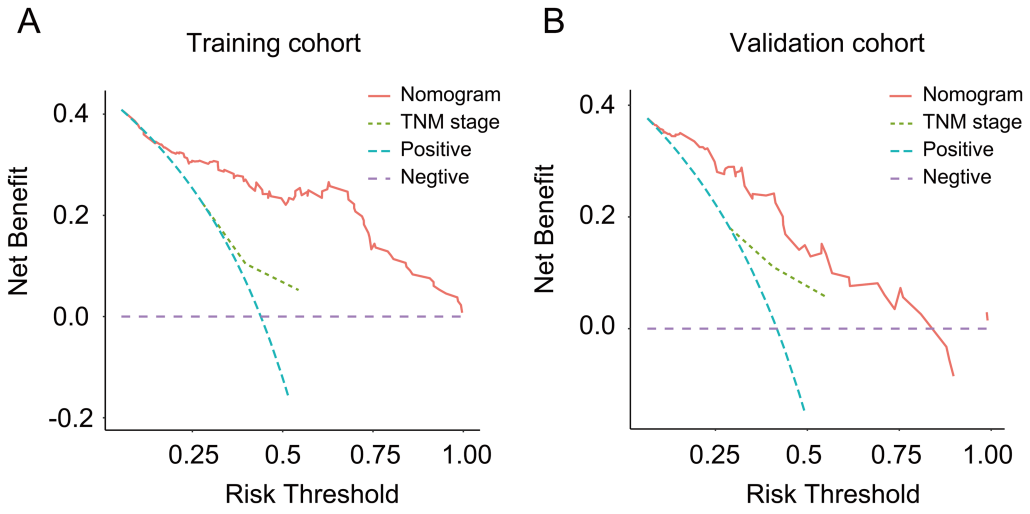

FIGURE 5
The decision curve analysis for the nomogram and TNM stage. **(A)** Decision curve analysis for the nomogram and TNM stage in the training cohort; **(B)** decision curve analysis for the nomogram and TNM stage in the validation cohort.

Conclusion

Multi-agent chemotherapy is recommended for PDAC patients after surgery. The single-agent chemotherapy also deserves consideration after tumor recurrence. The nomogram model provided a new way for PPFS prediction in recurrent PDAC patients. Moreover, the predictive value and accuracy of the present nomogram will be improved if validated in a larger and multi-center cohort.

Data availability statement

The datasets presented in this study can be found in online repositories. The names of the repository/repositories and accession number(s) can be found in the article/Supplementary material.

Ethics statement

The studies involving humans were approved by the Ethics Committee of Sun Yat-sen University. The studies were conducted in accordance with the local legislation and institutional requirements. The participants provided their written informed consent to participate in this study. The manuscript presents research on animals that do not require ethical approval for their study. Written informed consent was obtained from the individual(s) for the publication of any potentially identifiable images or data included in this article.

Author contributions

DQ: Writing – original draft. PX: Data curation, Formal analysis, Writing – original draft. KH: Methodology, Resources, Writing – original draft. LJ: Visualization, Writing – original draft. ZY: Software, Writing – original draft. RW: Writing – review & editing. SL: Funding acquisition, Supervision, Writing – review & editing.

Funding

The author(s) declare that financial support was received for the research, authorship, and/or publication of this article. This work was supported by the National Natural Science Funds (Nos. 81972299 and 81672390) and National Key Research and Development Plan (No. 2017YFC0910002).

Conflict of interest

The authors declare that the research was conducted in the absence of any commercial or financial relationships that could be construed as a potential conflict of interest.

Publisher's note

Supplementary material

The Supplementary material for this article can be found online at: https://www.frontiersin.org/articles/10.3389/fmed.2024.1486750/full#supplementary-material

References

1. Siegel R, Miller K, Jemal A. Cancer statistics, 2020. *CA Cancer J Clin*. (2020) 70:7–30. doi: 10.3322/caac.21590

2. Rawla P, Sunkara T, Gaduputi V. Epidemiology of pancreatic cancer: global trends, etiology and risk factors. *World J Oncol*. (2019) 10:10–27. doi: 10.14740/wjon1166

3. Ellison L, Wilkins K. An update on cancer survival. *Health Rep*. (2010) 21:55–60.

4. Rahib L, Smith B, Aizenberg R, Rosenzweig A, Fleshman J, Matrisian L. Projecting cancer incidence and deaths to 2030: the unexpected burden of thyroid, liver, and pancreas cancers in the United States. *Cancer Res*. (2014) 74:2913–21. doi: 10.1158/0008-5472.Can-14-0155

5. Ben-Josef E, Guthrie K, el-Khoueiry AB, Corless CL, Zalupski MM, Lowy AM, et al. SWOG S0809: A Phase II Intergroup Trial of Adjuvant Capecitabine and Gemcitabine Followed by Radiotherapy and Concurrent Capecitabine in Extrahepatic Cholangiocarcinoma and Gallbladder Carcinoma. *J Clin Oncol*. (2015) 33:2617–22. doi: 10.1200/jco.2014.60.2219

6. Suenaga M, Fujii T, Kanda M, Takami H, Okumura N, Inokawa Y, et al. Pattern of first recurrent lesions in pancreatic cancer: hepatic relapse is associated with dismal prognosis and portal vein invasion. *Hepatogastroenterology*. (2014) 61:1756–61.

7. Groot V, Rezaee N, Wu W, Cameron JL, Fishman EK, Hruban RH, et al. Patterns, timing, and predictors of recurrence following pancreatectomy for pancreatic ductal adenocarcinoma. *Ann Surg*. (2018) 267:936–45. doi: 10.1097/sla.0000000000002234

8. He C, Cai Z, Zhang Y, Lin X. Comparative recurrence analysis of pancreatic adenocarcinoma after resection. *J Oncol*. (2021) 2021:3809095–18. doi: 10.1155/2021/3809095

9. He C, Huang X, Zhang Y, Cai Z, Lin X, Li S. A quantitative clinicopathological signature for predicting recurrence risk of pancreatic ductal adenocarcinoma after radical resection. *Front Oncol*. (2019) 9:1197. doi: 10.3389/fonc.2019.01197

10. Lei P, Pereira E, Andersson P, Amoozgar Z, van Wijnbergen JW, O'Melia MJ, et al. Cancer cell plasticity and MHC-II-mediated immune tolerance promote breast cancer metastasis to lymph nodes. *J Exp Med*. (2023) 220:e20221847. doi: 10.1084/jem.20221847

11. Goldfarb Y, Sorski L, Benish M, Levi B, Melamed R, Ben-Eliyahu S. Improving postoperative immune status and resistance to cancer metastasis: a combined perioperative approach of immunostimulation and prevention of excessive surgical stress responses. *Ann Surg*. (2011) 253:798–810. doi: 10.1097/SLA.0b013e318211d7b5

12. Miyamoto D, Lee R, Kalinich M, LiCausi JA, Zheng Y, Chen T, et al. An RNA-based digital circulating tumor cell signature is predictive of drug response and early dissemination in prostate cancer. *Cancer Discov*. (2018) 8:288–303. doi: 10.1158/2159-8290.Cd-16-1406

13. Tempero M, Malafa M, al-Hawary M, Behrman SW, Benson AB, Cardin DB, et al. Pancreatic Adenocarcinoma, Version 2.2021, NCCN Clinical Practice Guidelines in Oncology. *J Natl Compr Canc Netw*. (2021) 19:439–57. doi: 10.6004/jnccn.2021.0017

14. He C, Sun S, Zhang Y, Lin X, Li S. A Novel Nomogram to Predict Survival in Patients With Recurrence of Pancreatic Ductal Adenocarcinoma After Radical Resection. *Front Oncol*. (2020) 10:1564. doi: 10.3389/fonc.2020.01564

15. Tiansong X, Xuebin X, Wei L, Lei C, Kefu L, Zhengrong Z. Prediction of postoperative recurrence in resectable pancreatic body/tail adenocarcinoma: a novel risk stratification approach using a CT-based nomogram. *Eur Radiol*. (2023) 33:7782–93. doi: 10.1007/s00330-023-10047-x

16. Tang TY, Li X, Zhang Q, Guo CX, Zhang XZ, Lao MY, et al. Development of a Novel Multiparametric MRI Radiomic Nomogram for Preoperative Evaluation of Early Recurrence in Resectable Pancreatic Cancer. *J Magn Reson Imaging*. (2020) 52:231–45. doi: 10.1002/jmri.27024

17. Ruiqiu C, Chaohui X, Shaoming S, Lin Z, Tianchen Z, Rong L. The optimal choice for patients underwent minimally invasive pancreaticoduodenectomy: a systematic review and meta-analysis including patient subgroups. *Surg Endosc*. (2024) 38:6237–53. doi: 10.1007/s00464-024-11289-6

18. Jiang L, Ning D, Chen XP. Improvement in distal pancreatectomy for tumors in the body and tail of the pancreas. *World J Surg Oncol*. (2021) 19:49. doi: 10.1186/s12957-021-02159-9

19. Chang D, Johns A, Merrett N, Gill AJ, Colvin EK, Scarlett CJ, et al. Margin clearance and outcome in resected pancreatic cancer. *J Clin Oncol*. (2009) 27:2855–62. doi: 10.1200/jco.2008.20.5104

20. Mathew G, Agha R, Albrecht J, Goel P, Mukherjee I, Pai P, et al. STROCSS 2021: Strengthening the reporting of cohort, cross-sectional and case-control studies in surgery. *Int J Surg*. (2021) 96:106165. doi: 10.1016/j.ijsu.2021.106165

21. Groot V, Gemenetzis G, Blair A, Rivero-Soto RJ, Yu J, Javed AA, et al. Defining and Predicting Early Recurrence in 957 Patients With Resected Pancreatic Ductal Adenocarcinoma. *Ann Surg*. (2019) 269:1154–62. doi: 10.1097/sla.0000000000002734

22. Bednar F, Pasca di Magliano M. Chemotherapy and Tumor Evolution Shape Pancreatic Cancer Recurrence after Resection. *Cancer Discov*. (2020) 10:762–4. doi: 10.1158/2159-8290.Cd-20-0359

23. Siegel R, Miller K, Jemal A. Cancer statistics, 2019. *CA Cancer J Clin*. (2019) 69:7–34. doi: 10.3322/caac.21551

24. Gillen S, Schuster T, Meyer Zum Büschenfelde C, Friess H, Kleeff J. Preoperative/neoadjuvant therapy in pancreatic cancer: a systematic review and meta-analysis of response and resection percentages. *PLoS Med*. (2010) 7:e1000267. doi: 10.1371/journal.pmed.1000267

25. Taniyama T, Morizane C, Nakachi K, Nara S, Ueno H, Kondo S, et al. Treatment outcome for systemic chemotherapy for recurrent pancreatic cancer after postoperative adjuvant chemotherapy. *Pancreatology*. (2012) 12:428–33. doi: 10.1016/j.pan.2012.07.016

26. Akhtar M, Haider A, Rashid S, Al-Nabet A. Paget's "Seed and Soil" Theory of Cancer Metastasis: An Idea Whose Time has Come. *Adv Anat Pathol*. (2019) 26:69–74. doi: 10.1097/pap.0000000000000219

27. Psaila B, Lyden D. The metastatic niche: adapting the foreign soil. *Nat Rev Cancer*. (2009) 9:285–93. doi: 10.1038/nrc2621

28. Herrmann R, Bodoky G, Ruhstaller T, Glimelius B, Bajetta E, Schüller J, et al. Gemcitabine plus capecitabine compared with gemcitabine alone in advanced pancreatic cancer: a randomized, multicenter, phase III trial of the Swiss Group for Clinical Cancer Research and the Central European Cooperative Oncology Group. *J Clin Oncol*. (2007) 25:2212–7. doi: 10.1200/jco.2006.09.0886

29. Conroy T, Desseigne F, Ychou M, Bouché O, Guimbaud R, Bécouarn Y, et al. FOLFIRINOX versus gemcitabine for metastatic pancreatic cancer. *N Engl J Med*. (2011) 364:1817–25. doi: 10.1056/NEJMoa1011923

30. Mavros M, Moris D, Karanicolas P, Katz M, O'Reilly E, Pawlik T. Clinical Trials of Systemic Chemotherapy for Resectable Pancreatic Cancer: A Review. *JAMA Surg*. (2021) 156:663–72. doi: 10.1001/jamasurg.2021.0149

31. von Hoff DD, Ervin T, Arena F, Chiorean EG, Infante J, Moore M, et al. Increased survival in pancreatic cancer with nab-paclitaxel plus gemcitabine. *N Engl J Med*. (2013) 369:1691–703. doi: 10.1056/NEJMoa1304369

32. Sohal D, Duong M, Ahmad S, Gandhi NS, Beg MS, Wang-Gillam A, et al. Efficacy of Perioperative Chemotherapy for Resectable Pancreatic Adenocarcinoma: A Phase 2 Randomized Clinical Trial. *JAMA Oncol*. (2021) 7:421–7. doi: 10.1001/jamaoncol.2020.7328

33. Xiong X, Mao Q, Yang J, Chen S, Li X. Clinical effectiveness of fluorouracil and cisplatin intraperitoneal perfusion combined with intravenous chemotherapy for peritoneal metastasis in gastric cancer. *Eur Rev Med Pharmacol Sci*. (2023) 27:8716–31. doi: 10.26355/eurrev_202309_33794

34. Inworn N, Senavat P, Aleenajitpong N, Chingchaimaneesri M, Siripoon T, Srirattanapong S, et al. Predictive Factors for the Survival Outcomes of Preoperative Chemotherapy in Patients with Resectable and Borderline Resectable Colorectal Cancer with Liver Metastasis. *Asian Pac J Cancer Prev*. (2023) 24:3037–47. doi: 10.31557/apjcp.2023.24.9.3037

35. Zeng Y, Zhang S, Li S, Song G, Meng T, Yuan H, et al. Normalizing Tumor Blood Vessels to Improve Chemotherapy and Inhibit Breast Cancer Metastasis by Multifunctional Nanoparticles. *Mol Pharm*. (2023) 20:5078–89. doi: 10.1021/acs.molpharmaceut.3c00381

36. Zhao X, Ren Y, Lawlor M, Shah BD, Park PMC, Lwin T, et al. BCL2 Amplicon Loss and Transcriptional Remodeling Drives ABT-199 Resistance in B Cell Lymphoma Models. *Cancer Cell*. (2019) 35:752–766.e9. doi: 10.1016/j.ccell.2019.04.005

37. Orgaz JL, Crosas-Molist E, Sadok A, Perdrix-Rosell A, Maiques O, Rodriguez-Hernandez I, et al. Myosin II Reactivation and Cytoskeletal Remodeling as a Hallmark and a Vulnerability in Melanoma Therapy Resistance. *Cancer Cell*. (2020) 37:85–103.e9. doi: 10.1016/j.ccell.2019.12.003

38. Mollaoglu G, Guthrie MR, Böhm S, Brägelmann J, Can I, Ballieu PM, et al. MYC Drives Progression of Small Cell Lung Cancer to a Variant Neuroendocrine Subtype with Vulnerability to Aurora Kinase Inhibition. *Cancer Cell*. (2017) 31:270–85. doi: 10.1016/j.ccell.2016.12.005

39. Yan W, Si L, Ding Y, Qiu S, Zhang Q, Liu L. Neoadjuvant chemotherapy does not improve the prognosis and lymph node metastasis rate of locally advanced cervical squamous cell carcinoma: A retrospective cohort study in China. *Medicine*. (2019) 98:e17234. doi: 10.1097/md.0000000000017234

40. Inoue Y, Fujii K, Tashiro K, Ishii M, Masubuchi S, Yamamoto M, et al. Preoperative Chemotherapy May Not Influence the Remnant Liver Regenerations and Outcomes After Hepatectomy for Colorectal Liver Metastasis. *World J Surg*. (2018) 42:3316–30. doi: 10.1007/s00268-018-4590-1

41. Hoyle M, Crathorne L, Peters J, Jones-Hughes T, Cooper C, Napier M, et al. The clinical effectiveness and cost-effectiveness of cetuximab (mono- or combination chemotherapy), bevacizumab (combination with non-oxaliplatin chemotherapy) and panitumumab (monotherapy) for the treatment of metastatic colorectal cancer after first-line chemotherapy (review of technology appraisal No.150 and part review of technology appraisal No. 118): a systematic review and economic model. *Health Technol Assess*. (2013) 17:1–237. doi: 10.3310/hta17140

42. Ranson M, Hersey P, Thompson D, Beith J, McArthur GA, Haydon A, et al. Randomized trial of the combination of lomeguatrib and temozolomide compared with temozolomide alone in chemotherapy naive patients with metastatic cutaneous melanoma. *J Clin Oncol*. (2007) 25:2540–5. doi: 10.1200/jco.2007.10.8217

43. Rosenberg S, Yang J, Schwartzentruber D, Hwu P, Marincola FM, Topalian SL, et al. Prospective randomized trial of the treatment of patients with metastatic melanoma

using chemotherapy with cisplatin, dacarbazine, and tamoxifen alone or in combination with interleukin-2 and interferon alfa-2b. *J Clin Oncol*. (1999) 17:968–75. doi: 10.1200/jco.1999.17.3.968

44. Varol U, Dirican A, Yildiz I, Oktay E, Degirmenci M, Alacacioglu A, et al. First-line mono-chemotherapy in frail elderly patients with metastatic colorectal cancer. *Asian Pac J Cancer Prev*. (2014) 15:3157–61. doi: 10.7314/apjcp.2014.15.7.3157

45. Yhim H, Lee J, Kim K, Kim SA, Lee JY, Hwang HG, et al. Increased risk of venous and arterial thromboembolism in patients with colorectal cancer receiving cetuximab-based combination chemotherapy: A population-based study in Korea. *Thromb Res*. (2023) 231:50–7. doi: 10.1016/j.thromres.2023.10.005

46. Sahin T, Fujii T, Kanda M, Nagai S, Kodera Y, Kanzaki A, et al. Prognostic implications of lymph node metastases in carcinoma of the body and tail of the pancreas. *Pancreas*. (2011) 40:1029–33. doi: 10.1097/MPA.0b013e3182207893

47. Murata Y, Ogura T, Hayasaki A, Gyoten K, Ito T, Iizawa Y, et al. Predictive risk factors for early recurrence in patients with localized pancreatic ductal adenocarcinoma who underwent curative-intent resection after preoperative chemoradiotherapy. *PLoS One*. (2022) 17:e0264573. doi: 10.1371/journal.pone.0264573

48. Kadera B, Sunjaya D, Isacoff W, Li L, Hines OJ, Tomlinson JS, et al. Locally advanced pancreatic cancer: association between prolonged preoperative treatment and lymph-node negativity and overall survival. *JAMA Surg*. (2014) 149:145–53. doi: 10.1001/jamasurg.2013.2690

49. Asiyanbola B, Gleisner A, Herman J, Choti MA, Wolfgang CL, Swartz M, et al. Determining pattern of recurrence following pancreaticoduodenectomy and adjuvant 5-flurouracil-based chemoradiation therapy: effect of number of metastatic lymph nodes and lymph node ratio. *J Gastrointest Surg*. (2009) 13:752–9. doi: 10.1007/s11605-008-0762-x

50. Åkerberg D, Ansari D, Andersson R. Re-evaluation of classical prognostic factors in resectable ductal adenocarcinoma of the pancreas. *World J Gastroenterol*. (2016) 22:6424–33. doi: 10.3748/wjg.v22.i28.6424

51. Sun Y, Chen Y, Li J, Huo YM, Liu DJ, Hua R, et al. A novel long non-coding RNA ENST00000480739 suppresses tumour cell invasion by regulating OS-9 and HIF-1α in pancreatic ductal adenocarcinoma. *Br J Cancer*. (2014) 111:2131–41. doi: 10.1038/bjc.2014.520

52. Liu C, Cheng H, Jin K, Fan Z, Gong Y, Qian Y, et al. Resected Pancreatic Cancer With N2 Node Involvement Is Refractory to Gemcitabine-Based Adjuvant Chemotherapy. *Cancer Control*. (2020) 27:1073274820915947. doi: 10.1177/1073274820915947

53. Zhao Y, Wang C. Clinicopathological Features, Recurrence Patterns, and Prognosis of Pancreatic Adenocarcinoma with Normal Serum CA19-9. A Consecutive Series of 154 Cases from a Single Institute. *J Gastrointest Surg*. (2020) 24:855–65. doi: 10.1007/s11605-019-04209-w

54. Kim N, Kim H. Preoperative risk factors for early recurrence in patients with resectable pancreatic ductal adenocarcinoma after curative intent surgical resection. *Hepatobiliary Pancreat Dis Int*. (2018) 17:450–5. doi: 10.1016/j.hbpd.2018.09.003

55. Vasan N, Baselga J, Hyman DM. A view on drug resistance in cancer. *Nature*. (2019) 575:299–309. doi: 10.1038/s41586-019-1730-1

56. Groot V, Gemenetzis G, Blair A, Ding D, Javed AA, Burkhart RA, et al. Implications of the Pattern of Disease Recurrence on Survival Following Pancreatectomy for Pancreatic Ductal Adenocarcinoma. *Ann Surg Oncol*. (2018) 25:2475–83. doi: 10.1245/s10434-018-6558-7

57. Groot V, Blair A, Gemenetzis G, Ding D, Burkhart RA, Yu J, et al. Recurrence after neoadjuvant therapy and resection of borderline resectable and locally advanced pancreatic cancer. *Eur J Surg Oncol*. (2019) 45:1674–83. doi: 10.1016/j.ejso.2019.04.007

58. Zhao J, Zhang W, Zhang J, Chen YT, Ma WJ, Liu SY, et al. Independent Risk Factors of Early Recurrence After Curative Resection for Perihilar Cholangiocarcinoma: Adjuvant Chemotherapy May Be Beneficial in Early Recurrence Subgroup. *Cancer Manag Res*. (2020) 12:13111–23. doi: 10.2147/cmar.S289094

59. Pulvirenti A, Javed AA, Michelakos T, Sekigami Y, Zheng J, Kalvin HL, et al. Recurring Pancreatic Neuroendocrine Tumor: Timing and Pattern of Recurrence and Current Treatment. *Ann Surg*. (2023) 278:e1063–7. doi: 10.1097/SLA.0000000000005809

60. Honselmann K, Pergolini I, Castillo C, Deshpande V, Ting D, Taylor MS, et al. Timing But Not Patterns of Recurrence Is Different Between Node-negative and Node-positive Resected Pancreatic Cancer. *Ann Surg*. (2020) 272:357–65. doi: 10.1097/sla.0000000000003123

61. Prassas D, Safi S, Stylianidi M, Telan LA, Krieg S, Roderburg C, et al. N, LNR or LODDS: Which Is the Most Appropriate Lymph Node Classification Scheme for Patients with Radically Resected Pancreatic Cancer? *Cancers*. (2022) 14:1834. doi: 10.3390/cancers14071834

frontiers | Frontiers in Medicine

TYPE Original Research
PUBLISHED 13 December 2024
DOI 10.3389/fmed.2024.1517001

OPEN ACCESS

EDITED BY
Hua Zhong,
University of Hawaii at Manoa, United States

REVIEWED BY
Ling Xiao,
Harvard Medical School, United States
Peng Wang,
Coriell Institute for Medical Research, United States
Pingze Zhang,
Yale University, United States
Yanping Qiu,
California Institute of Technology, United States

*CORRESPONDENCE
Qingyi Feng
fengqingyi2024@163.com
Qunqing Chen
chenqq1985@sina.com

†These authors have contributed equally to this work and share first authorship

RECEIVED 25 October 2024
ACCEPTED 28 November 2024
PUBLISHED 13 December 2024

CITATION
Xie X, Zhang H, He H, Wu B, Chen Y, Lin W, Feng Q and Chen Q (2024) Postoperative adjuvant immunotherapy for pathological stage II–IVa esophageal squamous cell carcinoma after radical surgery does not improve disease-free recurrence rates.
Front. Med. 11:1517001.
doi: 10.3389/fmed.2024.1517001

Postoperative adjuvant immunotherapy for pathological stage II–IVa esophageal squamous cell carcinoma after radical surgery does not improve disease-free recurrence rates

Xihao Xie[1,2†], Hai Zhang[2†], Haiquan He[2], Bomeng Wu[2], Ying Chen[2], Wanli Lin[2], Qingyi Feng[2*] and Qunqing Chen[1*]

[1]Department of Thoracic Surgery, Zhujiang Hospital, Southern Medical University, Guangzhou, China, [2]Department of Thoracic Surgery, Gaozhou People's Hospital Affiliated to Guangdong Medical University, Gaozhou, China

Background/objectives: Postoperative adjuvant therapy for esophageal squamous cell carcinoma (ESCC) primarily includes chemotherapy and chemoradiotherapy. The survival benefits of postoperative adjuvant therapy for R0-resected ESCC remain controversial. Immunotherapy is being gradually applied perioperatively for esophageal cancer, but the efficacy of postoperative immunotherapy in ESCC is unclear. This study aimed to evaluate the effectiveness of postoperative immunotherapy for esophageal cancer. Toward this goal, we explored the differences between postoperative immunotherapy combined with chemotherapy and postoperative adjuvant chemotherapy alone.

Methods: This retrospective study evaluated patients who underwent radical surgery for esophageal cancer at Gaozhou People's Hospital between January 2020 and August 2022 and received postoperative adjuvant therapy. Patients were divided into two groups according to the adjuvant treatment regimens: postoperative adjuvant chemotherapy (aCT) and postoperative adjuvant immunotherapy combined with chemotherapy (aICT) groups. Data on baseline characteristics, surgical-related indicators, adverse event rates during adjuvant therapy, and 2-year postoperative follow-up were collected for both groups.

Results: A total of 76 patients were included: 36 and 40 patients in the aICT and aCT groups, respectively. There were no significant differences in baseline data between the two groups. During the adjuvant treatment period, the incidence of hypothyroidism was significantly higher in the aICT group than in the aCT group (25.0% vs. 2.5%, $p = 0.007$). During the 2-year follow-up, local and recurrence rates were 17.5 and 12.5% in the aCT group and 13.9 and 5.6% in the aICT group, respectively, showing no significant difference between the two groups ($p = 0.489$).

Conclusion: For patients with pathologically confirmed locally advanced ESCC after surgery, postoperative immunotherapy did not confer better disease-free recurrence rates compared to postoperative adjuvant therapy. Nonetheless, with research advancements, the role of immunotherapy in the treatment of ESCC is likely to expand, offering new hope for these patients.

KEYWORDS

adjuvant, chemotherapy, esophageal cancer, immunotherapy, disease-free recurrence rates

1 Introduction

Surgery is the primary treatment modality for early- and mid-stage esophageal squamous cell carcinoma (ESCC). Surgical techniques have rapidly advanced over the past decade, with new technologies being increasingly applied in clinical practice, particularly in minimally invasive treatments and robotic surgeries for esophageal cancer (1). These advancements and innovations have significantly improved the patients' quality of life; however, long-term efficacy remains less than satisfactory (2, 3). Current research indicates that patients may still experience local recurrence or distant metastasis within 2 years after radical surgery for esophageal cancer. This directly affects their survival prognosis, with a 5-year survival rate of approximately 25–30% (4–6). Particularly, postoperative pathological findings indicating positive lymph nodes directly influence patient survival outcomes (7). To further improve long-term survival rates, perioperative neoadjuvant and adjuvant therapies for locally advanced esophageal cancer have become key research focuses (8, 9). Meta-analyses show that neoadjuvant chemoradiotherapy or neoadjuvant chemotherapy is beneficial in improving survival outcomes for patients with locally advanced esophageal cancer. In clinical practice, it is common to combine neoadjuvant treatment with surgery, combine surgery with adjuvant treatment, or implement a comprehensive treatment approach that includes perioperative adjuvant therapies (neoadjuvant treatment, surgery, and postoperative adjuvant treatment), although specific protocols may vary across different clinical centers (10–12).

Neoadjuvant therapy encompasses neoadjuvant chemoradiotherapy, neoadjuvant chemotherapy, and, increasingly, neoadjuvant immunotherapy adopted in clinical trials. These therapeutic approaches have been shown to enhance R0 resection rates, prolong disease-free survival, and potentially improve long-term survival rates (13, 14). Postoperative adjuvant therapy is routinely offered as a complementary treatment to mitigate the risk of postoperative recurrence and improve the survival of esophageal cancer patients with postoperative pathological stages of T2 or higher, N+, or other high-risk factors. Postoperative adjuvant chemotherapy is the most common adjuvant regimen, although some institutions also perform postoperative chemoradiotherapy (15). However, there exists some controversy regarding the ability of postoperative adjuvant therapy to improve long-term survival for esophageal cancer. For select patients with R0-resected T3, N+ ESCC, postoperative adjuvant radiotherapy can reduce postoperative recurrence and improve survival (16). Conversely, postoperative adjuvant chemotherapy may be a risk factor for poor disease-free survival (DFS) and overall survival (OS) (17). Immunotherapy has demonstrated promising efficacy in the treatment of advanced esophageal cancer, improving survival outcomes. Consequently, the exploratory application of immunotherapy in the perioperative period of esophageal cancer has become increasingly prevalent (18). Researchers are actively investigating whether immunotherapy can effectively identify and attack cancer cells in postoperative patients, thereby providing these patients with more comprehensive and durable therapeutic effects (19). However, there are fewer studies on the safety and efficacy of the novel treatment paradigm of postoperative adjuvant immunotherapy compared to those on traditional postoperative adjuvant chemotherapy. Hence, this study aimed to assess the real-world short-term efficacy of immunotherapy in the adjuvant setting for postoperative patients with ESCC.

2 Methods

2.1 Study design and patients

This retrospective study was approved by the Ethical Committee of Gaozhou People's Hospital and was conducted according to the tenets of the Declaration of Helsinki. The requirement for individual consent was waived.

Patients with esophageal cancer who underwent surgical resection and postoperative adjuvant therapy at Gaozhou People's Hospital between January 2020 and August 2022 were evaluated. The inclusion criteria were as follows: (1) age 18–75 years; (2) underwent minimally invasive Mckeown surgery; (3) postoperative pathological confirmation of ESCC; (4) postoperative pathological stage I–IVa ESCC; (5) received postoperative adjuvant chemotherapy or immune therapy combined with chemotherapy; and (6) complete clinical data. The exclusion criteria were as follows: (1) preoperative severe cardiovascular and cerebrovascular complications; (2) preoperative coexistence of other malignancies; (3) preoperative neoadjuvant therapy; (4) non-R0 resection of esophageal cancer; and (5) postoperative adjuvant radiotherapy. The patients were divided into two groups based on the adjuvant treatment regimen received: postoperative adjuvant chemotherapy (aCT) or postoperative adjuvant immunotherapy combined with chemotherapy (aICT).

2.2 Postoperative adjuvant treatment regimens

2.2.1 Postoperative adjuvant chemotherapy

Postoperative adjuvant chemotherapy was administered every 3 weeks for a total of 4 cycles. Chemotherapy drugs included docetaxel (75 mg/m^2), paclitaxel injection (135 mg/m^2), paclitaxel injection (albumin bound, 260 mg/m^2), fluorouracil injection (0.5–1 g, d1–5), and vinorelbine bitartrate injection (25–30 mg/m^2, d1 and d8) in combination with cisplatin (75 mg/m^2) or carboplatin injection (200–400 mg/m^2).

2.2.2 Postoperative adjuvant chemotherapy combined with immunotherapy

Postoperative adjuvant chemotherapy combined with immunotherapy was administered every 3 weeks for a total of 4 cycles. The chemotherapy regimen was the same as that in the postoperative adjuvant chemotherapy group. The immunotherapy drugs included sintilimab injection (200 mg every 3 weeks), tislelizumab injection

(200 mg every 3 weeks), camrelizumab injection (200 mg every 3 weeks), toripalimab (3 mg/kg, every 2 weeks), pembrolizumab injection (2 mg/kg every 2 weeks), or nivolumab injection (3 mg/kg every 2 weeks).

2.3 Observation indicators

Patient data, including demographic information, past medical history, personal history, tumor pathological stage, tumor location, surgery-related indicators (operative time, intraoperative blood loss, number of lymph node stations dissected, number of lymph nodes dissected, postoperative hospital stay, and postoperative complication rate), incidence of adverse events during postoperative adjuvant treatment, tumor recurrence pattern at 2 years after surgery, and recurrence-free survival time at 2 years after surgery, were collected. Postoperative pathological staging was based on the 8th edition of the American Joint Committee on Cancer/Union for International Cancer Control staging of cancers of the esophagus and esophagogastric junction. The incidence of adverse events during postoperative adjuvant treatment was assessed using the Common Terminology Criteria for Adverse Events version 5.0 Local recurrence and metastasis was defined as those involving the mediastinal lymph node, supraclavicular lymph node, and local anastomotic recurrence. However, distant metastasis was defined as metastasis to distant organs.

2.4 Statistical analysis

Age, operative time, intraoperative blood loss, number of lymph node dissection, number of lymph node dissection stations, and postoperative hospitalization days were expressed as the mean ± standard deviation and analyzed using Student's t-test. Sex, combined history of hypertension and diabetes, tumor location, postoperative pathological G-grade, postoperative pathological tumor stage, incidence of postoperative anastomotic fistula, pulmonary infections, myelosuppression during postoperative adjuvant therapy, liver function impairment, hypothyroidism, and diarrhea were analyzed. The rates of local recurrence and distant metastasis at 2 years after surgery were assessed using the Chi-square test. The DFS was calculated using the Kaplan–Meier method, and differences in relapse-free survival rates were evaluated with the log-rank test. Confidence intervals (CIs) were set at 95%. All statistical analyses were performed using SPSS (Version 23; IBM, Armonk, NY, USA) and GraphPad Prism version 9.0 software (GraphPad Software, La Jolla, CA, USA). A two-sided p-value <0.05 was considered statistically significant.

3 Results

A total of 76 patients were included; among them, 40 and 36 patients belonged to the aCT and aICT groups, respectively. The study flowchart is shown in Figure 1. The aICT group was older but the difference in age was not significant (mean: 61.850 ± 7.973 years vs. 65.194 ± 8.558 years, $p > 0.05$). There were also no significant between-group differences in sex, postoperative pathological G grading, pathological staging, perioperative surgical-related indicators, and the incidence of postoperative complications. The patient characteristics are shown in Table 1. The main complications during the adjuvant treatment period included bone marrow suppression, elevated liver transaminases, hypothyroidism, and diarrhea. The incidence rates of hypothyroidism were 2.5% ($n = 1$, grade 1) in the aCT group and 25% in the aICT group ($n = 9$, 2 [5.6%] patients with grade 2 hypothyroidism), with a significant difference ($p < 0.05$, Table 2). The median follow-up time for the overall population was 28.5 months. The rates of local recurrence and distant metastasis were higher in the aCT than in the aICT group, although the difference was not significant (Table 3). There was also no significant between-group difference in DFS (HR = 1.042, 95% CI = 0.378–2.871, $p = 0.934$). The survival curves for both groups are shown in Figure 2.

4 Discussion

The introduction of immune checkpoint inhibitors in clinical practice has led to notable advancements in the treatment of esophageal cancer. The KEYNOTE-590 study demonstrated that the first-line administration of immunotherapy significantly enhanced long-term survival rates (20). Furthermore, a meta-analysis confirmed the efficacy of immunotherapy as a first-line treatment for advanced esophageal cancer (21). The success of immunotherapy as first-line treatment for advanced esophageal cancer has prompted the focus on its clinical application in the perioperative setting. However, the controversy continues. Nevo et al. (22) reported negative outcomes associated with the combination of neoadjuvant immunotherapy and chemotherapy. In contrast, Zhang et al. (23) found that neoadjuvant immunotherapy may provide significant survival benefits for patients with resectable locally advanced ESCC. Postoperative adjuvant therapy is currently not a standard treatment modality for resectable esophageal cancer. There is relatively fewer research data on postoperative adjuvant immunotherapy than on neoadjuvant immunotherapy. There are ongoing clinical trials exploring the role of immune checkpoint inhibitors in postoperative adjuvant treatment, either alone or in combination with other therapies, in solid tumors (24). Given the high recurrence rate of esophageal cancer, there is hope for more clinical studies to further explore this new treatment model of postoperative adjuvant immunotherapy for esophageal cancer (25–27).

Immunotherapy can activate the patient's immune system and enhance its ability to attack cancer cells, but it also has side effects. Adjuvant therapy has clinical specificity, particularly for patients who have undergone R0 surgical resection, as the patient's physical condition postoperatively is worse than that preoperatively. In the current study, the addition of immunotherapy agents did not significantly increase the incidence of common hematological and biochemical complications (e.g., as bone marrow suppression and liver dysfunction) during the adjuvant chemotherapy period. However, the incidence of hypothyroidism during the postoperative immunotherapy period was higher in those receiving postoperative adjuvant immunotherapy combined with chemotherapy than in those receiving adjuvant chemotherapy alone, although this was limited to grade 1 hypothyroidism. For other common immune-related adverse events, no significant increase was found in this study, which may be due to the short postoperative immunotherapy cycle and the small study sample size. In the CheckMate 577 study, the incidence of grade ≥ 3 adverse events was less than 1% in the postoperative

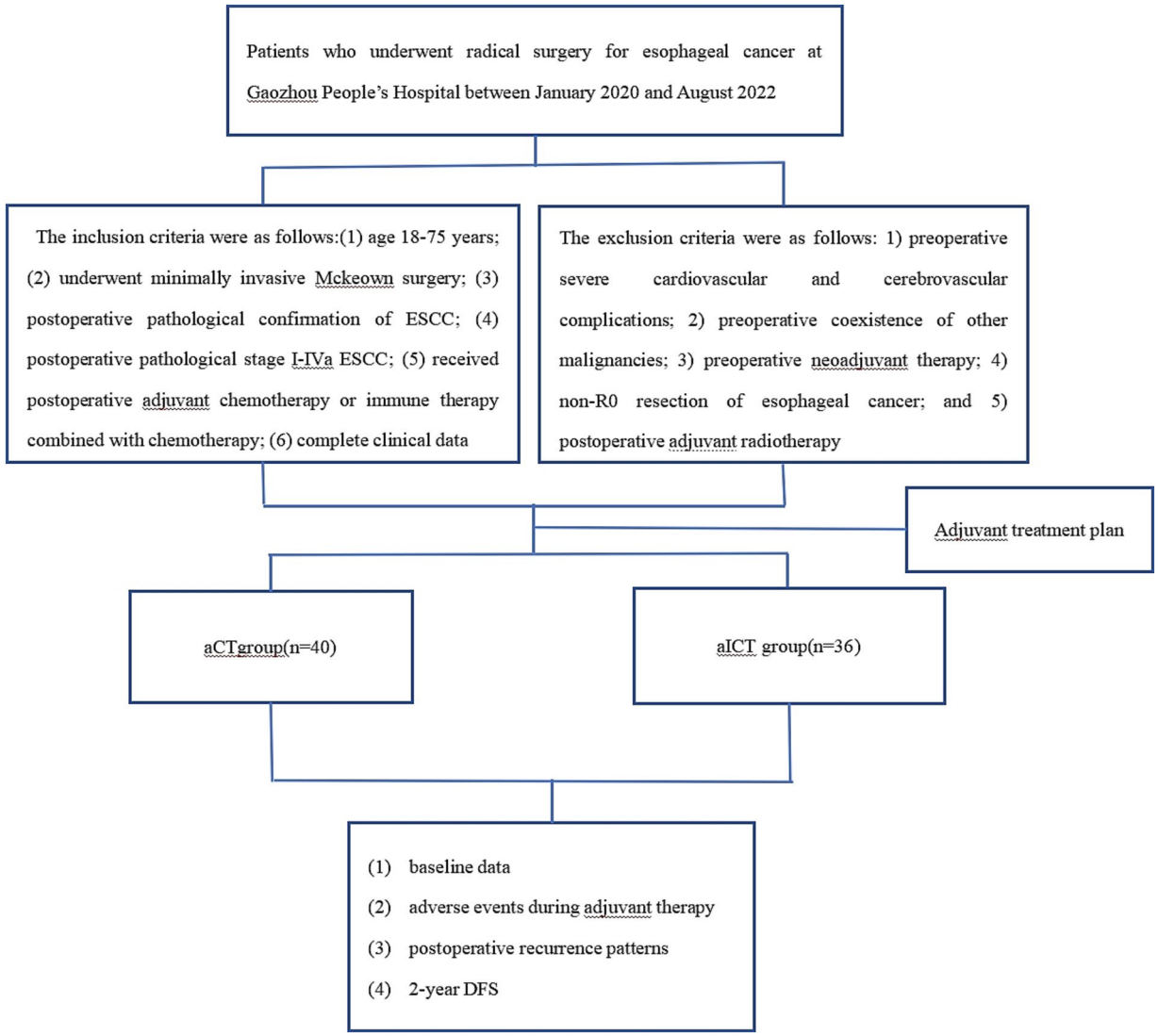

FIGURE 1
Study flowchart. aCT, adjuvant chemotherapy; aICT, adjuvant immunotherapy combined with chemotherapy; DFS, disease-free survival.

maintenance immunotherapy group (25). In a prospective clinical trial of patients with locally advanced esophageal cancer conducted by Park et al. (27), the immunotherapy-related complications following durvalumab maintenance after neoadjuvant chemoradiotherapy was largely limited to grades 1 and 2. Collectively, these findings indicate that adding immunotherapy to adjuvant treatment does not significantly increase the incidence of adverse events.

A meta-analysis on postoperative adjuvant treatment of gastric cancer that included 11 randomized controlled clinical studies reported better improvement in OS rates in patients who received postoperative adjuvant combined immunotherapy than in those who received surgery alone (HR = 0.72; 95% CI = 0.61–0.85; $p < 0.001$) (28). In the GERCOR NEONIPIGA study, which included patients with locally defective mismatch repair/high microsatellite instability gastric or gastroesophageal junction adenocarcinoma, no recurrences or metastases were observed after neoadjuvant treatment followed by postoperative adjuvant immunotherapy until the reporting cutoff date (29). These findings indicate that in patients with locally advanced esophageal cancer after R0 resection, whether postoperative immunotherapy can achieve good therapeutic effects remains an important question. In the current study, both patient groups experienced varying degrees of local recurrence and distant metastasis within 2 years postoperatively. However, the incidence rates of local recurrence and distant metastasis were lower in the patients who received postoperative immunotherapy combined with chemotherapy than in those who received postoperative adjuvant chemotherapy alone, although the difference was not significant. In the CheckMate 577 trial, patients who underwent R0 resection after preoperative neoadjuvant chemoradiotherapy and received nivolumab as postoperative adjuvant treatment demonstrated superior DFS compared to those who received placebo (25). However, a report by Park et al. indicated that using durvalumab as maintenance therapy postoperatively did not provide superior DFS or OS compared to placebo (27). Thus, the role of postoperative immunotherapy in improving survival outcomes for resectable

TABLE 1 Comparison of baseline data between the two groups.

Clinical features	aCT group (n = 40)	aICT group (n = 36)	χ^2/t	p
Age	61.850 ± 7.973	65.194 ± 8.558	−1.764	0.082
Sex (%)			0.045	0.831
Male	28 (70.0)	25 (72.2)		
Female	12 (30.0)	11 (27.8)		
History of hypertension (%)	4 (10.0)	3 (8.3)	0.062	0.802
History of diabetes (%)	1 (2.5)	1 (2.8)	0.006	0.940
Tumor location (%)			1.935	0.380
Upper	3 (7.5)	3 (8.3)		
Middle	13 (32.5)	17 (47.2)		
Lower	24 (60.0)	16 (44.4)		
G stage (%)			0.381	0.827
G_1	2 (5.0)	3 (8.3)		
G_2	21 (52.5)	19 (52.8)		
G_3	17 (42.5)	14 (38.9)		
Pathological stage (%)			0.663	0.718
II	9 (22.5)	6 (16.7)		
III	29 (72.5)	27 (75.0)		
IV	2 (5.0)	3 (8.3)		
Operation time (min)	288.475 ± 57.751	302.722 ± 59.100	−1.062	0.292
Intraoperative blood loss (mL)	88.000 ± 28.029	94.444 ± 35.411	−0.884	0.380
Number of lymph nodes dissected	28.825 ± 7.382	31.277 ± 12.427	−1.058	0.293
Number of lymph node dissection stations	11.625 ± 1.705	12.416 ± 2.622	−1.575	0.119
Postoperative hospital stay	12.250 ± 5.623	13.388 ± 10.340	−0.605	0.547
Postoperative pulmonary infection (%)	2 (5.0)	3 (8.3)	0.015	0.903
Anastomotic fistula (%)	2 (5.0)	1 (2.8)	2.47	0.619

Data are presented as n (%) or mean ± SD.
aCT, adjuvant chemotherapy; aICT, adjuvant immunotherapy combined with chemotherapy.

locally advanced esophageal cancer remains controversial. The PILOT trial aims to evaluate the efficacy of perioperative tislelizumab use, with hopes of achieving better 2-year DFS (30). Similarly, the multicenter phase III clinical trial NCT05495152 is further assessing the efficacy of postoperative immunotherapy in ESCC (31).

Neoadjuvant therapy combined with surgery is the standard treatment regimen for locally advanced esophageal malignancies. The efficacy of postoperative adjuvant therapy after R0 resection varies among different centers as the modalities used differ, with postoperative adjuvant chemotherapy being more frequently implemented in China. Early animal model studies suggest that neoadjuvant immunotherapy may be more effective than postoperative adjuvant treatments (32). In this study, patients in the aICT group did not achieve improved PFS compared to those in the aCT group. We posits that following primary tumor resection, the human body lacks specific antigens related to the primary tumor, resulting in ineffective postoperative immunotherapy. Therefore, whether postoperative adjuvant chemotherapy combined with immunotherapy can enhance antitumor efficacy and improve postoperative prognosis for esophageal cancer remains a matter of debate. As such, patients considering postoperative adjuvant immunotherapy must have a thorough understanding of relevant treatment information. This includes comprehensive knowledge of the treatment's purpose, potential effects, and risks and side effects, as well as alternative treatment options. Furthermore, to ensure the ethical and legal integrity of the treatment process, oversight and review by an ethics committee is required.

Postoperative adjuvant chemotherapy typically consists of four cycles. Currently, the number of cycles for postoperative immunotherapy has not been defined. Based on studies in lung cancer, postoperative immunotherapy maintenance treatment is commonly administered for a duration of 1 year (33, 34); however, a real-world study by Kwak et al. indicated that many patients are unable to complete the postoperative immunotherapy maintenance treatment on schedule (35). Therefore, further clinical trials are needed to verify the appropriate number of cycles of postoperative immunotherapy in esophageal cancer. Given the lack of imaging techniques targeting the

TABLE 2 Comparison of the incidence of adverse events during adjuvant therapy after surgery between the two groups of patients.

Variables	aCT group (*n* = 40)	aICT group (*n* = 36)	*Z*	*p*
Myelosuppression (%)			1.566	0.815
Grade 0	25 (62.5)	21 (58.3)		
Grade 1	5 (12.5)	7 (19.4)		
Grade 2	6 (15.0)	5 (13.9)		
Grade 3	3 (7.5)	3 (8.3)		
Grade 4	1 (2.5)	0 (0.0)		
Glutamic pyruvic transaminase increased (%)			1.134	0.567
Grade 0	31 (77.5)	24 (66.7)		
Grade 1	7 (17.5)	9 (25.0)		
Grade 2	2 (5.0)	3 (8.3)		
Glutamic oxaloacetic transaminase increased (%)			0.086	0.958
Grade 0	29 (72.5)	25 (69.4)		
Grade 1	8 (20.0)	8 (22.2)		
Grade 2	3 (7.5)	3 (8.3)		
Hypothyroidism (%)			9.818	0.007
Grade 0	39 (97.5)	27 (75.0)		
Grade 1	1 (2.5)	7 (19.4)		
Grade 2	0 (0.0)	2 (5.6)		
Diarrhea (%)			0.773	0.379
Grade 0	37 (92.5)	30 (83.3)		
Grade1	3 (7.5)	6 (16.7)		

aCT, adjuvant chemotherapy; aICT, adjuvant immunotherapy combined with chemotherapy.

TABLE 3 Comparison of postoperative recurrence patterns between the two groups.

Variables	aCT group (*n* = 40)	aICT group (*n* = 36)	*Z*	*p*
Tumor recurrence (%)			1.430	0.489
Mediastinal lymph nodes/esophagus	7 (17.5)	5 (13.9)		
Distant metastasis	5 (12.5)	2 (5.6)		

aCT, adjuvant chemotherapy; aICT, adjuvant immunotherapy combined with chemotherapy.

primary lesion as a main evaluation measure for effectiveness, Powles et al. reported the guiding role of ctDNA in adjuvant immunotherapy for urothelial carcinoma (36). It is essential to determine which patients will benefit from postoperative adjuvant immunotherapy for esophageal malignancies and to identify effective monitoring methods during the immunotherapy period of adjuvant treatment.

This study has some limitations. It was a single-center retrospective study with a small sample size, and the results may be influenced by specific factors related to the center's environment, equipment, and personnel, thereby limiting their generalizability and applicability. Nevertheless, retrospective studies can still hold significant value in certain contexts. Future research should consider expanding the sample size and adopting a multicenter design to enhance the study's representativeness and credibility.

In conclusion, based on our 2-year follow-up results, adjuvant chemotherapy combined with immunotherapy after R0 surgical resection does not provide superior DFS compared to postoperative chemotherapy alone for locally advanced esophageal malignancies.

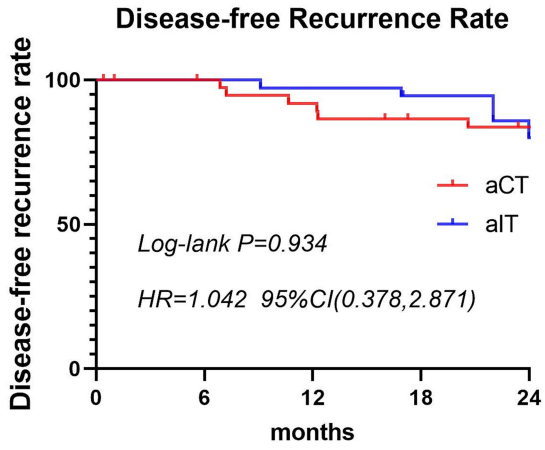

FIGURE 2
Comparison of 2-year disease-free survival between the two groups of patients after surgery. aCT, adjuvant chemotherapy; aICT, adjuvant immunotherapy combined with chemotherapy; DFS, disease-free survival.

Data availability statement

The original contributions presented in the study are included in the article/supplementary material, further inquiries can be directed to the corresponding authors.

Ethics statement

The studies involving humans were approved by the institutional review board of Ethical Committee of Gaozhou People's Hospital. The studies were conducted in accordance with the local legislation and institutional requirements. The ethics committee/institutional review board waived the requirement of written informed consent for participation from the participants or the participants' legal guardians/next of kin because this retrospective study was approved by the institutional review board of Ethical Committee of Gaozhou People's Hospital and was conducted according to the tenets of the Declaration of Helsinki. Individual consent for this retrospective analysis was waived.

Author contributions

XX: Writing – review & editing, Methodology. HZ: Writing – original draft, Conceptualization, Data curation, Software. HH: Data curation, Writing – original draft. BW: Conceptualization, Writing – original draft. YC: Resources, Writing – original draft. WL: Methodology, Supervision, Writing – original draft. QF: Formal analysis, Funding acquisition, Resources, Writing – original draft. QC: Formal analysis, Funding acquisition, Project administration, Writing – original draft.

Funding

The author(s) declare that no financial support was received for the research, authorship, and/or publication of this article.

Conflict of interest

The authors declare that the research was conducted in the absence of any commercial or financial relationships that could be construed as a potential conflict of interest.

Generative AI statement

The author(s) declare that no Generative AI was used in the creation of this manuscript.

Publisher's note

References

1. Sihag S. Advances in the surgical management of esophageal cancer. *Hematol Oncol Clin North Am*. (2024) 38:559–68. doi: 10.1016/j.hoc.2024.03.001

2. Eisner DC. Esophageal cancer: treatment advances and need for screening. *JAAPA*. (2024) 37:19–24. doi: 10.1097/01.JAA.0001007328.84376.da

3. Siaw-Acheampong K, Kamarajah SK, Gujjuri R, Bundred JR, Singh P, Griffiths EA. Minimally invasive techniques for transthoracic oesophagectomy for oesophageal cancer: systematic review and network meta-analysis. *BJS Open*. (2020) 4:787–803. doi: 10.1002/bjs5.50330

4. Chen D, Kong M, Sun J, Yang H, Chen Y, Fang W, et al. Prognostic value of recurrence pattern in locally advanced esophageal squamous cell carcinoma: results from the phase III trial NEOCRTEC5010. *J Thorac Cardiovasc Surg*. (2023) 165:888–97. doi: 10.1016/j.jtcvs.2022.08.009

5. Ni W, Yang J, Deng W, Xiao Z, Zhou Z, Zhang H, et al. Patterns of recurrence after surgery and efficacy of salvage therapy after recurrence in patients with thoracic esophageal squamous cell carcinoma. *BMC Cancer*. (2020) 20:144. doi: 10.1186/s12885-020-6622-0

6. Zhong J, Fang S, Chen R, Yuan J, Xie X, Lin T, et al. The patterns and risk factors for relapse in oesophageal squamous cell cancers that achieve pathological complete response to neoadjuvant chemoradiotherapy. *Eur J Cardiothorac Surg*. (2024) 65:ezae207. doi: 10.1093/ejcts/ezae207

7. Xu ZC, Su BA, Li JC, Cheng WF, Chen J. Pattern of relapse following three-field lymphadenectomy of esophageal carcinoma and related factors predictive of recurrence. *Cancer Radiother*. (2023) 27:189–95. doi: 10.1016/j.canrad.2022.09.001

8. Tsuji T, Matsuda S, Takeuchi M, Kawakubo H, Kitagawa Y. Updates of perioperative multidisciplinary treatment for surgically resectable esophageal cancer. *Jpn J Clin Oncol*. (2023) 53:645–52. doi: 10.1093/jjco/hyad051

9. Sun HB, Yan S, Liu XB, Xing WQ, Chen PN, Liu SL, et al. Neoadjuvant chemotherapy or adjuvant chemotherapy for esophageal squamous cell carcinoma. *Ann Surg Oncol*. (2024) 31:2443–50. doi: 10.1245/s10434-023-14581-2

10. Schröder W, Bruns CJ. Multimodal treatment of locally advanced esophageal adenocarcinoma-neoadjuvant chemoradiotherapy or perioperative chemotherapy? *Chirurgie (Heidelb)*. (2024) 95:587–8. doi: 10.1007/s00104-024-02119-5

11. Abdelhakeem A, Blum MM. Adjuvant therapies for esophageal cancer. *Thorac Surg Clin*. (2022) 32:457–65. doi: 10.1016/j.thorsurg.2022.06.004

12. Weiss JA, Jain S. Neoadjuvant and adjuvant therapy in esophageal cancer. *J Gastrointest Oncol*. (2023) 14:1927–32. doi: 10.21037/jgo-22-735

13. Zeng H, Zhang F, Sun Y, Li S, Zhang W. Treatment options for neoadjuvant strategies of esophageal squamous cell carcinoma (review). *Mol Clin Oncol*. (2024) 20:4. doi: 10.3892/mco.2023.2702

14. Csontos A, Fazekas A, Szakó L, Farkas N, Papp C, Ferenczi S, et al. Effects of neoadjuvant chemotherapy vs chemoradiotherapy in the treatment of esophageal adenocarcinoma: a systematic review and meta-analysis. *World J Gastroenterol*. (2024) 30:1621–35. doi: 10.3748/wjg.v30.i11.1621

15. Jin Z, Chen D, Chen M, Wang C, Zhang B, Zhang J, et al. (Neo)adjuvant chemoradiotherapy is beneficial to the long-term survival of locally advanced esophageal squamous cell carcinoma: a network meta-analysis. *World J Surg*. (2022) 46:136–46. doi: 10.1007/s00268-021-06301-2

16. Lin HN, Chen LQ, Shang QX, Yuan Y, Yang YS. A meta-analysis on surgery with or without postoperative radiotherapy to treat squamous cell esophageal carcinoma. *Int J Surg*. (2020) 80:184–91. doi: 10.1016/j.ijsu.2020.06.046

17. Zhao P, Yan W, Fu H, Lin Y, Chen KN. Efficacy of postoperative adjuvant chemotherapy for esophageal squamous cell carcinoma: a meta-analysis. *Thorac Cancer*. (2018) 9:1048–55. doi: 10.1111/1759-7714.12787

18. Shoji Y, Koyanagi K, Kanamori K, Tajima K, Ogimi M, Ninomiya Y, et al. Immunotherapy for esophageal cancer: where are we now and where can we go. *World J Gastroenterol*. (2024) 30:2496–501. doi: 10.3748/wjg.v30.i19.2496

19. Yao J, Tan X, Sha Y, Chen Y, Chen R, Shi D. An updated review of immunotherapy in esophageal cancer: PD-L1 footprint. *Cent Eur J Immunol*. (2024) 49:77–90. doi: 10.5114/ceji.2024.139269

20. Kato K, Kojima T, Hara H, Tsuji A, Yasui H, Muro K, et al. First-line pembrolizumab plus chemotherapy for advanced/metastatic esophageal cancer: 1-year extended follow-up in the Japanese subgroup of the phase 3 KEYNOTE-590 study. *Esophagus*. (2024) 21:306–18. doi: 10.1007/s10388-024-01053-z

21. Nian Z, Zhao Q, He Y, Xie R, Liu W, Chen T, et al. Efficacy and safety of first-line therapies for advanced unresectable oesophageal squamous cell cancer: a systematic review and network meta-analysis. *Clin Oncol (R Coll Radiol)*. (2024) 36:30–8. doi: 10.1016/j.clon.2023.09.011

22. Nevo Y, Tankel J, Zhao H, Ramirez J, Cools-Lartigue J, Muller C, et al. Influence of neoadjuvant immunotherapy-chemotherapy on perioperative outcomes in locally advanced esophageal adenocarcinoma. *Ann Surg Oncol*. (2024) 31:5666–73. doi: 10.1245/s10434-024-15186-z

23. Zhang Y, Li H, Yu B, Sun S, Hu Z, Wu X, et al. Neoadjuvant chemoimmunotherapy for locally advanced esophageal squamous cell carcinoma: data from literature review and a real-world analysis. *Thorac Cancer*. (2024) 15:1072–81. doi: 10.1111/1759-7714.15291

24. Moujaess E, Haddad FG, Eid R, Kourie HR. The emerging use of immune checkpoint blockade in the adjuvant setting for solid tumors: a review. *Immunotherapy*. (2019) 11:1409–22. doi: 10.2217/imt-2019-0087

25. Kelly RJ, Ajani JA, Kuzdzal J, Zander T, Van Cutsem E, Piessen G, et al. Adjuvant nivolumab in resected esophageal or gastroesophageal junction cancer. *N Engl J Med*. (2021) 384:1191–203. doi: 10.1056/NEJMoa2032125

26. Kita R, Matsuda S, Nomura M, Machida R, Sasaki K, Kato K, et al. Protocol digest of a randomized controlled phase III study comparing surgery alone versus adjuvant nivolumab versus adjuvant S-1 for locally advanced oesophageal squamous cell carcinoma with no pathological complete response after neoadjuvant chemotherapy followed by curative esophagectomy: Japan clinical oncology group study JCOG2206 (SUNRISE trial). *Jpn J Clin Oncol*. (2024) 54:212–6. doi: 10.1093/jjco/hyad150

27. Park S, Sun JM, Choi YL, Oh D, Kim HK, Lee T, et al. Adjuvant durvalumab for esophageal squamous cell carcinoma after neoadjuvant chemoradiotherapy: a placebo-controlled, randomized, double-blind, phase II study. *ESMO Open*. (2022) 7:100385. doi: 10.1016/j.esmoop.2022.100385

28. Wang Z, Dong L, Shi W, Gao L, Jiang X, Xue S, et al. Postoperative therapy for local-advanced gastric cancer: a systematic review and meta-analysis. *Adv Clin Exp Med*. (2024) 33:669–78. doi: 10.17219/acem/171616

29. André T, Tougeron D, Piessen G, de La Fouchardière C, Louvet C, Adenis A, et al. Neoadjuvant nivolumab plus ipilimumab and adjuvant nivolumab in localized deficient mismatch repair/microsatellite instability-high gastric or esophagogastric junction adenocarcinoma: the GERCOR neonipiga phase II study. *J Clin Oncol*. (2023) 41:255–65. doi: 10.1200/JCO.22.00686

30. Ding C, Guo Y, Zhou Y, He Y, Chen C, Zhang M, et al. Perioperative tislelizumab plus chemotherapy for locally advanced resectable thoracic esophageal squamous cell carcinoma trial: a prospective single-arm, phase II study (PILOT trial). *BMC Cancer*. (2023) 23:1237. doi: 10.1186/s12885-023-11747-9

31. Sun HB, Xing WQ, Liu XB, Yang SJ, Chen PN, Liu SL, et al. A multicenter randomized, controlled clinical trial of adjuvant sintilimab for esophageal squamous cell carcinoma. *Future Oncol*. (2023) 19:1777–84. doi: 10.2217/fon-2022-1255

32. Liu J, Blake SJ, Yong MCR, Harjunpää H, Ngiow SF, Takeda K, et al. Improved efficacy of neoadjuvant compared to adjuvant immunotherapy to eradicate metastatic disease. *Cancer Discov*. (2016) 6:1382–99. doi: 10.1158/2159-8290.CD-16-0577

33. Matsubara T, Yamaguchi M, Shimokawa M, Okamoto I. Phase II trial of adjuvant atezolizumab therapy in elderly patients with completely resected stage II/III non-small cell lung cancer: RELIANCE trial. *Clin Lung Cancer*. (2024) 25:280–3. doi: 10.1016/j.cllc.2024.01.009

34. Heymach JV, Mitsudomi T, Harpole D, Aperghis M, Jones S, Mann H, et al. Design and rationale for a phase III, double-blind, placebo-controlled study of neoadjuvant durvalumab + chemotherapy followed by adjuvant durvalumab for the treatment of patients with resectable stages II and III non-small-cell lung cancer: the Aegean trial. *Clin Lung Cancer*. (2022) 23:e247–51. doi: 10.1016/j.cllc.2021.09.010

35. Kwak HV, Banks KC, Hung YY, Alcasid NJ, Susai CJ, Patel A, et al. Adjuvant immunotherapy in curative intent esophageal cancer resection patients: real-world experience within an integrated health system. *Cancers (Basel)*. (2023) 15:5317. doi: 10.3390/cancers15225317

36. Powles T, Assaf ZJ, Davarpanah N, Banchereau R, Szabados BE, Yuen KC, et al. ctDNA guiding adjuvant immunotherapy in urothelial carcinoma. *Nature*. (2021) 595:432–7. doi: 10.1038/s41586-021-03642-9

frontiers | Frontiers in Medicine

TYPE Case Report
PUBLISHED 17 December 2024
DOI 10.3389/fmed.2024.1498290

OPEN ACCESS

EDITED BY
Yuanyuan Zheng,
Tongji University School of Medicine, China

REVIEWED BY
Guoli Zhu,
University of Pennsylvania, United States
Laixing Zhang,
University of California, Los Angeles, United States

*CORRESPONDENCE
Ana Karina Zambrano
anazambrano17@hotmail.com

†These authors have contributed equally to this work

RECEIVED 18 September 2024
ACCEPTED 22 November 2024
PUBLISHED 17 December 2024

CITATION
Guevara-Ramírez P, Ruiz-Pozo VA, Cadena-Ullauri S, Paz-Cruz E, Tamayo-Trujillo R, Gaviria A, Cevallos F and Zambrano AK (2024) Case report: Exploring Lynch Syndrome through genomic analysis in a mestizo Ecuadorian patient and his brother. *Front. Med.* 11:1498290. doi: 10.3389/fmed.2024.1498290

Case report: Exploring Lynch Syndrome through genomic analysis in a mestizo Ecuadorian patient and his brother

Patricia Guevara-Ramírez[1†], Viviana A. Ruiz-Pozo[1†], Santiago Cadena-Ullauri[1], Elius Paz-Cruz[1], Rafael Tamayo-Trujillo[1], Aníbal Gaviria[2], Francisco Cevallos[2] and Ana Karina Zambrano[1*†]

[1]Centro de Investigación Genética y Genómica, Facultad de Ciencias de la Salud Eugenio Espejo, Universidad UTE, Quito, Ecuador, [2]Hemocentro Nacional, Cruz Roja Ecuatoriana, Quito, Ecuador

Lynch Syndrome (LS) is a hereditary disorder characterized by genetic mutations in DNA mismatch repair genes, affecting approximately 0.35% of the population. LS primarily increases the risk of colorectal cancer (CRC), as well as various other cancer types like endometrial, breast, and gastric cancers. Microsatellite instability, caused by MMR gene mutations, is a key feature of LS, impacting genes such as *MLH1*, *MSH2*, *MSH6*, and *PMS2*. Pathology tests studying microsatellite instability and immunohistochemical staining are used to diagnose LS. Furthermore, next-generation sequencing (NGS) allows for a thorough investigation of cancer susceptibility genes. This approach is crucial for identifying affected individuals and managing their care effectively. This study evaluated two siblings who harbored a mutation in the *MLH1* gene associated with LS. The older brother was diagnosed with CRC at 24, while the younger brother remains asymptomatic at 7 years old. Genetic testing confirmed the presence of the *MLH1* mutation in both siblings. Ancestry analysis showed a mix of African, European, and Native American heritage, common among Ecuadorians. Both siblings shared a family history of cancer, suggesting hereditary factors. Treatment involved surgery and chemotherapy for the older brother, emphasizing the importance of genetic testing for siblings with a cancer family history. NGS plays a pivotal role in identifying genetic mutations and guiding treatment decisions, demonstrating its significance in managing LS and other hereditary cancers.

KEYWORDS

lynch syndrome, colorectal cancer, genomic, ancestral, Ecuadorian

Introduction

Lynch Syndrome (LS) is an autosomal dominant inherited disorder characterized by germline pathogenic variants in DNA mismatch repair (MMR) genes. LS carriers account for 0.35% of the general population (1). Furthermore, the lifetime risk of developing cancer in individuals LS varies depending on the mutated MMR gene, with estimates of 80% for high penetrance genes such as *MLH1* and *MSH2* (2). Individuals with LS have an elevated risk of various cancers, primarily colorectal cancer (CRC) (up to 80%), as well as other cancers, including endometrial cancer (approximately 60%) (3, 4).

Colorectal cancer is the third most frequent type of cancer worldwide (5). LS represents the predominant hereditary form of CRC. Individuals with LS have an estimated cumulative

lifetime risk of developing CRC of up to 52.2% in women and 68.7% in men (6). Approximately 15% of all CRCs exhibit a MMR-deficient phenotype, resulting in microsatellite instability (MSI) and lack of expression of MMR proteins (7, 8). Microsatellite instability is characterized by the accumulation of abnormal lengths of tandemly repeated mono- or dinucleotide sequences, which are caused by mutations in one or both alleles of MMR genes.

The primary MMR genes are *MLH1*, *MSH2*, *MSH6*, or *PMS2* and their function involves detecting and repairing DNA mismatches generated during DNA replication (9). The incidence of CRC varies based on the specific MMR gene mutation and the implementation of surveillance colonoscopies. Notably, higher cumulative incidence rates have been reported for individuals with mutations in *MLH1* (36–52%) and *MSH2* (30–50%) under surveillance, compared to those with mutations in *MSH6* (10–17%) and *PMS2* (3–11%) (10).

The diagnosis of LS typically relies on a combination of pathology tests including MSI testing and immunohistochemical staining. Furthermore, next-generation sequencing (NGS) has complemented this process by enabling simultaneous analysis of multiple cancer susceptibility genes through multiplex panels. This approach provides a cost-effective alternative compared to single-gene testing (11). Molecular testing, especially for LS, has garnered attention due to its ability to precisely identify affected individuals and its evolving significance in managing prognostic and therapeutic interventions (12, 13).

This study presents a case involving two young siblings from Ecuador, both harboring a mutation in the *MLH1* gene associated with LS. The older brother, aged 24 years, has been diagnosed with CRC, while the 7-year-old brother remains asymptomatic. Our study aims to highlight the role of NGS as a fundamental tool in the management and monitoring of cancer patients and their families.

Case presentation

This report presents a case involving two brothers, a 26-year-old man (Individual A) and an 8-year-old boy (Individual B), both of whom have a significant family history of cancer.

Individual A

Individual A reported alterations in his intestinal habits, muscle pain, and spots on the face. Hematological analysis and biochemical parameters revealed hemoglobin in the stool and anemia. A subsequent colonoscopy identified a tumor mass in the cecum, measuring approximately 6 cm. The tumor was partially obstructing the lumen of the cecum, with evidence of ulcers (Figure 1). Furthermore, a gastric biopsy revealed a well-differentiated tubulovillous adenocarcinoma of the colon. Lymph nodes were positive for malignancy, indicating lymphatic spread of the disease. The presumptive diagnosis was CRC. Genomic analyses were performed to confirm the diagnosis and assess the genetic predispositions, including LS.

Individual B

Individual B did not exhibit any symptoms. However, due to a family history of cancer, the parents authorized genomic testing to investigate potential mutations that could affect his health in the future.

Next generation sequencing (NGS)

The NGS analyses were conducted at the Centro de Investigación de Genética y Genómica (CIGG), Universidad UTE. Individual A and the legal guardians of individual B provided their informed consent before the process.

DNA extraction was performed from peripheral blood samples taken from individuals A and B, using the PureLink™ genomic DNA mini kit (Invitrogen, USA). In the case of Individual A, DNA was extracted from tissue samples in paraffin-embedded blocks with the same kit (PureLink™ genomic DNA mini kit).

The DNA concentrations were obtained using the Qubit™ fluorometer with the 1X dsDNA high-sensitivity (HS) and broad-range (BR) assay kits. NGS was performed on MiSeq platform (Illumina, USA), using the TruSight™ Cancer sequencing panel (Illumina, USA), which includes 255 kb and 94 genes related to different types of cancer. The bioinformatics analyses used were DRAGEN Enrichment v3.9.5, Annotation Engine v3.15, PolyPhen, Sift and Variant Interpreter v2.16.1.300.

Ancestry analysis

For ancestry analysis, a multiplex polymerase chain reaction (PCR) of 46 ancestry-informative INDEL markers (AIMs) was conducted, following the protocol of Zambrano et al. (2019) (14). Fragment detection was performed using Genetic Analyzer 3,500 (Applied Biosystems, USA) equipment. Data Collection v3.3 and Gene Mapper v.5 software were used for data collection and analysis, respectively. The STRUCTURE v.2.3.4 software was used for ancestry study.

Results

In individual A, genomic analyses identified a missense mutation in exon 4/19 (NM_000249.3:c.350C > T) of the *MLH1* gene and a Frameshift insertion–deletion (InDel) mutation in exon 8/9 (NM_000314.6c.968dup) of the *PTEN* gene, these mutations were detected in the paraffin-embedded tissue sample. In addition, the same *MLH1* gene mutation was observed in the DNA analysis from a blood sample. The Variant Interpreter Platform (Illumina) classified these mutations as Pathogenic for both the *MLH1* and *PTEN* genes. These analyses suggest a diagnosis consistent with LS, attributed to the variant in the *MLH1* gene.

For Individual B, who is asymptomatic and appears healthy, genomic testing revealed the presence of the same *MLH1* mutation as individual A (NM_000249.3:c.350C > T) and another mutation in the *FH* gene (NM_000143.3:c.580G > A). The latter mutation is classified as a variant of uncertain significance (VUS) and it is noteworthy because mutations in the *FH* gene have been implicated in predisposition to other cancer types (Table 1).

Furthermore, the ancestry test revealed that individual A carried 6.6% African, 13.2% European, and 80.2% Native American ancestry

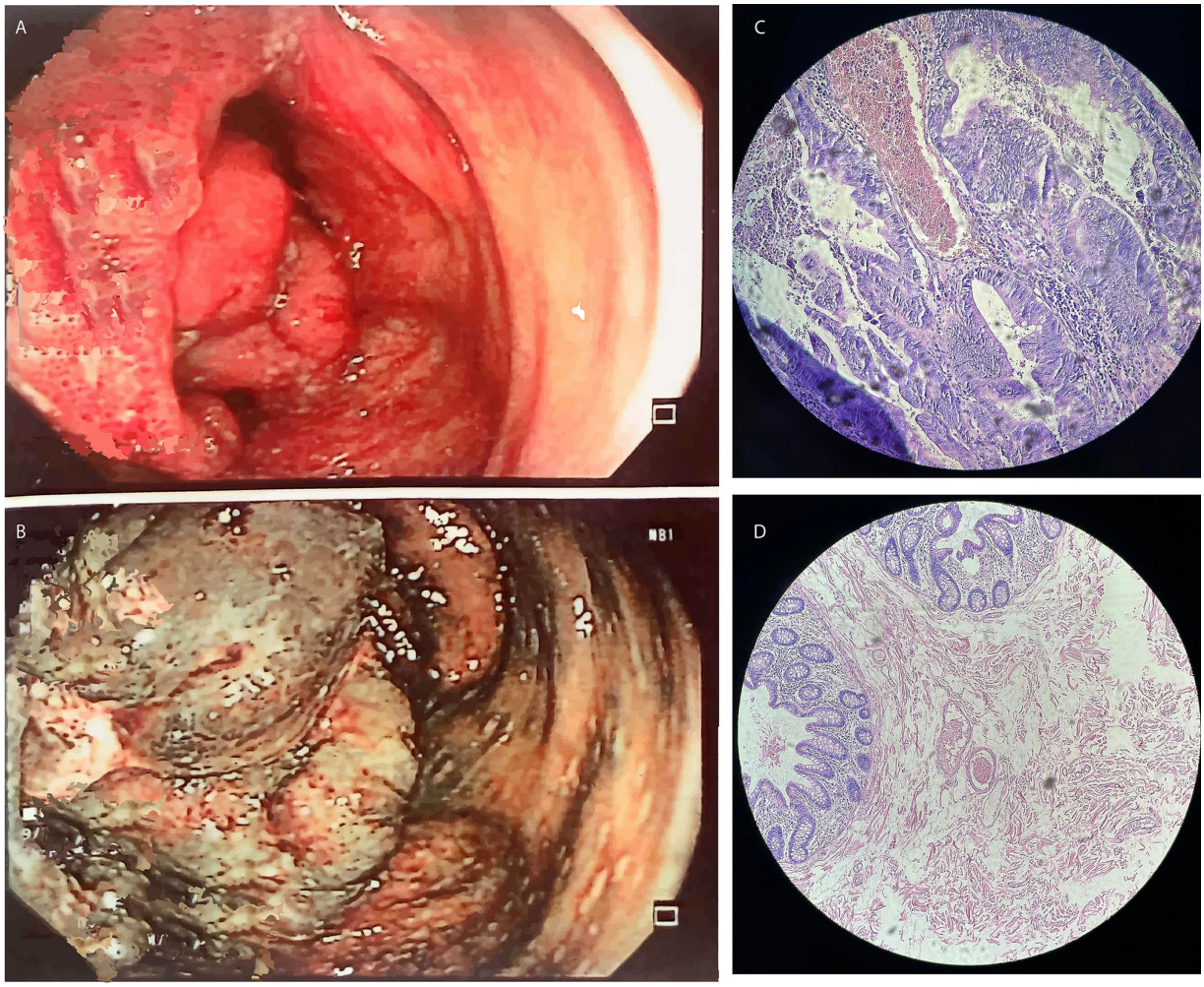

FIGURE 1
The results of the colonoscopy performed on Individual A indicated **(A,B)** Tumor mass in the cecum; **(C,D)** Hematoxylin and eosin-stained slides showing adenocarcinoma of the colon mucosa in Individual A.

proportions, while Individual B showed slightly different proportions with 5.4% African, 17.1% European, and 77.5% Native American ancestry (Supplementary Figure S1).

Family history

Both siblings shared a family history of cancer. Their maternal grandfather was diagnosed with stomach cancer, and their paternal relatives had been diagnosed with pancreatic, liver, esophageal, and breast cancer. The shared genetic mutation in the *MLH1* gene between the two siblings suggests hereditary cancer (Figure 2).

Treatment

After diagnosis, both patients were informed about the results of the genomic test and the implications of LS. Subsequently, individual A underwent an extended right hemicolectomy and ileotransverse isoperistaltic anastomosis. Individual A was subsequently treated with chemotherapy. On the other hand, Individual B was advised to continue with follow-up medical care. This case highlights the importance of genetic testing for siblings with a family history of cancer (Figure 3).

Discussion

Lynch Syndrome screening aims to enhance future cancer surveillance for the patient and offer germline variant testing for their at-risk relatives. However, traditional LS screening protocols, such as those based on clinical criteria like Amsterdam I and II or Bethesda guidelines, exhibit limited sensitivity, failing to detect over 40% of LS carriers (15). The advent of NGS has revolutionized clinical laboratory practices, enabling simultaneous sequencing of multiple cancer susceptibility genes with improved efficiency (11). In our investigation, we utilized NGS to analyze individuals with a familial cancer history, successfully identifying various variants, including a pathogenic mutation in the MutL Homolog 1 (*MLH1*) gene, present in two young siblings.

The *MLH1* gene encodes a protein essential for the DNA mismatch repair system forming heterodimer with the mismatch repair endonuclease PMS2, to generate MutL alpha complex. The encoded protein also participates in DNA damage signaling and can

TABLE 1 Genetic variants identified using TruSight™ Cancer sequencing panel.

Gene	Chr	HGVSP DNA reference	HGVS Protein reference	Consequence	Predicted effect	dbSNP/ dbVar ID	Genotype
MLH1⁺*	3	NM_000249.3 c.350C > T	NM_000249.3 p.(Thr117Met)	Missense variant	Pathogenic	rs63750781	Heterozygous
PTEN⁺	10	NM_000314.6 c.968dup	NM_000314.6 p.(Asn323LysfsTer2)	Frameshift Indels	Pathogenic	rs121913291	Heterozygous
*FH**	1	NM_000143.3 c.580G > A	NM_000143.3 p.(Ala194Thr)	Missense variant	VUS	rs587782215	Heterozygous

MLH1 variant found in both subjects A and B. *PTEN* variant found in subject A. *FH* variant found in subject B. VUS, variants of uncertain significance. ⁺Variants of subject A; *Variants of subject B.

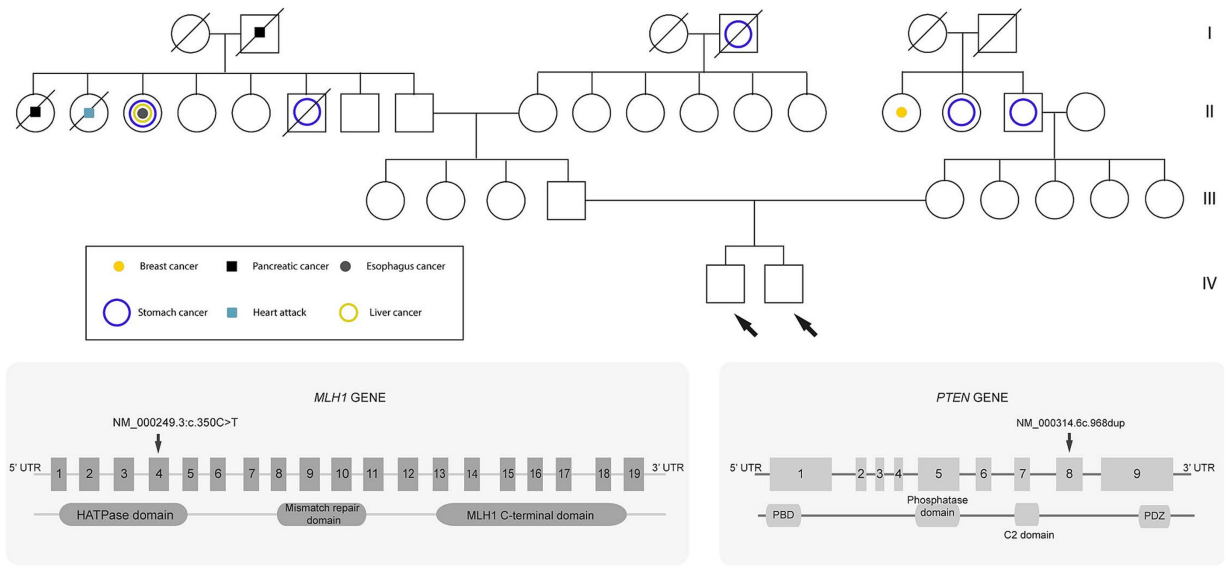

FIGURE 2
Genealogical tree of the family. Circles represent females, and squares represent males. Diagonal lines through a symbol indicate that the individual is deceased. The white circles or squares represent unaffected (healthy) individuals. Probands are indicated by the arrows.

heterodimerize with MLH3 protein to form MutL gamma, involved in meiosis (16, 17). Disruption of the MLH1-PMS2 heterodimer compromises MMR, leading to the accumulation of replication errors and increased microsatellite instability. Also, disruption of the heterodimer MLH1-MLH3 could contribute to tumor growth by accumulating errors during meiosis (18–20).

LS is an autosomal dominant disorder caused by germline mutations in MMR genes, primarily *MLH1* and *MSH2*. In families with LS, over 90% of the mutations are found in these two genes (10). Mutations in the *MLH1* gene impair the protein's ability to recognize and repair DNA damage. This leads to the accumulation of genetic errors and hinders apoptosis signaling, which could promote the development of cancer (16, 17). LS is associated with an increased predisposition to different cancer types, primarily colon cancer (occurring in 46–61% of individuals with a pathogenic *MLH1* variant) or endometrial cancer (occurring in 34–54% of individuals with a pathogenic *MLH1* variant) (2, 21). Colorectal cancer, associated with Lynch syndrome, tends to manifest at an earlier age, with an average age of diagnosis around 40 years (22).

In both subjects, the *MLH1* gene variant c.350C > T (p.Thr117Met) was identified, and notably, in Individual A, this variant was present in both blood and tissue samples. According to the InSiGHT classification, the *MLH1* variant is classified as class 5 (pathogenic) (23, 24). The c.350C > T variant affects a highly conserved domain in exon 4 of the *MLH1* gene. This genetic change arises from cytosine to thymine substitution at position 350 in the nucleotide sequence (25, 26), causing codon 117 undergoes a pathogenic transformation, replacing a polar threonine with a hydrophobic methionine in a highly conserved domain of the *MLH1* gene.

Different tests are used for the detection of LS associated with CRC, such as colonoscopy, genetic testing, MSI, immunohistochemistry (IHC) and others. Immunohistochemistry, used for screening patients with suspected LS, can detect approximately 74% of MLH1 germline mutations when using MLH1-specific antibodies (27). This test uses antibodies against four MMR proteins (MLH1, MS2, MSH6, and PMS2) to assess their expression in colorectal cancer tissue (28). For example, the biological interpretation of the *MLH1* gene mutation could be shown by IHC that has demonstrated a reduction in DNA repair activity in cells carrying the Thr117Met variant which is associated with increased MSI. Functional analyses reveal reduced protein expression and compromised mismatch repair (MMR) activity linked to the

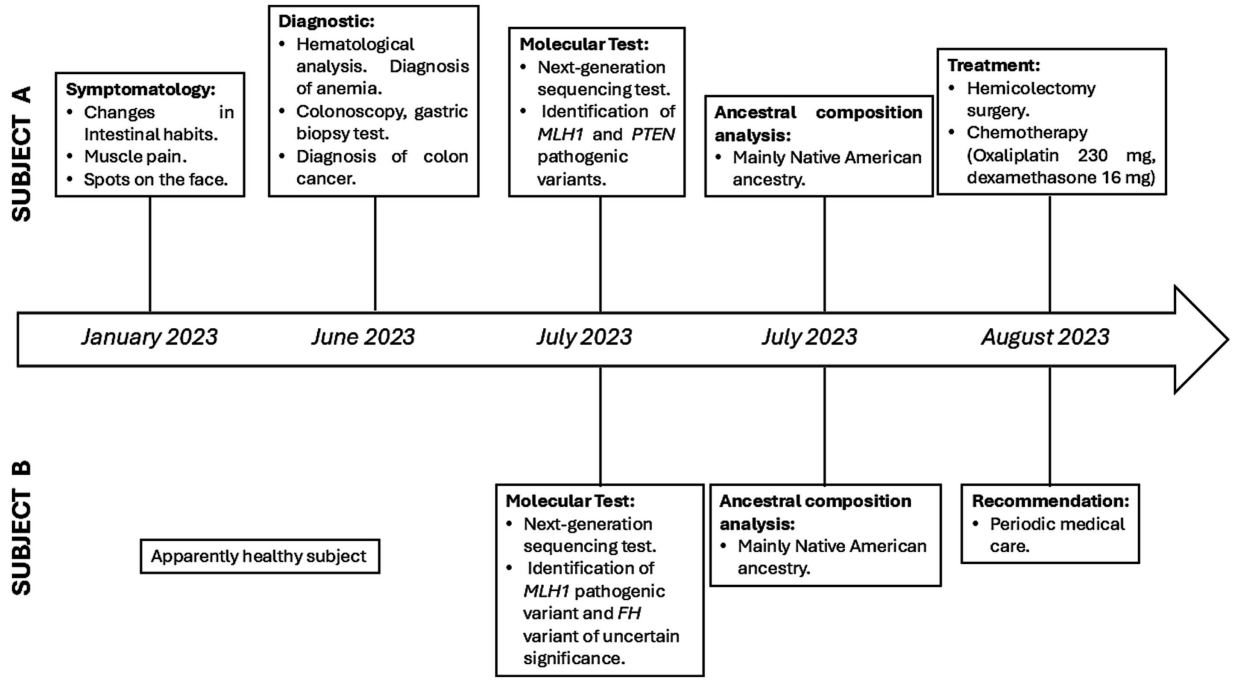

FIGURE 3
Timeline of subject A and B. The relevant episodes related to the siblings.

disruption caused by the Thr117Met variant (29, 30). Moreover, this missense mutation likely impairs mismatch repair function by affecting the mutant protein's ATP binding and hydrolysis, interfering with the formation of protein complex like hPMS2.

Considering that individual A has adenocarcinoma of the colon and carries a mutation in the *MLH1* gene, MSI analysis of the tumor samples is recommended. This test is essential not only for confirming the diagnosis of LS but also for its prognosis, as MSI has been established as a key biomarker in CRCs. In the general population, the rate of MSI varies between 12 and 17% but has been reported to be as high as 27 to 35% in patients younger than 30 years (31). In the case of 26-year-old A, an evaluation of MSI would not only contribute to a better understanding of his diagnosis but is also essential to guide appropriate follow-up and treatment for both him and his brother.

Determination of MSI has important prognostic value, as tumors with high instability are often associated with a better clinical prognosis. In addition, MSI has been established as a predictive biomarker in the context of immunotherapy, suggesting that immune checkpoint inhibitors may be more effective in these cases. This is because tumors with a higher mutational burden, characteristic of elevated MSI, generate a greater number of neoantigens (32). These neoantigens can stimulate an immune response, making MMR-deficient tumors particularly responsive to immune checkpoint inhibitors, such as anti-PD-1/PD-L1 therapies (33–35). In our case, the MLH1 c.350C > T variant, associated with increased microsatellite instability, could potentially create a pro-inflammatory tumor microenvironment. Understanding the interplay between mismatch repair gene mutations and immune response could lead to personalized immunotherapeutic strategies for Lynch Syndrome patients (14, 15). In this context, performing MSI analysis is not only crucial for the diagnosis and treatment of individual A, but also for the preventive management and follow-up of individual B, given the possible heritable involvement of mutations in the MLH1 gene (36).

This study marks the first report of this variant in Ecuadorian patients. Nevertheless, the variant has also been previously identified in unrelated families from Uruguay and Argentina, suggesting that the c.350C > T variant may be present within the broader Latin American gene pool (37). Notably, the reported frequency of the alternative allele T is 0,000 in the Latin American population (38).

Furthermore, this variant was identified in other populations. For instance, Yanus et al. (39) studied Russian individuals with either colorectal or endometrial cancer, who were referred for LS testing, revealing the *MLH1* c.350C > T variant. The results are consistent with the UMD-MMR database, which includes 55 entries for the mutation in French laboratories until 2015 (40). Moreover, another study focused on analyzing the *MLH1* gene in Polish and Baltic State families, revealing the mutation in one family with colon cancer (19). Another study reported the mutation in a hereditary nonpolyposis colorectal cancer patient in Slovakia (26). These studies collectively highlight the recurrent nature of the mutation across diverse geographical regions. Despite its global prevalence, the mutation has not been previously reported in Ecuador (14).

In the tumor sample from individual A, a *PTEN* c.968dup variant was identified. This variant results in a frameshift and a premature stop codon, probably producing absent or truncated PTEN protein. The truncation caused by c.968dup disrupts critical domains such as C2, C-tail, and PDZ, which play pivotal roles in protein localization, stability, and interaction with other proteins (41, 42).

PTEN is a tumor suppressor that regulates the PI3K/Akt signaling pathway, which is crucial for cell growth and survival. In colorectal cancer, loss of *PTEN* function leads to increased activity in this pathway, promoting tumorigenesis (43, 44). Other research suggests that loss of PTEN in CRC is closely associated with increased genomic instability and worse clinical outcomes, such as more advanced disease stages and the development of liver metastasis (45, 46). In this case study, the pathogenic

variants in the *PTEN* and *MLH1* genes identified in individual A could trigger an additive effect from mutations in different genes, leading to a more aggressive disease phenotype.

However, this relationship is not consistently observed across all studies, suggesting that the role of *PTEN* in tumor progression may be influenced by other genetic or epigenetic factors (45–48). Moreover, in an extensive study involving 1,093 cases of CRC, *PTEN* mutations were detected in 43 tumors. Among these mutations, 47.3% were identified as nonsense mutations, 38.2% as frameshift mutations, 9.1% as missense mutations, and 5.5% as splice site mutations. Notably, the c.968dup variant was among the frameshift mutations closely related to CRC (49). This variability highlights the molecular complexity of CRC, particularly in cases linked to LS, and underscores the importance of further investigation to fully understand the impact of *PTEN* on CRC development and progression.

On the other hand, individual B carries a *FH* c.580G > A mutation, which has been implicated in hereditary cancer predisposition (50). The variant frequency has not been reported among the Latin American population. The c.580G > A variant, also denoted as p.Ala194Thr, is situated within the coding sequence of exon 5 in the *FH* gene. This genetic alteration arises from the substitution of alanine for threonine at codon 194. Notably, alanine is characterized as neutral and non-polar, whereas threonine possesses a neutral and polar nature. Consequently, advanced protein modeling techniques, coupled with the scrutiny of their physical properties, have revealed that this missense variant disrupts the functionality of FH protein (51). Despite this, the variant has been categorized as a variant of uncertain significance, primarily due to findings from RNA analysis suggesting that its impact on mRNA splicing does not significantly alter splicing patterns. Furthermore, associations have been made between this variant and other types of cancer such as pheochromocytoma, paraganglioma, and renal cell cancer. However, its low population frequency (0.00007), mainly present in individuals of European descent, makes it uninformative for assessing its pathogenicity (51, 52).

Furthermore, the PTEN protein has a physical or functional interaction with MLH1, while the FH protein does not show any interaction with *PTEN* or MLH1 (Supplementary Figure S2). However, the coexistence of these variants in individuals could have synergistic effects, potentially increasing their cancer risk. Even though the assay employed in this investigation covered some genes implicated in mismatch repair, it would be interesting to utilize a multigene panel encompassing an extensive spectrum of genes or SNPs associated with LS.

The genetic analysis of the ancestral components of the two brothers harboring the *MLH1* c.350C > T variant, along with additional variants (*PTEN* c.968dup for individual A and *FH* c.580G > A for individual B), has provided a further understanding of the possible relationship between genetic ancestry and specific mutations associated with hereditary cancer predisposition.

Moreover, the ancestral composition of the individuals revealed a mosaic of African, European, and Native American components, as previously reported for the Ecuadorian (14). However, both siblings have high levels of Native American ancestry, which is notable given a lack of data on population specific genetic risks in this group. Although ancestry data does not directly elucidate cancer predisposition in this case, the Native American heritage may offer insights into underrepresented genetic variants relevant to Lynch Syndrome and cancer. Further studies on larger cohorts are needed to explore the relationship between ancestry and cancer risk in Latin American (14).

The *MLH1* c.350C > T variant, associated with Lynch syndrome, has been extensively studied and reported in different regions, such as Latin America (37) and Europe (19, 26, 39, 40). Besides, a study compared the racial differences in *MLH1* mutations between the Caucasian and East Asian races and found that this variant ranks among the top ten mutations in both ethnic groups (53). The prevalence of this mutation in individuals with predominantly Native American ancestry is of particular interest and has not been previously reported, which could provide insights into population-specific genetic risk factors. However, the *PTEN* and *FH* variants have not been previously described in other populations.

Consequently, employing multiple gene sequencing may benefit patients, especially those with personal or familial histories. The identification of individuals with hereditary cancer predispositions, such as Lynch syndrome, holds significant promise for reducing cancer incidence and mortality rates. Nonetheless, accessing comprehensive mutation screening may present challenges in certain scenarios. However, once mutations are identified, screening other family members for the same mutation can be achieved using relatively straightforward methods (15).

In this study, we used NGS panels that included the MMR genes (*MLH1, MSH2, MSH6, or PMS2*), identifying a pathogenic *MLH1* mutation in both siblings. This finding underscores the importance of genomic testing in detecting germline mutations within families. Clinically, it enables a more precise diagnosis and treatment for Individual A, who is symptomatic, while providing necessary follow-up for Individual B, who remains asymptomatic.

A limitation of this study is the budget constraint, because NGS could not be performed on all family members. Despite this constraint, the screening process remains informative and contributes significantly to continuous patient monitoring. Consequently, the adoption of massive sequencing approaches may provide valuable insights, enabling the implementation of effective cancer prevention strategies, personalized screening protocols, and tailored therapeutic interventions to mitigate cancer-related morbidity and mortality linked to Lynch Syndrome (11, 54).

In conclusion, the ancestral components, and associated variants of the two siblings provide the first data of a mainly Native American composition and mutations related to LS and cancer predisposition. Further studies on diverse populations and larger cohorts could improve the understanding of population-specific variants, their implications, and healthcare strategies.

Data availability statement

The original contributions presented in the study are included in the article/Supplementary material, further inquiries can be directed to the corresponding author/s.

Ethics statement

The studies involving humans were approved by Human Research Ethics Committee-University UTE. The studies were conducted in accordance with the local legislation and institutional requirements. Written informed consent for participation in this study was provided by the participants' legal guardians/next of kin. Written informed consent was obtained from the individual(s) for the publication of any potentially identifiable images or data included in this article.

Author contributions

PG-R: Conceptualization, Methodology, Writing – original draft, Writing – review & editing. VR-P: Conceptualization, Methodology, Writing – original draft, Writing – review & editing. SC-U: Methodology, Writing – review & editing. EP-C: Methodology, Writing – review & editing. RT-T: Methodology, Writing – review & editing. AG: Conceptualization, Writing – review & editing. FC: Conceptualization, Writing – review & editing. AZ: Conceptualization, Funding acquisition, Methodology, Supervision, Writing – original draft, Writing – review & editing.

Funding

The author(s) declare that financial support was received for the research, authorship, and/or publication of this article. The experimentation and publication fee of this article are funded by Universidad UTE.

Acknowledgments

We are grateful to Universidad UTE for supporting the researchers. Furthermore, the authors are grateful to Alex Tulcán Cuadros for his help during the project.

Conflict of interest

The authors declare that the research was conducted in the absence of any commercial or financial relationships that could be construed as a potential conflict of interest.

Publisher's note

Supplementary material

The Supplementary material for this article can be found online at: https://www.frontiersin.org/articles/10.3389/fmed.2024.1498290/full#supplementary-material

SUPPLEMENTARY FIGURE S1
Ancestral composition of the subjects under analysis (in yellow).

SUPPLEMENTARY FIGURE S2
Protein – protein physical and functional association (constructed with STRING).

References

1. Umemiya M, Horikawa N, Kanai A, Saeki A, Ida K, Makio S, et al. Endometrial Cancer diagnosed at an early stage during lynch syndrome surveillance: a case report. *Case Rep Oncol*. (2023) 16:634–9. doi: 10.1159/000531837

2. Peltomäki P, Nyström M, Mecklin JP, Seppälä TT. Lynch syndrome genetics and clinical implications. *Gastroenterology*. (2023) 164:783–99. doi: 10.1053/J.GASTRO.2022.08.058

3. Mukucha K-E, Manase MT, Muronda C, Whittaker J, Guzha BT. Challenges managing women with suspected lynch syndrome in Zimbabwe: a case report. *South African J Gynaecol Oncol*. (2021) 13:42–4. doi: 10.1080/20742835.2021.1991100

4. Ito T, Kono K, Eguchi H, Okazaki Y, Yamamoto G, Tachikawa T, et al. Prevalence of lynch syndrome among patients with upper urinary tract carcinoma in a Japanese hospital-based population. *Jpn J Clin Oncol*. (2020) 50:80–8. doi: 10.1093/jjco/hyz140

5. Sung H, Ferlay J, Siegel RL, Laversanne M, Soerjomataram I, Jemal A, et al. Global Cancer statistics 2020: GLOBOCAN estimates of incidence and mortality worldwide for 36 cancers in 185 countries. *CA Cancer J Clin*. (2021) 71:209–49. doi: 10.3322/caac.21660

6. Abu-Ghazaleh N, Kaushik V, Gorelik A, Jenkins M, Macrae F. Worldwide prevalence of lynch syndrome in patients with colorectal Cancer: systematic review and Meta-analysis. *Genet Med*. (2022) 24:971–85. doi: 10.1016/J.GIM.2022.01.014

7. Bohaumilitzky L, von Knebel Doeberitz M, Kloor M, Ahadova A. Implications of hereditary origin on the immune phenotype of mismatch repair-deficient cancers: systematic literature review. *J Clin Med*. (2020) 9:1741. doi: 10.3390/JCM9061741

8. Boland CR, Goel A. Microsatellite instability in colorectal Cancer. *Gastroenterology*. (2010) 138:2073–2087.e3. doi: 10.1053/J.GASTRO.2009.12.064

9. Evrard C, Tachon G, Randrian V, Karayan-Tapon L, Tougeron D. Microsatellite instability: diagnosis, heterogeneity, discordance, and clinical impact in colorectal Cancer. *Cancers (Basel)*. (2019) 11:1567. doi: 10.3390/CANCERS11101567

10. Helderman NC, van Leerdam ME, Kloor M, Ahadova A, Nielsen M. Emerge of colorectal Cancer in lynch syndrome despite colonoscopy surveillance: a challenge of Hide and Seek. *Crit Rev Oncol Hematol*. (2024) 197:104331. doi: 10.1016/J.CRITREVONC.2024.104331

11. Yurgelun MB, Hampel H. Recent advances in lynch syndrome: diagnosis, treatment, and Cancer prevention. *Am Soc Clin Oncol Educ Book*. (2018) 38:101–9. doi: 10.1200/EDBK_208341

12. Sobocińska J, Kolenda T, Teresiak A, Badziąg-Leśniak N, Kopczyńska M, Guglas K, et al. Diagnostics of Mutations in MMR/ EPCAM Genes and Their Role in the Treatment and Care of Patients with Lynch Syndrome. *Diagnostics*. (2020) 10:786. doi: 10.3390/diagnostics10100786

13. Yao ZG, Lv BB, Jing HY, Su WJ, Li JM, Fan H, et al. A practical screening strategy for lynch syndrome and lynch syndrome mimics in colorectal Cancer. *J Cancer Res Ther*. (2021) 17:790–6. doi: 10.4103/JCRT.JCRT_214_21

14. Zambrano AK, Gaviria A, Cobos-Navarrete S, Gruezo C, Rodríguez-Pollit C, Armendáriz-Castillo I, et al. The three-hybrid genetic composition of an Ecuadorian population using AIMs-InDels compared with autosomes, mitochondrial DNA and Y chromosome data. *Sci Rep*. (2019) 9:9247. doi: 10.1038/s41598-019-45723-w

15. Pasanen A, Loukovaara M, Kaikkonen E, Olkinuora A, Pylvänäinen K, Alhopuro P, et al. Testing for lynch syndrome in endometrial carcinoma: from universal to age-selective MLH1 methylation analysis. *Cancers*. (2022) 14:1348. doi: 10.3390/CANCERS14051348

16. Thompson BA, Goldgar DE, Paterson C, Clendenning M, Walters R, Arnold S, et al. A multifactorial likelihood model for MMR gene variant classification incorporating probabilities based on sequence bioinformatics and tumor characteristics: a report from the Colon Cancer family registry. *Hum Mutat*. (2013) 34:200–9. doi: 10.1002/humu.22213

17. Stelzer G, Rosen N, Plaschkes I, Zimmerman S, Twik M, Fishilevich S, et al. The GeneCards suite: from gene data mining to disease genome sequence analyses. *Curr Protoc Bioinformatics*. (2016) 54:1.30.1–1.30.33. doi: 10.1002/cpbi.5

18. Frostberg E, Petersen AH, Bojesen A, Rahr HB, Lindebjerg J, Rønlund K. The prevalence of pathogenic or likely pathogenic germline variants in a Nationwide cohort of Young colorectal Cancer patients using a panel of 18 genes associated with colorectal Cancer. *Cancers*. (2021) 13:5094. doi: 10.3390/cancers13205094

19. Kurzawski G, Suchy J, Kładny J, Safranow K, Jakubowska A, Elsakov P, et al. Germline MSH2 and MLH1 mutational spectrum in HNPCC families from Poland and the Baltic States. *J Med Genet*. (2002) 39:65e–665e. doi: 10.1136/jmg.39.10.e65

20. Talbot A, O'Donovan E, Berkley E, Nolan C, Clarke R, Gallagher D. The contribution of lynch syndrome to early onset malignancy in Ireland. *BMC Cancer*. (2021) 21:617. doi: 10.1186/s12885-021-08263-z

21. Massachusetts General Hospital Cancer Center. (2023). Lynch syndrome: information for families with a pathogenic variant in the MLH1 Gene Available at: https://www.massgeneral.org/assets/mgh/pdf/cancer-center/genetics/mlh1/mlh1_result_handout_2021.pdf.

22. Momma T, Gonda K, Akama Y, Endo E, Ujiie D, Fujita S, et al. MLH1 germline mutation associated with lynch syndrome in a family followed for more than 45 years. *BMC Med Genet*. (2019) 20:67. doi: 10.1186/S12881-019-0792-0

23. Pinto RM, Dragileva E, Kirby A, Lloret A, Lopez E, St Claire J, et al. Mismatch repair genes Mlh1 and Mlh3 modify CAG instability in Huntington's disease mice: genome-wide and candidate approaches. *PLoS Genet*. (2013) 9:e1003930. doi: 10.1371/journal.pgen.1003930

24. Global Variome shared LOVD. (2024). All variants in the MLH1 Gene Available at: https://databases.lovd.nl/shared/variants/MLH1?search_VariantOnGenome/Genetic_origin=SUMMARY#object_id=VariantOnTranscript%2CVariantOnGenome&id=MLH1&order=VariantOnTranscript%2FDNA%2CASC&search_transcriptid=00013676&search_VariantOnGenome/Genetic_origin=S (Accessed on 21 December 2024).

25. Bennett G, Rudzki Z, Cole S, Young G, Suthers G. The impact of molecular diagnosis on familial colorectal. *Cancer*. (1998) 36:641–4. doi: 10.1515/CCLM.1998.113

26. Zavodna K, Bujalkova M, Krivulcik T, Alemayehu A, Skorvaga M, Marra G, et al. Novel and recurrent germline alterations in the MLH1 and MSH2 genes identified in hereditary nonpolyposis colorectal Cancer patients in Slovakia*. *Neoplasma*. (2006) 53:269–76. doi: 10.5167/uzh-34290

27. Mojtahed A, Schrijver I, Ford JM, Longacre TA, Pai RK. A two-antibody mismatch repair protein immunohistochemistry screening approach for colorectal carcinomas, skin sebaceous tumors, and gynecologic tract carcinomas. *Mod Pathol*. (2011) 24:1004–14. doi: 10.1038/modpathol.2011.55

28. Sarode VR, Robinson L. Screening for lynch syndrome by immunohistochemistry of mismatch repair proteins: significance of indeterminate result and correlation with mutational studies. *Arch Pathol Lab Med*. (2019) 143:1225–33. doi: 10.5858/arpa.2018-0201-OA

29. Jäger AC, Rasmussen M, Bisgaard HC, Singh KK, Nielsen FC, Rasmussen LJ. HNPCC mutations in the human DNA mismatch repair gene HMLH1 influence assembly of HMutLα and HMLH1–HEXO1 complexes. *Oncogene*. (2001) 20:3590–5. doi: 10.1038/sj.onc.1204467

30. Trojan J, Zeuzem S, Randolph A, Hemmerle C, Brieger A, Raedle J, et al. Functional analysis of HMLH1 variants and HNPCC-related mutations using a human expression system. *Gastroenterology*. (2002) 122:211–9. doi: 10.1053/gast.2002.30296

31. Battaglin F, Naseem M, Lenz HJ, Salem ME. Microsatellite instability in colorectal Cancer: overview of its clinical significance and novel perspectives. *Clin Adv Hematol Oncol*. (2018) 16:735–45.

32. Shaikh R, Bhattacharya S, Prajapati BG. Microsatellite instability: a potential game-changer in colorectal Cancer diagnosis and treatment. *Results Chem*. (2024) 7:101461. doi: 10.1016/J.RECHEM.2024.101461

33. Zhao P, Li L, Jiang X, Li Q. Mismatch repair deficiency/microsatellite instability-high as a predictor for anti-PD-1/PD-L1 immunotherapy efficacy. *J Hematol Oncol*. (2019) 12:1–14. doi: 10.1186/S13045-019-0738-1/TABLES/5

34. Puccini A, Battaglin F, Iaia ML, Lenz HJ, Salem ME. Overcoming resistance to anti-PD1 and anti-PD-L1 treatment in gastrointestinal malignancies. *J Immunother Cancer*. (2020) 8:e000404. doi: 10.1136/JITC-2019-000404

35. Kim ST, Klempner SJ, Park SH, Park JO, Park YS, Lim HY, et al. Correlating programmed death ligand 1 (PD-L1) expression, mismatch repair deficiency, and outcomes across tumor types: implications for immunotherapy. *Oncotarget*. (2017) 8:77415–23. doi: 10.18632/ONCOTARGET.20492

36. Abidi A, Gorris MAJ, Brennan E, Jongmans MCJ, Weijers DD, Kuiper RP, et al. Challenges of Neoantigen targeting in lynch syndrome and constitutional mismatch repair deficiency syndrome. *Cancers (Basel)*. (2021) 13:2345. doi: 10.3390/CANCERS13102345

37. Rossi BM, Palmero EI, López-Kostner F, Sarroca C, Vaccaro CA, Spirandelli F, et al. A survey of the Clinicopathological and molecular characteristics of patients with suspected lynch syndrome in Latin America. *BMC Cancer*. (2017) 17:1–26. doi: 10.1186/s12885-017-3599-4

38. National Library of Medicine Rs63750781 RefSNP Report - DbSNP. (2022). Available at: https://www.ncbi.nlm.nih.gov/snp/rs63750781 (Accessed on 16 December 2023).

39. Yanus GA, Akhapkina TA, Iyevleva AG, Kornilov AV, Suspitsin EN, Kuligina ES, et al. The Spectrum of lynch syndrome-associated germ-line mutations in Russia. *Eur J Med Genet*. (2020) 63:103753. doi: 10.1016/j.ejmg.2019.103753

40. The French National Committee of Informatics and Liberty. (2014). Available at: http://www.umd.be/MLH1/4DACTION/DMD_EX1/4 (Accessed on 24 October 2024).

41. PTEN Regulatory functions in tumor suppression and cell biology - PubMed. (2004). Available at: https://pubmed.ncbi.nlm.nih.gov/15448614/ (Accessed on 22 April 2024).

42. Brito MB, Goulielmaki E, Papakonstanti EA. Focus on PTEN regulation. *Front Oncol*. (2015) 5:5. doi: 10.3389/FONC.2015.00166

43. Rascio F, Spadaccino F, Rocchetti MT, Castellano G, Stallone G, Netti GS, et al. The pathogenic role of PI3K/AKT pathway in Cancer onset and drug resistance: an updated review. *Cancers (Basel)*. (2021) 13:3949. doi: 10.3390/CANCERS13163949

44. Salvatore L, Calegari MA, Loupakis F, Fassan M, Di Stefano B, Bensi M, et al. PTEN in colorectal Cancer: shedding light on its role as predictor and target. *Cancers (Basel)*. (2019) 11:1765. doi: 10.3390/CANCERS11111765

45. Guanti G, Resta N, Simone C, Cariola F, Demma I, Fiorente P, et al. Involvement of PTEN mutations in the genetic pathways of colorectal Cancerogenesis. *Hum Mol Genet*. (2000) 9:283–7. doi: 10.1093/HMG/9.2.283

46. Molinari F, Frattini M. Functions and regulation of the PTEN gene in colorectal Cancer. *Front Oncol*. (2014) 3:326. doi: 10.3389/FONC.2013.00326

47. Zhou XP, Loukola A, Salovaara R, Nystrom-Lahti M, Peltomäki P, De la Chapelle A, et al. PTEN mutational spectra, expression levels, and subcellular localization in microsatellite stable and unstable colorectal cancers. *Am J Pathol*. (2002) 161:439–47. doi: 10.1016/S0002-9440(10)64200-9

48. List of Variants in Gene PTEN reported as pathogenic for hereditary Cancer-predisposing syndrome - ClinVar miner. (2024). Available at: https://clinvarminer.genetics.utah.edu/variants-by-gene/PTEN/condition/Hereditary%20cancer-predisposing%20syndrome/pathogenic (Accessed on 6 November 2024).

49. Day FL, Jorissen RN, Lipton L, Mouradov D, Sakthianandeswaren A, Christie M, et al. PIK3CA and PTEN gene and Exon mutation-specific Clinicopathologic and molecular associations in colorectal Cancer. *Clin Cancer Res*. (2013) 19:3285–96. doi: 10.1158/1078-0432.CCR-12-3614

50. NCBI. VCV000142075.34 - ClinVar. (2024). Available at:https://www.ncbi.nlm.nih.gov/clinvar/variation/142075/ (Accessed on 6 November 2024).

51. Jaime Castro-Vega L, Buffet A, De Cubas AA, Cascó A, lanie Menara M, Khalifa E, et al. Germline mutations in FH confer predisposition to malignant Pheochromocytomas and Paragangliomas. *Hum Mol Genet*. (2014) 23:2440–6. doi: 10.1093/hmg/ddt639

52. Zavoshi S, Lu E, Boutros PC, Zhang L, Harari A, Hatchell KE, et al. Fumarate hydratase variants and their association with Paraganglioma/Pheochromocytoma. *Urology*. (2023) 176:106–14. doi: 10.1016/J.UROLOGY.2022.11.053

53. Wei W, Liu L, Chen J, Jin K, Jiang F, Liu F, et al. Racial differences in MLH1 and MSH2 mutation: an analysis of yellow race and white race based on the Insight database. *J Bioinforma Comput Biol*. (2010) 8:111–25. doi: 10.1142/S0219720010005154

54. Tung N, Battelli C, Allen B, Kaldate R, Bhatnagar S, Bowles K, et al. Frequency of mutations in individuals with breast Cancer referred for BRCA1 and BRCA2 testing using next-generation sequencing with a 25-gene panel. *Cancer*. (2015) 121:25–33. doi: 10.1002/CNCR.29010

frontiers | Frontiers in Medicine

TYPE Original Research
PUBLISHED 26 February 2025
DOI 10.3389/fmed.2025.1516307

OPEN ACCESS

EDITED BY
Hua Zhong,
University of Hawaii at Manoa, United States

REVIEWED BY
Radhika Amaradhi,
University of Texas at San Antonio, United States
Zhanyang Luo,
Shanghai Pudong Hospital, China
Yiqian Zhang,
Tulane University, United States

*CORRESPONDENCE
Songpo Wang
✉ wsp_tcm@163.com

†These authors have contributed equally to this work

RECEIVED 24 October 2024
ACCEPTED 12 February 2025
PUBLISHED 26 February 2025

CITATION
Li Y, Chen K, Li Q, Liu Q, Han H, Liu H and Wang S (2025) Exploring the therapeutic potential of "Zhi-Zhen" formula for oxaliplatin resistance in colorectal cancer: an integrated study combining UPLC-QTOF-MS/MS, bioinformatics, network pharmacology, and experimental validation.
Front. Med. 12:1516307.
doi: 10.3389/fmed.2025.1516307

Exploring the therapeutic potential of "Zhi-Zhen" formula for oxaliplatin resistance in colorectal cancer: an integrated study combining UPLC-QTOF-MS/MS, bioinformatics, network pharmacology, and experimental validation

Yongjing Li[1,2†], Ke Chen[1†], Qin Li[3], Qiaoli Liu[1], Huijie Han[1], Hui Liu[1] and Songpo Wang[1*]

[1]Department of Traditional Chinese Medicine, Shanghai General Hospital, Shanghai Jiao Tong University School of Medicine, Shanghai, China, [2]Department of Traditional Chinese Medicine, Shuguang Hospital Affiliated to Shanghai University of Traditional Chinese Medicine, Shanghai, China, [3]Department of Pharmacy, Shanghai General Hospital, Shanghai Jiao Tong University School of Medicine, Shanghai, China

Background: Chemoresistance is a critical factor compromising the survival of patients with colorectal cancer (CRC). The "Zhi-Zhen" formula (ZZF), a traditional prescription developed by Chinese national medicine masters, has been extensively used in clinical practice to treat gastrointestinal cancer. Notably, ZZF has the potential to enhance tumor sensitivity to chemotherapy. Although previous *in vitro* studies have demonstrated the efficacy of ZZF in overcoming chemoresistance in colorectal cancer (CRC), its precise molecular mechanisms remain poorly understood.

Materials and methods: We used an integrated approach of bioinformatics and network pharmacology to predict the potential active ingredients and targets of ZZF in alleviating chemoresistance. The top five active ingredients identified by degree in the network analysis were validated using mass spectrometry. We then established an oxaliplatin-resistant CRC cell model to explore the potential targets and regulatory mechanisms through which ZZF overcomes chemoresistance at the cellular level.

Results: Network pharmacology and bioinformatics analyses jointly identified 29 active compounds and 13 potential key targets of ZZF, associated with chemoresistance. Among these targets, the differential expression of CASP7 significantly affected the progression-free survival of patients with CRC. We established two oxaliplatin-resistant CRC cell lines and observed an upregulation of CASP7 expression in these resistant cells. Furthermore, ZZF increases the expression and activation of CASP7 in resistant cells, promoting apoptosis, and thereby ameliorating chemoresistance. Additionally, β-catenin knockdown led to an upregulation of CASP7 expression, whereas activation of the Wnt/β-catenin signaling pathway reduced CASP7 protein levels. ZZF

decreases the activity of the Wnt/β-catenin signaling pathway by decreasing β-catenin transcription and nuclear localization.

Conclusion: ZZF has potential clinical value in the treatment of chemoresistance in CRC by inhibiting the transcription and nuclear localization of β-catenin, thereby increasing the expression of CASP7 and enhancing the apoptotic response in chemoresistant CRC cells.

KEYWORDS

traditional Chinese medicine, colorectal cancer, chemoresistance, caspase-7, Wnt/β-catenin signaling

1 Introduction

Colorectal cancer (CRC) is a prevalent malignant tumor with high morbidity (9.6%) and mortality (9.3%) rates among newly diagnosed cancer cases and cancer-related deaths, as reported by Global Cancer Statistics 2022 (1). Population-based data from the National Cancer Institute indicates that the 5-year survival rate of patients with metastatic CRC is approximately 14% (2). Recent advances in targeted therapy and immunotherapy, which have changed the treatment strategies for CRC. The combination of anti-PD-1 and chemotherapy has been the standard first-line treatment for advanced CRC (3). Additionally, chimeric antigen receptor (CAR)-T cell therapy has shown strong anti-tumor effects in CRC. However, treatment efficacy is limited by chemoresistance, the immunosuppressive microenvironment of solid tumors, the lack of tumor-specific antigens, and post-treatment side effects (4). Therefore, chemotherapy remains a key strategy in CRC treatment. It is the primary approach to reduce the risk of recurrence after curative surgery and serves as the cornerstone treatment for metastatic CRC. Oxaliplatin-based chemotherapy regimens (FOLFOX or CAPOX) are the standard first-line treatments for CRC (5). However, chemotherapy often results in acquired chemoresistance, leading to tumor progression and adverse effects on patient survival (6). Overall, acquired chemoresistance is a significant factor contributing to disease recurrence and metastasis, profoundly affecting the prognosis of patients with CRC. Enhancing the sensitivity of CRC to chemotherapy is crucial for improving clinical outcomes.

Chemoresistance arises from a complex interplay of biological processes including multidrug resistance gene expression, apoptosis, epigenetics, and the tumor microenvironment (7). Traditional Chinese medicine (TCM), with its multi-component, multi-target network, and diverse regulatory methods (8), has the potential to enhance the efficacy of chemotherapy. The "Zhi-Zhen" formula (ZZF), developed by the renowned TCM practitioner Zhang Jingren, is composed of herbs including Huang Qi, Nv Zhenzi, Shi Jianchuan, Teng Ligen, Xiang Fu, Ye Putaoteng, and Yi Yiren. Our preliminary studies suggest that ZZF, when combined with chemotherapy, enhances the therapeutic effects on gastrointestinal tumors. As a traditional Chinese herbal formula, ZZF contains numerous herbs and active ingredients with various mechanisms of action. Experimental research has shown that ZZF can reverse chemoresistance in CRC through several mechanisms (9–13): (1) inhibition of P-glycoprotein (P-gp) expression; (2) suppression of IκB-α phosphorylation, reducing NF-κB/p65 protein expression; (3) inhibition of the Hedgehog signaling pathway; (4) reduction of P-gp efflux function and inhibition of ERK pathway activity; (5) inhibition of cell proliferation in resistant cells; (6) modulation of M2 macrophage-derived exosomes to alter the immune microenvironment. However, the specific targets and mechanisms of ZZF require further investigation.

This study aims to elucidate the mechanisms and therapeutic targets of ZZF in reversing chemoresistance in CRC through an integrated analysis of bioinformatics, network pharmacology, and cellular experiments. The research aims to provide theoretical insights and empirical data to support the development of future treatment strategies for chemoresistance.

2 Materials and methods

2.1 Drugs and reagents

Herbs, including Huang Qi, Nv Zhenzi, Shi Jianchuan, Teng Ligen, Xiang Fu, Ye Putaoteng, and Yi Yiren, were procured from Cai Tongde (Shanghai, China). Oxaliplatin, MSAB, Wnt/β-catenin agonist 2, and Cell Counting Kit-8 (CCK-8) reagents were sourced from Haoyuan MedChemExpress (Shanghai, China). HyperScript III RT SuperMIX (with gDNA remover) and S6 Universal SYBR qPCR Mix were obtained from NovaBio (Shanghai, China). NE-PER Nuclear and Cytoplasmic Extraction reagents were acquired from Thermo Fisher Scientific (USA). Annexin V-adenomatous polyposis coli (APC)/7-AAD apoptosis kit was purchased from Multi Sciences (Hangzhou, China). Immunostaining Blocking Buffer, DAPI Stain Solution, and Alexa Fluor 594 AffiniPure goat anti-rabbit IgG (H + L) were obtained from Yeasen (Shanghai, China).

2.2 Identification of differentially expressed genes

Transcriptome sequencing data and corresponding annotation files from CRC tissues and adjacent normal tissues were acquired from The Cancer Genome Atlas (TCGA). Transcriptome sequencing data of HCT-116 cells with β-catenin (CTNNB1) knockdown were obtained from the Gene Expression Omnibus (GEO) database. Raw sequencing data, along with sample and platform information, were downloaded from the GEO database. Data annotation was performed using Python 3.9 (64-bit), resulting in a complete gene expression matrix. Differential expression analysis was conducted using the limma package in R 4.0.3, with genes considered differentially expressed if $\log2|FC| > 1$ and the adjusted p-value was <0.05. A volcano plot was generated for data visualization using the ggplot2 package in R 4.0.3.

2.3 Screening of candidate components and targets of ZZF

ZZF consists of Huang Qi (Astragali Radix), Nv Zhenzi (Ligustri Lucidi Fructus), Shi Jianchuan (Salvia Chinensis), Teng Ligen (Radix actinidiae), Xiang Fu (Cyperi rhizoma), Ye Putaoteng (Hairy grape stem), and Yi Yiren (Coicis semen). The chemical components of these herbs were obtained from the Traditional Chinese Medicine Systems Pharmacology Database (TCMSP) (14, 15). Additionally, compounds for Ye Putaoteng were obtained from the Chinese Academy of Sciences Chemistry Database and other research (16). These additional compounds were linked to specific TCMSP mol-IDs using their InChIKey and CAS codes. The active ingredients were selected based on the criteria of oral bioavailability (OB) being ≥30% and drug-like properties (DL) being ≥0.18. TCMSP predicts the potential targets of these candidate components. Finally, the protein names of all the targets were converted to gene names using the UniProt protein database.

2.4 Identification of chemoresistance targets

Chemoresistance-related targets were identified by searching the GeneCards and OMIM databases using "chemoresistance" and "chemoresistance." The GeneCards database assigns a score to each target reflecting its relevance to chemoresistance. When many targets were identified, they were filtered these potential targets based on their scores. To compile a comprehensive list of chemoresistance targets, the results from both databases were integrated and the duplicate entries were removed using R (version 4.0.3).

2.5 Construction of the network of potential targets of ZZF-herb-active ingredients

To identify candidate therapeutic targets, we analyzed the intersection of targets of the active ingredients of ZZF, DEGs in CRC, and targets related to chemoresistance. Using R (version 4.0.3), we created a Venn diagram to visualize this intersection. Overlapping genes are considered therapeutic targets for overcoming chemoresistance (hereafter referred to as therapeutic targets). Subsequently, we imported the data file into Cytoscape (version 3.7.0) software to construct and visualize the network of potential targets of ZZF-herb-active ingredients of chemoresistance. Furthermore, the network was treated as an undirected network using NetworkAnalyzer in Cytoscape (version 3.7.0).

2.6 Gene ontology and Kyoto encyclopedia of genes and genomes enrichment analysis of therapeutic targets

Enrichment analysis of therapeutic targets, including the Gene Ontology (GO) Biological Processes, GO Molecular Function, GO Cellular Components, and Kyoto Encyclopedia of Genes and Genomes (KEGG) Pathway, was performed using the "clusterProfiler" and "enrichplot" packages in R 4.0.3. The results were visualized using the "ggplot2" package to facilitate interpretation in R (version 4.0.3).

2.7 Survival analysis

The survival data of patients was downloaded from the TCGA database. The 'survival' and 'survminer' packages in R (version 4.0.3) were used for survival analysis and visualization.

2.8 Preparation of the extracts of ZZF

A total weight of 175 g of Huang Qi, Nv Zhenzi, Yi Yiren, Shi Jianchuan, Teng Ligen, Ye Putaoteng, and Xiang Fu was mixed in a ratio of 6:3:6:6:6:6:2. The mixture was then soaked in 95% ethanol for 20 min and refluxed for 2 h. After filtration, the solution was concentrated with a rotary steamer and converted into a powder by lyophilization, resulting in an ethanol extract of ZZF.

2.9 Cell lines and cell culture

Human CRC cell lines, HCT-116 and HCT-8 were acquired from Obio Technology (Shanghai, China) and verified through STR profiling. The cells were cultured in RPMI-1640 medium (Gibco, Carlsbad, CA, United States) supplemented with 10% fetal bovine serum and 1% antibiotics. To establish an oxaliplatin-resistant cell model, HCT-8 and HCT-116 cells were exposed to increasing concentrations of oxaliplatin, ranging from 0.5 μM to 10 μM. The established oxaliplatin-resistant cell lines, HCT-8/LOHP and HCT-116/LOHP were maintained in a complete medium containing 4 μg/mL and 3 μg/mL oxaliplatin, respectively. All cell cultures were maintained at 37°C in a 5% CO_2 humidified atmosphere.

2.10 Real-time quantitative PCR

Total RNA was extracted with the TRIzol reagent and reverse-transcribed into cDNA using HyperScript III RT SuperMIX (with gDNA remover). Real-time quantitative PCR (RT-qPCR) was conducted using the S6 Universal SYBR qPCR Mix according to the instructions of the manufacturer. The primer pairs are shown in Supplementary Table S1. Gene expression levels were calculated as follows:

$$\Delta\Delta CT = \Delta CT\_treated - \Delta CT\_control, \text{Relative expression} = 2\,\hat{}\,(\Delta\Delta CT).$$

2.11 Drug inhibition analysis

Cells were seeded in 96-well plates at a density of 10,000 cells/well and incubated in fresh medium with or without ZZF for 24 h. Next, the medium was replaced with fresh medium containing various concentrations of oxaliplatin, and the cells were cultured for an additional 24 h. Subsequently, the cells were treated with a medium containing 10% CCK-8 solution for 1 h, and the absorbance at 450 nm was measured using a microplate reader. The inhibition rate was calculated using the following formula:

$$\text{Inhibition rat} = (1 - (\text{OD\_treated} - \text{OD\_blank}) / (\text{OD\_control} - \text{OD\_blank}) * 100\%$$

The half-maximal inhibitory concentration (IC50) was determined using GraphPad Prism 8.

2.12 Colony formation assay

Cells were diluted to different concentrations, seeded into 6-well plates, and incubated in a growth medium for 48 h. Oxaliplatin was then added to the growth medium and incubated for 10 d. The plates were washed with PBS, fixed with 4% paraformaldehyde, and stained with crystal violet. Finally, images were obtained using a camera and the established colonies were manually counted.

2.13 Protein extraction

To obtain total protein, cells were lysed in RIPA buffer containing protease and phosphatase inhibitors. The lysate was then centrifuged, and the supernatant was collected.

Nuclear and cytosolic proteins were extracted using the NE-PER Nuclear and Cytoplasmic Extraction Kit. Briefly, cells were harvested using trypsin and washed with PBS, and the supernatant was discarded to leave the cell pellet. Cells were lysed with Cytoplasmic Extraction Reagent I (CERI), vortexed, and incubated on ice. The supernatant containing cytoplasmic proteins was collected after the addition of Cytoplasmic Extraction Reagent II (CER II) and centrifugation. The remaining pellet was resuspended in Nuclear Extraction Reagent (NER), vortexed, and incubated on ice multiple times to extract nuclear proteins. Following the final centrifugation, the supernatant containing the nuclear proteins was collected. All protein solutions were boiled in 5× loading buffer at 100°C for 10 min.

2.14 Western blotting

Proteins were separated by 10% SDS-PAGE and transferred to PVDF membranes. Membranes were blocked with 2% skim milk for 1.5 h at room temperature. Subsequently, the membranes were incubated with primary antibodies overnight at 4°C. The following day, the membranes were incubated with horseradish peroxidase-conjugated secondary antibodies for 1.5 h at room temperature. After washing with TBST, the bands were visualized. The intensities of the bands were analyzed for grayscale values using ImageJ software. The antibodies in this experiment were as follows: Anti-Caspase-7(1:1000, ABclonal), Anti-Bax (1:1000, CST), Anti-Bcl2 (1:1000, CST), Anti-Cleaved-Caspase-7 (1:1000, CST), Anti-Caspase-3 (1:1000, CST), Anti-Cleaved-Caspase-3 (1:1000, CST), Anti-Cleaved-PARP (1:1000, CST), Anti-*β*-catenin (1:1000, CST), Anti-Lamin A/C (1:1000, CST), Anti-GSK-3β (1:1000, CST), Anti-phospho-GSK-3β(Ser9) (1:1000, CST), and Anti-GADPH (1:1000, CST).

2.15 Flow cytometry analysis of apoptosis

The cells were seeded in 6-well plates and treated with various reagents for 24 h. Subsequently, the cells were trypsinized, washed twice, and immediately stained with Annexin V-APC and 7-AAD. The apoptosis rate was visualized using the BD Accuri C6 software (BD Biosciences, United States).

2.16 Immunofluorescence

A total of 1×10^4 cells were seeded in glass-bottomed cell culture dishes for 24 h before treatment for an additional 24 h. The cells were then fixed with 4% paraformaldehyde for 15 min, washed three times with PBS buffer, and blocked in blocking buffer for 1 h. Subsequently, the cells were incubated with an anti-*β*-catenin antibody (1:100, CST) overnight at 4°C. The next day, cells were washed and incubated with Alexa Fluor 594 AffiniPure goat anti-rabbit IgG (H + L) (1:200, Yeasen) for 1.5 h at room temperature. DAPI staining was performed, and the cells were photographed using a laser scanning confocal microscope (Leica, Italy).

2.17 UPLC-QTOF-MS/MS analysis

ZZF (1 mg) was thoroughly dissolved in 1 mL 95% ethanol by ultrasonication for 20 min (50 kHz, 300 W), followed by vortexing and shaking for 30 s. After centrifugation at 4°C and 12,000 rpm for 5 min, the supernatant (800 μL) was used for UPLC-QTOF-MS/MS analysis. Chromatographic separation was performed on a Waters ACQUITY UPLC system using an ACQUITY UPLC BEH C18 column (2.1 mm × 100 mm, 1.7 μm). The mobile phase consisted of eluent A (0.1% formic acid aqueous solution, v/v) and eluent B (acetonitrile). The gradient elution program was as follows: 0–8 min, 10–11% B; 8–14 min, 11–21% B; 14–20 min, 21–27% B; 20–24 min, 27–38% B; 24–31 min, 38–53.5% B; 31–38 min, 53.5–90% B; 38–40 min, 90–10% B. The flow rate was adjusted to 0.4 mL/min, with the column temperature kept steady at 40°C, and an injection volume of 2 μL was used.

The UPLC system was coupled with a Synaptic Q-TOF mass spectrometer. An electrospray ionization source (ESI) was used in both positive and negative ion modes. The MS and MS/MS scan range was m/z 100–1700. The temperatures of the drying gas and sheath gas were 350°C. The capillary voltage was set at 3500 V. The flow rate of the drying gas was 8 L/min. The collision voltage was 150 V and the collision energies were set to 5, 20, 35, and 50 eV. The nebulizer pressure was 50 psi (1 psi, 6.895 kPa).

An Excel table was created to record the compound names, molecular formulae, precise molecular weights of the adducts, and CAS registry numbers (Supplementary Table S2). The table was imported into the PCDL database using PCDL Manager B.08.00. Qualitative Analysis software (version 10.0) was used to identify the components of ZZF based on the chemical structure formula, charge-to-mass ratio, and secondary fragment ion information.

10.3389/fmed.2025.1516307

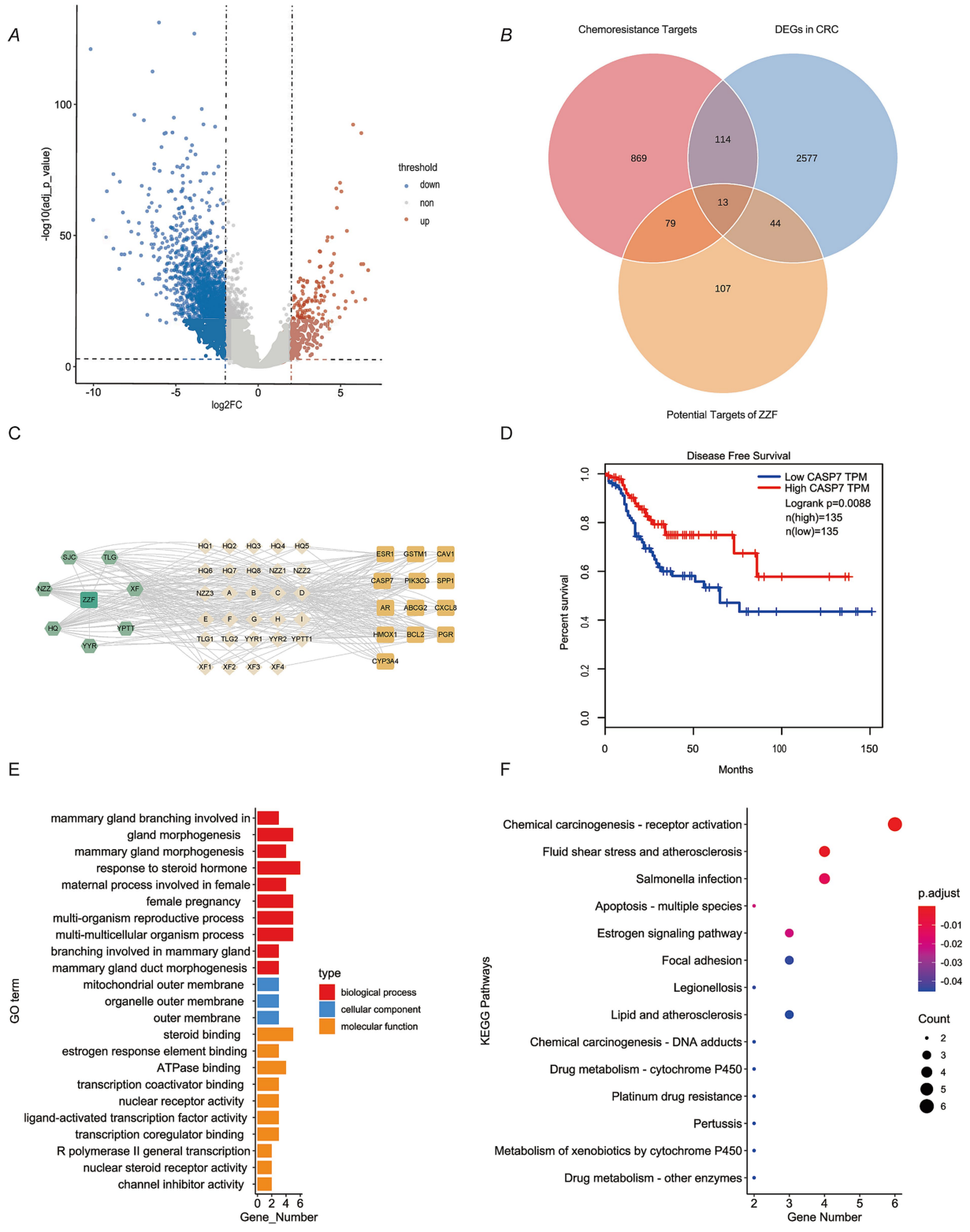

FIGURE 1
Caspase-7 presented as a potential target in the mechanism of ZZF against colorectal cancer chemoresistance. **(A)** Characterization of differentially expressed genes (DEGs) between colorectal cancer (CRC) and normal tissues in the TCGA database. DEGs were screened with log2 (FC) ≥ 1 and adjusted *p*-value ≤0.01. Blue, significantly downregulated genes; red, markedly upregulated genes. **(B)** Venn diagram shows the overlap of DEGs in CRC, chemoresistance targets, and potential targets of ZZF. **(C)** ZZF-herb-active ingredient-potential targets network diagram. **(D)** Survival analysis of CRC patients grouped based on CASP7 expression level. Data from the TCGA database. **(E)** GO enrichment analysis of therapeutic targets. **(F)** KEGG pathway enrichment analysis of therapeutic targets.

TABLE 1 Mass spectrometry identification of the top five ingredients in the ZZF-herb-active ingredient-potential target network.

Sheared Name	Chemical name	Degree	Formula	CAS	RT (min)	Adduct [M + H]+	MS/MS fragments
D	Quercetin	90	C15H10O7	117–39-5	5.328	303.0445	229.0471, 165.0189, 153.0184
C	Kaempferol	42	C15H10O6	520–18-3	6.914	287.0542	213.0546, 153.0167, 135.0360, 115.0542
F	Beta-sitosterol	30	C29H50O	83–46-5	11.974	415.2104	119.0853
E	Luteolin	16	C15H10O6	491–70-3	6.911	285.0385	151.0030, 133.0286
B	Isorhamnetin	12	C16H12O7	491–70-3	-		

2.18 Statistical analysis

Differences between the two groups were assessed using the Student's t-test. For data involving more than two groups, we used a one-way analysis of variance (ANOVA) followed by Dunnett's t-test for multiple comparisons. Differences were considered statistically significant at a p-value <0.05. Statistical analyses were performed using GraphPad Prism version 8 for Windows. Each experiment was repeated at least three times.

3 Results

3.1 Caspase-7 presented as a potential target in the mechanism of ZZF against CRC chemoresistance

To elucidate how ZZF relieves chemoresistance in CRC, we used bioinformatics and network pharmacology tools in a preliminary study. A total of 2,748 DEGs were identified by analysis of the differences in RNA-seq data between CRC tissues and adjacent normal mucosal tissues in TCGA (Figure 1A). An aggregate of 1,074 chemoresistance-related genes were identified in the databases. By intersecting these genes, we identified 127 potential chemoresistance targets. Additionally, we identified 42 potential active ingredients and 243 potential targets of ZZF from various databases. Intersecting these with 127 chemoresistance targets resulted in 13 potential targets in chemoresistant CRC (Figure 1B). Based on these data, we constructed a ZZF-herbs-active ingredients-potential targets network, comprising 50 nodes (one formula, seven herbs, 29 potential ingredients, and 13 therapeutic targets) and 280 edges (Figure 1C). Network analysis ranked the top five active ingredients by degree, which was validated by mass spectrometry (Table 1; Supplementary Figure S1). To further explore the mechanism of ZZF, we conducted analyses for GO and KEGG enrichment to investigate the common biological functions of the 13 therapeutic targets (Figures 1E,F). We performed KEGG enrichment analysis on the candidate genes and identified several pathways associated with tumorigenesis and drug metabolism. Notably, the "Platinum drug resistance" pathway was enriched among those. A deeper analysis of this pathway revealed the inclusion of BCL2 and GSTM1, both of which are involved in. Furthermore, we found several genes in this pathway closely related to apoptosis, including CASP3, CASP8, CASP9, and BAX. However, the role of CASP7 was not prominently represented. In line with this, Patients with low caspase-7 expression had higher progression-free survival in survival analysis ($p = 0.0088$) (Figure 1D). These findings suggest that caspase-7 is a crucial target for the anti-chemoresistant effect of ZZF in CRC.

3.2 ZZF enhanced the apoptotic response of oxaliplatin-resistant cells by upregulating the expression and activation of caspase-7

With the aim of ascertaining the role of caspase-7 in ZZF's effects on chemoresistance, we established two oxaliplatin-resistant CRC cell lines, HCT-116/LOHP and HCT-8/LOHP, by sequential drug administration (Figure 2A). The IC50 of oxaliplatin was significantly higher in HCT-116/LOHP cells at 234.17 ± 47.3 μM compared to 30.28 ± 6.46 μM in HCT-116 cells ($p < 0.05$). Similarly, HCT-8/LOHP cells exhibited an IC50 of 142.80 ± 4.30 μM, much higher than 32.62 ± 4.37 μM in HCT-8 cells ($p < 0.05$) (Figure 2B). The colony formation assay confirmed that HCT-116/LOHP and HCT-8/LOHP cells exhibited a greater ability to form colonies in the presence of oxaliplatin than the parental cell lines, indicating increased resistance (Figure 2D). Preconditioning with ZZF reduced the IC50 of oxaliplatin in drug-resistant cells ($p < 0.05$) (Figure 2C), suggesting that ZZF could potentiate chemotherapy sensitivity in CRC. Consistent with previous findings that identified caspase-7 as a putative target of ZZF in reversing chemoresistance, we found that the expression of caspase-7 was significantly lower in oxaliplatin-resistant cells compared to parental cells ($p < 0.05$) (Figures 2E,F). Treatment with ZZF reversed this downregulation, leading to an increase in the expression and activation of caspase-7 in resistant cell lines (Figures 2G,H). Consequently, ZZF treatment combined with oxaliplatin resulted in higher caspase-7 expression and activation, which increased apoptosis in oxaliplatin-resistant cell lines (Figures 2I–K).

3.3 ZZF regulated caspase-7 expression by the upstream Wnt/β-catenin pathway

To further explore the upstream pathways through which ZZF regulates CASP7-expression, we searched the UALCAN database using the keyword "CASP7," and subsequently selected the colon cancer dataset for further analysis. The results revealed that activating Wnt/β-catenin signaling led to a significant reduction in caspase-7 expression ($p < 0.05$) (Figure 3A). Conversely, the knockdown of β-catenin, a vital component of the Wnt/β-catenin pathway (17), significantly elevated the transcript level of caspase-7 (FC = 2.15, $p < 0.05$) (Figure 3B). Western blotting results indicated higher

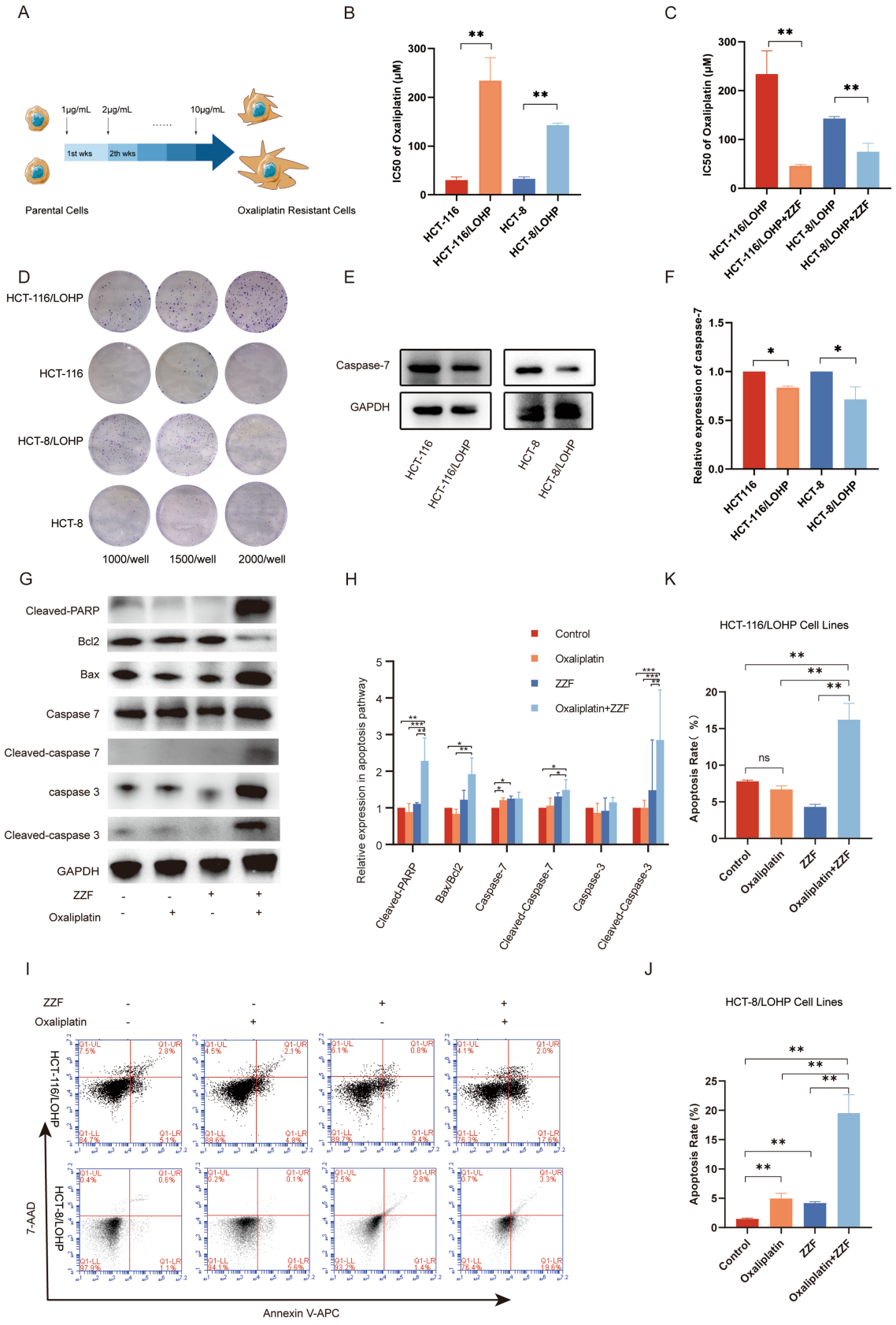

FIGURE 2
ZZF enhanced the apoptotic response of oxaliplatin-resistant cells by upregulating the expression and activation of caspase-7. **(A)** Schematic diagram of the construction of the oxaliplatin-resistant cell model, HCT-8/LOHP and HCT-116/LOHP, with "wks" denoting weeks. **(B)** The IC50 values of

(Continued)

FIGURE 2 (Continued)
oxaliplatin in parental and resistant cell lines were calculated using GraphPad Prism 8. **(C)** The IC50 of oxaliplatin in drug-resistant cell lines with or without ZZF pretreatment. **(D)** Colony formation assays of the parental and oxaliplatin-treated resistant cell lines. **(E,F)** Expression levels of caspase-7 in parental and resistant cell lines. **(G,H)** Expression levels of apoptosis-related proteins of HCT-116/LOHP in different groups. **(I–K)** Flow cytometry analysis of apoptosis rate of oxaliplatin-resistant cell lines in different groups. *$p < 0.05$, **$p < 0.01$, ***$p < 0.001$ ($n = 3$); ns, no significance ($n = 3$).

expression of β-catenin in HCT-116/LOHP and HCT-8/LOHP than parental cells ($p < 0.05$) (Figures 3C,D), along with the observed downregulation of caspase-7 in chemoresistant cells. Furthermore, activators of the Wnt/β-catenin signaling pathway were observed to downregulate caspase-7 expression in HCT-116 and HCT-8 ($p < 0.05$) (Figures 3E,F). These findings suggest that the Wnt/β-catenin pathway is an upstream regulator of CASP7 expression. Moreover, ZZF downregulated β-catenin expression in chemoresistant cells ($p < 0.05$) (Figures 3G,H). Flow cytometry results further demonstrated that ZZF and a specific β-catenin inhibitor, MSAB, had a synergistic effect, significantly enhancing oxaliplatin-induced apoptosis ($p < 0.05$), respectively (Figures 3I–K). Conversely, Wnt/β-catenin agonist 2, a specific β-catenin activator, antagonized the chemosensitization effect of ZZF, inhibiting apoptosis in a concentration gradient ($p < 0.05$) (Figures 3L–N). These results support the role of Wnt/β-catenin as an upstream regulator of CASP7-expression in the ZZF mechanism to reverse chemoresistance.

3.4 ZZF regulated the Wnt/β-catenin pathway by modulating β-catenin during transcription and localization

For a more comprehensive understanding of the regulatory mechanisms of ZZF, we investigated the transcription, degradation, and cellular localization of β-catenin. The qRT-PCR results indicated that ZZF markedly decreased the mRNA expression of CTNNB1 in chemoresistant cells ($p < 0.05$) (Figures 4A,B). Additionally, GSK3β is a crucial component of the Wnt/β-catenin signaling pathway, contributing to forming the β-catenin degradation complex and promoting β-catenin degradation (18). Western blotting showed that neither ZZF nor oxaliplatin significantly impacted the levels of GSK3β or p-GSK3β (Figures 4E,F). Moreover, the subcellular localization of β-catenin closely links to its function (18). Western blotting revealed that ZZF decreased β-catenin expression, mainly in the nucleus ($p < 0.05$) (Figures 4C,D). Immunofluorescence results demonstrated that the nuclear aggregation of β-catenin was diminished in the ZZF group compared to the control group. Additionally, the nuclear distribution of β-catenin was further decreased in the oxaliplatin combined with the ZZF group versus the oxaliplatin group (Figure 4G). These results indicate that ZZF regulates the Wnt/β-catenin pathway by influencing the transcription and cellular localization of β-catenin.

4 Discussion

CRC, with complex pathogenesis and regulatory circuits, stands as one of the most lethal malignancies (19). For decades, oxaliplatin has been the cornerstone chemotherapeutic agent for CRC (20, 21). However, chemoresistance continues to be a significant obstacle that greatly reduces the effectiveness of CRC treatments. Although the mechanisms underlying chemoresistance have been studied to some extent, further investigations are necessary to develop more effective therapeutic strategies (22).

As research on TCM has progressed, scientists have recognized its potential to enhance tumor sensitivity to chemotherapy by modulating cell survival, metabolism, and death through multiple mechanisms (23). ZZF is clinically used to treat CRC owing to its potentiating and detoxifying effects. However, unlike monomolecules, ZZF comprises complex active components that modulate diverse targets, making it challenging to ascertain its pharmacological mechanisms. Network pharmacology and bioinformatics offer tools for investigating the active components and underlying targets of TCM formulae, such as ZZF (24, 25). Utilizing these methodologies, we analyzed and identified the active ingredients and targets of ZZF involved in CRC chemoresistance. We constructed a ZZF–herb–compound–target network and performed mass spectrometry identification of the top five ingredients in the network based on the degree value. The mass spectrometry results demonstrated a certain degree of reliability. However, isorhamnetin, a flavonoid, was not identified in the mass spectrometry ions of ZZF, possibly because of its very low water solubility than quercetin [<3.5 μg/mL (26) and 2.15 mg/L (27) at 25°C]. Further annotation of the targets revealed that the critical targets of ZZF's anti-chemoresistance effects in CRC were related to platinum-based chemoresistance. This suggests that ZZF regulates platinum resistance through these specific targets. In this study, we established an oxaliplatin-resistant cell model and confirmed the chemosensitizing effects of ZZF in drug-resistant cells.

Additionally, survival analysis identified CASP7, a member of the caspase family involved in apoptosis signaling pathways (28), as a potential target for ZZF to overcome chemoresistance in CRC in our study. The caspase family of proteases is essential for the execution of apoptosis, which is the process of programmed cell death. In both the extrinsic and intrinsic pathways of apoptosis, caspase-3 and caspase-7 are hydrolytically activated and processed by effector cysteine asparaginases to promote the degradation of cellular components and execute cell death (29). Chemoresistance is associated with the evasion of apoptosis through the downregulation of caspase-3 (30). XIAP, belonging to the inhibitor of apoptosis (IAP) protein family, inhibits the activity of caspase-9, caspase-7, and caspase-3, thereby preventing cell death. XIAP is highly expressed in various chemoresistant cancer cells (31, 32). The XIAP/caspase-7 complex has been linked to chemoresistance in caspase-3-deficient breast cancer (33). Inhibition of this complex and reactivation of caspase-7 can sensitize cancer cells to chemotherapy-induced apoptosis (34, 35). Conversely, caspase-7 deficiency confers resistance to endotoxin-induced lymphocyte apoptosis and increases the tolerance of chicken lymphoma cells to chemotherapeutic agents (36). Therefore, reactivating caspase-7 may be a practical approach to overcome chemoresistance. However, the specific mechanism through which caspase-7 affects CRC chemosensitivity remains unclear. Notably, we verified the difference

10.3389/fmed.2025.1516307

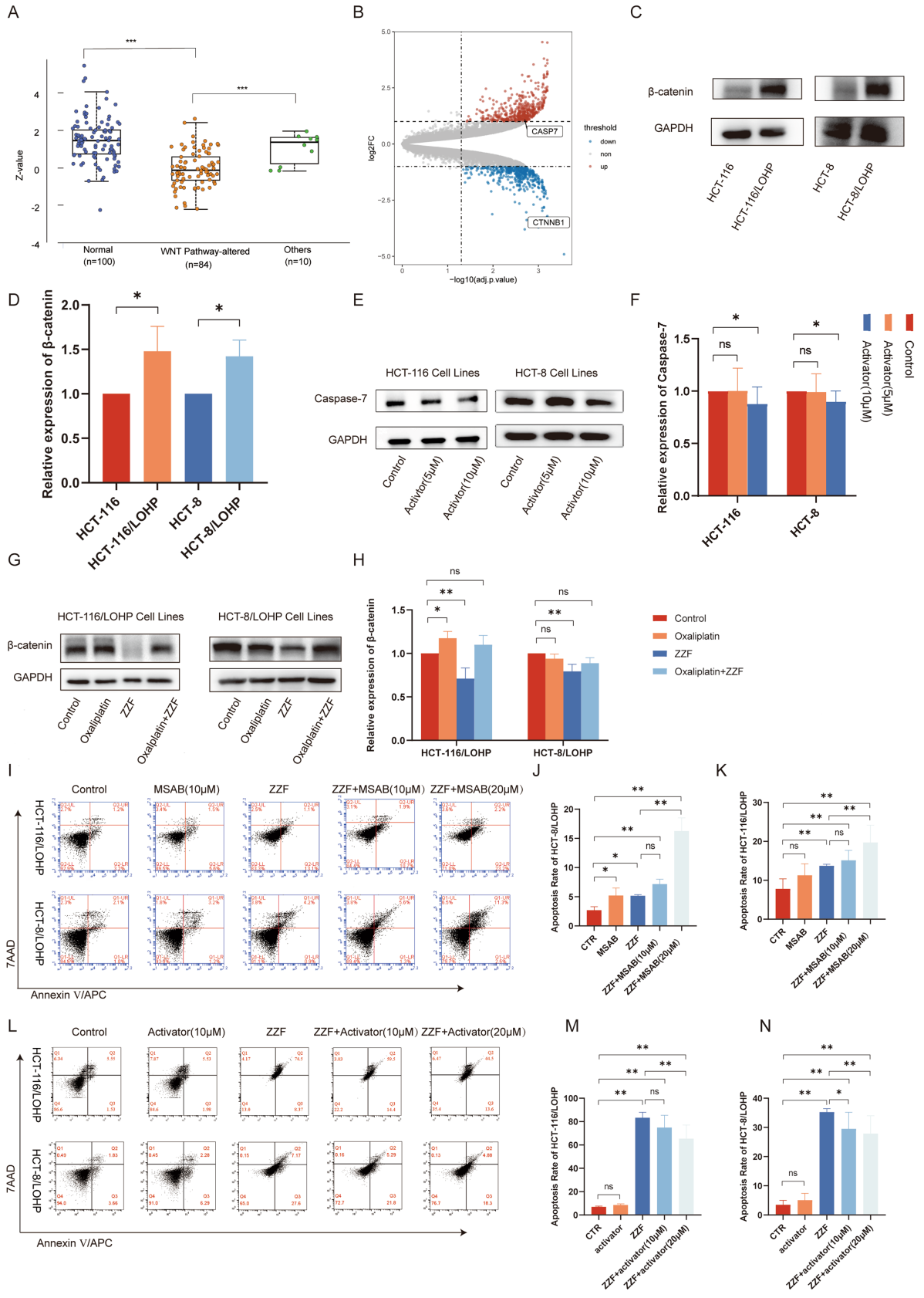

FIGURE 3
ZZF regulated caspase-7 expression by the upstream Wnt/β-catenin pathway. **(A)** Proteomic data for CASP7 were retrieved from the UALCAN database by selecting the CPTAC colon cancer dataset. Expression profiles were analyzed under the "Total Protein" section based on Wnt pathway status, and a

(Continued)

FIGURE 3 (Continued)
Jitter Plot visualization was generated. Statistical data, including *p*-values, were obtained and used for result interpretation. **(B)** DEGs between wild-type HCT-116 cells and β-catenin knockdown HCT-116 cells in GSE87429. DEGs screened with log2(FC) ≥ 1 and adjusted *p*-value ≤0.01. **(C,D)** β-expression between drug-resistant and parental cell lines was detected by Western blotting (WB). **(E,F)** Effect of Wnt/β-catenin agonist 2 on caspase-7 expression in parental cell lines. **(G,H)** Effect of different treatments on the expression level of β-catenin in drug-resistant cell lines. **(I–K)** Resistant cells were treated with different agents, and flow cytometry was used to investigate the effect of MSAB on ZZF and oxaliplatin-induced apoptosis. The groups were as follows: CTR, the group treated with oxaliplatin alone; MASB, the group treated with both MSAB and oxaliplatin; ZZF, the group treated with ZZF and oxaliplatin; ZZF + MASB represents, the group treated with varying concentrations of MSAB, ZZF, and oxaliplatin in combination. **(L–N)** Flow cytometry analysis of the effect of Wnt/β-catenin agonist 2 on apoptosis induced by the combination of ZZF and oxaliplatin in the resistant cell lines, with the grouping method consistent with figures **(I–K)**. $*p < 0.05$, $**p < 0.01$ ($n = 3$); ns, no significance ($n = 3$).

in the expression of caspase-7 between the resistant and parental cell lines. These findings revealed a significant downregulation of caspase-7 in drug-resistant cells, indicating that cancer cells proactively decreased the levels of caspase-7 to gain tolerance to apoptotic stimuli. Moreover, treatment with ZZF in combination with oxaliplatin upregulated caspase-7 expression, ultimately increasing apoptosis in drug-resistant cells. These results suggest that ZZF modulates caspase-7 expression and restores the sensitivity to chemotherapeutic agents.

The Wnt/*β*-catenin signaling pathway is essential for both embryogenesis and maintaining adult tissue homeostasis (37). This pathway regulates the proliferation and differentiation of intestinal epithelial cells (38) and is intricately involved in the initiation and advancement of CRC (39). Aberrant signaling of the Wnt/*β*-catenin pathway has been implicated in chemoresistance in several tumors (40, 41). The β-catenin, a key molecule in the Wnt/*β*-catenin signaling pathway, also functions as an adhesion junction protein (42), but when APC proteins are mutated, *β*-catenin accumulates in the cytoplasm and then shuttles to the nucleus, where it acts as a transcriptional cofactor interacting with TCF family members (e.g., TCF4) to regulate target gene expression (43). Dominant negative TCF/LEF induced the expression of caspase proteins, suggesting that the Wnt/*β*-catenin signaling pathway may participate in the regulation of caspase-7 (44). This hypothesis is corroborated by observations of a negative correlation between *β*-catenin and caspase-7 in CRC, and the knockdown of *β*-catenin upregulates the transcription of caspase-7. Furthermore, activation of the Wnt/β-catenin signaling pathway induced the downregulation of caspase-7 expression. These results indicate that the Wnt/β-catenin signaling pathway is an upstream regulator of caspase-7 expression. From the perspective of cellular function, inhibitors and activators of the Wnt/*β*-catenin signaling pathway exhibited significant interactions alongside ZZF and directly influenced ZZF-induced sensitization of resistant tumor cells to apoptosis. This implies that ZZF can regulate the expression level of caspase-7 by affecting the Wnt/*β*-catenin signaling pathway, thereby enhancing sensitivity for CRC chemotherapy.

The Wnt /*β*-catenin signaling pathway, which is regulated by multiple cellular signals, is primarily influenced by the abundance, activity, and subcellular localization of β-catenin. We discovered that the decrease in *β*-catenin expression mediated by ZZF was attributed to reduced transcription instead of increased protein degradation. This regulatory mechanism may circumvent the activation of other oncogenic factors caused by GSK3β upregulation (45). In addition, ZZF reduced the intranuclear amount and distribution of *β*-catenin. This indicates that ZZF influences the intracellular localization of β-catenin, thereby impeding its functionality.

The Wnt signaling pathway is a complex regulatory network, with the Wnt/β-catenin pathway being the most well-studied component. β-catenin, as a key effector molecule in this pathway, directly influences various biological properties of tumors through its stability and nuclear localization, making it a critical therapeutic target for inhibiting this pathway (46). However, *β*-catenin is considered an "undruggable" molecule due to its inherent challenges in directly targeted by drugs. Current efforts to develop β-catenin inhibitors primarily focus on identifying compounds that can disrupt its interactions with other proteins. For example, the natural compound PKF115-584 has been identified as capable of disrupting the interaction between β-catenin and TCF complexes, thereby inhibiting the proliferation of CRC cells (47). Additionally, Sec62 binds to β-catenin, inhibiting its degradation and enhancing Wnt signaling, which promotes CRC stemness and chemoresistance (48). Despite promising preclinical and clinical results, no drugs targeting the Wnt/β-catenin pathway have been approved (49). Challenges include unknown mechanisms, regulatory factors, and potential safety risks (50). Multi-target strategies offer new directions. ZZF, a traditional Chinese medicine formula, has shown unique multi-target advantages. This study demonstrates that ZZF suppresses *β*-catenin activity, increases Caspase-7 expression, and enhances the apoptotic response in chemotherapy-resistant colorectal cancer cells, overcoming the limitations of single-target therapies and improving chemoresistance.

Although this study delivers valuable insights into the effects of ZZF on ameliorating oxaliplatin resistance in CRC by regulating the Wnt/β-catenin/Caspase-7 signaling pathway, it is essential to acknowledge certain limitations. This study primarily relied on *in vitro* experiments, and the effects of ZZF have not been validated in animal models. The *in vivo* environment is more complex, with factors such as the tumor microenvironment and drug metabolism potentially influencing the efficacy of ZZF. Therefore, the lack of in vivo validation may limit the generalizability of the results. ZZF is a multi-component herbal formula, and variations in ingredient composition across different batches may affect its therapeutic efficacy. Factors such as cultivation, harvesting, and storage conditions can influence the concentration of active compounds, leading to variability in therapeutic outcomes. Future research should focus on optimizing and standardizing its composition to ensure consistent and reliable therapeutic effects. Although a correlation between *β*-catenin and caspase-7 has been observed, its precise mechanism remains unclear. Future research should aim to

10.3389/fmed.2025.1516307

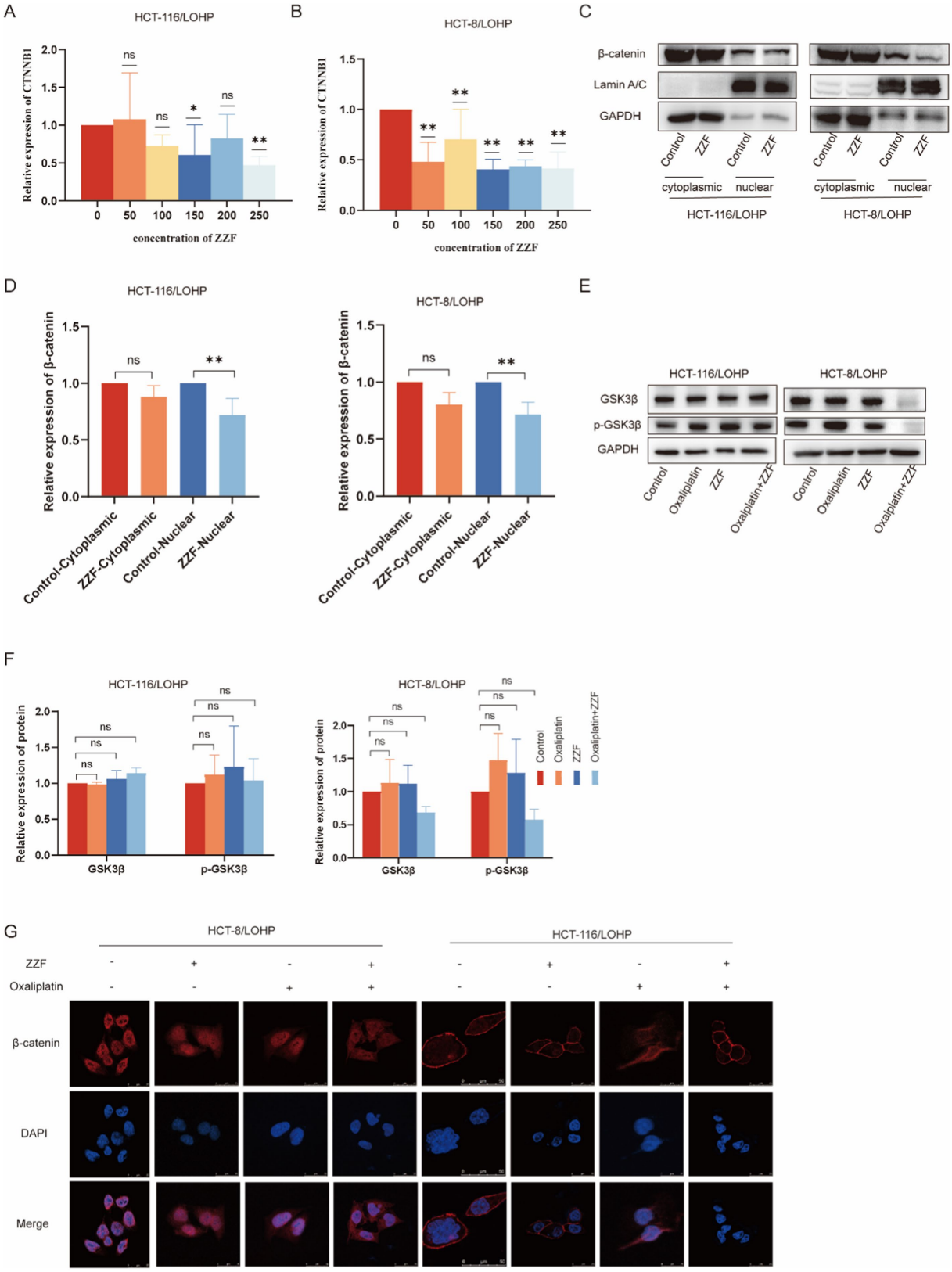

FIGURE 4
ZZF regulates the Wnt/β-catenin pathway by modulating β-catenin during transcription and localization. **(A,B)** GSK3β and p-GSK3β expression with different treatments in the resistant cell lines. **(C)** ZZF treatment at different concentrations followed by qRT-PCR to assess the mRNA expression level of β-catenin (CTNNB1) in the resistant cell lines. **(D–F)** The resistant cell lines were treated with ZZF for 24 h. Nuclear and cytoplasmic proteins were isolated from the samples, followed by the analysis of β-catenin expression using WB. **(G)** Immunofluorescence image of cells to detect the subcellular localization of β-catenin in the resistant cell lines treated with different treatments. *$p < 0.05$, **$p < 0.01$ ($n = 3$); ns, no significance ($n = 3$).

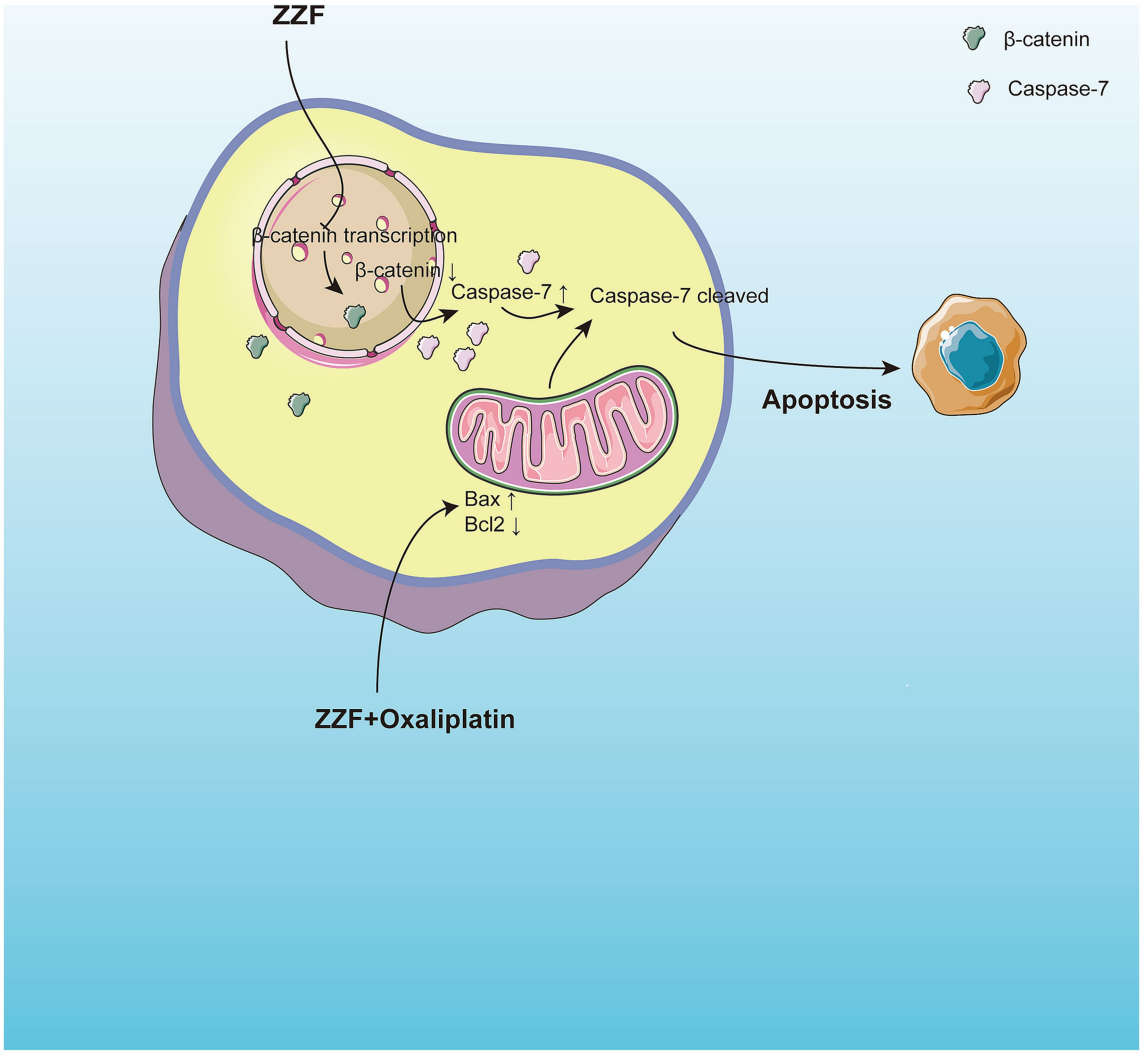

FIGURE 5
ZZF reinstates apoptotic capacities via regulating β-catenin and caspase-7 in chemoresistant colorectal cancer. ZZF regulates the nonconstitutive expression of caspase-7 and the expression and nuclear localization of β-catenin to influence the sensitivity of chemoresistant CRC cells to apoptosis.

elucidate this mechanism to understand better how the Wnt/β-catenin pathway regulates caspase-7 and its role in CRC chemoresistance. Additionally, future studies could explore the therapeutic potential of various combinations of chemical components from the ethanol extract of ZZF to determine whether specific combinations or individual components are primarily responsible for its effects and provide new insights for formulation optimization and novel drug development.

5 Conclusion

In this study, we utilized bioinformatics and network pharmacology to identify the active components and potential target genes of the traditional herbal formula ZZF involved in overcoming chemoresistance in colorectal cancer. These findings offer a novel perspective on addressing chemoresistance. Validation experiments using an oxaliplatin-resistant CRC cell model demonstrated that ZZF enhances the response of chemoresistant CRC cells to apoptosis by inhibiting the transcription and nuclear localization of β-catenin and increasing the expression of caspase-7 to reverse chemoresistance. Additionally, an analysis of ZZF components highlighted the unique role of traditional Chinese medicine in multi-target, multi-level regulation, emphasizing the need for further research to fully elucidate the molecular mechanisms by which ZZF reverses chemoresistance. Such insights could pave the way for the development of new adjuvant therapeutic strategies for chemotherapy (Figure 5).

Data availability statement

The raw data supporting the conclusions of this article will be made available by the authors, without undue reservation.

Ethics statement

Ethical approval was not required for the studies on humans in accordance with the local legislation and institutional requirements because only commercially available established cell lines were used.

Author contributions

YL: Data curation, Formal analysis, Investigation, Methodology, Software, Validation, Visualization, Writing – original draft, Writing – review & editing. KC: Data curation, Visualization, Writing – review & editing. QinL: Writing – review & editing. QiaL: Writing – review & editing. HH: Writing – review & editing. HL: Writing – review & editing. SW: Conceptualization, Funding acquisition, Project administration, Resources, Supervision, Writing – review & editing.

Funding

The author(s) declare financial support was received for the research, authorship, and/or publication of this article. This study was supported by Shanghai Three-Year Action Plan to Further Accelerate the Development of Chinese Medicine (Zhang's Internal Medicine School of Spleen and Stomach Disease Inheritance and Innovation Team) (no: 2021LPTD-010), Training Program for the Fifth Batch of National Outstanding Clinical Talents in Traditional Chinese Medicine (China TCM Human Education Letter [2022-1]).

Conflict of interest

The authors declare that the research was conducted in the absence of any commercial or financial relationships that could be construed as a potential conflict of interest.

Generative AI statement

The author(s) declare that no Gen AI was used in the creation of this manuscript.

Publisher's note

Supplementary material

The Supplementary material for this article can be found online at: https://www.frontiersin.org/articles/10.3389/fmed.2025.1516307/full#supplementary-material

SUPPLEMENTARY FIGURE S1
Mass spectrometry identification of the top five ingredients in the ZZF-herb-active ingredient-potential target network.

References

1. Bray F, Laversanne M, Sung H, Ferlay J, Siegel RL, Soerjomataram I, et al. Global cancer statistics 2022: GLOBOCAN estimates of incidence and mortality worldwide for 36 cancers in 185 countries. *CA Cancer J Clin*. (2024) 74:229–63. doi: 10.3322/caac.21834

2. Rumpold H, Niedersüß-Beke D, Heiler C, Falch D, Wundsam HV, Metz-Gercek S, et al. Prediction of mortality in metastatic colorectal cancer in a real-life population: a multicenter explorative analysis. *BMC Cancer*. (2020) 20:1149. doi: 10.1186/s12885-020-07656-w

3. Chong X, Madeti Y, Cai J, Li W, Cong L, Lu J, et al. Recent developments in immunotherapy for gastrointestinal tract cancers. *J Hematol Oncol*. (2024) 17:65. doi: 10.1186/s13045-024-01578-x

4. Cao Y, Efetov SK, He M, Fu Y, Beeraka NM, Zhang J, et al. Updated clinical perspectives and challenges of chimeric antigen receptor-T cell therapy in colorectal Cancer and invasive breast Cancer. *Arch Immunol Ther Exp*. (2023) 71:19. doi: 10.1007/s00005-023-00684-x

5. Biller LH, Schrag D. Diagnosis and treatment of metastatic colorectal cancer. *JAMA*. (2021) 325:669–85. doi: 10.1001/jama.2021.0106

6. Douillard JY, Cunningham D, Roth AD, Navarro M, James RD, Karasek P, et al. Irinotecan combined with fluorouracil compared with fluorouracil alone as first-line treatment for metastatic colorectal cancer: a multicentre randomised trial. *Lancet*. (2000) 355:1041–7. doi: 10.1016/s0140-6736(00)02034-1

7. Marin JJ, Sanchez de Medina F, Castano B, Bujanda L, Romero MR, Martinez-Augustin O, et al. Chemoprevention, chemotherapy, and chemoresistance in colorectal cancer. *Drug Metab Rev*. (2012) 44:148–72. doi: 10.3109/03602532.2011.638303

8. Wang S, Wang H, Lu Y. Tianfoshen oral liquid: a CFDA approved clinical traditional Chinese medicine, normalizes major cellular pathways disordered during colorectal carcinogenesis. *Oncotarget*. (2017) 8:14549–69. doi: 10.18632/oncotarget.14675

9. Chen Z, Kong L, Sun Y, Wang S. Reversal of multidrug resistance and expression of P-gp on human colorectal Cancer cell line HCT-8/VCR by Zhizhen recipe. *Prog Modern Biomed*. (2010) 10:1242–6. doi: 10.13241/j.cnki.pmb.2010.07.043

10. Cai S, Zhang X, Chen Z, Kong L, Wang S. Medicated serum prepared with Chinese herbal medicine Zhizhen recipe down-regulates activity of nuclear factor-κB and expression of P-glycoprotein in human colorectal cancer multidrug-resistant cell line HCT-8/VCR. *Zhong Xi Yi Jie He Xue Bao*. (2011) 9:1353–9. doi: 10.3736/jcim20111212

11. Duan P-w, Wang H, Fu J, Wang S-p. ZZR reverses the multidrug resistance of colorectal cancer cells through hedgehog/ABCG2 signaling pathway. *Chin J Integ Trad Western Med Digestion*. (2018) 26:270–4. doi: 10.3969/j.issn.1671-038X.2018.03.11

12. Liang W, Chen Z-x, Wang H-j, Wang S. Research on the role of ERK signaling pathway in the reversing effect of Zhizhen recipe on multidrug resistance in human colorectal cancer cell lines. *Chin J Integ Trad Western Med Digestion*. (2015) 23:315–20. doi: 10.3969/j.issn.1671-038X.2015.05.04

13. Qian Y, hua S, Han H, Li Y, Li Q, Wang S. Mechanism of Zhizhenfang regulation of M2 macrophages derived exosomes to improve drug resistance in colorectal cancer. Chinese journal of integrated traditional and Western medicine on. *Digestion*. (2021) 29:193–8. doi: 10.3969/j.issn.1671-038X.2021.03.08

14. Ru J, Li P, Wang J, Zhou W, Li B, Huang C, et al. TCMSP: a database of systems pharmacology for drug discovery from herbal medicines. *J Cheminform*. (2014) 6:13. doi: 10.1186/1758-2946-6-13

15. Chang X. J. Research on anti-colon Cancer active constituents of hairy grape stem. [Master's thesis]. South China University of Technology. (2012). Available at: https://kns.cnki.net/kcms2/article/abstract?v=xEDmK2-VgJgKXgJx8CZH9rnzEucbiMERfh2hN6gmStNQKBf-yXvkmOUF8CY4XAO27XrZZxht9UKQHLU5VbCGtA6ocQo44fGSSOVPLgJKEBK2uZwC-vG-k-JoQs6lkLnIRtyvKlqLRpZyfMHuOA5Xf6C4NA7YmIC04rZcj-9K-NQ2Xu9ZTVu9yycjFcz2kOU3lmxqz1yox3M=&uniplatform=NZKPT&language=CHS

16. Wu MJ, Yen JH, Wang L, Weng CY. Antioxidant activity of Porcelainberry (*Ampelopsis brevipedunculata* (maxim.) Trautv.). *Am J Chin Med*. (2004) 32:681–93. doi: 10.1142/S0192415X04002387

17. Ohtsuka M, Ling H, Ivan C, Pichler M, Matsushita D, Goblirsch M, et al. H19 noncoding RNA, an independent prognostic factor, regulates essential Rb-E2F and

CDK8-β-catenin signaling in colorectal Cancer. *EBioMedicine*. (2016) 13:113–24. doi: 10.1016/j.ebiom.2016.10.026

18. Nusse R, Clevers H. Wnt/β-catenin signaling, disease, and emerging therapeutic modalities. *Cell*. (2017) 169:985–99. doi: 10.1016/j.cell.2017.05.016

19. Kim JC, Bodmer WF. Genomic landscape of colorectal carcinogenesis. *J Cancer Res Clin Oncol*. (2022) 148:533–45. doi: 10.1007/s00432-021-03888-w

20. National Health Commission of the People's Republic of C. Chinese Protocol of Diagnosis and Treatment of Colorectal Cancer. *Zhonghua Wai Ke Za Zhi*. (2020) 2020:561–85. doi: 10.3760/cma.j.cn112139-20200518-00390

21. Kanemitsu Y, Shimizu Y, Mizusawa J, Inaba Y, Hamaguchi T, Shida D, et al. Hepatectomy followed by mFOLFOX6 versus hepatectomy alone for liver-only metastatic colorectal Cancer (JCOG0603): a phase II or III randomized controlled trial. *J Clin Oncol*. (2021) 39:3789–99. doi: 10.1200/JCO.21.01032

22. Szakacs G, Paterson JK, Ludwig JA, Booth-Genthe C, Gottesman MM. Targeting multidrug resistance in cancer. *Nat Rev Drug Discov*. (2006) 5:219–34. doi: 10.1038/nrd1984

23. Khatoon E, Banik K, Harsha C, Sailo BL, Thakur KK, Khwairakpam AD, et al. Phytochemicals in cancer cell chemosensitization: current knowledge and future perspectives. *Semin Cancer Biol*. (2022) 80:306–39. doi: 10.1016/j.semcancer.2020.06.014

24. Hopkins AL. Network pharmacology: the next paradigm in drug discovery. *Nat Chem Biol*. (2008) 4:682–90. doi: 10.1038/nchembio.118

25. Zhao L, Zhang H, Li N, Chen J, Xu H, Wang Y, et al. Network pharmacology, a promising approach to reveal the pharmacology mechanism of Chinese medicine formula. *J Ethnopharmacol*. (2023) 309:116306. doi: 10.1016/j.jep.2023.116306

26. Tian R, Wang H, Xiao Y, Hu P, Du R, Shi X, et al. Fabrication of Nanosuspensions to improve the Oral bioavailability of Total flavones from *Hippophae rhamnoides* L. and their comparison with an inclusion complex. *AAPS PharmSciTech*. (2020) 21:249. doi: 10.1208/s12249-020-01788-9

27. Srinivas K, King JW, Howard LR, Monrad JK. Solubility and solution thermodynamic properties of quercetin and quercetin dihydrate in subcritical water. *J Food Eng*. (2010) 100:208–18. doi: 10.1016/j.jfoodeng.2010.04.001

28. Sahoo G, Samal D, Khandayataray P, Murthy MK. A review on caspases: key regulators of biological activities and apoptosis. *Mol Neurobiol*. (2023) 60:5805–37. doi: 10.1007/s12035-023-03433-5

29. Shi Y. Mechanisms of caspase activation and inhibition during apoptosis. *Mol Cell*. (2002) 9:459–70. doi: 10.1016/S1097-2765(02)00482-3

30. Devarajan E, Sahin AA, Chen JS, Krishnamurthy RR, Aggarwal N, Brun A-M, et al. Down-regulation of caspase 3 in breast cancer: a possible mechanism for chemoresistance. *Oncogene*. (2002) 21:8843–51. doi: 10.1038/sj.onc.1206044

31. Devi GR, Finetti P, Morse MA, Lee S, de Nonneville A, Van Laere S, et al. Expression of X-linked inhibitor of apoptosis protein (XIAP) in breast Cancer is associated with shorter survival and resistance to chemotherapy. *Cancers (Basel)*. (2021) 13:2807. doi: 10.3390/cancers13112807

32. Miyamoto M, Takano M, Iwaya K, Shinomiya N, Kato M, Aoyama T, et al. X-chromosome-linked inhibitor of apoptosis as a key factor for chemoresistance in clear cell carcinoma of the ovary. *Br J Cancer*. (2014) 110:2881–6. doi: 10.1038/bjc.2014.255

33. Twiddy D, Cohen GM, MacFarlane M, Cain K. Caspase-7 is directly activated by the ~700-kDa Apoptosome complex and is released as a stable XIAP-Caspase-7 ~200-kDa complex*. *J Biol Chem*. (2006) 281:3876–88. doi: 10.1074/jbc.M507393200

34. Guicciardi ME, Gores GJ. Unshackling caspase-7 for cancer therapy. *J Clin Invest*. (2013) 123:3706–8. doi: 10.1172/JCI71440

35. Lin Y-F, Lai T-C, Chang C-K, Chen C-L, Huang M-S, Yang C-J, et al. Targeting the XIAP/caspase-7 complex selectively kills caspase-3–deficient malignancies. *J Clin Invest*. (2013) 123:3861–75. doi: 10.1172/JCI67951

36. Korfali N, Ruchaud S, Loegering D, Bernard D, Dingwall C, Kaufmann SH, et al. Caspase-7 gene disruption reveals an involvement of the enzyme during the early stages of apoptosis. *J Biol Chem*. (2004) 279:1030–9. doi: 10.1074/jbc.M306277200

37. Liu J, Xiao Q, Xiao J, Niu C, Li Y, Zhang X, et al. Wnt/β-catenin signalling: function, biological mechanisms, and therapeutic opportunities. *Signal Transduct Target Ther*. (2022) 7:3. doi: 10.1038/s41392-021-00762-6

38. van de Wetering M, Sancho E, Verweij C, de Lau W, Oving I, Hurlstone A, et al. The beta-catenin/TCF-4 complex imposes a crypt progenitor phenotype on colorectal cancer cells. *Cell*. (2002) 111:241–50. doi: 10.1016/s0092-8674(02)01014-0

39. Clevers H, Nusse R. Wnt/β-catenin signaling and disease. *Cell*. (2012) 149:1192–205. doi: 10.1016/j.cell.2012.05.012

40. Mohapatra P, Shriwas O, Mohanty S, Ghosh A, Smita S, Kaushik SR, et al. CMTM6 drives cisplatin resistance by regulating Wnt signaling through the ENO-1/AKT/GSK3β axis. *JCI Insight*. (2021) 6:143643. doi: 10.1172/jci.insight.143643

41. Zhou C, Yi C, Yi Y, Qin W, Yan Y, Dong X, et al. LncRNA PVT1 promotes gemcitabine resistance of pancreatic cancer via activating Wnt/β-catenin and autophagy pathway through modulating the miR-619-5p/Pygo2 and miR-619-5p/ATG14 axes. *Mol Cancer*. (2020) 19:118. doi: 10.1186/s12943-020-01237-y

42. Peifer M. Cancer, catenins, and cuticle pattern: a complex connection. *Science*. (1993) 262:1667–8. doi: 10.1126/science.8259511

43. Morin PJ. β-Catenin signaling and cancer. *BioEssays*. (1999) 21:1021–30. doi: 10.1002/(SICI)1521-1878(199912)22:1<1021::AID-BIES6>3.0.CO;2-P

44. Chen T, Yang I, Irby R, Shain KH, Wang HG, Quackenbush J, et al. Regulation of caspase expression and apoptosis by adenomatous polyposis coli. *Cancer Res*. (2003) 63:4368–74.

45. Mancinelli R, Carpino G, Petrungaro S, Mammola CL, Tomaipitinca L, Filippini A, et al. Multifaceted roles of GSK-3 in Cancer and autophagy-related diseases. *Oxidative Med Cell Longev*. (2017) 2017:4629495. doi: 10.1155/2017/4629495

46. He K, Gan W-J. Wnt/β-catenin signaling pathway in the development and progression of colorectal Cancer. *Cancer Manag Res*. (2023) 15:435–48. doi: 10.2147/CMAR.S411168

47. Lepourcelet M, Chen Y-NP, France DS, Wang H, Crews P, Petersen F, et al. Small-molecule antagonists of the oncogenic Tcf/beta-catenin protein complex. *Cancer Cell*. (2004) 5:91–102. doi: 10.1016/s1535-6108(03)00334-9

48. Su G, Yan Z, Deng M. Sevoflurane inhibits proliferation, invasion, but enhances apoptosis of lung cancer cells by Wnt/β-catenin signaling via regulating lncRNA PCAT6/miR-326 axis. *Open Life Sci*. (2020) 15:159–72. doi: 10.1515/biol-2020-0017

49. Liu C, Takada K, Zhu D. Targeting Wnt/β-catenin pathway for drug therapy. *Med Drug Disc*. (2020) 8:100066:100066. doi: 10.1016/j.medidd.2020.100066

50. Kahn M. Can we safely target the WNT pathway? *Nat Rev Drug Discov*. (2014) 13:513–32. doi: 10.1038/nrd4233

frontiers | Frontiers in Medicine

TYPE Study Protocol
PUBLISHED 20 March 2025
DOI 10.3389/fmed.2025.1523913

OPEN ACCESS

EDITED BY
Hua Zhong,
University of Hawaii at Manoa, United States

REVIEWED BY
Chuang Li,
AbbVie, United States
Yifei Yang,
Cornell University, United States

*CORRESPONDENCE
Hanchen Xu
✉ hanson0702@126.com;
✉ hcxu@shutcm.edu.cn
Guang Ji
✉ jiliver@vip.sina.com;
✉ jg@shutcm.edu.cn

RECEIVED 06 November 2024
ACCEPTED 10 March 2025
PUBLISHED 20 March 2025

CITATION
Nie S, Su Y, Lu L, Jing Y, Jiang Z, Xu Y, Wu T, Zhong Y, Wu H, Chen J, Ruan M, Zheng L, Wang L, Gong Y, Ji G and Xu H (2025) Sijunzi decoction granules for the treatment of advanced refractory colorectal cancer: study protocol for a multicenter, randomized, double-blind, placebo-controlled trial. *Front. Med.* 12:1523913.
doi: 10.3389/fmed.2025.1523913

Sijunzi decoction granules for the treatment of advanced refractory colorectal cancer: study protocol for a multicenter, randomized, double-blind, placebo-controlled trial

Shuchang Nie[1], Yingyu Su[1], Lu Lu[1,2,3], Yanhua Jing[1,2], Zenghua Jiang[4], Yangxian Xu[4], Tingting Wu[5], Yi Zhong[5], Hao Wu[6], Junming Chen[6], Ming Ruan[7], Lan Zheng[7], Liyu Wang[8], Yabin Gong[8], Guang Ji[1,2,3]* and Hanchen Xu[1,2,3]*

[1]Institute of Digestive Diseases, Longhua Hospital, China-Canada Center of Research for Digestive Diseases (ccCRDD), Shanghai University of Traditional Chinese Medicine, Shanghai, China, [2]State Key Laboratory of Integration and Innovation of Classic Formula and Modern Chinese Medicine (Shanghai University of Traditional Chinese Medicine), Shanghai, China, [3]Shanghai Frontiers Science Center of Disease and Syndrome Biology of Inflammatory Cancer Transformation, Shanghai, China, [4]Department II of General Surgery, Longhua Hospital, Shanghai University of Traditional Chinese Medicine, Shanghai, China, [5]Oncology Department, Shanghai Traditional Chinese Medicine - Integrated Hospital, Shanghai University of Traditional Chinese Medicine, Shanghai, China, [6]Minhang Hospital, Fudan University, Shanghai, China, [7]Department of Traditional Chinese Medicine, Ruijin Hospital, Shanghai Jiao Tong University School of Medicine, Shanghai, China, [8]Oncology Department, Yueyang Hospital of Integrated Traditional Chinese and Western Medicine, Shanghai University of Traditional Chinese Medicine, Shanghai, China

Background: Colorectal cancer (CRC) ranks among the most common gastrointestinal cancers globally, with both its incidence and mortality rates showing an upward trend. In particular, the 5-year survival rate for stage IV CRC patients is only 14%. Conventional treatments such as chemotherapy and immunotherapy can lead to drug resistance, exacerbate gastrointestinal function damage, and induce immunosuppression. Sijunzi decoction (SJZD), as a fundamental formula of Traditional Chinese medicine (TCM), has been demonstrated to confer distinct advantages in treatment of CRC. Therefore, we designed this trial to explore the efficacy of SJZD for the treatment of advanced refractory CRC.

Methods: A multicenter, randomized, double-blind, placebo-controlled trial is being conducted to assess the effectiveness of SJZD combined with standard therapy for treating advanced refractory CRC. Patients with advanced CRC will be recruited and randomly allocated to either the SJZD treatment group or the placebo group in a 1:1 ratio. Both groups will receive standard treatment. The intervention period will last for 6 months, with follow-up assessments every 8 to 10 weeks. Progression-free survival (PFS) is the main outcome measure. And the secondary outcomes contain duration of disease control (DDC), overall survival (OS), completion rate of chemotherapy, incidence of treatment-related adverse events, quality of survival scale score for tumor patients and changes in spleen deficiency patient-reported outcome (PRO) scores following the intervention.

Expected outcomes: To the best of our knowledge, this trial marks the first clinical investigation into the therapeutic potential of SJZD for managing

advanced refractory CRC. The primary aim of this study is to provide robust clinical evidence to support the integration of TCM with Western medicine in the treatment of advanced refractory CRC.

Trial registration: The trial was registered at Chinese Clinical Trial Registry, http://www.chictr.org.cn (Registration No: ChiCTR2200065434); Date: 2022-11-04.

KEYWORDS

traditional Chinese medicine, Sijunzi decoction, randomized controlled trial, colorectal cancer, spleen deficiency syndrome

Introduction

Colorectal cancer (CRC) is among the most common gastrointestinal malignancies worldwide (1, 2) and ranks third among the most common tumors in China, with increasing incidence and mortality rates (3, 4). Early stage CRC can be treated with radical surgery, with a 5-year survival rate of more than 90% (5). However, postoperative recurrence occurs in at least 40% of CRC patients (6, 7), and most patients are initially diagnosed at an advanced stage (8, 9), with unsatisfactory 5-year survival and overall mortality rates (10). In particular, the 5-year survival rate for patients with stage IV CRC is only 14% (11), and patients with RAS mutations have an even worse prognosis. Consequently, to identify effective treatment strategies for stage IV CRC patients with RAS mutations holds significant clinical importance.

Currently, for advanced CRC patients with RAS mutations, chemotherapy combined with targeted therapy has become the primary treatment. Nevertheless, standard medicine treatment has serious side effects, drug resistance and a poor prognosis. The long-standing history and proven efficacy of traditional Chinese medicine (TCM) make it a prominent treatment option for CRC in China. TCM has been demonstrated to confer distinct advantages in reducing toxicity, enhancing efficacy, preventing recurrence and metastasis, prolonging survival, and improving quality of life (12, 13).

Spleen deficiency syndrome (SDS) is recognized as one of the most common TCM syndromes in patients with CRC (14), and it mainly includes gastrointestinal symptoms such as anorexia and diarrhea, as well as systemic symptoms such as fatigue, perspiration, and aversion to cold. To enhance the accuracy of diagnosing this syndrome, a patient-reported outcome (PRO) scale specific to SDS has been developed. It includes 10 symptoms, each with its own weighting factor (Table 1) (15). A diagnosis of SDS is confirmed when the cumulative score of all symptoms exceeds 20. And our previous clinical study demonstrated the feasibility of this scoring scale (16).

Sijunzi decoction (SJZD), consisting of four key ingredients—Radix Ginseng (Renshen), Rhizoma Atractylodis Macrocephalae (Baizhu), Poria (Fuling), and Radix Glycyrrhizae Preparata (Gancao)—is a foundational formula used in the clinical treatment of SDS. The standard dosages, as prescribed by classical texts and the 2015 Chinese Pharmacopoeia, are 9 g, 9 g, 9 g, and 6 g. Our preliminary clinical study showed that a Chinese herbal formula based on SJZD could extend the disease-free survival (DFS) of CRC patients after curative surgery. Chinese researchers have shown that SJZD can promote the apoptosis and autophagy of CRC cells through the PI3K/Akt/mTOR pathway, thus exerting a therapeutic effect on CRC (17). Several researchers have confirmed the effectiveness of SJZD in preventing and treating advanced CRC and studied its therapeutic targets and relevant mechanisms (17, 18). However, there are few clinical trials on SJZD for the treatment of CRC, so we designed a randomized, double-blind, placebo-controlled clinical trial to assess the efficacy and safety of SJZD-based integrated TCM combined with Western medicine for treating advanced refractory CRC.

Methods and analysis

Study design and setting

This study protocol was approved by the Medical Ethics Committee of Longhua Hospital, affiliated with Shanghai University of Traditional Chinese Medicine (approval number: 2022LCSY082).

TABLE 1 Spleen deficiency rating scale.

Questions	Scoring weight (%)
Do you feel tired and too lazy to speak?	20
Do you sweat easily?	5
Do you feel food is tasteless?	10
Are your stools thin and shapeless?	20
Do you drool a lot?	5
Do you have bleeding gums?	5
Do you feel your hands and feet are not warm?	10
Do you suffer from insomnia?	5
Do you feel you can easily catch a cold?	10
Do you have any abnormal changes in your eating habits recently, such as decreased appetite and abdominal distension after eating?	10

Abbreviations: CRC, Colorectal cancer; TCM, traditional Chinese medicine; SDS, spleen deficiency syndrome; SJZD, Sijunzi decoction; PFS, progression-free survival; DDC, duration of disease control; OS, overall survival; PRO, patient-reported outcome; DFS, disease-free survival; INR, International Normalized Ratio; ULN, upper limit of normal; aPTT, activated partial thromboplastin time; LLN, lower limit of normal; NCCN, National Comprehensive Cancer Network; CRF, case report form; DMC, data monitoring committee; ITT, intention-to-treat; MSI-H, microsatellite instability-high; ICIs, immune checkpoint inhibitors.

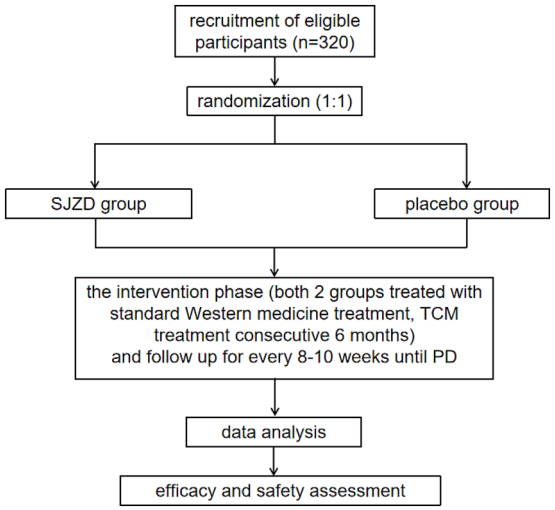

FIGURE 1
The flowchart of the trial.

And it was also registered with the Chinese Clinical Trial Registry (ChiCTR2200065434) on November 4, 2022.[1] The trial flowchart is illustrated in Figure 1.

This is a multicenter, double-blind, randomized controlled trial involving two parallel groups. A total of 320 participants will be recruited through advertisements and referrals from clinicians in outpatient and inpatient settings. Patients who meet the inclusion criteria will be informed about the opportunity to participate in this study during their outpatient visits or upon admission. Detailed interviews will be conducted to explain the study's objectives, interventions, examinations, and follow-up procedures. After obtaining informed consent, patients will be randomly allocated to either the SJZD group or the placebo group at a 1:1 ratio. During the intervention period, both groups will receive standard therapy. Additionally, the SJZD group will be administered SJZD granules, while the control group will receive a placebo as part of the treatment simulation. The key components of SJZD are outlined in Table 2. Treatment will continue for 6 months or until disease progression, resectable lesions are identified, patients are unable to tolerate the drug toxicity, patients withdraw their consent, patients are lost to follow-up, or patients die. Follow-up appointments will be scheduled every 8 to 10 weeks, as detailed in Table 3.

Objectives

The primary goal of this study is to assess the efficacy of integrating TCM with Western medicine, using the SJZD formula, in extending progression-free survival (PFS) and enhancing the quality of life for patients with advanced refractory CRC.

1 http://www.chictr.org.cn/listbycreater.aspx

TABLE 2 Main components of Sijunzi decoction.

Chinese name	Latin name	Source plant	Amount (g)
Renshen	Ginseng Radix et Rhizoma	*Panax ginseng* C. A. Mey.	9
Baizhu	Atractylodis Macrocephalae Rhizoma	*Atractylodes macrocephala* Koidz.	9
Fuling	Poria	*Poria cocos(Schw.)*Wolf	9
Gancao	Glycyrrhizae Radix et Rhizoma	*Glycyrrhiza uralensis* Fisch.	6

Participants

Patients will be enrolled from oncology departments and Chinese Medicine departments in 5 hospitals—3 hospitals affiliated with the Shanghai University of Traditional Chinese Medicine, namely, Longhua Hospital, Yueyang Hospital of Integrated Traditional Chinese and Western Medicine, and Shanghai Traditional Chinese Medicine-Integrated Hospital; 1 hospital affiliated with the Shanghai Jiaotong University School of Medicine, Ruijin Hospital; and 1 hospital affiliated with Fudan University, Minhang Hospital.

Inclusion criteria

Participants will be eligible if they meet all of the following inclusion criteria:

(1) Patients with stage IV CRC and a definitive pathologic diagnosis of adenocarcinoma;
(2) Presence of at least one clearly measurable tumor lesion as defined by RECIST 1.1 criteria;
(3) Individuals aged over 18 years and of either sex;
(4) Molecular pathology test results showing the RAS (including KRAS, NRAS and HRAS) mutant phenotype;
(5) Organ function levels must meet the following requirements: (a) normal hematologic function: neutrophil count $\geq 1.5 \times 10^9$/L, white blood cell count $\geq 3 \times 10^9$/L, hemoglobin $\geq$90 g/L, and platelet count $\geq 75 \times 109$/L. (b) Hepatic function: total bilirubin $\leq 1.5 \times$ upper limit of normal (ULN), ALT and AST $\leq 2.5 \times$ ULN ($\leq 5 \times$ ULN for patients with liver metastases). (c) Renal function: serum creatinine $\leq 1.5 \times$ ULN, and estimated creatinine clearance >50 mL/min. (d) Coagulation function: prothrombin time (PT) $\leq 1.5 \times$ ULN, activated partial thromboplastin time (aPTT) $\leq 1.5 \times$ ULN, and International Normalized Ratio (INR) $\leq 1.5 \times$ ULN. (e) Electrolyte levels: serum magnesium and potassium $\geq$lower limit of normal (LLN); electrolyte correction is permitted during the screening period.
(6) Patients who are proposed to receive first-line therapy or who have previously withdrawn from first-line therapy (regardless of molecularly targeted agent) due to intolerance of drug toxicity or imaging-confirmed disease progression or who have relapsed within 6 months of adjuvant chemotherapy completion;

TABLE 3 Schedule of trial.

Visit	Screening	Drug intervention period (weeks)			After drug withdrawal	Further follow-up (months)			
	0d	9 ± 1	18 ± 1	24 ± 1	6 month	9	12	15	18
Informed consent form	×								
Demographic information	×								
Inclusion and exclusion criteria	×								
General information	×								
Vital signs	×								
History of CRC and its treatment	×								
History of other diseases and their treatments	×								
Spleen deficiency rating scale	×	×	×	×		×	×	×	×
ECOG score	×	×	×	×		×	×	×	×
Routine blood tests	×	×	×	×		×	×	×	×
Routine urine test	×	×	×	×		×	×	×	×
Routine stool test	×	×	×	×		×	×	×	×
Liver function	×	×	×	×		×	×	×	×
Renal function	×	×	×	×		×	×	×	×
Coagulation function	×	×	×	×		×	×	×	×
Electrocardiograph	×	×	×	×		×	×	×	×
Quality of Survival Scale Score (EORTC QLQ-CR30)	×	×	×	×		×	×	×	×
Serum and stool samples collection	×				×				
Adverse events		×	×	×		×	×	×	×
Release drugs/placebo	×	×	×						
Retrieve empty packages		×	×	×	×				
Drug combination	×	×	×	×	×	×	×	×	×
Survival				×	×	×	×	×	×

(7) Patients assessed as having spleen deficiency prior to enrolment for treatment;
(8) ECOG performance status of 0 or 1;
(9) Estimated life expectancy of at least 3 months;
(10) Patients who have provided informed consent and are willing to participate in long-term follow-up.

Exclusion criteria

Participants will be excluded if they meet any of the following criteria:

(1) Histologic type of CRC other than adenocarcinoma;
(2) Patients with wild-type RAS (including KRAS, HRAS and NRAS);
(3) Bowel obstruction (except for patients whose obstruction has been relieved by fistula or stent placement) or active inflammatory bowel disease (patients who currently require medical intervention or are symptomatic) prior to study entry;
(4) Pregnant women and lactating women;
(5) Patients with mental disorders or other conditions that impede cooperation;
(6) Active cardiovascular disease, such as cerebrovascular events, myocardial infarction, unstable angina, NYHA class II-IV congestive heart failure, or severe arrhythmias requiring

medication that occurred within 6 months before the initiation of treatment in this study;
(7) Uncontrollable high blood pressure;
(8) Long-term use of high-dose aspirin (>325 mg/d);
(9) Bleeding tendency or severe coagulation disorders;
(10) Patients who cannot take medications orally, have structural abnormalities of the upper gastrointestinal tract, or suffer from malabsorption syndromes or other conditions that the investigators deem likely to interfere with gastrointestinal motility or absorption;
(11) Patients with severe proteinuria (nephrotic syndrome);
(12) Patients with a history of active tuberculosis (*Mycobacterium tuberculosis*) infection;
(13) Patients with severe, nonhealing wounds, ulcers or fractures;
(14) Patients with brain metastases, spinal cord compression, or primary brain tumors;
(15) Patients with a history or physical evidence of uncontrolled central nervous system disorders (e.g., epilepsy or stroke);
(16) Patients who have undergone surgery or open biopsy within 28 days prior to the initiation of study treatment;
(17) Patients with a history of other malignancies within the past 5 years, excluding basal cell carcinoma of the skin and/or cervical carcinoma *in situ* following radical surgery;
(18) Patients currently participating in other clinical trials;
(19) Any other conditions where investigators determine the patient is unsuitable for participation.

Withdrawal/termination criteria

Participants will be withdrawn or terminated from the trial if any of the following conditions are met:

(1) Serious adverse events occur at any time, rendering patients unable to continue;
(2) Patients decline to proceed with the clinical trial;
(3) Patients who do not formally withdraw but discontinue medication and testing and are lost to follow-up.

Additionally, researchers will document the last date of drug administration and collect assessment data for participants who discontinue or deviate from the intervention protocols.

Interventions

Drug intervention

TCM intervention: The intervention phase will span 6 months. Both the SJZD and placebo are formulated as granules, each weighing 1.77 g per pack and packaged identically to ensure uniform appearance, texture, smell, and taste. However, the placebo granules lack therapeutic effects. Patients will be instructed to dissolve each pack of granules in 200 mL of hot water and take two packs orally twice daily (totaling 3.54 g/day). The dosage and frequency will remain constant throughout the study. The SJZD and placebo granules are supplied by Sichuan Neo-green Pharmaceutical Technology Development Co., Ltd. (Sichuan, China).

The ingredients of the placebo are a one-tenth dose of SJZD (Radix ginseng, Rhizoma Atractylodis macrocephalae, Poria and Radix Glycyrrhizae Preparata) and maltodextrin. All of the processing and preparation of the medications and placebo will be conducted by qualified personnel.

Participants experiencing severe adverse events (AEs) related to this trial will receive posttrial care along with additional compensation if necessary. For participants who have adverse reactions unrelated to the trial medication, the relevant medical interventions will be implemented based on the comprehensive information of the patients, including their previous medical history, symptoms and signs, and laboratory, imaging and other examination results.

The placebo composition includes a one-tenth dose of SJZD along with maltodextrin. All processing and preparation of both the medications and placebo will be conducted by qualified personnel.

Participants who experience severe adverse events (AEs) related to this trial will receive post-trial care and additional compensation if necessary. For participants with adverse reactions not associated with the trial medication, appropriate medical interventions will be implemented based on comprehensive patient information, including their medical history, symptoms, signs, and results from laboratory tests, imaging, and other examinations.

Standard medicine intervention: The standard treatment will follow the recommendations outlined in the National Comprehensive Cancer Network (NCCN) Guidelines (2022 edition).

1. **First-line chemotherapy regimen:**
   (1) FOLFOX+ Bevacizumab [oxaliplatin 85 mg/m^2, ivgtt for 2 h, Day 1; calcium folinate 400 mg/m^2, ivgtt for 2 h, Day 1; fluorouracil 400 mg/m^2, i.v., Day 1, 1,200 mg/(m^{2}d) × 2 d, continuous ivgtt]; (total 2,400 mg/m^2 for 46–48 h); bevacizumab 5 mg/kg, ivgtt, Day 1; a course of 14 days, with an expected total of 12 chemotherapy treatments;
   (2) FOLFIRI+ Bevacizumab [irinotecan 180 mg/m^2, ivgtt for 30–90 min, Day 1; calcium folinate 400 mg/m^2, ivgtt for 2 h, Day 1; fluorouracil 400 mg/m^2, i.v., Day 1, 1,200 mg/(m^{2}d) × 2 d, continuous ivgtt]; (total 2,400 mg/m^2 for 46–48 h); bevacizumab 5 mg/kg, ivgtt, Day 1; a course of 14 days, with an expected total of 12 chemotherapy treatments;
   (3) CAPEOX+ Bevacizumab (oxaliplatin 130 mg/m^2, ivgtt for more than 2 h, Day 1); capecitabine was taken orally 1,000 mg/m^2 twice a day (once in the morning and once after meals) for the 1st to 14th days; bevacizumab 5 mg/kg, ivgtt, Day 1; a course of 21 days, with an expected total of 8 chemotherapy treatments.
2. **Second-line chemotherapy regimen:**
   (1) First-line treatment with oxaliplatin: FOLFIRI+ Bevacizumab;
   (2) First-line treatment with irinotecan: FOLFOX/CAPEOX+ Bevacizumab;
   (3) First-line treatment without irinotecan or oxaliplatin: FOLFOX/FOLFIRI/CAPEOX+ Bevacizumab.
3. **Maintenance therapy:** Maintenance therapy is given to patients whose disease has not progressed and who tolerate the drug well after the completion of standard chemotherapy. Maintenance therapy is continued until the disease has progressed, the lesion is resectable, the patient is unable to tolerate the toxic effects of the drug, or the patient withdraws consent, is lost to follow-up, or dies.

Maintenance treatment options:

(1) FOLFOX+ Bevacizumab [calcium folinate 400 mg/m^2, ivgtt for 2 h, Day 1; fluorouracil 400 mg/m^2, i.v., Day 1, 1,200 mg/(m^{2}d) × 2 d, continuous ivgtt]; (total 2,400 mg/m^2 for 46–48 h); bevacizumab 5 mg/kg, ivgtt, Day 1; 14 days for each course of treatment;
(2) FOLFOX+ Bevacizumab [calcium folinate 400 mg/m^2, ivgtt for 2 h, Day 1; fluorouracil 400 mg/m^2, i.v., Day 1, 1,200 mg/(m^{2}d) × 2 d, continuous ivgtt]; (total 2,400 mg/m^2 for 46–48 h); bevacizumab 5 mg/kg, ivgtt, Day 1; 14 days for each course of treatment;
(3) CAPEOX+ Bevacizumab (capecitabine taken orally 1,000 mg/m^2 twice a day; once in the morning and once after meals) for the 1st to 14th days; bevacizumab 7.5 mg/kg, ivgtt, Day 1; 21 days for each course of treatment.

Concomitant treatment regulations

During the trial, participants will be prohibited from using any other medications or interventions that could influence the evaluation of efficacy and safety. For participants with coexisting chronic conditions requiring ongoing treatment, any concurrent interventions must be documented in the case report form (CRF).

Outcomes

The primary outcome measure is PFS. This is defined as the time interval from the date of patient enrollment to the first occurrence of malignant tumor progression or death from any cause.

The secondary outcomes include the following: (1) duration of disease control (DDC); (2) overall survival (OS); (3) completion rate of chemotherapy; (4) incidence of treatment-related adverse events; (5) quality of survival scale score for tumor patients, European Organization for Research and Treatment of Cancer Quality of Life Questionnaire-Colorectal 30 (EORTC QLQ-CR30); and (6) changes in the spleen deficiency PRO scores following the intervention.

The safety assessment will include physical examinations, monitoring of vital signs, and laboratory tests at each visit, along with ongoing surveillance of AEs during the intervention period. The laboratory assessments will include routine blood, urine, and stool analyses; evaluations of liver and renal function; and electrocardiograms (ECGs). AEs will be defined and graded in accordance with the National Cancer Institute's Common Terminology Criteria for Adverse Events (CTCAE), Version 5.0 (US Department of Health and Human Services, 2017).

Randomization and blinding

To ensure balanced allocation, a permuted block randomization method, stratified by the recruitment locations, will be employed to assign participants to either the SJZD group or the placebo group in a 1:1 ratio using the SAS statistical software. Each medication dose will be placed in identical opaque envelopes marked with distinct randomized identification numbers. Participants will be enrolled sequentially by clinical staff and assigned an envelope based on their order of entry into the study. An independent statistician will manage the randomization procedure. All individuals involved in the trial—including clinicians, nurses, researchers, and patients—will remain unaware of the treatment assignments. The randomization codes and treatment allocations will be securely stored by the principal investigators until the trial and data analysis are completed, except in cases of serious AEs. In the event of such occurrences, sealed emergency letters containing unblinding information will be distributed to each recruitment site as needed. These letters will provide details about the treatment assignment and any urgent conditions. If any serious AEs arise, the emergency letter will be opened, and the affected participant will be withdrawn from the study. A report of any serious AEs must be submitted to the principal investigators within 24 h. After the follow-up period ends, the treatment codes will be disclosed, and the specific interventions associated with these codes will be revealed following the completion of data analysis.

Sample size

The sample size for this study was calculated based on the primary efficacy indicators. According to previous cohort studies conducted by the research team of Longhua Hospital, it was found that patients with advanced CRC who received a combination of traditional Chinese medicine and standard Western medicine had a median PFS of 9.21 months. In contrast, the median PFS for patients treated solely with standard Western medicine was 7.5 months. Following the 1:1 parallel control principle, SAS statistical analysis software was used to generate the sample size with a double-sided significance level of 0.05 and a power of 80% ($\alpha = 0.05$, $\beta = 0.2$). Assuming that the dropout rate in each group will be 10%, 320 patients are required ($n = 160$ in each group). In accordance with the 1:1 parallel control design, we utilized SAS statistical software to calculate the required sample size, considering a two-sided significance level of 0.05 and a power of 80% ($\alpha = 0.05$, $\beta = 0.2$). Anticipating a dropout rate of approximately 10% in each group, the total number of patients needed is 320, with 160 patients in each arm of the study.

Data collection and registration

Information will be documented in CRF and subsequently uploaded to REDcap,[2] a web-based electronic data management system. All clinical investigators will receive training on patient communication, information collection, and inputting data into the electronic database. Researchers will secure informed consent from participants, evaluate their general and demographic details, and gather baseline biomedical and tumor-related data.

Individuals meeting the NAE criteria will be recruited and started chemotherapy in combination with the herbal/placebo treatment. After enrolment and initiation of treatment, participants will undergo follow-up assessments every 8 to 10 weeks, and the treatment will

2 http://longhua.site/redcap3

be continued until the disease progresses, the lesions are resectable, the patients cannot tolerate the toxic side effects of drugs, or the patients withdraw their consent, are lost to follow-up, or die. During the course of the study, if the patient's CEA level continues to increase abnormally or if other evidence of a suspected recurrence is found, the frequency of follow-up will be accelerated promptly. Additionally, physical examination, colonoscopy, chest/abdominal/pelvic CT scanning with enhancement, and PET-CT will be performed if necessary.

The initial data and collected samples will be retained for a minimum of 5 years following the completion of the trial. An independent Data Monitoring Committee (DMC) will be formed, consisting of clinical epidemiologists, data monitors, and statisticians who are not involved in the trial and have no affiliation with the sponsors. This committee will ensure there are no conflicts of interest. The DMC will conduct biannual reviews of documents, CRFs, and relevant data to oversee trial safety, verify the accuracy of participant profiles, and safeguard the confidentiality of participants' information. Additionally, the DMC will offer recommendations regarding potential modifications to the study design or considerations for trial termination.

Statistical analysis

Data analysis will be conducted using SAS statistical software. The efficacy and safety of the study will be evaluated according to the intention-to-treat (ITT) principle. Missing data will be imputed using the last-observation-carried-forward method. Continuous variables will be presented as means ± standard deviations or medians (interquartile ranges), depending on the distribution and uniformity of variance. Categorical variables will be compared between the SJZD and placebo groups using the χ^2 test. Within-group comparisons will be analyzed using paired t-tests, while between-group comparisons will employ independent sample t-tests. Logistic regression analysis will be utilized to assess factors influencing the recurrence rate. An interim analysis is planned after 50% of the sample has been collected. Subgroup analyses will be conducted based on participant characteristics such as sex, chemotherapy regimen, and tumor stage. A p-value of less than 0.05 will be considered statistically significant.

Trial status

Participant enrollment is scheduled to begin in January 2023 and conclude by March 2025. Follow-up assessments are expected to be finalized by December 2025. Clinical data will be secured and locked in January 2026. This study protocol was submitted prior to the completion of participant recruitment.

Ethics and dissemination

This research adheres to the guidelines outlined in the Declaration of Helsinki, the Standard Protocol Items: Recommendations for Interventional Trials (SPIRIT) 2013 Statement, and the Standard Protocol Items for Clinical Trials with Traditional Chinese Medicine: Recommendations, Explanation and Elaboration (SPIRIT-TCM) Extension 2018 Statement. The study protocol received approval from the ethics committee of Longhua Hospital, affiliated with Shanghai University of Traditional Chinese Medicine (Approval No. 2022LCSY082), and is registered with the Chinese Clinical Trial Registry (ChiCTR2200065434). Any modifications to the study design will be promptly reported to the ethics committee. Enrollment will be restricted to individuals who have provided written informed consent.

Upon completion of the study, the findings will be submitted for publication in a peer-reviewed journal. Clinical insights and trial experiences will be shared with participants and the broader public via conferences and publications. Authorship of the final report will be determined based on individual contributions to the study.

Discussion

The incidence of CRC remains a significant global health challenge, with over 1.9 million cases reported worldwide in 2020, resulting in approximately 935,000 deaths, accounting for approximately one-tenth of all cancer cases and deaths (19). Furthermore, the burden of CRC is projected to increase to 3.2 million new cases and 1.6 million deaths by 2040 (20). Consequently, the management of CRC presents an urgent clinical challenge. Current standard therapies for CRC encompass a range of approaches, including surgical intervention, chemotherapy, immunotherapy, targeted therapy, radiation therapy, and various combinations thereof.

Surgery is the primary treatment for CRC; however, serious complications, such as anastomotic leakage, intestinal obstruction, and hernia, are common after surgery (21) and can lead to gastrointestinal dysfunction and abnormal nutrient metabolism.

Recent advances in tumor immunotherapy have been remarkable. Pembrolizumab improves the median survival time of patients with metastatic CRC from 8.2 to 16.5 months and has become the standard first-line treatment for microsatellite instability-high (MSI-H) and mismatch repair-deficient (dMMR) metastatic CRC (22). However, immune checkpoint inhibitors (ICIs) are only effective in CRC patients with MSI-H/dMMR, which accounts for only about 15% of CRC cases (23). Targeted therapies such as cetuximab and bevacizumab have significantly improved OS for patients, but resistance can easily develop (24).

In recent years, scientists have studied novel molecular factors (KRASs, BRAFs, and microsatellite instability markers) to improve the prognostic stratification and personalized treatment of CRC (25). KRAS mutations are found in approximately 40% of CRC patients (all stages) and are associated with a poor prognosis. According to the National Comprehensive Cancer Network (NCCN) guidelines, only patients with wild-type RAS should be treated with anti-EGFR inhibitors after evaluation of RAS mutations, as BRAF and RAS mutations (including mutations in KRAS and NRAS) are associated with primary resistance to EGFR therapy (26, 27). Unfortunately, until recently, no drugs were available to directly target mutant KRAS (28). Currently, the most effective treatment for advanced CRC is based on the combination of fluorouracil and oxaliplatin (FOLFOX/XELOX) or fluorouracil and irinotecan (FOLFIRI) (29, 30). With the development of targeted drugs such as bevacizumab and cetuximab, a standardized treatment scheme for advanced CRC involving the combination of chemotherapy with targeted therapy has been developed (31).

However, chemotherapy can cause drug resistance, worsen gastrointestinal function damage, and cause immunosuppression (32, 33), leading to a series of adverse reactions in elderly or weak patients and preventing them from tolerating further chemotherapy, ultimately resulting in a poor prognosis (34).

TCM is an important component of comprehensive treatment for cancer, and it has accumulated rich experience in the long-term treatment of malignancies (35, 36). TCM has unique advantages in reducing toxicity, enhancing efficacy, preventing recurrence and metastasis, prolonging survival, improving the quality of life for patients treated with chemotherapy, reducing adverse reactions, and enhancing immunity (12, 13). Patients with advanced CRC are mostly in the pathological stage of deficiency of positive qi and residual evils, which is in line with the pathological mechanism and clinical manifestations of SDS. Treatment is mainly based on supporting positive qi, and the nutritional status and immune function of patients can be improved through tonic formulae. SDS is recognized as one of the most common TCM syndromes in patients with CRC (14). Additionally, a study suggested that patients with advanced CRC had higher SDS scores than patients with early-stage CRC (37).

SJZD, a classical prescription for treating SDS in China for centuries, has been widely used for gastrointestinal diseases and is favored by clinicians due to its adaptability with the addition of other Chinese herbs under different pathological conditions (38). Wu and Xuan reported that SJZD could enhance the clinical symptoms of CRC patients, improve their quality of life and survival rate, and decrease the risk of tumor recurrence and metastasis (39). Shang demonstrated that SJZD induces autophagy and apoptosis in HCT116 and LOVO cancer cells by modulating PI3K/Akt/mTOR signaling in CRC (17). Another study confirmed that the core genes HSPB1, SPP1, IGFBP3 and TGFB1, which are involved in the therapeutic mechanism of SJZD in the CRC TME, affect CRC development and prognosis by regulating hypoxia, protein binding and EMT in the extracellular matrix (40). Modified SJZ was observed to have a suppressive impact on liver metastasis of colon cancer *in vivo*, both as a standalone treatment and in combination with 5-Fu. The potential mechanism may be attributed to its ability to stimulate cytokines such as GM-CSF, leading to an increase in the number of macrophages in the spleen and the timely clearance of colon cancer cells from the vascular system (41).

Nevertheless, randomized clinical trials evaluating the combination of TCM with standard therapies for advanced CRC remain limited. Consequently, we designed this study to investigate the efficacy and safety of SJZD in treating patients with refractory advanced CRC.

This study has several limitations. Firstly, the design does not include planned dose reduction or escalation, precluding a comparison of dose–response effects. Secondly, all participating sites are located in Shanghai, which limits the generalizability of the findings. Future studies should aim for a larger and more diverse sample size to enhance external validity.

In conclusion, this trial will employ a randomized, double-blind, placebo-controlled design to investigate a combination of TCM and Western medicines for the treatment of advanced refractory CRC, using SJZD as the foundational formula. The study aims to assess the efficacy and safety of this combined approach in managing advanced CRC, with PFS serving as the primary efficacy endpoint, aiming to provide a robust scientific foundation for the clinical application of TCM and Western medicine in the diagnosis and treatment of CRC.

Ethics statement

This study received approval from the Medical Ethics Committee of Longhua Hospital, affiliated with Shanghai University of Traditional Chinese Medicine (approval number: 2022LCSY082). It was also registered with the Chinese Clinical Trial Registry (ChiCTR2200065434) on November 4, 2022 (http://www.chictr.org.cn/listbycreater.aspx). All participants will be required to provide written informed consent prior to enrollment.

Author contributions

SN: Writing – original draft. YS: Writing – original draft. LL: Writing – review & editing. YJ: Writing – review & editing. ZJ: Writing – review & editing. YX: Writing – review & editing. TW: Writing – review & editing. YZ: Writing – review & editing. HW: Writing – review & editing. JC: Writing – review & editing. MR: Writing – review & editing. LZ: Writing – review & editing. LW: Writing – review & editing. YG: Writing – review & editing. GJ: Writing – review & editing. HX: Writing – review & editing.

Funding

The author(s) declare that financial support was received for the research and/or publication of this article. This work was supported by National Nature Science Foundation of China, Nos. 82322076 and 82320108022; Shanghai "Science and Technology Innovation Action Plan" medical innovation research special project of major difficult disease diagnosis and treatment strategy clinical research (22Y31920100); Young Elite Scientists Sponsorship Program by CACM (2021-QNRC2-B26); Construction of Traditional Chinese Medicine Inheritance and Innovation Development Demonstration Pilot Projects in Pudong New Area -High-Level Research-Oriented Traditional Chinese Medicine Hospital Construction (YC-2023-0901).

Conflict of interest

The authors declare that the research was conducted in the absence of any commercial or financial relationships that could be construed as a potential conflict of interest.

Generative AI statement

The author(s) declare that no Gen AI was used in the creation of this manuscript.

Publisher's note

References

1. Huo C, Wu D, Li X, Zhang Y, Hu B, Zhang T, et al. Eif3a mediates malignant biological behaviors in colorectal Cancer through the Pi3k/Akt signaling pathway. *Cancer Biol Ther*. (2024) 25:2355703. doi: 10.1080/15384047.2024.2355703

2. Xi Y, Xu P. Global colorectal Cancer burden in 2020 and projections to 2040. *Transl Oncol*. (2021) 14:101174. doi: 10.1016/j.tranon.2021.101174

3. Chen H, Lu B, Dai M. Colorectal Cancer screening in China: status, challenges, and prospects - China, 2022. *China CDC Wkly*. (2022) 4:322–8. doi: 10.46234/ccdcw2022.077

4. Wang Z, Dan W, Zhang N, Fang J, Yang Y. Colorectal Cancer and gut microbiota studies in China. *Gut Microbes*. (2023) 15:2236364. doi: 10.1080/19490976.2023.2236364

5. Shinji S, Yamada T, Matsuda A, Sonoda H, Ohta R, Iwai T, et al. Recent advances in the treatment of colorectal Cancer: a review. *J Nippon Med Sch*. (2022) 89:246–54. doi: 10.1272/jnms.JNMS.2022_89-310

6. Wang J, Song Z. Analysis of risk factors for postoperative recurrence of stage I colorectal Cancer: a retrospective analysis of a large population. *Front Surg*. (2024) 11:1388250. doi: 10.3389/fsurg.2024.1388250

7. Renouf DJ, Woods R, Speers C, Hay J, Phang PT, Fitzgerald C, et al. Improvements in 5-year outcomes of stage ii/iii rectal Cancer relative to Colon Cancer. *Am J Clin Oncol*. (2013) 36:558–64. doi: 10.1097/COC.0b013e318256f5dc

8. Ni R, Jiang J, Zhao M, Huang S, Huang C. Knockdown of Ubqln1 functions as a strategy to inhibit Crc progression through the Erk-C-Myc pathway. *Cancers (Basel)*. (2023) 15:3088. doi: 10.3390/cancers15123088

9. Meng S, Li M, Qin L, Lv J, Wu D, Zheng D, et al. The Onco-embryonic antigen Ror1 is a target of chimeric antigen T cells for colorectal Cancer. *Int Immunopharmacol*. (2023) 121:110402. doi: 10.1016/j.intimp.2023.110402

10. Zhao J, Quan J, Chen W, Xie X. Grid2 interacting protein is a potential biomarker related to immune infiltration in colorectal Cancer. *Eur J Med Res*. (2023) 28:511. doi: 10.1186/s40001-023-01468-x

11. Shin AE, Giancotti FG, Rustgi AK. Metastatic colorectal Cancer: mechanisms and emerging therapeutics. *Trends Pharmacol Sci*. (2023) 44:222–36. doi: 10.1016/j.tips.2023.01.003

12. Wang Y, Zhang Q, Chen Y, Liang CL, Liu H, Qiu F, et al. Antitumor effects of immunity-enhancing traditional Chinese medicine. *Biomed Pharmacother*. (2020) 121:109570. doi: 10.1016/j.biopha.2019.109570

13. Wang K, Chen Q, Shao Y, Yin S, Liu C, Liu Y, et al. Anticancer activities of Tcm and their active components against tumor metastasis. *Biomed Pharmacother*. (2021) 133:111044. doi: 10.1016/j.biopha.2020.111044

14. Sun L, Mao JJ, Yan Y, Xu Y, Yang Y. Patient reported traditional Chinese medicine spleen deficiency syndrome (Tcm-Sds) scale for colorectal Cancer: development and validation in China. *Integr Cancer Ther*. (2021) 20:15347354211020105. doi: 10.1177/15347354211020105

15. Dai L, Xu JJ, Zhou WJ, Lu AP, Ji G. Appraisal of treatment outcomes in integrative medicine using Metabonomics: taking non-alcoholic fatty liver disease with spleen deficiency syndrome as an example. *J Integr Med*. (2022) 20:524–33. doi: 10.1016/j.joim.2022.08.002

16. Dai L, Zhou WJ, Wang M, Zhou SG, Ji G. Efficacy and safety of Sijunzi decoction for chronic fatigue syndrome with spleen deficiency pattern: study protocol for a randomized, double-blind, placebo-controlled trial. *Ann Transl Med*. (2019) 7:587. doi: 10.21037/atm.2019.09.136

17. Shang L, Wang Y, Li J, Zhou F, Xiao K, Liu Y, et al. Mechanism of Sijunzi decoction in the treatment of colorectal Cancer based on network pharmacology and experimental validation. *J Ethnopharmacol*. (2023) 302:115876. doi: 10.1016/j.jep.2022.115876

18. Jie Y, He W, Yang X, Chen W. Kruppel-like factor 4 acts as a potential therapeutic target of Sijunzi decoction for treatment of colorectal Cancer. *Cancer Gene Ther*. (2017) 24:361–6. doi: 10.1038/cgt.2017.25

19. Sung H, Ferlay J, Siegel RL, Laversanne M, Soerjomataram I, Jemal A, et al. Global Cancer statistics 2020: Globocan estimates of incidence and mortality worldwide for 36 cancers in 185 countries. *CA Cancer J Clin*. (2021) 71:209–49. doi: 10.3322/caac.21660

20. Morgan E, Arnold M, Gini A, Lorenzoni V, Cabasag CJ, Laversanne M, et al. Global burden of colorectal Cancer in 2020 and 2040: incidence and mortality estimates from Globocan. *Gut*. (2023) 72:338–44. doi: 10.1136/gutjnl-2022-327736

21. Chern YJ, Tsai WS, Hung HY, Chen JS, Tang R, Chiang JM, et al. The dark side of laparoscopic surgery for colorectal Cancer patients aged 75 years or older. *Int J Color Dis*. (2018) 33:1367–71. doi: 10.1007/s00384-018-3130-7

22. Trullas A, Delgado J, Genazzani A, Mueller-Berghaus J, Migali C, Muller-Egert S, et al. The Ema assessment of Pembrolizumab as monotherapy for the first-line treatment of adult patients with metastatic microsatellite instability-high or mismatch repair deficient colorectal Cancer. *ESMO Open*. (2021) 6:100145. doi: 10.1016/j.esmoop.2021.100145

23. Lu W, Yu W, He J, Liu W, Yang J, Lin X, et al. Reprogramming immunosuppressive myeloid cells facilitates immunotherapy for colorectal Cancer. *EMBO Mol Med*. (2021) 13:e12798. doi: 10.15252/emmm.202012798

24. Ohishi T, Kaneko MK, Yoshida Y, Takashima A, Kato Y, Kawada M. Current targeted therapy for metastatic colorectal Cancer. *Int J Mol Sci*. (2023) 24:1702. doi: 10.3390/ijms24021702

25. Tonello M, Baratti D, Sammartino P, Di Giorgio A, Robella M, Sassaroli C, et al. Prognostic value of specific Kras mutations in patients with colorectal peritoneal metastases. *ESMO Open*. (2024) 9:102976. doi: 10.1016/j.esmoop.2024.102976

26. Benson AB, Venook AP, Al-Hawary MM, Arain MA, Chen YJ, Ciombor KK, et al. Colon Cancer, version 2.2021, Nccn clinical practice guidelines in oncology. *J Natl Compr Cancer Netw*. (2021) 19:329–59. doi: 10.6004/jnccn.2021.0012

27. Sepulveda AR, Hamilton SR, Allegra CJ, Grody W, Cushman-Vokoun AM, Funkhouser WK, et al. Molecular biomarkers for the evaluation of colorectal Cancer: guideline summary from the American Society for Clinical Pathology, College of American Pathologists, Association for Molecular Pathology, and American Society of Clinical Oncology. *J Oncol Pract*. (2017) 13:333–7. doi: 10.1200/JOP.2017.022152

28. Gmeiner WH. Recent advances in therapeutic strategies to improve colorectal Cancer treatment. *Cancers (Basel)*. (2024) 16:1029. doi: 10.3390/cancers16051029

29. Marmol I, Sanchez-de-Diego C, Pradilla Dieste A, Cerrada E, Rodriguez Yoldi MJ. Colorectal carcinoma: a general overview and future perspectives in colorectal Cancer. *Int J Mol Sci*. (2017) 18:197. doi: 10.3390/ijms18010197

30. Modest DP, Pant S, Sartore-Bianchi A. Treatment sequencing in metastatic colorectal Cancer. *Eur J Cancer*. (2019) 109:70–83. doi: 10.1016/j.ejca.2018.12.019

31. Messersmith WA. Nccn guidelines updates: management of metastatic colorectal Cancer. *J Natl Compr Cancer Netw*. (2019) 17:599–601. doi: 10.6004/jnccn.2019.5014

32. Islam MR, Akash S, Rahman MM, Nowrin FT, Akter T, Shohag S, et al. Colon Cancer and colorectal Cancer: prevention and treatment by potential natural products. *Chem Biol Interact*. (2022) 368:110170. doi: 10.1016/j.cbi.2022.110170

33. Huang X, Ke K, Jin W, Zhu Q, Zhu Q, Mei R, et al. Identification of genes related to 5-fluorouracil based chemotherapy for colorectal Cancer. *Front Immunol*. (2022) 13:887048. doi: 10.3389/fimmu.2022.887048

34. Lund CM, Vistisen KK, Dehlendorff C, Ronholt F, Johansen JS, Nielsen DL. The effect of geriatric intervention in frail elderly patients receiving chemotherapy for colorectal Cancer: a randomized trial (Gerico). *BMC Cancer*. (2017) 17:448. doi: 10.1186/s12885-017-3445-8

35. Xie YH, Chen YX, Fang JY. Comprehensive review of targeted therapy for colorectal Cancer. *Signal Transduct Target Ther*. (2020) 5:22. doi: 10.1038/s41392-020-0116-z

36. Zhang X, Qiu H, Li C, Cai P, Qi F. The positive role of traditional Chinese medicine as an adjunctive therapy for Cancer. *Biosci Trends*. (2021) 15:283–98. doi: 10.5582/bst.2021.01318

37. Yan Y, Yang Y, Ning C, Wu N, Yan S, Sun L. Role of traditional Chinese medicine syndrome type, gut microbiome, and host immunity in predicting early and advanced stage colorectal Cancer. *Integr Cancer Ther*. (2023) 22:15347354221144051. doi: 10.1177/15347354221144051

38. Ni W, Liu T, Liu Y, Lu L, Zhou B, Dai Y, et al. Sijunzi decoction granules in the prevention and treatment of recurrence of colorectal adenoma: study protocol for a multicenter, randomized, double-blind, placebo-controlled trial. *Front Pharmacol*. (2023) 14:1175811. doi: 10.3389/fphar.2023.1175811

39. Wu B, Xuan ZR. Progress in research on applying Sijunzi decoction in treating digestive malignant tumor. *Chin J Integr Med*. (2007) 13:156–9. doi: 10.1007/s11655-007-0156-z

40. Du J, Tao Q, Liu Y, Huang Z, Jin H, Lin W, et al. Assessment of the targeted effect of Sijunzi decoction on the colorectal Cancer microenvironment via the estimate algorithm. *PLoS One*. (2022) 17:e0264720. doi: 10.1371/journal.pone.0264720

41. Zhou JY, Chen M, Wu CE, Zhuang YW, Chen YG, Liu SL. The modified Si-Jun-Zi decoction attenuates Colon Cancer liver metastasis by increasing macrophage cells. *BMC Complement Altern Med*. (2019) 19:86. doi: 10.1186/s12906-019-2498-4

frontiers | Frontiers in Medicine

TYPE Systematic Review
PUBLISHED 01 May 2025
DOI 10.3389/fmed.2025.1527829

OPEN ACCESS

EDITED BY
Hua Zhong,
University of Hawaii at Manoa, United States

REVIEWED BY
Yiqian Zhang,
Tulane University, United States
H. -S. Chen,
University of California, Irvine, United States
Chuang Li,
AbbVie, United States

*CORRESPONDENCE
Yang Wang
✉ Wangyang669811@163.com

RECEIVED 13 November 2024
ACCEPTED 10 March 2025
PUBLISHED 01 May 2025

CITATION
Zou X and Wang Y (2025) Predictive value of osteopenia as prognostic marker for survival and recurrence in patients with gastrointestinal cancers: a systematic review and meta-analysis.
Front. Med. 12:1527829.
doi: 10.3389/fmed.2025.1527829

Predictive value of osteopenia as prognostic marker for survival and recurrence in patients with gastrointestinal cancers: a systematic review and meta-analysis

Xinmei Zou and Yang Wang*

Ward 13 (Respiratory Digestive Geriatrics), Huzhou Third Municipal Hospital, The Affiliated Hospital of Huzhou University, Huzhou, Zhejiang, China

Background: Early detection, systematic prevention, and personalized therapy are crucial to reduce mortality in patients with gastrointestinal (GI) cancers. This systematic review and meta-analysis aimed to clarify the predictive value of osteopenia and osteosarcopenia as prognostic markers of survival and recurrence in patients with GI cancers.

Methods: Medline, Google Scholar, and Science Direct databases were searched for English-language studies that included patients who underwent surgical resection following a pathologically diagnosed GI cancer and reported the association between osteopenia and osteosarcopenia on the overall survival (OS) and recurrence-free survival (RFS). Meta-analysis was done using STATA 14.2, and the results were reported as pooled hazard ratios (HR) with 95% confidence intervals (CI). Heterogeneity was assessed using the I2 statistic and the Chi-square test. Study quality was evaluated using the Newcastle Ottawa Scale (NOS).

Results: A comprehensive literature search yielded 23 eligible studies, primarily from Japan. Osteopenia emerged as a significant risk factor for both OS (pooled HR 2.20, 95% CI: 1.74–2.79) and RFS (pooled HR 2.15, 95% CI: 1.60–2.89). Patients with osteosarcopenia exhibited threefold higher mortality rates (pooled HR 2.96, 95% CI: 1.99–4.40) and heightened risk of recurrence (pooled HR 2.75, 95% CI: 1.79–4.24). Subgroup analyses underscored the consistency of these associations across diverse contexts.

Conclusion: This meta-analysis establishes osteopenia and osteosarcopenia as robust prognostic indicators for survival and recurrence in GI cancers. Integrating musculoskeletal assessments into routine oncological care is imperative for timely interventions and optimized patient outcomes.

KEYWORDS

osteopenia, GI cancers, overall survival, recurrence-free survival, osteosarcopenia

Introduction

Gastrointestinal (GI) cancers include malignancies of the esophagus, stomach, pancreas and biliary apparatus, liver and colon (1). GI cancers represent a formidable global health challenge, contributing significantly to morbidity and mortality (2). The prognosis of GI cancers may be influenced by many factors, such as tumor size, extent of metastases, and musculoskeletal status of patients that emerges as a critical determinant of overall well-being (3, 4).

Numerous studies have focused on the relationship between body composition and cancer prognosis. Recent reports have shown that osteopenia, characterized by low bone mineral density [BMD], sarcopenia, marked by loss of skeletal muscle mass, and osteosarcopenia, defined as the coexistence of osteopenia along with sarcopenia in cancer patients, are conditions that may potentially impact GI cancer outcomes (5, 6). Low BMD is often linked with an increased risk of falls, fractures, hospitalization, and even death, thereby negatively impacting the health-related quality of life (5). Additionally, bone loss in cancer patients may reflect osteopenia, malnutrition, and systemic inflammation (7). Recent studies demonstrated that in cancer patients, sarcopenia may be viewed not just as a malnutritional alteration but also as a systemic inflammatory change (8, 9). Furthermore, cancer-induced changes in metabolism, inflammatory status, and hormonal regulation may in turn contribute to the development and progression of osteopenia and sarcopenia (9).

The intricate relationship between osteopenia, sarcopenia, and cancer outcomes is still unclear. Existing studies often focus on individual components—tumor characteristics, treatment modalities, and patient demographics—neglecting the combined impact of bone and muscle health on patient outcomes (10, 11). GI cancers often impair nutrient absorption, leading to deficiencies that contribute to bone loss and worse clinical outcomes. Osteopenia is linked to increased chemotherapy toxicity, poor surgical recovery, and higher recurrence rates, making it a valuable early predictor of prognosis (7, 12). Therefore, due to the strong association of osteopenia with malnutrition, sarcopenia, and cancer cachexia, all of which are prevalent in GI cancer patients, it is crucial to further assess its value as a potential prognostic marker in this type of cancer. This comprehensive systematic review and meta-analysis aim to evaluate the predictive value of osteopenia and osteosarcopenia as prognostic markers of survival and recurrence in patients with GI cancers. Our results may contribute to developing tailored interventions and improving the prognostic accuracy of GI cancer outcomes.

Materials and methods

Research questions

Is there an association between osteopenia and osteosarcopenia with outcomes such as overall survival (OS) and recurrence-free survival (RFS) among patients with gastrointestinal cancers?

Objective

To evaluate the predictive value of osteopenia and osteosarcopenia as prognostic markers of survival and recurrence in patients with GI cancers.

Inclusion and exclusion criteria (PECO)

Population

Cancer patients who underwent surgical resection following a pathologically diagnosed digestive tract cancer (gastric, colorectal, esophageal, liver, biliary tract, pancreatic, and gallbladder) were chosen as study participants.

Exposure

Preoperative osteopenia was the main exposure of interest. Osteopenia was defined using the BMD, in accordance with the individual studies (The individual author's cut-offs for BMD were considered to categorize osteopenia). This study also included osteosarcopenia (coexistence of osteopenia and sarcopenia together). The definitions used for osteopenia and sarcopenia are elaborated in Table 1.

Outcome

The primary outcomes of interest were OS and RFS. OS was defined as the patient's death between the date of resection and the last point of contact with the patient. RFS was calculated from the date of the tumor's resection to the first recurrence at any site.

Study design

The review included all analytical designs, including cross-sectional, prospective, and retrospective studies.

Exclusion criteria

Studies not reported in English, studies that were not retrievable, case reports, case series, and grey literature were excluded. The search was not restricted to a specific region or publication year.

Our literature search encompassed three databases: Medline, Google Scholar, and Science Direct, from inception until December 2023.

Primary and secondary data screenings were independently conducted by both authors. Any conflicts that arose between them were resolved through mutual consensus. The reporting of our review adhered to the Preferred Reporting Items for Systematic Reviews and Meta-Analyses (PRISMA) framework (13). During the primary screening, both authors screened titles and abstracts of the studies, removing any duplicates. In the subsequent secondary screening, full texts of the selected studies were reviewed using the inclusion criteria, and relevant information was extracted.

Both authors created and meticulously checked a data extraction template to ensure completeness and accuracy. Information such as author details, region, study design, inclusion criteria, type of cancer, sample size, definition of OS, SP, OSP, and the cut-offs used were extracted from individual studies and entered into the template.

The databases and PROSPERO were examined to ascertain the absence of prior systematic reviews on the same topic, confirming the novelty of our review (CRD42023493216).

Search strategy

The following Medical subject heading (MeSH) terms were used: "Digestive tract cancer" OR "Digestive tract tumours" OR

TABLE 1 Characteristics of included studies, *n* = 23.

Study	Country	Cancer type	Sample size	Study type	Measurement of osteopenia	Measurement of sarcopenia	Formula for osteopenia	Formula for sarcopenia	Age (median and range/ Mean (SD))	Inclusion criteria	Outcomes	Quality of study (NOS)
Takeda et al. (16)	Japan	Biliary tract cancer (BTC)	306	Retrospective	Non-contrast CT scan images at the level of the 11th thoracic vertebra were used	SMI analyzed at the level of L3 vertebra before surgery	cut-off of <135 HU	SMI < 42 cm2 /m2 for men and SMI < 38 cm2 /m2 for women	70 (64–76)	Patients diagnosed with unresectable or recurrent BTC	OS, DFS	8
Matsumoto et al. (17)	Japan	Extrahepatic biliary cancer (EHBC)	138	Retrospective	Non-contrast CT scan images at the level of the 11th thoracic vertebra were used	PMA at 3rd lumber vertebra	men = [308.82–2.49 × age]; women = [311.84–2.41 × age]	length of the major axes × length of the minor axes × π	71 (35–87)	Patients with EHBC underwent resection	OS, DFS	8
Miki et al. (18)	Japan	Intrahepatic Cholangiocarcinoma (IHCC)	71	Retrospective	Non-contrast CT scan images at the level of the 11th thoracic vertebra were used	CT scan images at the third lumbar spine (L3) level were used to measure the psoas muscle mass index (PMI)	cut-off of <160 HU	6.36 for men and 3.92 for women	68.3 ± 8.6	Adult patients who underwent hepatectomy for IHCC	Overall Survival (OS), Recurrence Free Survival (RFS)	8
Kato et al. (19)	Japan	Colorectal cancer (CRC)	1,086	Retrospective	Non-contrast CT scans at the level of the 11th thoracic vertebra were used to measure BMD	Not evaluated	308.82–2.49 × age in men and 311.84–2.41 × age in women	Not evaluated	69 (59–76)	Patients who underwent curative surgical resection of stage I to III CRC	OS, RFS	8
Yanagaki et al. (20)	Japan	Hepatocellular cancer (HCC)	227	Retrospective	Average pixel density within a circle in the mid-vertebral core at the bottom of the 11th thoracic vertebra (Th11) on preoperative computed tomography	Lengths of the major and minor axes of the psoas muscle at the caudal end of the third lumbar vertebra and calculated the area of the psoas muscle	308.82–2.49 × age in men and 311.84–2.41 × age in women	Skeletal muscle index (SMI) cut off of 11.0 cm2/m2 for men and 7.4 cm2/ m2 for women	69 (62–74)	Patients with HCC who underwent primary hepatic resection	OS, RFS	8
Taniai et al. (21)	Japan	IHCC	41	Retrospective	BMD was measured in trabecular bone at the bottom of 11th thoracic vertebra (Th11) by calculating average pixel density within a circle	Psoas muscle mass area (PMA) below the sex-specific cutoffs level determined by a receiver-operating characteristics (ROC)	308.82–2.49 × age in men and 3.11.84–2.41 × age in female	major axis × the minor axis × π at the level of the 3rd lumber vertebra	63 (55–68)	Patients with IHCC undergoing hepatic resection	OS, RFS	7

(Continued)

10.3389/fmed.2025.1527829

TABLE 1 (Continued)

Study	Country	Cancer type	Sample size	Study type	Measurement of osteopenia	Measurement of sarcopenia	Formula for osteopenia	Formula for sarcopenia	Age (median and range/ Mean (SD))	Inclusion criteria	Outcomes	Quality of study (NOS)
Abe et al. (22)	Japan	Pancreatic ductal adenocarcinoma (PDAC)	265	Retrospective	Average pixel density within an oval core at the level of the Th11 vertebra before surgery	SMI analyzed at the level of L3 vertebra before surgery	men: 308.82–2.49 × age (yr) and women: 311.84–2.41 × age (yr)	Cut-off preoperative SMI value of 47.1 and 36.6 for male and female patients	68.2 ± 8.3	Patients with no evidence of distant metastases and underwent surgical resection for PDAC	OS, RFS	9
Meister et al. (23)	Germany	HCC	176	Retrospective	At the level of 11th Thoracic vertebra	Not evaluated	cut-off of <175 HU	Not evaluated	79 (75, 84)	All patients who underwent partial hepatectomy for HCC	OS, RFS	7
Fukushima et al. (24)	Japan	Gastric cancer (GC)	224	Retrospective	Average pixel density within a circle of the mid-vertebral core at the bottom of the 11th thoracic vertebra (Th11) on preoperative plain CT	PMA at 3rd lumber vertebra	men = [308.82–2.49 × age]; women = [311.84–2.41 × age]	length of the major axes × length of the minor axes × π	73 (66–79)	Patients with GC underwent initial gastrectomy	OS, RFS	8
Takano et al. (25)	Japan	CRC	136	Retrospective	Average pixel density within a circle in the mid-vertebral core at the bottom of the Th11 on the preoperative plain CT image	Cross-sectional area (cm2) of skeletal muscle at the level of the third lumbar vertebra and normalizing it by the patient's height (cm2/m2)	308.82–2.49 × age in men and 311.84–2.41 × age in women	SMI of ≤43.75 cm2/m2 for men and ≤ 41.10 cm2/m2 for women	72.6 (16.6) years	Stage I-III CRC aged 65–98 y who underwent curative resection.	OS, RFS	7
Watanabe et al. (26)	Japan	Perihilar Cholangiocarcinoma (PHCC)	256	Retrospective	Non-contrast CT scan images at the 11th thoracic (T11) vertebral level	Preoperative CT scan images at the level of the third lumbar (L3) vertebra	Cut-off of <160 HU	6.36 in males and 3.92 in females	70.3 ± 7.2	Patients who underwent resection of PHCC	OS	7
Cameron et al. (27)	United States	PDAC	152	Case control	Lumbar vertebral radiodensity (LVR)	An axial image at the level of the third lumbar (L3) vertebra	Not provided	Not provided	64.2 ± 12.6	Patients who underwent resection for histologically proven PDAC	OS	7
Kamada et al. (28)	Japan	CRC	230	Retrospective	Non-contrast CT images obtained at the 11th thoracic vertebra (Th11)	PMA at 3rd lumber vertebra	men = [308.82–2.49 × age]; women = [311.84–2.41 × age]	length of the major axes × length of the minor axes × π	67 (32–89 years)	Patients who underwent surgical resection for CRC	OS, RFS	7

(Continued)

10.3389/fmed.2025.1527829

TABLE 1 (Continued)

Study	Country	Cancer type	Sample size	Study type	Measurement of osteopenia	Measurement of sarcopenia	Formula for osteopenia	Formula for sarcopenia	Age (median and range/ Mean (SD))	Inclusion criteria	Outcomes	Quality of study (NOS)
Ikuta et al. (29)	Japan	Colorectal liver metastases (CRLM)	281	Retrospective	Non-contrast CT images obtained at the 11th thoracic vertebra	Not evaluated	BMD <141 HU	Not evaluated	66 (35–88 years)	Patients with CRLM underwent initial hepatic resection	OS, RFS	7
Furukawa et al. (30)	Japan	Colorectal liver metastases (CRLM)	118	Retrospective	Non-contrast CT images obtained at the 11th thoracic vertebra (Th11)	PMA at 3rd lumber vertebra	men = [308.82–2.49 × age]; women = [311.84–2.41 × age]	length of the major axes × length of the minor axes × π	Not provided	Patients with CRLM underwent initial hepatic resection	OS, RFS	8
Takahashi et al. (31)	Japan	Esophageal cancer (EC)	229	Retrospective	Average pixel density (HU) within a circle in the midvertebral core at the bottom of the 11th thoracic vertebra on preoperative CT	Cross-sectional area of the total skeletal muscle volume (cm2) at the bottom level of L3	Any	SMI < 41.1 cm2/m2 in females, and SMI < 43.0 cm2/m2 in males	65.3 ± 8.0	Patients with EC who underwent McKeown esophagectomy	OS, RFS	9
Tamura et al. (32)	Japan	EHCC	111	Retrospective	Non-contrast CT images obtained at the 11th thoracic vertebra (Th11)	The skeletal muscle area at the level of the third lumbar vertebra (L3) using transverse CT	308.82–2.49 × age in men and 311.84–2.41 × age in women	Not provided	Not provided	Patients who underwent PD	OS, RFS	7
Abe et al. (33)	Japan	PC	56	Retrospective	Non-contrast CT images obtained at the 11th thoracic vertebra (Th11)	The skeletal muscle area at the level of the third lumbar vertebra (L3) using transverse CT	Cut-off of <160 HU	The cut-off values were 38 cm2/m2 for women and 42 cm2/m2 for men	73 years	Patients who underwent pancreaticoduodenectomy (PD) or distal pancreatectomy (DP)	OS, RFS	9
Toshima et al. (34)	Japan	HCC	193	Retrospective	trabecular bone by calculating average pixel density within a circle in midvertebral core at the bottom of 11th thoracic vertebra	Cross-sectional areas (cm2) of skeletal muscles in L3 region	308.82–2.49 × age in men and 311.84–2.41 × age in women	126.9 x body surface area (BSA)–66.2 in men and 125.6 x BSA–81.1 in women	58 ± 6	Patients who underwent living donor liver transplantation	OS	8
Motomura et al. (35)	Japan	Pancreatic cancer (PC)	109	Retrospective	Non-contrast CT images at the Th11 level, using the entire vertebra body as the region of interest (ROI)	SMI analyzed at the level of L3 vertebra before surgery	Cut-off of <148 HU	Not provided	75 (49–90)	Patients who underwent resection for PC	OS, RFS	8

(Continued)

10.3389/fmed.2025.1527829

TABLE 1 (Continued)

Study	Country	Cancer type	Sample size	Study type	Measurement of osteopenia	Measurement of sarcopenia	Formula for osteopenia	Formula for sarcopenia	Age (median and range/ Mean (SD))	Inclusion criteria	Outcomes	Quality of study (NOS)
Sharshar et al. (36)	Japan	PC	181	Retrospective	BMD measurements were taken at the level of the 11th thoracic vertebra through calculation of the average pixel density within a circle	Psoas Muscle Index (PMI)	Males (137.5 HU) and females (128.8 HU)	Not provided	68 years (33–84)	Patients who underwent resection for PC	OS, RFS	7
Yao et al. (37)	Japan	EHBC	181	Case control	BMD measured by the CT attenuation value in the trabecular bone at the eleventh thoracic vertebral (Th11)	Psoas Muscle Index (PMI)	cut-off of <169 HU	Not provided	68 years (33–84)	Patients who underwent resection for EHBC	OS, RFS	7
Miyachi et al. (38)	Japan	HCC	465	Retrospective	BMD measured by the CT attenuation value in the trabecular bone at the eleventh thoracic vertebral (Th11)	Psoas Muscle Index (PMI)	cut-off of <160 HU	≤6.089	69 (62–75)	Patients underwent primary hepatectomy for HCC	OS, RFS	7

10.3389/fmed.2025.1527829

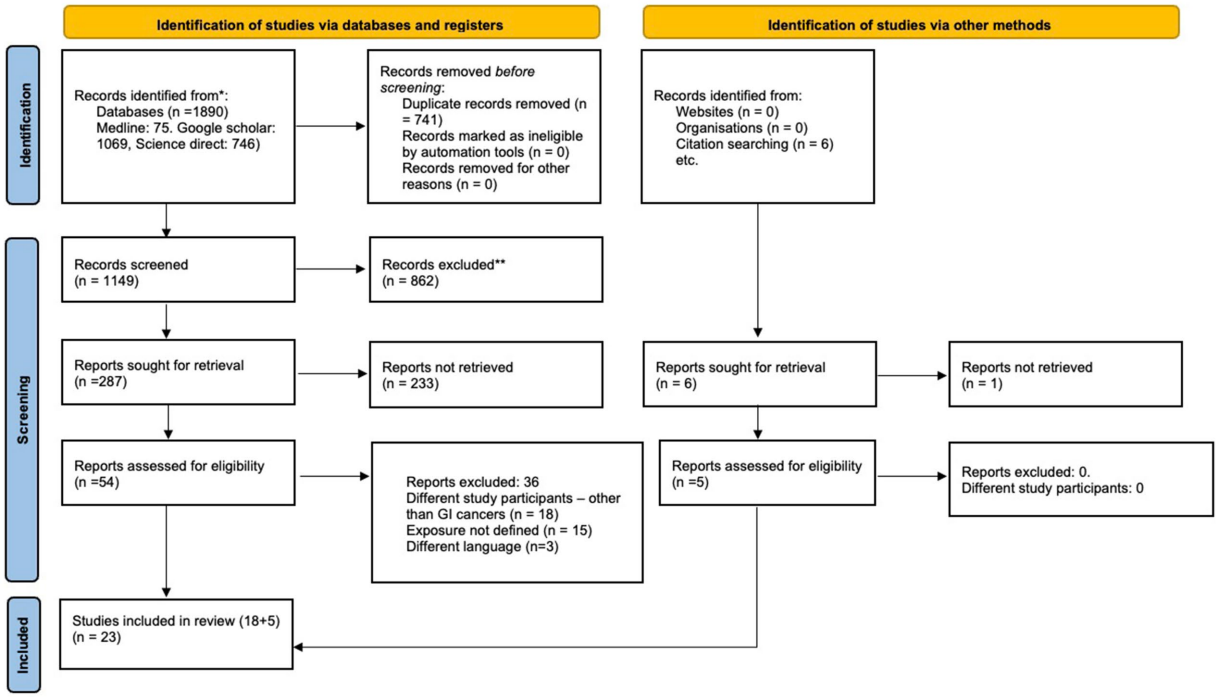

FIGURE 1
PRISMA 2020 flow diagram explaining the search flow.

"Gastrointestinal neoplasms" AND "Osteopenia" OR "Low BMD" AND "Osteosarcopenia" AND "Survival" OR "Death" AND "Outcome" AND "Recurrence free survival" AND "Disease free survival" AND "Observational studies" OR "Cohort studies" OR "Prospective studies." Reference list of included articles were screened for any potentially relevant studies. The detailed search strategy is provided as Supplementary material.

Statistical analysis

All statistical analyses were performed using STATA 14.2. Binary outcomes (OS, DFS & RFS) were analyzed using the inverse variance method to combine effects across various studies, expressing outcomes as pooled hazards ratios (HR) with 95% confidence intervals (CIs). The Freeman-Tukey double arcsine transformation was applied to mitigate the potential influences of both large and small studies on pooled estimates. Diligent attempts were made to contact the authors for missing data. Results, presented as pooled effect sizes, were visually depicted through forest plots. Publication bias was assessed using funnel plots, and statistical tests were conducted using Egger's test (14). Heterogeneity was assessed by I^2 statistic and the Chi-square heterogeneity test. Heterogeneity levels were categorized as mild ($I^2 < 25\%$), moderate (I^2 between 25 and 75%), and substantial ($I^2 > 75\%$). Due to expected heterogeneity in study definition and population, a random-effects model was used to account for the variation in effect sizes among the included studies. The between-study variance (τ^2) was estimated using the Der Simonian and Laird technique, and the pooled hazard ratios (HRs) for survival outcomes were calculated using the inverse variance approach. $p < 0.05$ was statistically significant.

Quality assessment of included studies

The Newcastle Ottawa Scale (NOS) (15) was used to evaluate study quality. This scale assesses studies based on outcomes, selection of study groups, and comparability, with a maximum score of nine for each study.

Results

Study selection

The initial search identified 1890 articles. After primary screening, 741 studies were removed as duplicates, and an additional 862 studies were removed at the stage of titles and abstracts evaluation. Of the remaining 287 articles, 54 free full-texts were retrieved for secondary screening, and 23 articles were ultimately selected for this systematic review and meta-analysis (16–38).

The reasons for exclusion were as follows: 18 studies reported on patients with other cancers, 15 did not define the exposure clearly, and 3 were not in English.

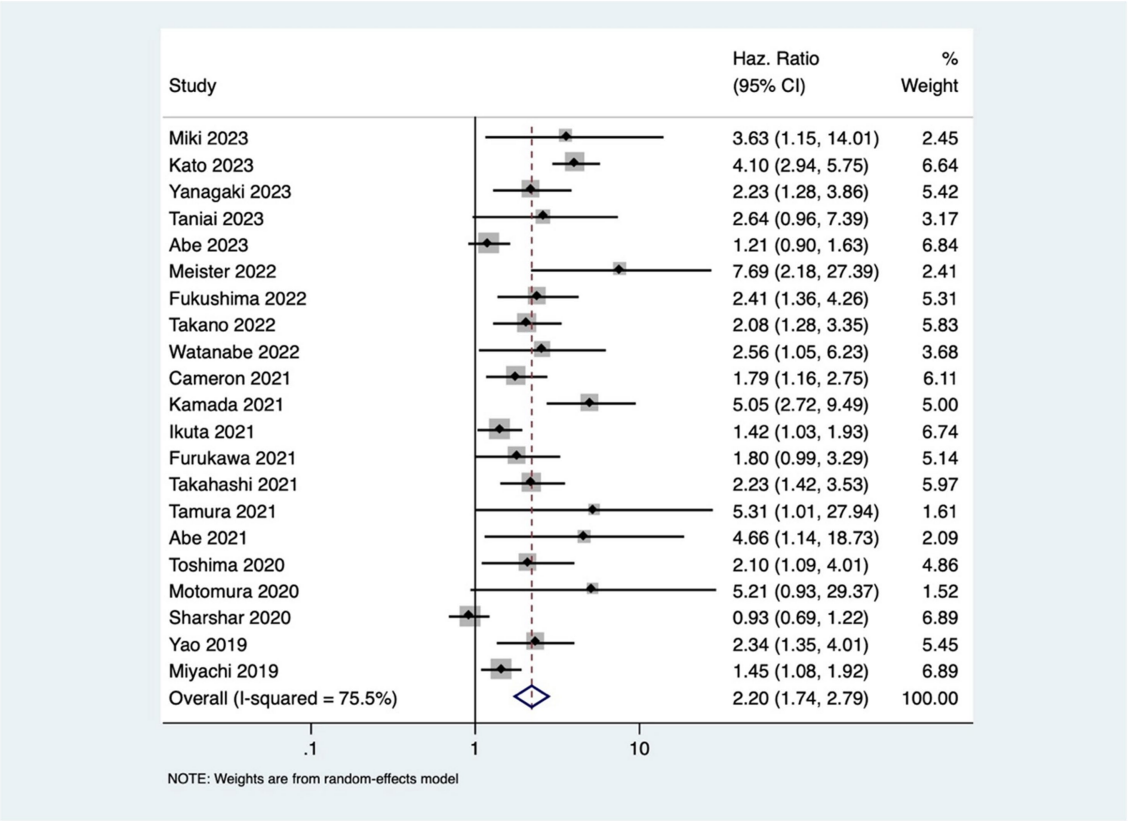

FIGURE 2
Forest plot of overall survival for osteopenia.

Characteristics of the included studies

The general characteristics of the included studies are outlined in Table 1. Of 23 studies, 21 were from Japan, and one study each was from Germany and the United States. Sample sizes of included studies ranged from 41 to 1,086. A majority (21/23) were retrospective. Figure 1 explains the study selection process. Twenty-one articles reported on the association between osteopenia and OS (18–38), 18 reported on the association between osteopenia and RFS (18–25, 28–33, 35–38). The association between OS and osteosarcopenia was reported by six studies (16, 17, 20–22, 25), RFS and osteosarcopenia were reported by five studies (17, 20–22, 25) and thus were pooled for the meta-analysis.

Association between osteopenia (low BMD) with OS and DFS

Patients with osteopenia or low BMD had significantly poorer OS (pooled HR of 2.20, 95% CI: 1.74–2.79, with high heterogeneity I^2=75.5, p-value <0.001) (Figure 2). The osteopenia was associated with lower RFS (pooled HR of 2.15, 95% CI: 1.60–2.89, with high heterogeneity I^2=88.4, p-value <0.001) (Figure 3). Due to the high heterogeneity observed across the studies, subgroup analysis was done to investigate the reasons for clinical heterogeneity. The type of GI cancer, geographical region of included studies, and sample size showed a significant association between incidences of osteopenia and survival outcomes (except for the association between low BMD with OS and low BMD with RFS among pancreatic cancer patients) (Supplementary Figures 1–6).

Association between osteosarcopenia with OS and DFS

GI cancer patients with osteosarcopenia had three 3 times higher mortality risk compared to patients without osteosarcopenia (pooled HR 2.96, 95% CI: 1.99–4.40, with high heterogeneity I^2=73.9, p-value <0.001) (Figure 4). Osteosarcopenia was a significant risk factor for poor RFS (pooled HR of 2.75, 95% CI: 1.79–4.24, with high heterogeneity I^2=74.8, p-value <0.001) (Figure 5).

Risk of bias

The asymmetric funnel plot showed evidence of publication bias for the association between osteopenia with OS and RFS (Supplementary Figures 7, 8).

Table 1 summarizes the risk of bias in the included studies, as assessed by NOS. Supplementary Figures 9, 10 show the effect of the risk of bias on the association between OS and RFS with osteopenia.

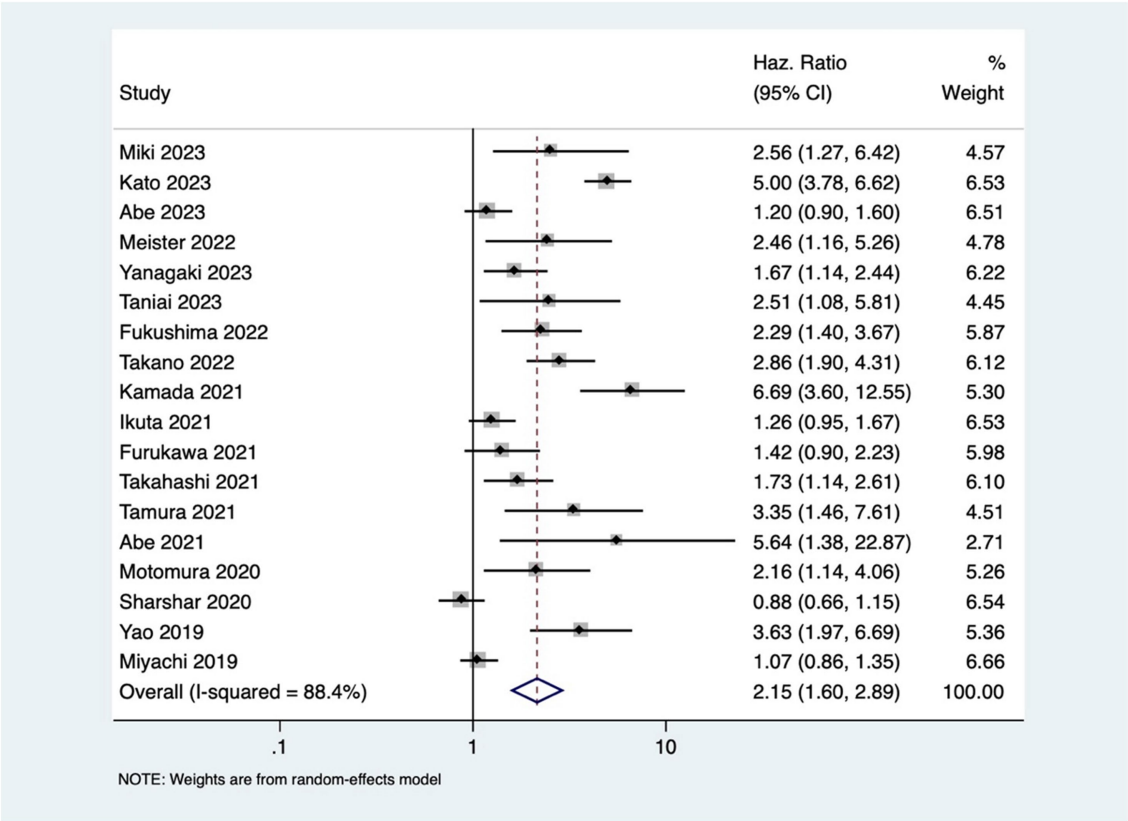

FIGURE 3
Forest plot of recurrence free survival for osteopenia.

Discussion

This meta-analysis showed that low BMD, osteopenia, and osteosarcopenia are potentially significant risk factors for poor OS and RFS among GI cancer patients. These findings highlight the need for preoperative assessment of GI cancer patients for timely interventions that may improve patient outcomes.

Together with genetics and ethnicity, BMD is a composite indicator reflecting exposure to multiple factors over the course of a patient's life (19). BMD positively correlates with patient's levels of estrogens, calcium and vitamin D intake, weight, and physical activity (39). Low BMD, therefore, is closely associated with factors that influence GI cancers either positively (calcium, vitamin D, oral contraceptives, physical activity) or negatively (age, BMI, smoking, alcohol) (40).

This study showed that GI cancer patients with osteopenia have 2-fold higher risk of death [pooled HR of 2.20, 95% CI: 1.74–2.79] and cancer recurrence [pooled HR of 2.15, 95% CI: 1.60–2.89]. These findings are comparable to the previous study done by Watanabe et al. that reported pooled HR of 2.02 and 1.96 for OS and RFS, respectively (41) The observed high heterogeneity in the association between osteopenia/osteosarcopenia and the outcomes might be attributed to variations in cancer types and stages, reflecting the heterogeneous nature of GI cancers. Despite the increased risk, the mechanism underlying osteopenia's negative impact on prognosis is still unclear. One possible mechanism of this effect may be osteoclast stimulation brought on by cancer cachexia (severe, unintentional loss of weight, muscle mass, and strength due to chronic inflammation and metabolic dysfunction), resulting in bone loss (42). The compromised structural integrity of bones in patients with osteopenia may render them more susceptible to the skeletal complications of cancer (such as osteoporosis, fracture, and bone loss), contributing to the observed increased rates of mortality and cancer recurrence. Additionally, cytokines produced from cancer cells, such as PTHrP, interleukin (IL)-1, IL-6, and IL-8, create and activate osteoclasts through activating the RANK/RANKL receptors, and subsequently, NF-κB (43), which leads to muscle loss and sarcopenia (5, 44, 45). This study revealed that osteosarcopenia that encompasses both bone and muscle deficits was associated with 3-times higher mortality in GI cancer patients.

The interplay between chronic inflammation (increased IL-6 and TNF-α leading to osteoclast activation and muscle protein breakdown, increased NF-κB and RANKL expression), muscle-bone crosstalk dysregulation (myostatin overexpression, irisin and osteocyte dysfunction), metabolic dysfunction, and tumor microenvironment alterations (IGF-1 suppression and adipokines and endocrine dysfunction) underlies the association between osteopenia/osteosarcopenia and poor survival in GI cancers (44, 45).

The results of this study further corroborate other reports highlighting the compounded impact of this complex condition (46). While our findings were comparable with previous reports (16, 17,

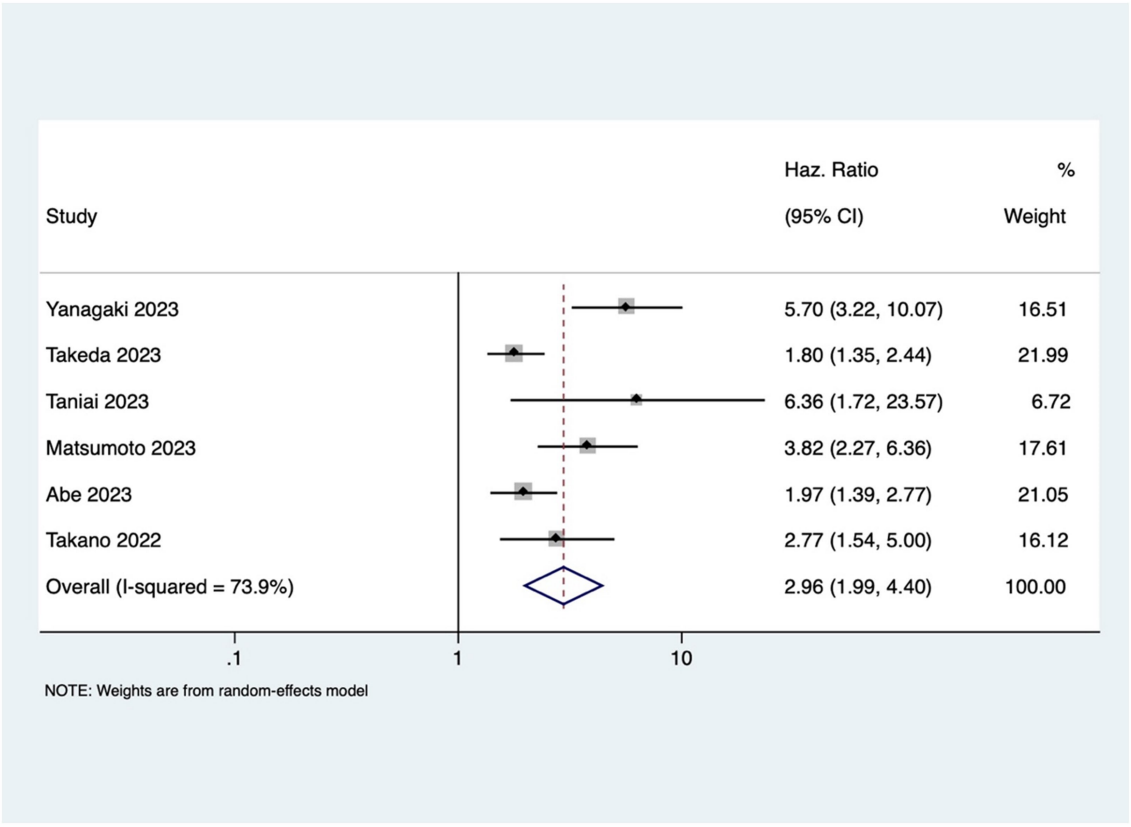

FIGURE 4
Forest plot of overall survival for osteosarcopenia.

22), the observed mortality rates associated with osteosarcopenia were slightly lower compared to other studies [HR >5] (20, 21). It is plausible that variations in study design, sample size, patient demographics, and follow-up period could cause this disparity. It's possible that selection bias was more likely to affect earlier research with smaller sample numbers, which resulted in inflated hazard ratios. Inconsistencies between studies may have also been caused by differences in diagnostic thresholds, imaging modalities, and definitions of osteosarcopenia (47).

Additionally, this study showed that osteosarcopenia was associated with poorer RFS (pooled HR of 2.75; $p < 0.001$). This observation further emphasizes the need for a comprehensive assessment that includes both musculoskeletal aspects.

The subgroup analysis showed that osteopenia was associated with poor OS in patients with colorectal cancer (HR of 2.5) and lower RFS in patients with bile duct and colorectal cancer (HR of 3 and 2.75, respectively). These results are in agreement with the previous meta-analysis by Watanabe et al. that showed the highest mortality rates in patients with colorectal cancer in combination with osteopenia and a maximum risk for recurrence in patients with osteopenia and colorectal or bile duct cancer (41).

However, no association was detected in pancreatic cancer patients. This discrepancy may be due to the aggressive tumor biology and early metastatic spread of pancreatic cancer, which may overshadow the impact of osteopenia on survival. Additionally, treatment-related malabsorption (Whipple surgery leading to malabsorption, etc), cachexia, and vitamin D deficiencies might have confounded the relationship between survival and low bone mineral density. Variations in assessment methods, such as computer tomography (CT) vs. dual-energy X-ray absorptiometry (DXA) and heterogeneity in patient cohorts could also contribute to the inconsistency (48, 49).

It is also important to consider that cancer chemotherapies, including alkylating agents, FOLFIRI, antimetabolites, glucocorticoids, and platinum-derived cisplatin, cause direct dysregulation of bone turnover and nephrotoxicity, which expedite bone loss (46, 50). Additionally, low BMD-specific outcomes, especially frailty fractures, could significantly impair functional status and physical activity. This, in turn, could result in non-cancer mortality or non-adherence to cancer treatment, which triggers recurrence (51).

Strengths and limitations

The main strengths of this review and meta-analysis are the inclusion of a substantial number of studies, rigorous screening processes, and comprehensive subgroup analyses that enhance the robustness of our findings.

However, this study has certain limitations. The high heterogeneity between the studies might impact the precision of our estimates.

One major limitation is the lack of standardized definitions for osteopenia and sarcopenia, which varied across the included

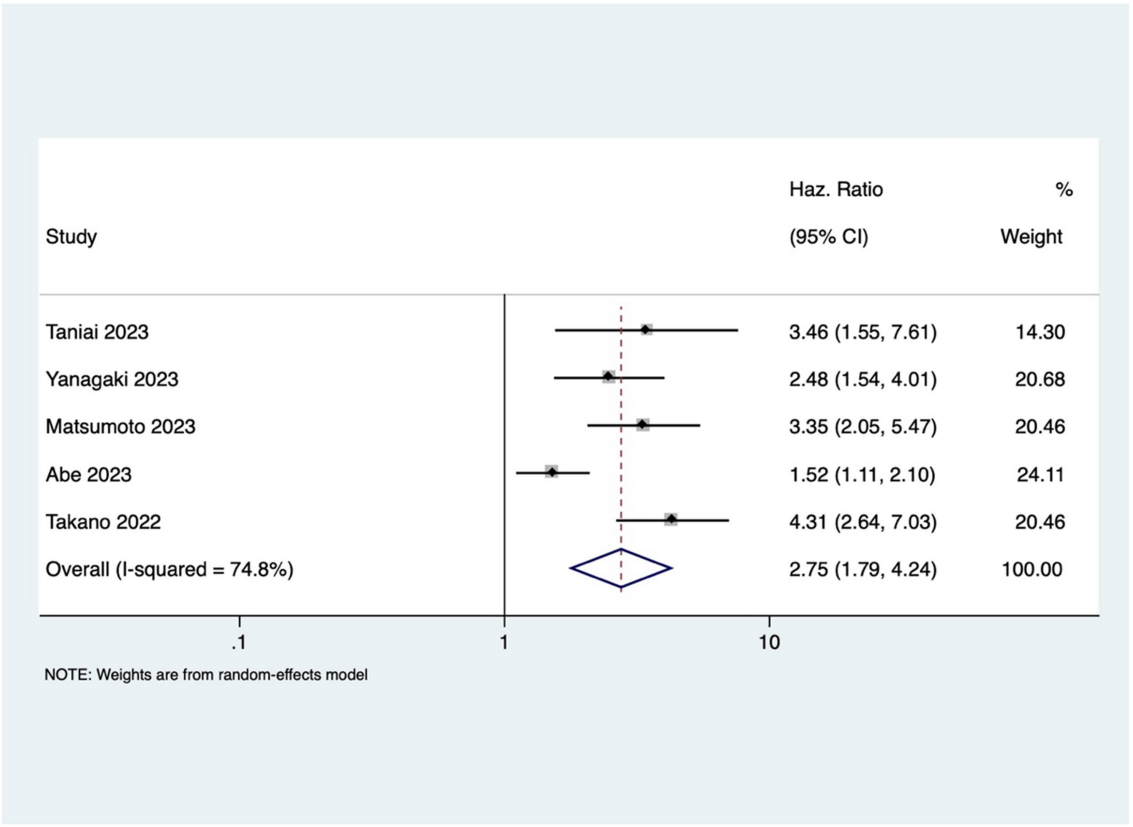

FIGURE 5
Forest plot of recurrence free survival for osteosarcopenia.

studies. This might have introduced heterogeneity in the findings, affecting the comparability of results. Additionally, while DXA is considered a gold standard for diagnosing osteopenia, all studies included in this review diagnosed osteopenia using preoperative CT. Thus, over-reliance on CT-based measurements instead of DXA to assess BMD presents another challenge. Moreover, different studies used different threshold values for defining osteopenia. Most included studies were from Japan, thus limiting the generalisability of the findings. The predominance of Japanese studies in this meta-analysis raises concerns about the generalizability of our findings due to cultural, genetic, dietary, and healthcare system differences. Traditional Japanese diets, lower obesity rates, and distinct genetic factors influencing bone and muscle metabolism may affect the prevalence and impact of osteopenia differently than in Western populations. Finally, this study was unable to rule out the potential publication and language biases (since the review included only studies published in English).

Conclusion and recommendations

In conclusion, this systematic review and meta-analysis show that osteopenia and osteosarcopenia are associated with significantly worse outcomes in patients with GI cancers. These results shed light on the intricate interplay between musculoskeletal health and outcomes in this population of patients. This study provides a robust foundation for integrating musculoskeletal assessments such as routine sarcopenia and osteopenia screening using tools like CT-based body composition analysis or DXA into the prognostic considerations for these cancers, and further strengthens the need of a holistic approach to GI cancer management that considers not only tumor characteristics but also patient's bone and muscle health. Future research should also explore interventional strategies aimed at mitigating the negative impact of osteopenia and sarcopenia in GI cancer patients. Trials investigating the use of exercise therapies (resistance training and muscle mass training) nutritional supplementation, and pharmacological interventions (such as anti-resorptive agents like bisphosphonates or denosumab) among cancer patients with osteopenia and osteosarcopenia with standardized diagnostic criteria are necessary.

Data availability statement

Publicly available datasets were analyzed in this study. This data can be found here: Medline, Google Scholar, and Science Direct, from inception until December 2023.

Author contributions

XZ: Conceptualization, Data curation, Formal analysis, Writing – original draft, Methodology. YW: Data curation, Formal analysis,

Methodology, Writing – original draft, Writing – review & editing, Project administration, Validation, Visualization.

Funding

The author(s) declare that no financial support was received for the research and/or publication of this article.

Conflict of interest

The authors declare that the research was conducted in the absence of any commercial or financial relationships that could be construed as a potential conflict of interest.

Generative AI statement

The authors declare that no Gen AI was used in the creation of this manuscript.

Publisher's note

Supplementary material

The Supplementary material for this article can be found online at: https://www.frontiersin.org/articles/10.3389/fmed.2025.1527829/full#supplementary-material

SUPPLEMENTARY FIGURE 1
Forest plot of overall survival for osteopenia grouped by cancer type.

SUPPLEMENTARY FIGURE 2
Forest plot of overall survival for osteopenia grouped by country.

SUPPLEMENTARY FIGURE 3
Forest plot of overall survival for osteopenia grouped by sample size.

SUPPLEMENTARY FIGURE 4
Forest plot of recurrence free survival for osteopenia grouped by cancer type.

SUPPLEMENTARY FIGURE 5
Forest plot of recurrence free survival for osteopenia grouped by country.

SUPPLEMENTARY FIGURE 6
Forest plot of recurrence free survival for osteopenia grouped by sample size.

SUPPLEMENTARY FIGURE 7
Funnel plot of overall survival for osteopenia.

SUPPLEMENTARY FIGURE 8
Funnel plot of recurrence free survival for osteopenia.

SUPPLEMENTARY FIGURE 9
Funnel plot of overall survival for osteopenia by quality of included studies.

SUPPLEMENTARY FIGURE 10
Funnel plot of recurrence free survival for osteopenia by quality of included studies.

References

1. Siegel RL, Miller KD, Fuchs HE, Jemal A. Cancer statistics, 2021. *CA Cancer J Clin*. (2021) 71:7–33. doi: 10.3322/caac.21654

2. Peery AF, Crockett SD, Murphy CC, Lund JL, Dellon ES, Williams JL, et al. Burden and cost of gastrointestinal, liver, and pancreatic diseases in the United States: update 2018. *Gastroenterology*. (2019) 156:254–272.e11. doi: 10.1053/j.gastro.2018.08.063

3. Cruz-Jentoft AJ, Bahat G, Bauer J, Boirie Y, Bruyère O, Cederholm T, et al. Sarcopenia: revised European consensus on definition and diagnosis. *Age Ageing*. (2019) 48:601. doi: 10.1093/ageing/afz046

4. Su H, Ruan J, Chen T, Lin E, Shi L. CT-assessed sarcopenia is a predictive factor for both long-term and short-term outcomes in gastrointestinal oncology patients: a systematic review and meta-analysis. *Cancer Imaging*. (2019) 19:82. doi: 10.1186/s40644-019-0270-0

5. Verschueren S, Gielen E, O'Neill TW, Pye SR, Adams JE, Ward KA, et al. Sarcopenia and its relationship with bone mineral density in middle-aged and elderly European men. *Osteoporos Int*. (2013) 24:87–98. doi: 10.1007/s00198-012-2057-z

6. Kirk B, Zanker J, Duque G. Osteosarcopenia: epidemiology, diagnosis, and treatment-facts and numbers. *J Cachexia Sarcopenia Muscle*. (2020) 11:609–18. doi: 10.1002/jcsm.12567

7. Pin F, Bonewald LF, Bonetto A. Role of myokines and osteokines in cancer cachexia. *Exp Biol Med*. (2021) 246:2118–27. doi: 10.1177/15353702211009213

8. Lavalle S, Valerio MR, Masiello E, Gebbia V, Scandurra G. Unveiling the intricate dance: how Cancer orchestrates muscle wasting and sarcopenia. *In Vivo*. (2024) 38:1520–9. doi: 10.21873/invivo.13602

9. Looijaard SMLM, Te Lintel Hekkert ML, Wüst RCI, Otten RHJ, Meskers CGM, Maier AB. Pathophysiological mechanisms explaining poor clinical outcome of older cancer patients with low skeletal muscle mass. *Acta Physiol*. (2021) 231:e13516. doi: 10.1111/apha.13516

10. Clemente-Suárez VJ, Redondo-Flórez L, Rubio-Zarapuz A, Martínez-Guardado I, Navarro-Jiménez E, Tornero-Aguilera JF. Nutritional and exercise interventions in Cancer-related Cachexia: an extensive narrative review. *Int J Environ Res Public Health*. (2022) 19:4604. doi: 10.3390/ijerph19084604

11. Prado CM, Purcell SA, Laviano A. Nutrition interventions to treat low muscle mass in cancer. *J Cachexia Sarcopenia Muscle*. (2020) 11:366–80. doi: 10.1002/jcsm.12525

12. Hirase Y, Arigami T, Matsushita D, Shimonosono M, Tsuruda Y, Sasaki K, et al. Prognostic significance of osteosarcopenia in patients with stage IV gastric cancer undergoing conversion surgery. *Langenbeck's Arch Surg*. (2024) 410:7. doi: 10.1007/s00423-024-03574-8

13. Page MJ, McKenzie JE, Bossuyt PM, Boutron I, Hoffmann TC, Mulrow CD, et al. The PRISMA 2020 statement: an updated guideline for reporting systematic reviews. *BMJ*. (2021) 372:n71. doi: 10.1136/bmj.n71

14. Egger M, Davey Smith G, Schneider M, Minder C. Bias in meta-analysis detected by a simple, graphical test. *BMJ*. (1997) 315:629–34. doi: 10.1136/bmj.315.7109.629

15. Lo CK-L, Mertz D, Loeb M. Newcastle-Ottawa scale: comparing reviewers' to authors' assessments. *BMC Med Res Methodol*. (2014) 14:45. doi: 10.1186/1471-2288-14-45

16. Takeda T, Okamoto T, Sasaki T, Hirai T, Ishitsuka T, Yamada M, et al. The impact of osteosarcopenia in patients with unresectable or recurrent biliary tract cancer receiving palliative chemotherapy. *Jpn J Clin Oncol*. (2023) 53:1051–7. doi: 10.1093/jjco/hyad097

17. Matsumoto M, Onda S, Igarashi Y, Hamura R, Uwagawa T, Furukawa K, et al. Osteosarcopenia is a significant predictor of recurrence and the prognosis after resection for extrahepatic bile duct cancer. *Surg Today*. (2023) 54:407–18. doi: 10.1007/s00595-023-02747-0

18. Miki A, Sakuma Y, Watanabe J, Endo K, Sasanuma H, Teratani T, et al. Osteopenia is associated with shorter survival in patients with intrahepatic cholangiocarcinoma. *Curr Oncol*. (2023) 30:1860–8. doi: 10.3390/curroncol30020144

19. Kato H, Seishima R, Mizuno S, Matsui S, Shigeta K, Okabayashi K, et al. The prognostic impact of preoperative osteopenia in patients with colorectal Cancer. *Dis Colon Rectum*. (2023) 66:e1225–33. doi: 10.1097/DCR.0000000000002961

20. Yanagaki M, Haruki K, Taniai T, Igarashi Y, Yasuda J, Furukawa K, et al. The significance of osteosarcopenia as a predictor of the long-term outcomes in

hepatocellular carcinoma after hepatic resection. *J Hepatobiliary Pancreat Sci*. (2023) 30:453–61. doi: 10.1002/jhbp.1246

21. Taniai T, Haruki K, Yanagaki M, Igarashi Y, Furukawa K, Onda S, et al. Osteosarcopenia predicts poor prognosis for patients with intrahepatic cholangiocarcinoma after hepatic resection. *Surg Today*. (2023) 53:82–9. doi: 10.1007/s00595-022-02550-3

22. Abe T, Nakata K, Nakamura S, Ideno N, Ikenaga N, Fujita N, et al. Prognostic impact of preoperative Osteosarcopenia for patients with pancreatic ductal adenocarcinoma after curative resection. *Ann Surg Oncol*. (2023) 30:6673–9. doi: 10.1245/s10434-023-13936-z

23. Meister FA, Verhoeven S, Mantas A, Liu W-J, Jiang D, Heij L, et al. Osteopenia is associated with inferior survival in patients undergoing partial hepatectomy for hepatocellular carcinoma. *Sci Rep*. (2022) 12:18316. doi: 10.1038/s41598-022-21652-z

24. Fukushima N, Tsuboi K, Nyumura Y, Hoshino M, Masuda T, Suzuki T, et al. Prognostic significance of preoperative osteopenia on outcomes after gastrectomy for gastric cancer. *Ann Gastroenterol Surg*. (2023) 7:255–64. doi: 10.1002/ags3.12635

25. Takano Y, Kodera K, Tsukihara S, Takahashi S, Kobayashi Y, Koyama M, et al. Prognostic significance of osteosarcopenia in older adults with colorectal cancer. *Ann Gastroenterol Surg*. (2023) 7:637–44. doi: 10.1002/ags3.12663

26. Watanabe J, Miki A, Sakuma Y, Shimodaira K, Aoki Y, Meguro Y, et al. Preoperative osteopenia is associated with significantly shorter survival in patients with Perihilar cholangiocarcinoma. *Cancers*. (2022) 14:2213. doi: 10.3390/cancers14092213

27. Cameron ME, Underwood PW, Williams IE, George TJ, Judge SM, Yarrow JF, et al. Osteopenia is associated with wasting in pancreatic adenocarcinoma and predicts survival after surgery. *Cancer Med*. (2022) 11:50–60. doi: 10.1002/cam4.4416

28. Kamada T, Furukawa K, Takahashi J, Nakashima K, Nakaseko Y, Suzuki N, et al. Prognostic significance of osteopenia in patients with colorectal cancer: a retrospective cohort study. *Ann Gastroenterol Surg*. (2021) 5:832–43. doi: 10.1002/ags3.12491

29. Ikuta S, Aihara T, Nakajima T, Kasai M, Yamanaka N. Computed tomography-measured bone mineral density as a surrogate marker of survival after resection of colorectal liver metastases. *Ann Transl Med*. (2021) 9:21. doi: 10.21037/atm-20-3751

30. Furukawa K, Haruki K, Taniai T, Hamura R, Shirai Y, Yasuda J, et al. Osteosarcopenia is a potential predictor for the prognosis of patients who underwent hepatic resection for colorectal liver metastases. *Ann Gastroenterol Surg*. (2021) 5:390–8. doi: 10.1002/ags3.12428

31. Takahashi K, Nishikawa K, Furukawa K, Tanishima Y, Ishikawa Y, Kurogochi T, et al. Prognostic significance of preoperative osteopenia in patients undergoing Esophagectomy for esophageal Cancer. *World J Surg*. (2021) 45:3119–28. doi: 10.1007/s00268-021-06199-w

32. Tamura S, Ashida R, Sugiura T, Okamura Y, Ito T, Yamamoto Y, et al. The prognostic impact of skeletal muscle status and bone mineral density for resected distal cholangiocarcinoma. *Clin Nutr*. (2021) 40:3552–8. doi: 10.1016/j.clnu.2020.12.011

33. Abe K, Furukawa K, Okamoto T, Matsumoto M, Futagawa Y, Haruki K, et al. Impact of osteopenia on surgical and oncological outcomes in patients with pancreatic cancer. *Int J Clin Oncol*. (2021) 26:1929–37. doi: 10.1007/s10147-021-01986-w

34. Toshima T, Yoshizumi T, Kosai-Fujimoto Y, Inokuchi S, Yoshiya S, Takeishi K, et al. Prognostic impact of osteopenia in patients who underwent living donor liver transplantation for hepatocellular carcinoma. *World J Surg*. (2020) 44:258–67. doi: 10.1007/s00268-019-05206-5

35. Motomura T, Uchiyama H, Iguchi T, Ninomiya M, Yoshida R, Honboh T, et al. Impact of osteopenia on oncologic outcomes after curative resection for pancreatic Cancer. *In Vivo*. (2020) 34:3551–7. doi: 10.21873/invivo.12198

36. Sharshar M, Kaido T, Shirai H, Okumura S, Yao S, Miyachi Y, et al. Impact of the preoperative bone mineral density on the outcomes after resection of pancreatic cancer. *Surg Today*. (2020) 50:757–66. doi: 10.1007/s00595-019-01954-y

37. Yao S, Kaido T, Okumura S, Iwamura S, Miyachi Y, Shirai H, et al. Bone mineral density correlates with survival after resection of extrahepatic biliary malignancies. *Clin Nutr*. (2019) 38:2770–7. doi: 10.1016/j.clnu.2018.12.004

38. Miyachi Y, Kaido T, Yao S, Shirai H, Kobayashi A, Hamaguchi Y, et al. Bone mineral density as a risk factor for patients undergoing surgery for hepatocellular carcinoma. *World J Surg*. (2019) 43:920–8. doi: 10.1007/s00268-018-4861-x

39. Dawson-Hughes B, Harris SS. Calcium intake influences the association of protein intake with rates of bone loss in elderly men and women. *Am J Clin Nutr*. (2002) 75:773–9. doi: 10.1093/ajcn/75.4.773

40. Ganry O, Lapôtre-Ledoux B, Fardellone P, Dubreuil A. Bone mass density, subsequent risk of colon cancer and survival in postmenopausal women. *Eur J Epidemiol*. (2008) 23:467–73. doi: 10.1007/s10654-008-9256-0

41. Watanabe J, Saitsu A, Miki A, Kotani K, Sata N. Prognostic value of preoperative low bone mineral density in patients with digestive cancers: a systematic review and meta-analysis. *Arch Osteoporos*. (2022) 17:33. doi: 10.1007/s11657-022-01060-6

42. Sakuma K, Hamada K, Yamaguchi A, Aoi W. Current nutritional and pharmacological approaches for attenuating sarcopenia. *Cells*. (2023) 12:2422. doi: 10.3390/cells12192422

43. Ham SL, Nasrollahi S, Shah KN, Soltisz A, Paruchuri S, Yun YH, et al. Phytochemicals potently inhibit migration of metastatic breast cancer cells. *Integr Biol*. (2015) 7:792–800. doi: 10.1039/C5IB00121H

44. Zain NM, Seriramulu VP, Chelliah KK. Bone mineral density and breast Cancer risk factors among premenopausal and postmenopausal women a systematic review. *Asian Pac J Cancer Prev*. (2016) 17:3229–34. doi: 10.14456/apjcp.2016.80/APJCP.2016.17.7.3229

45. Stewart A, Kumar V, Torgerson DJ, Fraser WD, Gilbert FJ, Reid DM. Axial BMD, change in BMD and bone turnover do not predict breast cancer incidence in early postmenopausal women. *Osteoporos Int*. (2005) 16:1627–32. doi: 10.1007/s00198-005-1886-4

46. Dolly A, Lecomte T, Bouché O, Borg C, Terrebonne E, Douillard J-Y, et al. Concurrent losses of skeletal muscle mass, adipose tissue and bone mineral density during bevacizumab / cytotoxic chemotherapy treatment for metastatic colorectal cancer. *Clin Nutr*. (2020) 39:3319–30. doi: 10.1016/j.clnu.2020.02.017

47. Xu F, Xi H, Liao M, Zhang Y, Ma H, Wu M, et al. Repurposed antipsychotic chlorpromazine inhibits colorectal cancer and pulmonary metastasis by inducing G2/M cell cycle arrest, apoptosis, and autophagy. *Cancer Chemother Pharmacol*. (2022) 89:331–46. doi: 10.1007/s00280-021-04386-z

48. Cao Y, Efetov SK, He M, Fu Y, Beeraka NM, Zhang J, et al. Updated clinical perspectives and challenges of chimeric antigen receptor-T cell therapy in colorectal Cancer and invasive breast Cancer. *Arch Immunol Ther Exp*. (2023) 71:19. doi: 10.1007/s00005-023-00684-x

49. Khalilieh S, Iyer A, Hammelef E, Zohar N, Gorgov E, Yeo TP, et al. Major pancreatic resection increases bone mineral density loss, osteoporosis, and fractures. *Ann Surg*. (2024). doi: 10.1097/SLA.0000000000006326. Epub ahead of print

50. Sturgeon KM, Mathis KM, Rogers CJ, Schmitz KH, Waning DL. Cancer- and chemotherapy-induced musculoskeletal degradation. *JBMR Plus*. (2019) 3:e10187. doi: 10.1002/jbm4.10187

51. Cawthon PM, Patel S, Ewing SK, Lui L, Cauley JA, Lyons JG, et al. Bone loss at the hip and subsequent mortality in older men: The osteoporotic fractures in men (MrOS) study. *JBMR Plus*. (2017) 1:31–5. doi: 10.1002/jbm4.10006

frontiers | Frontiers in Medicine

TYPE Case Report
PUBLISHED 18 June 2025
DOI 10.3389/fmed.2025.1517325

OPEN ACCESS

EDITED BY
Hua Zhong,
University of Hawaii at Manoa, United States

REVIEWED BY
Lingzhang Meng,
Guangxi Academy of Medical Sciences, China
Audrius Dulskas,
National Cancer Institute, Lithuania
Yifei Yang,
Cornell University, United States

*CORRESPONDENCE
Jinchang Huang
✉ zryhhuang@163.com
Qiaoli Zhang
✉ zhangqiaoli1009@126.com

RECEIVED 25 October 2024
ACCEPTED 23 May 2025
PUBLISHED 18 June 2025

CITATION
Li W, Yang M, Huang J and Zhang Q (2025) Long-term electroacupuncture for low anterior resection syndrome in postoperative rectal cancer patients: case reports.
Front. Med. 12:1517325.
doi: 10.3389/fmed.2025.1517325

Long-term electroacupuncture for low anterior resection syndrome in postoperative rectal cancer patients: case reports

Wenna Li[1,2], Ming Yang[1,2], Jinchang Huang[1,2]* and Qiaoli Zhang[1,2]*

[1]The Third Affiliated Hospital, Beijing University of Chinese Medicine, Beijing, China, [2]Institute of Acupuncture and Moxibustion in Cancer Care, Beijing University of Chinese Medicine, Beijing, China

This study reports two cases of rectal cancer patients who developed low anterior resection Syndrome (LARS) following rectal cancer surgery. Both patients presented with significant bowel dysfunction, including frequent defecation, urgency, fecal incontinence, and incomplete evacuation. Current treatments for LARS are limited by variable responses, high costs, and adherence issues, highlighting the need for practical, safe therapies with minimal side effects. The patients underwent a 6-month electroacupuncture treatment targeting Baliao points. Assessments were conducted using the LARS score, Wexner fecal incontinence score, and the EORTC QLQ-C30 scale. Results indicated a marked reduction in bowel frequency, significant relief of fecal incontinence symptoms, and improvement in overall health status and quality of life. In addition, emotional and cognitive functions were enhanced. These case reports suggest that electroacupuncture may be a valuable adjunctive treatment for managing LARS and improving patient emotional status and quality of life. Further high-quality research is necessary to evaluate the long-term efficacy of this treatment fully.

KEYWORDS

rectal cancer, low anterior resection, electroacupuncture, case report, Baliao points

1 Introduction

Low Anterior Resection Syndrome (LARS) is a common complication after rectal cancer surgery, with a high incidence rate of up to 42–44% (1). After resection of rectal cancer, patients often present with LARS-related clinical symptoms, including frequent defecation, urgency, evacuation difficulties, and fecal incontinence (2). Low anterior resection syndrome is characterized as a functional disorder of the bowel following rectal resection, resulting in a decline in quality of life (3). Bowel dysfunction is associated with quality of life, especially for overall health status, social functioning, and role functioning (4, 5). Improving intestinal function and promoting overall well-being in postoperative patients with rectal cancer is a critical challenge.

Currently, there is still a lack of standardized and comprehensive treatment plans for LARS internationally (6). Interventions mainly include symptomatic treatment of defecation, pelvic floor rehabilitation, transanal irrigation, and sacral nerve stimulation therapy (7). Available treatment strategies have significant limitations, such as poor adherence and significant individual variability in treatment response, or high costs and the risk of infection (8). Recent researches highlight the development of new strategies for LARS management. The MANUEL project proposed evidence-based algorithms for LARS management, emphasizing personalized interventions (9). Therefore, a safe and effective therapy with few adverse effects is urgently needed (10).

Anal sphincter dysfunction and nerve injury are major causes of Low Anterior Resection Syndrome (LARS) in rectal cancer patients after surgery (11). Recent studies have indicated that traditional acupuncture may be a safe and effective approach to alleviate symptoms of LARS (12). The anatomical location of Baliao points corresponds to the posterior sacral foramina. The Shangliao (BL31), Ciliao (BL32), Zhongliao (BL33), and Xialiao (BL34) points are anatomically aligned with the first, second, third, and fourth posterior sacral foramina, respectively. The anterior and posterior sacral foramina are connected to the sacral canal, through which the anterior and posterior branches of the sacral nerves pass, respectively (13). The Baliao points are close to the sacral nerves, which innervate the muscles around the anus. Acupuncture at the Baliao points has been demonstrated to reduce anorectal pressure (14), improve pelvic floor nerve and muscle modulation, and promote recovery from defecation dysfunction (15). This could potentially help relieve symptoms in LARS patients, such as increased stool frequency and fecal incontinence (16). Electroacupuncture, an advancement of traditional acupuncture, enables controlled adjustment of intensity, frequency, and duration of stimulation, providing continuous stimulation, resulting in longer-lasting therapeutic effects (17). Electroacupuncture offers a promising option to clinical research on LARS, with advantages of high patient acceptance, minor trauma, and few adverse effects (18). This study presents two patients with rectal cancer showing severe LARS symptoms, including increased bowel frequency, fecal incontinence, urgency, and incomplete evacuation, demonstrating the potential of electroacupuncture treatment in improving symptoms of LARS, while also enhancing patients' quality of life. This study was approved by the Institutional Review Board of the Third Hospital affiliated to Beijing University of Chinese Medicine (no. ECHBZYYSL-ZYDSY2024-13).

2 Study intervention and evaluation protocol

2.1 Electroacupuncture treatment protocol

One well-trained person (T.A.) executed the electroacupuncture treatment. The patient was placed in a prone position, and the skin at the acupuncture points was disinfected. Disposable sterile acupuncture needles (0.30 × 75 mm) and an SDZ-V Hwato-brand electroacupuncture device were used during the treatment. The selected acupuncture points were Baliao points, including bilateral Shangliao (BL31), Ciliao (BL32), Zhongliao (BL33), and Xialiao (BL34) (Figure 1A). The needles were inserted in order from Xialiao to Shangliao. For Xialiao points, the needles were inserted vertically. For Zhongliao points, the needles were inserted obliquely at an approximate 70-degree angle to the skin, directed inferomedially. For Ciliao points, the insertions were at an approximate 50-degree angle, also directed inferomedially. Finally, for Shangliao points, the insertions were at an approximate 30-degree angle, pointing inferomedially. The patient experienced mild sensations of soreness, numbness, or distention, radiating toward the anus and perineum. Afterward, the SDZ-V electroacupuncture device was connected, with electrodes placed longitudinally, and a continuous wave with a frequency of 50 Hz was applied. The needles were retained for 30 min. Additionally, the Changqiang point (GV1) was obliquely needled for 30 min (Figure 1B). The 50 Hz continuous stimulation and 30-minute treatment duration have been used in electroacupuncture for postoperative gastrointestinal and bowel dysfunction, including rectal cancer patients (19, 20). These specific parameters have been demonstrated to improve bowel function improve bowel and enhance pelvic floor function (21). Based on our previous clinical experience and expert recommendations, these specific parameters may consistently improve bowel frequency, fecal incontinence, and overall quality of life. Our research team has applied the same electroacupuncture protocol targeting LARS in rectal cancer patients. This protocol has been executed in a single-arm trial, further supporting the efficacy of the parameters in our study (18). Furthermore, the acupuncture angles applied in our case reports are appropriate. The Baliao points are situated within the sacral foramina and must be inserted obliquely or perpendicularly to reach the sacral nerve branches. The acupuncture angles of the Baliao points can be adjusted based on clinical expertise (20, 22).

2.2 Clinical assessment tools

This study primarily utilized three scales to assess postoperative recovery in rectal cancer patients, including the LARS score (LARSS), the Wexner incontinence score, and the European Organization for Research and Treatment of Cancer Quality of Life Questionnaire Core 30 (EORTC QLQ-C30). These scales assessed defecation function, fecal incontinence, and overall quality of life.

LARSS is the only recognized tool globally used explicitly for assessing bowel function following LAR in rectal cancer patients. The total score ranges from 0 to 42, and is categorized into three severity levels, with 0–20 as no LARS, 21–29 as mild LARS, and 30–42 as severe LARS (23). We utilized the Chinese-translated and validated version, which has been previously adopted within the Chinese population and demonstrated high validity and reliability (24). The validated Chinese version has been widely used in research on bowel dysfunction following rectal cancer surgery.

The Wexner incontinence score offers a more comprehensive assessment of fecal incontinence. It evaluates symptoms related to incontinence for flatus, liquid stool, solid stool, wears pad usage and lifestyle alteration (25). This allows for a more detailed evaluation of changes in fecal incontinence symptoms (26). Wexner fecal incontinence score has been extensively applied in Chinese patient

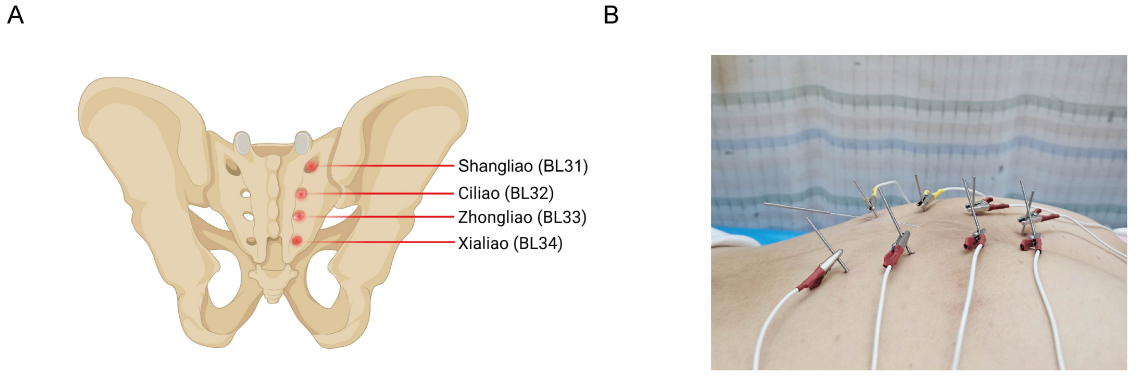

FIGURE 1
Anatomical locations of Baliao points and corresponding electroacupuncture needle placements. **(A)** Shows the anatomical locations of Baliao points, including Shangliao (BL31), Ciliao (BL32), Zhongliao (BL33), and Xialiao (BL34). **(B)** Shows positioning of electroacupuncture needles at Baliao points.

populations (27), including in postoperative patients of colorectal cancer, confirming its clinical feasibility and acceptability (28).

EORTC QLQ-C30 scale is a tool specifically designed for cancer patients that provides high specificity. It can evaluate multiple dimensions, including functional scales, symptom scales, and global health status, to comprehensively assess the quality of life in cancer patients (29). EORTC QLQ-C30 scale has been culturally adapted and psychometrically validated in China. It has demonstrated high reliability and validity (30, 31), and has been widely applied in clinical research among Chinese colorectal cancer patients (32).

3 Case presentation

3.1 Case no. 1

3.1.1 Management of rectal carcinoma

A 66-year-old male patient was diagnosed with rectal adenocarcinoma with a TNM stage of pT3N2M0. The patient had no prior history of gastrointestinal disease, diabetes, or neurological disease and had not undergone abdominal surgery or pelvic intervention. He denied prior abdominal operations and did not have significant cardiovascular and endocrine comorbidities. In September 2023, the patient underwent abdominal computed tomography (CT) and colonoscopy due to increased bowel movement frequency and hematochezia. The examinations revealed a rectal mass 5 cm from the anal verge without distant metastasis. Pathological examination confirmed rectal tubular adenocarcinoma. A multidisciplinary team recommended neoadjuvant chemotherapy followed by surgery. The patient received two cycles of neoadjuvant chemotherapy with the capecitabine and oxaliplatin (CAPOX) regimen. The specific dosage included oxaliplatin 200 mg administered via intravenous infusion on day 1 of each cycle and capecitabine 1.5 g orally, twice daily from days 1 to 14, followed by a 7-day drug withdrawal. The patient received a total of two chemotherapy cycles. The patient completed neoadjuvant chemotherapy without any grade $\geq$ 3 toxicities, and the regimen was generally well tolerated. In November 2023, the patient underwent a sphincter-sparing proctectomy. The postoperative pathology revealed a poorly differentiated adenocarcinoma of the rectum (protruding type, size 6 $\times$ 6 $\times$ 3 cm). The tumor invaded the muscularis and extended into the perirectal adipose tissue, forming one cancerous nodule. Perineural invasion and intravascular emboli were noted. Metastasis was identified in 1 of 20 pericolic lymph nodes, and 5 of 10 no. 253 lymph nodes located at the root of the inferior mesenteric artery showed metastatic involvement. Immunohistochemistry results showed negative HER-2 expression (4B5: 0) and a high proliferative index (Ki-67 > 75%). The tumor exhibited positive staining for MLH1, MSH2, MSH6, and PMS2. From January to June 2024, the patient underwent six cycles of chemotherapy, with the regimen consisting of oxaliplatin 180 mg on day 1 and capecitabine 1.5 g orally, twice daily, from day 1 to day 14. The chemotherapy was well tolerated, with no significant adverse reactions observed. The patient did not undergo any interventions for LARS prior to electroacupuncture, including sacral nerve stimulation (SNS) or transanal irrigation.

3.1.2 Electroacupuncture treatment and outcomes

The patient was severely affected by LARS symptoms after surgery, including frequent defecation, with up to 10 times a day, severely impacting his quality of life. In addition, frequent nocturnal bowel movements led to sleep disruption and considerable distress. Due to the persistence of LARS symptoms, the first patient, a 65-year-old male, began electroacupuncture treatment in February 2024, with a frequency of twice a week for a total of 6 months. The patients felt only minor discomfort from electrical stimulation. The discomfort was temporary and can be alleviated by modifying the electrical current. During the first 4 weeks after rectal cancer surgery, the patient followed a low-fiber, low-fat, and easily digestible soft diet, with adequate fluid intake. After six weeks, the diet gradually returned to normal, while caffeine, alcohol, and spicy foods were avoided. These measures followed the routine postoperative management of rectal

cancer and did not constitute structured interventions targeting LARS. No other LARS-related interventions were implemented during the treatment period, including structured dietary or lifestyle interventions, PFR, TAI, or SNS. Therefore, the clinical improvements observed in both cases are more likely attributable to electroacupuncture alone.

After rectal cancer surgery, the patient experienced more than ten bowel movements per day, accompanied by urgency and incomplete evacuation, with a LARSS score of 41. During the initial 3 months of electroacupuncture treatment, the frequency of bowel movements decreased from 10 times per day to approximately 5 times. Night-time bowel movements also decreased, allowing the patient to sleep better. By the end of the 6-month treatment, the symptoms of fecal incontinence, urgency and incomplete evacuation had improved significantly, with bowel frequency stabilizing 1 to 3 times per day, which was manageable for the patient. The patient's LARSS rating was assessed after 6 months of electroacupuncture treatment, and it improved from severe LARS (41 points) to no LARS (0 points) (Figure 2A). The Wexner score also improved, dropping from 17 before treatment to 0 (Figure 2B). In addition, according to the EORTC QLQ-C30 scale, we found that electroacupuncture treatment led to significant improvements in functional dimensions, including physical, emotional, cognitive, and social functions, with post-treatment scores increasing to 100. Symptoms such as fatigue, pain, and nausea were completely alleviated, with scores dropping to 0. Furthermore, sleep quality improved, and anxiety and depressive feelings related to bowel urgency were reduced. The patient's overall health and quality of life were significantly enhanced (Table 1). Follow-up in February 2025 showed that the patient had 1–2 bowel movements per day. There were no bowel movements at night, and sleep was not disturbed. Stool appearance was normal, and bowel movements were regular. There was no more fecal incontinence or urgency. Both the LARSS and Wexner scores were 0, signifying the resolution of intestinal dysfunction. The EORTC QLQ-C30 questionnaire indicated that the patient sustained a positive status in all dimensions, including physical, emotional, cognitive and social functioning. The global health score increased from 75 after treatment to 83. Symptoms like fatigue and pain did not come back. Sleep quality stayed good. The patient felt emotionally stable and reported a better quality of life. Case no. 1 outcomes at different time points are shown in Table 2.

3.2 Case no. 2

3.2.1 Management of rectal carcinoma

A 65-year-old male patient underwent a colonoscopy in April 2022 due to bloody stools and perianal pain. The colonoscopy showed a rectal mass located 6 cm from the anal verge, and pathological examination confirmed rectal tubular adenocarcinoma. Contrast-enhanced abdominal CT and pelvic MRI revealed a mid-rectal tumor extending beyond the muscularis propria, with no signs of regional lymphadenopathy or distant metastases. The patient had no prior history of gastrointestinal, neurological, cardiovascular, or endocrine disorders. He had not undergone any previous abdominal or pelvic surgery. The patient underwent proctectomy in May 2022. The postoperative pathology revealed a moderately differentiated adenocarcinoma of the rectum (protruding type, size 5.5 × 5 × 2.5 cm). The tumor invaded the muscularis and extended into the perirectal adipose tissue. Perineural invasion was noted, but no evidence of vascular invasion was detected. No regional lymph node metastasis was observed. Immunohistochemistry results showed negative HER-2 expression (4B5: 0) and a moderate proliferative index (Ki-67: 75%). The tumor exhibited positive staining for MLH1, MSH2, MSH6, and PMS2 with a TNM stage of pT3N0M0. After surgery, the patient received eight cycles of a capecitabine chemotherapy regimen. The specific dose was 1.25 g, orally twice daily from days 1 to 14 (d1–d14) of each chemotherapy cycle, followed by a 7-day drug withdrawal. Each cycle lasted 21 days, and the patient completed eight cycles. During chemotherapy, the patient experienced nausea and fatigue. No grade $\geq$ 3 hematologic or gastrointestinal toxicities were observed. The patient did not undergo any LARS intervention postoperatively, including SNS or transanal irrigation.

3.2.2 Electroacupuncture treatment and outcomes

The patient's primary postoperative symptoms included an increased frequency of defecation, up to 20 times a day, which was difficult to control, accompanied by anal pain and discomfort, as well as periodic intestinal fluid leakage. The patient had generalized weakness, affecting daily life seriously. The patient underwent 6 months of electroacupuncture therapy at our hospital 1 year after the operation, with treatments administered twice per week. The electroacupuncture protocol was the same as that used for the first patient. Following 30 min of stimulation, the patient felt mild skin irritation at the needling sites. The current intensity (1–5 mA) was adjusted to induce slight skin twitching around the acupoint without pain. Additionally, each treatment session was limited to 30 min to minimize the risk of side effects caused by extended electrical stimulation. The patient followed general postoperative recommendations after rectal cancer surgery, including consuming a light diet, avoiding irritant foods, and maintaining a regular daily routine. During the treatment period, no additional interventions for LARS were implemented, such as structured dietary or lifestyle interventions, PFR, TAI, or SNS.

Following the rectal cancer surgery, the patient had significant bowel dysfunction, with more than twenty bowel movements per day, accompanied by a feeling of anal discomfort. The LARSS score was 34, indicating severe LARS. The patient's symptoms gradually improved during the first 3 months of electroacupuncture treatment. The daily frequency of bowel movements gradually decreased from over twenty to about 10, while the comfortlessness and pain diminished, and urgency was significantly reduced. The patient's overall emotional state improved, which further enhanced the patients confidence in the treatment and provided a strong foundation for continued care. After 6 months of electroacupuncture treatment, a reassessment of the patient's LARSS score showed a reduction from severe LARS (34 points) to mild LARS (9 points), indicating that the patient's bowel function had nearly returned to normal (Figure 3A). Bowel frequency stabilized at 2–3 times per day, with the sensation of anal discomfort and pain nearly disappearing, and complete restoration of strength. The Wexner scale score decreased from 20 before treatment to 0 (Figure 3B). The patient's ability to control bowel movements has improved significantly,

10.3389/fmed.2025.1517325

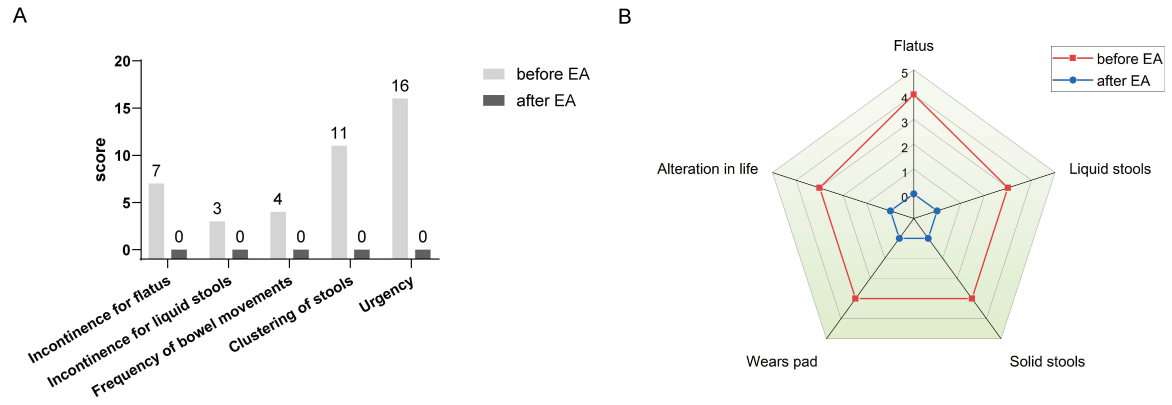

FIGURE 2
LARSS and Wexner incontinence score before and after electroacupuncture treatment in the first patient. **(A)** Shows LARSS scores of incontinence for flatus and liquid stools, frequency of bowel movements, clustering of stools, and urgency before and after treatment. **(B)** Shows Wexner incontinence scores before and after treatment, including incontinence for flatus, liquid stool, and solid stool, as well as wears pad usage and lifestyle alteration. EA, electroacupuncture.

TABLE 1 EORTC QLQ-C30 scores before and after electroacupuncture treatment for the first patient.

Dimension	Item numbers	Pre-treatment score	Post-treatment score
Functioning subscale			
Physical functioning	Q1–Q5	27	100
Role functioning	Q6–Q7	33	100
Emotional functioning	Q21–Q24	33	100
Cognitive functioning	Q20, Q25	33	100
Social functioning	Q26–Q27	83	100
Symptom subscale			
Fatigue	Q10, Q12, Q18	88	0
Nausea and vomiting	Q14, Q15	50	0
Pain	Q9, Q19	83	0
Dyspnea	Q8	100	0
Insomnia	Q11	100	0
Appetite loss	Q13	100	0
Constipation	Q16	67	0
Diarrhea	Q17	100	0
Financial difficulties	Q28	0	0
Global health status subscale			
Global health status	Q29–Q30	17	75

and fecal incontinence has completely disappeared, which has dramatically improved his quality of life. The results of the EORTC QLQ-C30 scale showed that prior to treatment, the patient had severe dysfunction in multiple dimensions, especially fatigue, pain, and diarrhea, which seriously affected daily life and overall health. Following electroacupuncture treatment, the patient's physical function recovered significantly, scoring 93. Role function improved to 67, emotional function improved to 83, cognitive function score improved to 50, and social function remained at 50. Most notably, the symptoms of fatigue, pain, and diarrhea completely alleviated, with scores dropping to 0. The patient's overall health status improved significantly, with the global health score rising from 0 to 100, indicating a substantial improvement in quality of life and health following treatment (Table 3). At the November 2024 follow-up, the patient maintained a bowel movement frequency of 2–3 times per day and regular bowel movements, with no incontinence or urgency. The LARSS score remained at 9 points, and the Wexner score remained at 0. According to the EORTC QLQ-C30, the patient's physical function remained good, emotional status was positive, and the global health score remained 100 points. The patient's quality of life was not affected by intestinal issues, with overall health status. Case no. 2 outcomes at different time points are shown in Table 4.

TABLE 2 Case no. 1: patient bowel function and symptoms at different time points.

Time points	Bowel frequency*	Fecal incontinence*	Fecal urgency*	Sleep quality	Emotional state	LARSS score	Wexner score	EORTC QLQ-C30 (Global Health Score)
Before EA (Feb 2024)	10–15 times/day	1–3 times/day	3–5 times/day	Poor	Anxiety/ depression	41	17	17
After EA (Aug 2024)	1–3 times/day	None	None	Good	Positive	0	0	75
Follow-up (Feb 2025)	1–2 times/day	None	None	Good	Positive	0	0	83

*Bowel Frequency, The daily frequency of bowel movements, including both daytime and nocturnal occurrences; Fecal Incontinence, The frequency of involuntary expulsion of a large volume of fecal material; Fecal Urgency, The frequency when the patient experiences an immediate compulsion to defecate, accompanied by an inability to postpone bowel movement.

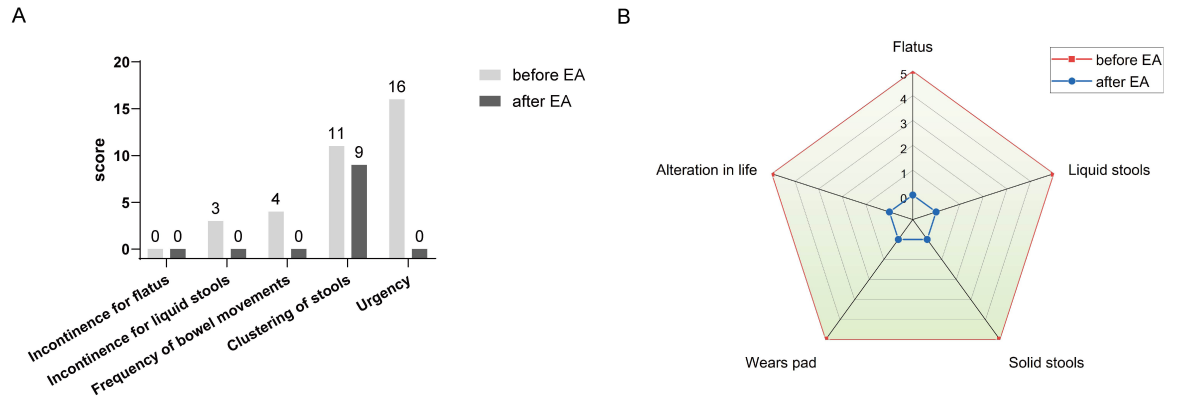

FIGURE 3
LARSS and Wexner incontinence score before and after electroacupuncture treatment in the second patient. **(A)** Shows scores of incontinence for flatus and liquid stools, frequency of bowel movements, clustering of stools, and urgency before and after treatment. **(B)** Wexner incontinence scores before and after treatment, including incontinence for flatus, liquid stool, and solid stool, as well as wears pad usage and lifestyle alteration. EA, electroacupuncture.

4 Discussion

Electroacupuncture is generally considered a safe treatment in rectal cancer patients (33). In this study, no needling-related adverse reactions were observed in all subjects. Patients were closely monitored throughout the treatment period, particularly during the initial electroacupuncture session, to prevent potential adverse reactions. The findings revealed that side effects from electroacupuncture on Baliao points were mild and temporary, consistent with the safety profiles observed in previous studies (14). Compared to conventional interventions, electroacupuncture offers a minimally invasive approach with fewer associated risks. Sacral nerve stimulation (SNS) involves the surgical implantation of a device to stimulate the S3 sacral nerve. This process carries risks such as infection, device failure, and the need for ongoing maintenance (34). Electroacupuncture is non-invasive and does not involve surgery, hence eliminating these risks. Furthermore, electroacupuncture shows distinct advantages in patient adherence. SNS requires permanent implantation and intricate parameter adjustments (35), while electroacupuncture is non-invasive and allows adaptable stimulation according to patient tolerance (36). Transanal irrigation demands daily use, frequently resulting in suboptimal compliance due to pain and discomfort (37). Conversely, electroacupuncture causes minimal interference with daily life and is better accepted. Pelvic floor rehabilitation requires active participation and prolonged training, restricting its use in patients with severe symptoms (38). Electroacupuncture works via neuromodulation and does not depend on patient effort, offering broader accessibility.

In addition to its positive safety and good adherence, electroacupuncture may ameliorate nerve injury and alleviate frequent defecation symptoms in postoperative LARS by sustained neural stimulation (16). Intraoperative damage to the sympathetic and parasympathetic nerves is a key factor contributing to postoperative LARS in patients with rectal cancer (39). Low anterior resection for rectal cancer leads to loss of autonomous control of the anal sphincter and incoordination of the rectal smooth muscles with the pelvic floor muscles (40). Pelvic floor rehabilitation effectively improved bowel control by strengthening the pelvic muscles (41). In contrast, acupuncture is recognized as a neuromodulatory therapy that activates somatic sensory afferents and modulates autonomic and neurochemical pathways involved in visceral regulation (42). It exerts broader neuromodulatory effects, potentially leading to faster and more pronounced robust improvements in the bowel (43). Colonic motility may be

TABLE 3 EORTC QLQ-C30 scores before and after electroacupuncture treatment for the second patient.

Dimension	Item numbers	Pre-treatment score	Post-treatment score
Functioning subscale			
Physical functioning	Q1–Q5	20	93
Role functioning	Q6–Q7	33	67
Emotional functioning	Q21–Q24	25	83
Cognitive functioning	Q20, Q25	17	50
Social functioning	Q26–Q27	50	50
Symptom subscale			
Fatigue	Q10, Q12, Q18	100	0
Nausea and vomiting	Q14, Q15	0	0
Pain	Q9, Q19	100	0
Dyspnea	Q8	0	0
Insomnia	Q11	0	0
Appetite loss	Q13	0	0
Constipation	Q16	0	0
Diarrhea	Q17	100	0
Financial difficulties	Q28	0	0
Global health status subscale			
Global health status	Q29–Q30	0	100

TABLE 4 Case no. 2: patient bowel function and symptoms at different time points.

Time points	Bowel frequency*	Fecal incontinence*	Fecal urgency*	Sleep quality	Emotional state	LARSS score	Wexner score	EORTC QLQ-C30 (Global Health Score)
Before EA (May 2023)	20–30 times/day	3–5 times/day	4–5 times/day	Fair	Anxiety/ depression	34	20	0
After EA (Nov 2023)	2–3 times/day	None	<1 time/week	Good	Positive	9	0	100
Follow-up (Nov 2024)	2–3 times/day	None	<1 time/week	Good	Positive	9	0	100

*Bowel Frequency, The daily frequency of bowel movements, including both daytime and nocturnal occurrences; Fecal Incontinence, The frequency of involuntary expulsion of a large volume of fecal material; Fecal Urgency, The frequency when the patient experiences an immediate compulsion to defecate, accompanied by an inability to postpone bowel movement.

altered through the modulation of enteric nervous system with acupuncture, lowering urgency symptoms of LARS (44).

Changqiang (GV1), located near the coccyx, is richly innervated. The deeper layers are penetrated by branches of the pudendal, perineal, and inferior rectal nerves. Stimulation of the GV1 via acupuncture will enhance coordination between reflexes of the pelvic floor and rectal sensation to improve bowel control and minimize fecal incontinence (45). Shangliao (BL31) is at the origin of the sacrospinalis and gluteus maximus muscles, under which the first sacral nerve (S1) passes. Ciliao (BL32) and Zhongliao (BL33) are at the gluteus maximus origin, and are passed through the posterior branches of the second (S2) and third (S3) sacral nerves, respectively. Xialiao (BL34) is at the similar muscular origin, with the fourth sacral nerve (S4) lying along with it (46). Baliao points are close to the sacral plexus, which innervates the pelvic floor muscles, including the levator ani, the external anal sphincter, and the internal anal sphincter through autonomic fibers (47). Deep needling of these points will directly stimulate the sacral nerve roots and potentially modulate both the somatic and the autonomic pathways used in anorectal function (20). Further, stimulation of the nerve via these points could increase the contractility of the external anal sphincter and thus enhance fecal continence control (48). Electroacupuncture has some advantages over traditional acupuncture. Electroacupuncture provides rhythmic microcurrent stimulation to the rectal surrounding muscles, inducing rhythmic contraction and enhancing the coordination of the muscles (21). Electroacupuncture at the Baliao acupoint was found to activate the sacral nerves (49), thus ensuring the regulation of the function of defecation (50). Sacral nerve stimulation (SNS) mainly treats fecal incontinence by implanting electrodes into the sacral foramina and stimulating the sacral nerves using low-frequency pulses (51, 52). SNS typically targets only the S3 nerve. In comparison, electroacupuncture at Baliao points stimulates the S1-S4 nerves, modulating defecation function via the sacral

nerves. Therefore, in this study, electroacupuncture at Baliao points was used as the primary intervention to explore its efficacy in treating LARS.

Although the initiation time of electroacupuncture treatment differed, with Case 1 initiating at 3 months and case 2 initiating at 12 months after rectal cancer surgery. Both of them demonstrated improvement in bowel function. It has been shown that spontaneous improvement in symptoms of LARS may occur within the first 12 months after rectal cancer surgery (53). However, this spontaneous improvement does not exclude a potential therapeutic effect of electroacupuncture. In case no. 2, electroacupuncture commenced 12 months after surgery, the patient's symptoms have stabilized. Therefore, the subsequent improvement observed may be more directly attributed to the effects of electroacupuncture. After intervention, the LARS score decreased from severe to mild, accompanied by a reduction in bowel movement frequency and urgency. These observations imply that delayed electroacupuncture can have potential therapeutic benefits in LARS patients. Indeed, electroacupuncture restores bowel function instead of relying on spontaneous recovery (54, 55). As stated above, electroacupuncture at the points of Baliao can stimulate the sacral roots of the nerves (S1–S4), thereby controlling the anorectal muscles and the pelvic floor. The ongoing neural stimulation enhances the neuromuscular coordination and gradually enhances the function of defecation. The extensive neural effects imply that early intervention with electroacupuncture, as in Case no. 1, may have the potential to prevent further deterioration. Even in later stages, as in case no. 2, its impact is significant. Our earlier work has demonstrated that neuroprotection with electroacupuncture results in neurogenesis (56). These observations provide mechanistic insight for the nerve restoration and support the therapeutic role of electroacupuncture. Ultimately, we underscore the patient-centered rationale for the various start times. Our aim was to not only alleviate physical symptoms but also enhance quality of life and improve mood. LARS symptoms, including frequent bowel movements, fecal incontinence, and urgency, can severely impact quality of life. Patient's urgent requirement for relief prompted the early electroacupuncture therapy in case no. 1. By intervening at 3 months after surgery, we facilitated the spontaneous recuperation of bowel function and alleviated physical discomfort earlier, possibly preventing further deterioration in mental health and daily functioning (9). Clinical research emphasizes the importance of intervention during early period when symptoms are severe, and patients are distressed (57). Numerous therapeutic methods, such as transanal irrigation and early drug interventions, are recommended to begin around 3–12 months after surgery to optimally manage LARS symptoms and help patients return to a normal daily routine (58, 59). Early electroacupuncture intervention can significantly reduce the severity of symptoms and improve psychological health (60). This aligns with the results of the EORTC QLQ-C30 scale in our case reports. On the other hand, the decision of the patient in case no. 2 to pursue electroacupuncture suggests that even after 12 months, persistent LARS symptoms continued to affect daily life, prompting the search for additional therapy. From a clinical perspective, therapy should be provided when the patient needs it most. In summary, despite the different timings of intervention, both patients benefited from electroacupuncture, which reduces bowel dysfunction and improves overall quality of life. This suggests the flexibility and efficacy of electroacupuncture at different stages following rectal cancer surgery. Early electroacupuncture may relieve LARS symptoms and avoid a deterioration in quality of life, while late electroacupuncture could still produce enhancements beyond the spontaneous improvement phase. Electroacupuncture demonstrates potential in the treatment of LARS at different postoperative phases, additional research is required to determine the most effective period for its application in LARS management.

In both cases, the patients' LARSS scores improved from severe (30–42) to no LARS (0–20), suggesting complete remission of symptoms such as frequent defecation, urgency, and incomplete evacuation. The Wexner scores were significantly reduced in both cases, reflecting an improvement in bowel control. Since the changes in bowel function following rectal cancer surgery have unpredictable negative impacts on patients' daily lives, emotions, and spirits, resulting in a decline in quality of life (33). Thus, managing LARS should not only focus on the intestinal symptoms but also address the broader effects on quality of life. Accordingly, this study further investigated the EORTC QLQ-C30 scale. Results showed that patients' EORTC QLQ-C30 functional and overall health status subscale scores increased significantly after a 6-month electroacupuncture treatment targeting Baliao points. This indicates enhancements in physical strength, emotional status, social interaction, and overall health status. Symptom relief was most prominent in fatigue, pain, and diarrhea, suggesting that acupuncture therapy may enhance the quality of life in LARS patients by improving bowel symptoms, which is beneficial for both physical and psychological health. Long-term follow-up results suggest that electroacupuncture may have a sustained effect on improving LARS symptoms. After 6 months of treatment, both patients maintained stable bowel function. LARS-related symptoms did not recur during the follow-up period, and quality of life remained largely unaffected. The follow-up revealed the initial effects of electroacupuncture treatment. The lack of a control group in these case reports generated potential bias. Moreover, the absence of blinding in the evaluation process may affect the outcomes. In future randomized controlled trials, we should incorporate sham acupuncture as a comparator and utilize independent blinded assessors for outcome evaluations. Additionally, extended follow-up periods are necessary to confirm the sustained efficacy of electroacupuncture in the management of LARS.

5 Conclusion

These two case reports highlight the potential of electroacupuncture as adjuvant therapy in the management of LARS symptoms following low anterior resection for rectal cancer. As a non-invasive therapy, electroacupuncture has demonstrated potential efficacy in relieving severe LARS symptoms, improving bowel function, and enhancing patients' quality of life. Electroacupuncture may be a valuable adjuvant treatment option for LARS, but future randomized controlled trials with rigorous design are needed to validate its long-term efficacy.

Data availability statement

The original contributions presented in the study are included in the article/Supplementary material, further inquiries can be directed to the corresponding authors.

Ethics statement

The studies involving humans were approved by Institutional Review Board of the third Hospital affiliated to Beijing University of Chinese Medicine. The studies were conducted in accordance with the local legislation and institutional requirements. The participants provided their written informed consent to participate in this study. Written informed consent was obtained from the individual(s) for the publication of any potentially identifiable images or data included in this article.

Author contributions

WL: Conceptualization, Data curation, Investigation, Methodology, Writing – original draft. MY: Data curation, Investigation, Writing – original draft. JH: Funding acquisition, Supervision, Writing – review & editing. QZ: Conceptualization, Funding acquisition, Supervision, Writing – review & editing.

Funding

The author(s) declare that financial support was received for the research and/or publication of this article. This research was funded by the Scientific Research Project of Hebei Province Administration of Traditional Chinese Medicine (B2025037) and Project of Beijing University of Chinese Medicine (2023-JYB-JBZD-038).

Acknowledgments

We would like to thank the patients' participation and cooperation. Figure 1A was created using BioRender.com.

Conflict of interest

The authors declare that the research was conducted in the absence of any commercial or financial relationships that could be construed as a potential conflict of interest.

Generative AI statement

The authors declare that no Generative AI was used in the creation of this manuscript.

Publisher's note

Supplementary material

The Supplementary Material for this article can be found online at: https://www.frontiersin.org/articles/10.3389/fmed.2025.1517325/full#supplementary-material

References

1. Varghese C, Wells C, O'Grady G, Christensen P, Bissett I, Keane C. The longitudinal course of low-anterior resection syndrome: An individual patient meta-analysis. *Ann Surg.* (2022) 276:46–54. doi: 10.1097/sla.0000000000005423

2. Haas S, Mikkelsen A, Kronborg C, Oggesen B, Møller P, Fassov J, et al. Management of treatment-related sequelae following colorectal cancer. *Colorectal Dis.* (2023) 25:458–88. doi: 10.1111/codi.16299

3. Mekhael, M, Kristensen H, Borre M, Drewes A, Emmertsen K, Fassov J, et al. Treatment of low anterior resection syndrome in specialized multidisciplinary late sequelae clinics: A prospective cohort study. *Ann Surg.* (2025). doi: 10.1097/sla.0000000000006714 [Epub ahead of print].

4. Sinimäki S, Elfeki H, Kristensen M, Laurberg S, Emmertsen K. Urinary dysfunction after colorectal cancer treatment and its impact on quality of life – a national cross-sectional study in women. *Colorectal Dis.* (2021) 23:384–93. doi: 10.1111/codi.15541

5. Bräuner A, Avellaneda N, Christensen P, Drewes A, Emmertsen K, Krogh K, et al. Prospective evaluation of bowel function and quality of life after colon cancer surgery–is it time for routine screening for late sequelae? *Acta Oncol.* (2023) 62:1132–42. doi: 10.1080/0284186x.2023.2246102

6. Sharp G, Findlay N, Clark D, Hong J. Systematic review of the management options available for low anterior resection syndrome (Lars). *Techn Coloproctol.* (2025) 29:58. doi: 10.1007/s10151-024-03090-3

7. Zhou L, Zhang Z, Wang L. Treatment of anterior resection syndrome: A systematic review and network meta-analysis. *Eur J Surg Oncol.* (2024) 50:108336. doi: 10.1016/j.ejso.2024.108336

8. Martellucci J, Falletto E, Ascanelli S, Bondurri A, Borin S, Bottini C, et al. Consensus-driven protocol for transanal irrigation in patients with low anterior resection syndrome and functional constipation. *Tech Coloproctol.* (2024) 28:153. doi: 10.1007/s10151-024-03033-y

9. Christensen P, Im Baeten C, Espín-Basany E, Martellucci J, Nugent K, Zerbib F, et al. Management guidelines for low anterior resection syndrome - the manuel project. *Colorectal Dis.* (2021) 23:461–75. doi: 10.1111/codi.15517

10. Ansar M, Boddeti S, Noor K, Malireddi A, Abera M, Suresh S, et al. A systematic review of comparative effectiveness of interventions for low anterior resection syndrome: Impacts on bowel function and quality of life. *Cureus.* (2024) 16:e72772. doi: 10.7759/cureus.72772

11. Miyo M, Akizuki E, Okuya K, Noda A, Ishii M, Miura R, et al. Diagnosis and treatment of low anterior resection syndrome. *J Anus Rectum Colon.* (2025) 9:1–9. doi: 10.23922/jarc.2024-069

12. Dulskas A, Aukstikalnis T, Kavaliauskas P, Samalavicius N. The role of traditional acupuncture in low anterior resection syndrome treatment: A pilot study. *Dis Colon Rectum.* (2022) 65:93–9. doi: 10.1097/dcr.0000000000002060

13. Wang X, Guan L. Effect of percutaneous electrical stimulation at the Baliao point on preventing postpartum urinary retention after labor analgesia. *World J Clin Cases.* (2024) 12:2758–64. doi: 10.12998/wjcc.v12.i16.2758

14. Shen J, Zhou X, Zhao J, Wang H, Ye T, Chen W, et al. Electroacupuncture at Baliao point alleviates post-operative pain and anal distension after procedure for prolapse and hemorrhoids (stapled hemorrhoidopexy): A prospective randomized clinical trial. *Int J Colorectal Dis.* (2023) 38:104. doi: 10.1007/s00384-023-04403-y

15. Ye S, Zhou J, Guo X, Jiang X. Three acupuncture methods for postoperative pain in mixed hemorrhoids: A systematic review and network meta-analysis. *Comput Math Methods Med.* (2022) 2022:5627550. doi: 10.1155/2022/5627550

16. Xu L, Xiang N, Cheng T, Li Y, Chen P, Jiang Z, et al. Application of electroacupuncture in the prevention of low anterior resection syndrome after rectal cancer surgery. *World J Gastrointest Surg.* (2023) 15:2765–73. doi: 10.4240/wjgs.v15.i12.2765

17. Wan Y, Qi X, Lian Y, Liu Z, Wang H, Qiu Y, et al. Electroacupuncture facilitates vascular normalization by inhibiting glyoxalase1 in endothelial cells to attenuate glycolysis and angiogenesis in triple-negative breast cancer. *Cancer Lett.* (2024) 598:217094. doi: 10.1016/j.canlet.2024.217094

18. Yang M, Jiang H, Xu L, Zhang Q, Li X, Han L, et al. Acupuncture for rectal cancer patients with low anterior resection syndrome: A mixed method pilot study protocol. *Perspect Integr Med.* (2023) 2:195–201. doi: 10.56986/pim.2023.10.008

19. Zhao J, Cai Y, Wang H, Zhou Y, Zhang Y, Chen W, et al. Comparison of pelvic autonomic nerve function recovery between the group only with surgery and group with additional acupuncture and electrotherapy for treatment in patients with rectal cancer after anus-preserving operation. *Acupunct Electro Ther Res.* (2018) 43:103–18. doi: 10.3727/036012918X15353852193131

20. Yang L, Yang M, Wan Y, Que C, Huang J. [Summary of professor Huang Jinchang's experience of electroacupuncture at Baliao acupoints for low anterior resection syndrome of rectal cancer]. *Zhongguo Zhen Jiu.* (2024) 44:1289–93. doi: 10.13703/j.0255-2930.20231212-k0001

21. Liu Z, Liu Y, Xu H, He L, Chen Y, Fu L, et al. Effect of electroacupuncture on urinary leakage among women with stress urinary incontinence: A randomized clinical trial. *JAMA.* (2017) 317:2493–501. doi: 10.1001/jama.2017.7220

22. Cheng X. *Chinese acupuncture and moxibustion*. Beijing: Foreign Languages Press (2019). 164.

23. Zhu Y, Ding X, Xiong W, Yang G, Si M, Yan H. Low anterior resection syndrome in total mesorectal excision: Risk factors and its relationship with quality of life. *J Laparoendosc Adv Surg Tech A.* (2024) 34:199–206. doi: 10.1089/lap.2023.0414

24. Hou X, Pang D, Lu Q, Yang P, Jin S, Zhou Y, et al. Validation of the Chinese version of the low anterior resection syndrome score for measuring bowel dysfunction after sphincter-preserving surgery among rectal cancer patients. *Eur J Oncol Nurs.* (2015) 19:495–501. doi: 10.1016/j.ejon.2015.02.009

25. Mahjoob D, Knol-de Vries G, de Boer M, van Koeveringe G, Blanker M. The association of fecal incontinence, constipation, and pelvic pain with the course of lower urinary tract symptoms in community-dwelling men and women. *Neurourol Urodyn.* (2024) 43:1566–73. doi: 10.1002/nau.25492

26. Essangri H, Majbar M, Benkabbou A, Amrani L, Mohsine R, Souadka A. Transcultural adaptation and validation of the moroccan arabic dialect version of the wexner incontinence score in patients with low anterior resection syndrome after rectal surgery. *Surgery.* (2021) 170:47–52. doi: 10.1016/j.surg.2021.01.029

27. Hsu L, Hung C, Kuo L, Tsai P. An abbreviated faecal incontinence quality of life scale for chinese-speaking population with colorectal cancer after surgery: Cultural adaptation and item reduction. *Eur J Cancer Care.* (2017) 26:1–10. doi: 10.1111/ecc.12547

28. Yuan Y, Qiu L, Li Z, Zhang L, Xu T, Lang J, et al. An epidemiology study of fecal incontinence in adult Chinese women living in urban areas. *Chin Med J.* (2020) 133:262–8. doi: 10.1097/cm9.0000000000000552

29. Zang Y, Qiu Y, Sun Y, Fan Y. Baseline functioning scales of Eortc Qlq-C30 predict overall survival in patients with gastrointestinal cancer: A meta-analysis. *Qual Life Res.* (2024) 33:1455–68. doi: 10.1007/s11136-023-03591-y

30. Shen M, Chen L, Ho T, Shih Y, Huang C, Chie W, et al. Validation of the Taiwan Chinese version of the Eortc Qlq-Cr29 to assess quality of life in colorectal cancer patients. *BMC Cancer.* (2018) 18:353. doi: 10.1186/s12885-018-4312-y

31. Magaji B, Moy F, Roslani A, Law C, Sagap I. Psychometric validation of the Malaysian Chinese version of the Eortc Qlq-C30 in colorectal cancer patients. *Asian Pac J Cancer Prev.* (2015) 16:8107–12. doi: 10.7314/apjcp.2015.16.18.8107

32. Peng J, Shi D, Goodman K, Goldstein D, Xiao C, Guan Z, et al. Early results of quality of life for curatively treated rectal cancers in Chinese patients with Eortc Qlq-Cr29. *Radiat Oncol.* (2011) 6:93. doi: 10.1186/1748-717X-6-93

33. Xu G, Xiao Q, Lei H, Fu Y, Kong J, Zheng Q, et al. Effectiveness and safety of acupuncture and moxibustion for defecation dysfunction after sphincter-preserving surgery for rectal cancer: Protocol for systematic review and meta-analysis. *BMJ Open.* (2020) 10:e034152. doi: 10.1136/bmjopen-2019-034152

34. Wynn J, Kelsey E, McLeod K. Treatment of the infected sacral nerve stimulator: A scoping review. *Neurourol Urodyn.* (2024) 43:579–94. doi: 10.1002/nau.25411

35. Thaha M, Abukar A, Thin N, Ramsanahie A, Knowles C. Sacral nerve stimulation for faecal incontinence and constipation in adults. *Cochrane Database Syst Rev.* (2015) 2015:Cd004464. doi: 10.1002/14651858.CD004464.pub3

36. Yang M, Zhu L, Yao H, Chen Y, Liu Z. Effects of electroacupuncture on chronic urinary retention after pelvic or lumbosacral tumor resection surgeries: A retrospective cohort study. *Transl Androl Urol.* (2024) 13:397–405. doi: 10.21037/tau-23-468

37. Boman E, Nylander M, Oja J, Olofsson B. Transanal irrigation for people with neurogenic bowel dysfunction: An integrative literature review. *Gastroenterol Nurs.* (2022) 45:211–30. doi: 10.1097/sga.0000000000000645

38. Bosch N, Kalkdijk-Dijkstra A, Broens P, van Westreenen H, Pierie J, Klarenbeek B, et al. Implementation of pelvic floor rehabilitation after rectal cancer surgery: A qualitative study guided by the consolidated framework for implementation research (Cfir). *PLoS One.* (2024) 19:e0301518. doi: 10.1371/journal.pone.0301518

39. Koda K, Yamazaki M, Shuto K, Kosugi C, Mori M, Narushima K, et al. Etiology and management of low anterior resection syndrome based on the normal defecation mechanism. *Surg Today.* (2019) 49:803–8. doi: 10.1007/s00595-019-01795-9

40. Park E, Baik S. Functional outcomes after sphincter-preserving surgeries for low-lying rectal cancer: A review. *Precis Future Med.* (2021) 5:164–74. doi: 10.23838/pfm.2021.00142

41. Zhou L, Zhong C, Su Y, Zhang Z, Wang L. Application of pelvic floor rehabilitation in patients with colorectal cancer: A scoping review. *Tech Coloproctol.* (2024) 28:141. doi: 10.1007/s10151-024-03017-y

42. Pang L, Chen X, Lan Y, Huang Q, Yu X, Qi L, et al. Research progress of acupuncture analgesia based on autonomic nerve regulation pathway. *Acupunct Herb Med.* (2023) 3:285–95. doi: 10.1097/HM9.0000000000000087

43. Yang X, He M, Cao J, Tang Q, Yang B, Li T, et al. Acupuncture and moxibustion for inflammatory bowel disease: Regulatory mechanisms revealed by microbiome and metabolomic analysis. *Am J Chin Med.* (2024) 52:1891–923. doi: 10.1142/s0192415x24500745

44. Yu Z. Neuromechanism of acupuncture regulating gastrointestinal motility. *World J Gastroenterol.* (2020) 26:3182–200. doi: 10.3748/wjg.v26.i23.3182

45. Huang Z, Liu Y, Su Z, Su J, Wu Q. [Effects of electroacupuncture at "Changqiang" (Gv 1) on expression of nerve growth factor and brain derived neurotrophic factor in rats after acute spinal cord injury]. *Zhongguo Zhen Jiu.* (2018) 38:399–404. doi: 10.13703/j.0255-2930.2018.04.015

46. Liu Y, Liu L, Wang X. Electroacupuncture at points Baliao and Huiyang (Bl35) for post-stroke detrusor overactivity. *Neural Regen Res.* (2013) 8:1663–72. doi: 10.3969/j.issn.1673-5374.2013.18.004

47. Wu G, Wang W. [Indication rules of Baliao points based on the clinical literature research]. *Zhongguo Zhen Jiu.* (2019) 39:96–102. doi: 10.13703/j.0255-2930.2019.01.024

48. Yang, S, Xin X, Liu J, Li Z. [Efficacy of spastic pelvic floor syndrome treated with electroacupuncture at Baliao (Bl 31, Bl 32, Bl 33 and Bl 34)]. *Zhongguo Zhen Jiu.* (2014) 34:869–72.

49. Zou Y, Ding S, Zhou H, Ye J, Xu X, Hu G, et al. [Development of researches on the underlying mechanism of acupuncture stimulation of Baliao-points for improving outlet obstruction constipation]. *Zhen Ci Yan Jiu.* (2015) 40:427–30.

50. Xue Y, Zhou H, Zeng Y, Wang C, Yang Y, Wang X, et al. Efficacy of electroacupuncture therapy in patients with functional anorectal pain: Study protocol for a multicenter randomized controlled trial. *Int J Colorectal Dis.* (2024) 39:55. doi: 10.1007/s00384-024-04628-5

51. Doshi D, Tambe D, Raina D. Sacral nerve stimulation for bladder dysfunction and pain-our experience. *Neuromodulation.* (2023) 26:S6. doi: 10.1016/j.neurom.2023.02.011

52. Weledji E, Marti L. A Historical perspective of sacral nerve stimulation (Sns) for bowel dysfunction. *IJS Short Rep.* (2021) 6:e25. doi: 10.1097/sr9.0000000000000025

53. Emmertsen K, Laurberg S. Impact of Bowel dysfunction on quality of life after sphincter-preserving resection for rectal cancer. *Br J Surg.* (2013) 100:1377–87. doi: 10.1002/bjs.9223

54. Liu Y, May B, Zhang A, Guo X, Lu C, Xue C, et al. Acupuncture and related therapies for treatment of postoperative ileus in colorectal cancer: A systematic review and meta-analysis of randomized controlled trials. *Evid Based Complement Alternat Med.* (2018) 2018:3178472. doi: 10.1155/2018/3178472

55. Yang Y, Pang F, Zhou M, Guo X, Yang Y, Qiu W, et al. Electroacupuncture reduces inflammatory Bowel disease in obese mice by activating the Nrf2/Ho-1 signaling pathways and repairing the intestinal barrier. *Diabetes Metab Syndr Obes.* (2024) 17:435–52. doi: 10.2147/dmso.S449112

56. Tian Y, Qiu X, Qi X, Dong Z, Zhao J, Huang J, et al. Electroacupuncture promotes apoptosis and inhibits axonogenesis by activating p75 neurotrophin receptor

for triple-negative breast xenograft in mice. *J Chem Neuroanat.* (2022) 124:102133. doi: 10.1016/j.jchemneu.2022.102133

57. van der Heijden J, Kalkdijk-Dijkstra A, Pierie J, van Westreenen H, Broens P, Klarenbeek B. Pelvic floor rehabilitation after rectal cancer surgery: A multicenter randomized clinical trial (force trial). *Ann Surg.* (2022) 276:38–45. doi: 10.1097/sla.0000000000005353

58. Rosen H, Boedecker C, Fürst A, Krämer G, Hebenstreit J, Kneist W. "Prophylactic" transanal irrigation (Tai) to prevent symptoms of low anterior resection syndrome (Lars) after rectal resection: Results at 12-month follow-up of a controlled randomized multicenter trial. *Tech Coloproctol.* (2020) 24:1247–53. doi: 10.1007/s10151-020-02261-2

59. Lin K, Granger C, Denehy L, Frawley H. Pelvic floor muscle training for bowel dysfunction following colorectal cancer surgery: A systematic review. *Neurourol Urodyn.* (2015) 34:703–12. doi: 10.1002/nau.22654

60. Shen L, Li W, Liu Z, Wang N, Liu Y, Miao L. Evaluating the clinical application and effect of acupuncture therapy in anal function rehabilitation after low-tension rectal cancer surgery. *World J Clin Cases.* (2024) 12:3476–81. doi: 10.12998/wjcc.v12.i18.3476

Frontiers in Medicine

Translating medical research and innovation into improved patient care

A multidisciplinary journal which advances our medical knowledge. It supports the translation of scientific advances into new therapies and diagnostic tools that will improve patient care.

Discover the latest Research Topics

See more →

Frontiers

Avenue du Tribunal-Fédéral 34
1005 Lausanne, Switzerland
frontiersin.org

Contact us

+41 (0)21 510 17 00
frontiersin.org/about/contact